



# Electrolytes polymère nano-structurés à base de liquides ioniques pour les piles à combustible hautes températures

Rakhi Sood

## ► To cite this version:

Rakhi Sood. Electrolytes polymère nano-structurés à base de liquides ioniques pour les piles à combustible hautes températures. Autre. Université de Grenoble, 2012. Français. NNT : 2012GRENI060 . tel-00819818

**HAL Id: tel-00819818**

**<https://theses.hal.science/tel-00819818>**

Submitted on 2 May 2013

**HAL** is a multi-disciplinary open access archive for the deposit and dissemination of scientific research documents, whether they are published or not. The documents may come from teaching and research institutions in France or abroad, or from public or private research centers.

L'archive ouverte pluridisciplinaire **HAL**, est destinée au dépôt et à la diffusion de documents scientifiques de niveau recherche, publiés ou non, émanant des établissements d'enseignement et de recherche français ou étrangers, des laboratoires publics ou privés.

## THESIS

To obtain the degree of

## DOCTOR OF UNIVERSITY OF GRENOBLE

Speciality: « **Materials, Mechanics, Civil Engineering, Electrochemistry** »

Arrêté ministériel : 7 août 2006

Presented by

« **Rakhi SOOD** »

Thesis directed by « **Cristina IOJOIU** » and

Co-directed by « **Eliane ESPUCHE** »

Prepared in the **Laboratory of Electrochemistry and Physical Chemistry of Materials and Interfaces (LEPMI)**

In the Doctoral School « **Engineering-Materials, Mechanics, Energy, Environment, Production (IMEP2)** »

# Nano-structured Polymer Electrolytes based on Ionic Liquids for High-Temperature PEMFCs

Thesis defended publically on « **06.12.2012** »,

In front of the esteemed jury comprising of:

**Mr. Jacques Rozière**

Professor, Montpellier II University

Reviewer

**Mr. Vito di Noto**

Professor, University of Padova

Reviewer

**Mr. Jean-Marc Zanutti**

Dr., CEA Saclay

Examiner

**Mr. Frédéric Bossard**

Professor, Joseph Fourier University

Examiner

**Mr. Jean Le Bideau**

Professor, Institut des Matériaux Jean Rouxel (IMN)

Examiner

**Ms. Hakima Mendil-Jakani**

Dr., CEA-Grenoble

Co-supervisor

**Ms. Eliane Espuche**

Professor, Claude Bernard University Lyon 1

Co-director

**Ms. Cristina Iojoiu**

CR-CNRS, LEPMI

Director



# **Acknowledgement**

*This thesis work would have not been possible without the guidance and the help of several individuals who in one way or another contributed and extended their valuable assistance in the preparation and completion of this study.*

*First and foremost, I would like to express my profound gratitude to **Dr. Cristina IOJOIU**, the director of my thesis work, whose constant advice, constructive criticism and encouragement immensely helped me in hurdling all the obstacles in the completion of this research work. I would equally like to thank **Prof. Eliane ESPUCHE**, the co-director of my thesis work, for her valuable suggestions and unfailing support throughout the course of my thesis work. I would also like to record my sincere thanks to **Dr. Hakima MEDIL-JAKANI**, the co-adviser of my thesis work, for her constructive discussions, valuable support and friendly attitude from the beginning to the very end of my thesis work.*

***Dr. Sandrine LYONNARD** not only for sharing her valuable insights in the relevance of the work but also for great moral support, friendly discussions, steadfast encouragement and immensely guiding the redaction of the manuscript of my thesis work.*

***Dr. Gerard GEBEL** for sharing his vision and giving precious suggestions on the interpretation of many important results despite his very tight schedule.*

***Dr. Laurent GONON** for providing his assistance, expertise and worthy contribution to one of the important parts of my thesis work.*

***Dr. Fabrice GOUANVE** for his great help and support in carrying out various experiments as well as his patience in explaining plenty of basics concerning a large part of my thesis work.*

***Prof. Jean-Yves SANCHEZ, Dr. Fannie ALLOIN and Prof. Jean-Claude LEPRETRE** for their kind concern, valuable advices and discussions from time to time which helped many times in the troubleshooting of various issues encountered during the course of my thesis work.*

***Dr. Armel GUILLERMO, Dr. Jacques JESTIN and Dr. Manuel MARECHAL** for their assistance and technical support in various experiments carried out during this research work.*

***Dr. Laure COINTEAUX and Ms. Denise FOSCALLO** for their help in handling many instruments utilized during my thesis work.*

***Dr. Jacques GUINET** for his timely assistance on installing various softwares required to treat many results as well as for sorting out problems encountered with instruments few times.*

*The technicians, **Ms. Virginie SZEFLINSKI** and **Ms. Emilie DUBARD**, for greatly assisting many experiments which had to be launched for long periods of time.*

*All my colleagues at **LEPMI** and **CEA-Grenoble** for providing me with moral support, cheerful environment as well as relaxing discussions.*

*Last but not the least, my **parents**, my **life partner**, my **brother** and **three friends** who gave me inestimable strength and inspired me to be optimistic in the times when I wanted to give up and decay. Without their support, I would have not been able to see this day when I have the title of “Doctor” in front of my name...*



# Contents

<b>Introduction</b> .....	1
<b>Chapter 1: State of the Art</b> .....	4
<b>1.1: Introduction to the Fuel cells</b> .....	5
<b>1.2: Types of Fuel cells</b> .....	5
<b>1.3: Fuel cells based on proton conduction</b> .....	7
1.3.1: DMFC.....	8
1.3.2: PEMFC.....	9
<b>1.4: Polymer Electrolyte Membranes (PEM)</b> .....	13
1.4.1: Perfluorosulfonic acid (PFSA) based membranes.....	16
1.4.2: Partially perfluorinated polymers and Polysiloxanes.....	29
1.4.3: Polymers based on Aromatic hydrocarbons.....	32
<b>1.5: Polymer Electrolyte Membranes for High temperature-PEMFCs</b> .....	42
1.5.1: Hygroscopic organic-inorganic membranes.....	42
1.5.2: Anhydrous proton conducting membranes.....	44
<b>a. Acid-Base complexes</b> .....	44
<b>b. Heterocycles</b> .....	46
<b>c. Proton conducting ionic liquids (PCIL)</b> .....	47
<b>Motivation of the thesis work</b> .....	54
 <b>Chapter 2: Triethylammonium Triflate doped Nafion<sup>®</sup> membranes based on swelling method</b> .....	64
<b>2.1: Polymer matrix: effect of neutralization</b> .....	66
a. Morphology.....	67
b. Thermo-mechanical properties.....	70
c. Conductivity.....	73

<i>d. Gas-permeability properties</i> .....	74
<i>e. Water sorption</i> .....	75
<i>Conclusion</i> .....	79
<b>2.2: TFTEA doped Nafion-TEA membranes</b> .....	80
<i>a. Membrane stability</i> .....	80
<i>b. Morphology</i> .....	81
<i>c. Differential Scanning Calorimetry</i> .....	85
<i>d. Thermo-mechanical properties</i> .....	85
<i>e. Conductivity</i> .....	88
<i>f. Gas-permeability properties</i> .....	89
<i>g. Water sorption</i> .....	89
<i>Conclusion</i> .....	96
<b>2.3: TFTEA doped Nafion-TEA in the presence of water</b> .....	97
<i>a. Morphology</i> .....	97
<i>b. Conductivity</i> .....	98
<i>Conclusion</i> .....	102
<b>2.4: General Conclusion</b> .....	103
 <b>Chapter 3: Elaboration of Triethylammonium Triflate doped Nafion<sup>®</sup> membranes: Swelling and Casting</b> .....	106
<b>3.1. Nafion-TEA by casting method</b> .....	107
<i>a. Morphology</i> .....	107
<i>b. Thermo-mechanical properties</i> .....	112
<i>c. Conductivity</i> .....	116
<i>d. Gas-permeability properties</i> .....	117

e. Water sorption.....	118
Conclusion.....	120
<b>3.2: TFTEA doped Nafion-TEA membranes: comparison of properties based on elaboration method.....</b>	<b>121</b>
a. Morphology.....	121
b. Differential Scanning Calorimetry.....	131
c. Thermo-mechanical properties.....	131
d. Conductivity.....	136
e. Gas-permeability properties.....	137
f. Water sorption.....	137
Conclusion.....	140
<b>3.3: Fuel cell performance and degradation study.....</b>	<b>141</b>
a. Fuel cell performance.....	141
b. Degradation in the presence of peroxy radicals.....	144
Conclusion.....	161
<b>3.4: General Conclusion.....</b>	<b>161</b>
 <b>Chapter 4: Casting based Nafion-TEA membranes doped with different per-fluorinated anion based ionic liquids.....</b>	 <b>166</b>
<b>4.1. Characterization and comparison of Nafion-TEA membranes based on different PCILs.....</b>	<b>167</b>
a. Morphology.....	168
b. Differential Scanning Calorimetry.....	180
c. Thermo-mechanical properties.....	184
d. Conductivity.....	190
e. Gas-permeability properties.....	194

<i>f. Water sorption</i> .....	195
<b>4.2: General Conclusion</b> .....	202
 <b>Chapter 5: TFTEA doped membranes based on Polysulfones</b> .....	206
<b>5.1. Synthesis of PSPF-TEA</b> .....	208
<i>a. Synthesis of the side chain function</i> .....	208
<i>b. Bromination of Polysulfone (Udel form) at ortho-ether-position</i> .....	210
<i>c. Grafting of side-chain function on the backbone of brominated Polysulfones</i> .....	213
<i>d. Neutralization of PSPF-acid form with triethylamine</i> .....	216
<b>5.2. PSPF-TEA+TFTEA</b> .....	217
<i>a. Morphology</i> .....	218
<i>b. Thermo-mechanical properties</i> .....	220
<i>c. Conductivity</i> .....	221
<b>5.3: General Conclusion</b> .....	223
 <b>General conclusions and perspectives</b> .....	226
 <b>Chapter 6: Experimental part</b> .....	232
<b>6.1. Synthesis</b> .....	232
<i>a. PCIL synthesis</i> .....	232
<i>b. Preparation of Nafion-TEA</i> .....	233
<i>c. Preparation of PSPF-TEA</i> .....	234
<i>d. PCIL-based-membrane elaboration</i> .....	237
<b>6.2: Membrane characterization</b> .....	238
<i>a. Study of leaching phenomenon</i> .....	238

<i>b. Density measurements.....</i>	<i>238</i>
<i>c. Wide Angle X-ray Scattering (WAXS).....</i>	<i>238</i>
<i>d. Small Angle Neutron Scattering (SANS).....</i>	<i>239</i>
<i>e. Differential Scanning Calorimetry (DSC).....</i>	<i>239</i>
<i>f. Dynamic Mechanical Analysis (DMA).....</i>	<i>240</i>
<i>g. Conductivity in anhydrous conditions.....</i>	<i>240</i>
<i>h. Conductivity in humid conditions.....</i>	<i>240</i>
<i>i. Gas-permeation Analysis.....</i>	<i>241</i>
<i>j. Water sorption Analysis.....</i>	<i>241</i>
<i>k. Fuel cell test.....</i>	<i>241</i>
<i>l. Degradation study.....</i>	<i>242</i>
 <b><i>Résumé (in French).....</i></b>	 <b><i>245</i></b>
<b><i>ANNEXES (I-3).....</i></b>	<b><i>265-267</i></b>

## Introduction

---

The thesis work presented in this manuscript is based on *the elaboration and characterization of PCIL doped nano-structured polymer electrolytes membranes* for the application of Polymer Electrolyte Membrane Fuel Cell (PEMFC) above 100°C.

The thesis project has been financed by *The Academic Community of Research (ARC) ENERGIES Rhone Alpes* (formerly known as *MACODEV Rhone Alpes*).

The work accomplished during the course of the thesis has been carried out in collaboration among three laboratories which include: *LEPMI* (The Laboratory of Electrochemistry and Physicochemistry of Materials and Interfaces), *LMPB/IMP* (The Laboratory of Polymer Materials and Bio-materials/Engineering of Polymer Materials) and *INAC-SPrAM* (The Laboratory of Structure and Properties of Molecular Architectures). The thesis work has been effectuated under the guidance of Cristina IOJOIU (LEPMI), Eliane ESPUCHE (LMPB/IMP) and Hakima MENDIL-JAKANI (INAC-SPrAM).

Proton exchange membranes (PEMs) have been extensively studied for application in fuel cells (PEMFC). Currently, the “state of the art” PEMFC technology is based on PEM and electrode active layers made of perfluorinated ionomers, most of which belong to the Nafion® family. Such PEMFCs are limited to an upper operating temperature close to 80°C, with ionomer performance dropping sharply at higher temperatures. Since the electric yield of a PEMFC is no more than 50%, the thermal management of a PEMFC in a small- to medium-size car is a real issue. Therefore, for most of the car manufacturers, the upper operating temperature needs to be increased to temperatures higher than 100°C.

A few approaches have been explored by the scientific community in this regard. These approaches include combination of polymer electrolytes with phosphoric acid, high boiling solvents such as imidazoles or proton conducting ionic liquids (*PCIL*).

The membranes containing PCILs are promising systems owing to their good ionic conductivity under high temperature and anhydrous conditions. Thus, this work is dedicated to such type of system i.e. Polymer Electrolyte + PCILs. However, the performance of such membrane strongly depends on the polymer and PCIL structures, concentration and particularly on the interactions of PCIL with the polymer to avoid the PCIL leaching phenomena and to assure an optimal dispersion of PCIL into polymer matrix. In addition to a good conductivity and stability at high temperature, good thermo-

mechanical strength, low gas permeability, limited water sorption are required for a PEMFC membrane. Thus, to overcome all these requirements, a nano-structured membrane must possess percolated hydrophobic nano-domains, responsive mainly for mechanical strength, and percolated ionic nano-domains, responsive for ionic conductivity.

Therefore, in this work, a deep study on the evolution of morphology and consequent functional properties of the polymer electrolytes in function of PCIL concentration and structure has been performed. Moreover, a study of the impact of the elaboration method on the properties of these doped membranes has been done. In addition, preliminary studies on the evaluation of fuel cell performance and degradation phenomenon in the presence of hydrogen peroxide for these doped membranes have been carried out. The polymer electrolyte chosen for this study is mainly Nafion<sup>®</sup> due to its known nano-structured morphology. Apart from Nafion<sup>®</sup>, new polymer electrolyte based on modified Polysulfone has been explored to some extent due its high thermal and mechanical stability required for high temperature-PEMFC applications.

The work related to the synthesis (of PCILs and polymer electrolytes) and elaboration of the membranes, evaluation of their thermal, electro-chemical thermo-mechanical properties and fuel cell performance has been carried out at LEPMI. The work at INAC-SPrAM was focused on the study of morphology of these doped membranes as well as the degradation phenomenon associated with these doped systems. Finally, at LMPB/IMP, the work involved the study of transport properties such as water sorption and gas-permeability of these PCIL based PEMs.

The manuscript of the thesis work has been divided into 6 chapters.

The *first chapter* is based on the bibliographical study of various features of fuel cell systems and more precisely of PEMFCs. The chapter will begin with brief discussion on the global features followed by a brief comparison of different types of fuel cells. Afterwards, the focus will be on the important aspects and key issues related specifically to the fuel cells based on proton conduction and the membranes used in this framework. In particular, the main features of Nafion<sup>®</sup> membranes, which are often considered as the reference membranes, will be recalled. Subsequently, different polymers and different routes proposed in the literature to improve the initial as well as long term properties of the membranes will be described.

The *second chapter* will be focused on the influence of PCIL addition on the morphology as well as the functional properties of Nafion<sup>®</sup> based PCIL doped membranes elaborated by swelling method. In this work, polymer electrolytes have been utilized in neutralized form (neutralized with an amine). Thus, in the first part of this chapter, the impact of neutralization on various characteristics (morphology and functional properties) of Nafion<sup>®</sup> 117 membrane will be presented since the

neutralized membrane (denoted as Nafion-TEA) will serve as the Reference membrane for the PCIL doped membranes. In the second part, influence of PCIL addition and its concentration on the nano-structuration of Nafion-TEA will be discussed. This will be followed by a profound discussion on the impact of PCIL addition/concentration on the thermo-mechanical, electro-chemical and transport properties of Nafion-TEA. Moreover, a co-relation among the evolution of morphology and functional properties will be attempted. In the last part of this chapter, the focus will be on the study of impact of presence of water on the morphology and properties of these PCIL doped Nafion-TEA membranes since the membranes were characterized in anhydrous state in the preceding sections of this chapter.

The *third chapter* will detail the impact of elaboration method on the characteristics of these PCIL doped Nafion-TEA membranes. The membranes elaborated by casting and swelling method will be compared with each other from the point of view of morphology at different length scales as well as the functional properties. This comparison will be followed by preliminary studies on the fuel cell performance and degradation phenomena associated with these PCIL doped systems.

The *fourth chapter* will be focused on the influence of the chemical structure of the PCIL on the properties of Nafion-TEA. A deep discussion on the morphology of membranes doped with PCILs based on different perfluorinated anions will be presented. Afterwards, the impact of the particular morphologies acquired by these doped membranes (based on different PCILs) on their functional properties will be discussed.

The *fifth chapter* will explore the possibility of replacing Nafion<sup>®</sup> with a synthetically modified high-performance aromatic polymer i.e. Polysulfone in these PCIL doped membranes. In the first part, the various steps involved in the modification of Polysulfone with perfluoro alkyl sulfonic acid functions will be discussed. The second part will be concentrated on the study of morphology and functional properties of PEMs based on the modified Polysulfone and PCILs.

After presenting all the chapters associated with different parts of this thesis work, *general conclusions and perspectives* of the work will be discussed.

In the *last chapter* i.e. sixth chapter, the details of experimental methods employed to carry out this thesis work will be given.



# 1. State of the Art

---

**T**his bibliographical chapter primarily underlines various features associated with fuel cells and more precisely with High Temperature-Polymer Electrolyte Membrane Fuel Cells (HT-PEMFC). The chapter will begin with brief discussion on the global features followed by a brief comparison of different types of fuel cells. Afterwards, the focus will be on the important aspects and key issues related specifically to the fuel cells based on proton conduction and the membranes used in this framework. In particular, the main features of Nafion<sup>®</sup> membranes, which are often considered as the reference membranes, will be recalled. Subsequently, different polymers and different routes proposed in the literature to improve the initial as well as long term properties of the membranes will be described. The objective of this analysis is to be able to draw guidelines that would guide the synthesis of new membranes which subject to the experimental work of the thesis.

### ***1.1: Introduction to Fuel Cells***

Worldwide energy consumption is acknowledged as the main source of human contribution to greenhouse gas emission. Moreover, it has had a dominating contribution to the exhaustion of fossil fuel resources. Therefore, development of alternative sources of energy which are both environment friendly and fossil fuel-free have recently garnered huge attention. Among these alternatives, Fuel cells have been considered as an interesting and promising alternative. A fuel cell is basically an electro-chemical device which can directly convert the chemical energy into electrical energy. It has become of great interest as a potential economical, clean and efficient means of producing electricity in a variety of commercial and industrial applications. Fuel cell systems offer several advantages<sup>(1,2)</sup> compared with conventional generation methods such as:

- a). Efficiency** - Fuel cells are generally more efficient than combustion engines as they are not limited by temperature as is the heat engine.
- b). Simplicity** - Fuel cells are essentially simple with few or no moving parts. High reliability may be attained with operational lifetimes exceeding 40,000 hours (the operational life is formally over when the rated power of the fuel cell is no longer satisfied).
- c). No emissions** - Fuel cells running on direct hydrogen and air produce only water as the byproduct.
- d). Silence** - The operation of fuel cell systems are very quiet with only a few moving parts if any. This is in strong contrast with present combustion engines.
- e). Flexibility** - Modular installations can be used to match the load and increase reliability of the system.

### ***1.2: Types of Fuel Cells***<sup>{2,4,5}</sup>

Fuel cells are classified ***primarily by the kind of electrolyte they employ***. This determines the kind of chemical reactions that take place in the cell, the kind of catalysts required, the temperature range in which the cell operates, the fuel required, and other factors. These characteristics, in turn, affect the applications for which these cells are the most suitable. There are several types of fuel cells currently under development, each with its own advantages, limitations, and potential applications. Table 1 describes various important features of different fuel cell technologies. Broadly, fuel cells can be

divided into *two categories*: **High Temperature-Fuel Cells** such as Solid Oxide Fuel Cell (SOFC), Molten Carbonate Fuel Cell (MCFC) and Phosphoric Acid Fuel Cell (PAFC); **Low Temperature-Fuel Cells** such as Alkaline Fuel Cell (AFC), Direct Methanol Fuel Cell (DMFC) and Proton Exchange Membrane Fuel Cell (PEMFC).

Considering Low Temperature Fuel Cells, AFC is based on the conduction of hydroxyl ions using potassium hydroxide as an electrolyte while DMFC and PEMFC are based on conduction of protons using a polymer electrolyte membrane.

<i>Type of Fuel Cell</i>	<i>Electrolyte</i>	<i>Charge Carrier</i>	<i>Operation Temperature (°C)</i>	<i>Fuel</i>	<i>Electric Efficiency (%)</i>	<i>Area of Application</i>
<b>AFC</b>	<i>KOH in H<sub>2</sub>O</i>	<i>OH<sup>-</sup></i>	<i>60-120</i>	<i>H<sub>2</sub> (pure)</i>	<i>35-55</i>	<i>Space, Mobile</i>
<b>PEMFC</b>	<i>Polymer</i>	<i>H<sup>+</sup></i>	<i>50-100</i>	<i>H<sub>2</sub> (pure, CO<sub>2</sub> tolerance)</i>	<i>35-45</i>	<i>Portable: Mobile, Stationary</i>
<b>DMFC</b>	<i>Polymer</i>	<i>H<sup>+</sup></i>	<i>0-60</i>	<i>Methanol</i>	<i>35-45</i>	<i>Portable: Mobile*</i>
<b>PAFC</b>	<i>Phosphoric acid</i>	<i>H<sup>+</sup></i>	<i>~220</i>	<i>H<sub>2</sub> (pure, CO<sub>2</sub>, 1% CO tolerance)</i>	<i>40</i>	<i>Distributed power</i>
<b>MCFC</b>	<i>Molten Lithium &amp; Potassium Carbonate</i>	<i>CO<sub>2</sub><sup>3-</sup></i>	<i>~650</i>	<i>H<sub>2</sub>, CO, CH<sub>4</sub></i>	<i>&gt;50</i>	<i>Distributed power generation</i>
<b>SOFC</b>	<i>Solid oxide electrolyte</i>	<i>O<sup>2-</sup></i>	<i>~1000</i>	<i>H<sub>2</sub>, CO</i>	<i>&gt;50</i>	<i>Base load power generation</i>

*Table 1: Characteristics of various Fuel Cell technologies*

This bibliographic chapter is principally focused on the **Polymer Electrolyte Membranes (PEM)**. Firstly, a short introduction to the important features, working and shortcomings of Low Temperature-Fuel cells based on proton conduction i.e. **PEMFC** and **DMFC** will be given. This will be followed by a global and thorough discussion on various polymer electrolyte systems developed and/or commercialized so far.

### 1.3: Fuel Cells based on proton conduction

In this section, various aspects such as design and features, schematic working, shortcomings and their solutions will be discussed in regard of low-temperature fuel cells involving proton conduction. Higher attention and hence *thorough discussion will be on PEMFCs due to their promising nature and better performance* for the moment.

Low temperature fuel cells have garnered great interest in regards to portable energy devices due to their potential of generating much higher power densities compared to lithium-ion batteries<sup>(6)</sup> in addition to the low temperature of their operation. Based on proton conducting polymer electrolyte, Direct Methanol Fuel Cell (DMFC) is the most developed Alcohol based fuel cell which uses *methanol as a fuel* directly in the fuel cell while Polymer Electrolyte Membrane Fuel Cells (PEMFC) utilizes *hydrogen as a fuel*. These fuel cells have been designed in the form of *Membrane Electrode Assembly (MEA)*. The key components of an MEA are illustrated in figure 1.

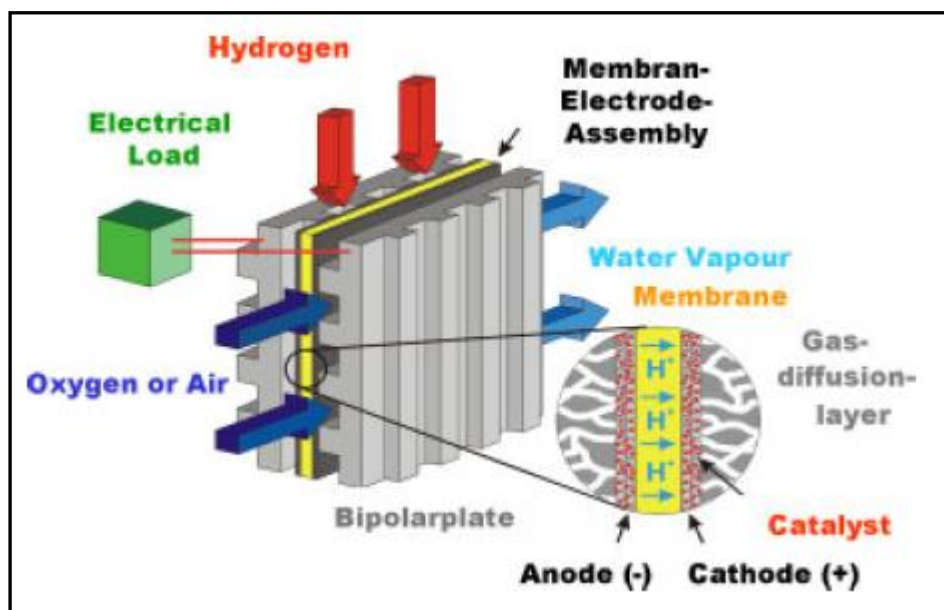


Figure 1: Schematic illustration of a Membrane Electrode Assembly (MEA)<sup>(7)</sup>

An MEA is manufactured by hot-pressing of the electrodes onto a polymer electrolyte membrane of very small thickness which is, hence, present between the two electrodes. A very porous electrode with a spherical microstructure is employed to achieve maximum area of contact between the electrodes, electrolyte and gas thus increasing the efficiency and current of the fuel cell. Materials commonly used for these electrodes are carbon cloth or carbon fibre paper. The electrodes are embedded with an electro-catalyst layer at the electrode-membrane interface in order to improve the

electrode reaction kinetics. This electro-catalyst layer consists of catalyst in the form of nano-particles as well as a proton conducting ionomer and consists of two types of channels (represented in figure 2): an electronic channel provided by the support (i.e. carbon) to the current collector; a protonic channel provided by incorporated proton conducting ionomer to/from the polymer electrolyte membrane or the purpose of both the channels provided by an electron and proton conducting polymer as proposed recently<sup>[8-10]</sup>. There should be a **high interfacial contact between polymer electrolyte membrane and electro-catalyst layer at the triple-phase boundary (TPD)** in order to acquire fast kinetics of electrode reactions<sup>[9]</sup>. In addition to polymer electrolyte membrane and electrodes, an MEA consists of gas diffusion layers before the electrodes for better transport of the reactants to the electrodes, more efficient elimination of water out the system and for better heat conduction.

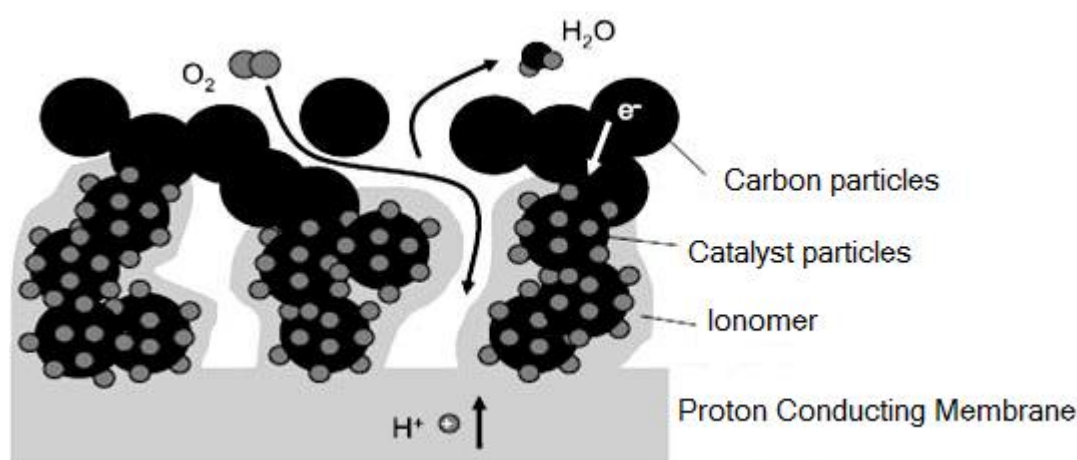


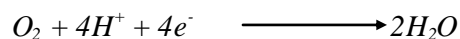
Figure 2: Illustration of co-existence of ionic-electronic-gaseous phase (Triple-phase Boundary) at the triple point contact; Reaction at the cathode i.e. reduction of oxygen and formation of water is shown<sup>[7,10]</sup>

### 1.3.1: DMFC

In a DMFC, methanol directly undergoes catalytic oxidation at the anode in the presence of water and produces electrons and protons along with carbon dioxide as a byproduct. The electrons are transferred through an external circuit and protons pass through the polymer electrolyte membrane and hence both reunite at the cathode.



At the cathode (positive terminal), oxygen reacts with the protons and electrons to produce electrical energy with water as a byproduct.



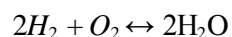
DMFCs present an overall *efficiency of 20-25%* and have been proposed for the application of automobiles and mobile phones<sup>(11)</sup>. However, there are certain *key issues* related to this technology which hinder its overall efficiency and commercialization mentioned below<sup>(11-16)</sup>:

1. High *crossover rate of methanol* through the polymer electrolyte membrane leading to low energy efficiency
2. Limited fuel cell performance and lifetime
3. Slow *oxidation kinetics of methanol* due to low activity of the electro-catalyst at the anode side (as formaldehyde and formic acid are produced as intermediate products during methanol oxidation which diminish catalyst activity) and *CO poisoning of the catalyst* (as CO and other gases are produced during methanol oxidation)
4. Low activity of electro-catalysts at the cathode side due to their low tolerance to methanol resulting in *slower oxygen reduction rate*.

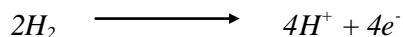
It has been proposed that these problems can be resolved to some extent by increasing the operating temperature of the fuel cell and by developing alternative electro-catalysts<sup>(11)</sup>.

### 1.3.2: PEMFC

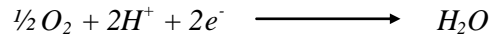
PEMFC technology is based upon the simple combustion reaction given below:



In order to understand this reaction, reactions occurring at the two electrodes have to be considered. Hydrogen fuel is supplied to the anode (negative terminal) of the fuel cell where it gets oxidized liberating electrons and creating protons along with the production of heat. Each takes a different path to the cathode. The electrons are transferred through an external circuit and protons pass through the polymer electrolyte and both reunite at the cathode.



At the cathode (positive terminal), the electron, proton, and oxygen combine to form the water as a byproduct.



PEMFCs have been envisioned primarily for transportation applications and some stationary applications. Due to their fast start-up time, low sensitivity to orientation, tolerance to shock and vibrations, immediate response to changes in the demand for power and favorable power-to-weight ratio, PEMFCs are particularly suitable for use in passenger vehicles, such as cars and buses<sup>{5,17}</sup>. However, there are certain key issues related to PEMFC technology which act as constraints for its large-scale commercialization. These **key issues** are listed below<sup>{18-20}</sup>.

1. The conduction of protons takes place with the help of water molecules present in the ionic domains through the polymer electrolyte membrane, hence hydration of the membrane is the key factor for fuel cell functioning. ***Presence of water limits the operational temperature*** of PEMFCs.
2. Moreover, water molecules are present not only due to the humidification of gases but also due to its production as a product at the cathode. As a result, there are ***different diffusion phenomena*** associated with water in the system which include: self-diffusion; diffusion from anode to cathode due to electro-osmotic drag causing dehydration of anode side leading to heterogenous swelling of the membrane which can affect the membrane-electrode interface or even cause membrane failure; diffusion phenomenon due to the concentration gradient created between the electrodes since water is in excess at cathode due to its production there. A balance has to be created among all these diffusion phenomena for the proper functioning of fuel cell. ***An excess of water in the system inhibits the transport of reactant gases, while it's deficiency leads to poor proton conductivity***<sup>{21}</sup>. Recently, it has been demonstrated in a study using neutron scattering that the distribution of water in the MEA depends on the relative humidity of the reactant gases, functioning temperature, water production at the cathode etc.<sup>{22}</sup>. Hence, ***water management, being complex in nature, is even more difficult when water is present in liquid and vapor phases***. In addition, presence of liquid water in the stack can limit the use of PEMFC under the environment with freezing conditions due to the fact that exterior conditions with sub-zero temperatures can cause phase and hence volume change of water which could eventually lead to the deformation of the catalytic layer and hence mechanical failures.

3. A **significant barrier** to using these fuel cells in vehicles is **hydrogen storage**. Most fuel cell vehicles (FCVs) powered by pure hydrogen must store the hydrogen onboard as a compressed gas in pressurized tanks. Due to the low energy density of hydrogen, it is difficult to store enough hydrogen onboard to allow vehicles to travel the same distance as gasoline-powered vehicles before refueling, typically 300-400 miles. Although, there have been certain approaches explored in literature to increase the hydrogen storage capacity, eg. Hydrogen storage based on complex hydrides. However, operating temperature of the fuel cell is the main hurdle in adopting this technology since the temperature required for desorption of Hydrogen from these metal hydrides require temperature between 100-200°C. Another viable solution is to use hydrogen produced by reforming of fuels such as natural gas, alcohols or gasoline using various reforming reactions such as water-gas shift reaction, preferential oxidation, methanol oxidation etc.. However, **gases produced from reforming reactions contain traces of CO which adsorbs on the surface of the catalyst at the anode thereby hindering the activity of catalyst** for the hydrogen oxidation reaction and hence greatly affect the fuel cell performance which only deteriorates with time<sup>[23]</sup>. Moreover, the CO gas passes through the membrane and poisons the cathode as well<sup>[24]</sup>. A lot of study is undergoing on other catalyst systems eg. platinum/ruthenium **catalysts that are more resistant to CO**. In addition, this approach would increase cost and weight, would reduce reliability and responsive capacity of the fuel cell.
  
4. **Heat management** is another key issue related to the technology. Since a large amount of heat is produced during fuel cell functioning which has to be rejected to maintain the operating temperature of the fuel cell, this task is almost completely dependent on the cooling systems. Hence, in order **to improve the efficiency of the system, increasing the operation temperature of PEMFC is necessary**. Moreover, increased working temperature would lead to higher amount of heat production which in turn could be recovered for the direct heating of PEMFC or could be utilized for the steam-reforming processes or for pressurized operation leading to an overall improved energy efficiency of the system.

As a way to **solve/minimize these shortcomings, high working temperature (100°C ≤ T < 200°C) of PEMFCs has been proposed**<sup>[18,19]</sup>. Key **advantages associated with high operating temperature** of PEMFCs are discussed as follows:

1. Increase in temperature would result in **faster reaction kinetics at both the electrodes especially in Oxygen reduction reaction**<sup>[25,26]</sup>. Moreover, improved reaction kinetics at the



electrodes can significantly help in replacing platinum based catalysts with other non-platinum based catalysts which would help in overall cost reduction<sup>{27,28}</sup>.

2. Higher temperature of fuel cell functioning would lead to a greater difference of temperature between the fuel cell and ambient atmosphere thereby facilitating *easier heat-rejection*. In this way, cooling systems can be simplified thereby increasing the mass-specific and volume-specific power density of the fuel cell.
3. The diffusion coefficient of hydrogen is one order higher than that of oxygen in air at certain pressure and temperature. Hence, slower diffusion of oxygen is a limiting factor in the functioning of PEMFC in regard of reactant transport. It has been observed that *oxygen transport is slower in liquid water than in water vapor*<sup>{4}</sup>. Hence, by increasing the operating temperature, the percentage of water vapor could be increased in the gas diffusion layer and catalyst layer of cathode, thereby, improving oxygen transport and hence, fuel cell performance.
4. Increasing operation temperature of the fuel cell has been observed as a solution to the problem of CO poisoning of the electro-catalysts due to *increased tolerance of the catalyst towards adsorption of CO*. According to literature, the CO tolerance of the catalyst can be greatly improved from, 20 ppm at 80°C, to 1000 ppm at 130°C, to 30000 ppm at 200°C<sup>{18}</sup>. This would allow the removal of CO separator for CO clean up from the fuel processing unit.
5. Presence of water in dual state i.e. liquid and vapor complicates the functioning of fuel cell and can affect the chemical stability of the membrane as well. In addition, presence of water in vapor state would increase the overall exposed surface area of electro-catalysts and hence *improve the ability of the reactants to diffuse into the reaction layer*<sup>{29}</sup>.

However, many research groups have also pointed out certain *disadvantages of using high temperature* which are listed below<sup>{20,25}</sup>:

1. Durability of the system will decrease due to *increased liability to structural and chemical degradation*<sup>{30,31}</sup>.
2. The already existing problems of *corrosion of carbon support can aggravate* with the increase in operating temperature of PEMFCs<sup>{32}</sup>. It has been reported that the corrosion rate of the carbon support increases with increasing platinum loading and increasing temperature. Moreover *agglomeration of Pt nano-particles* (reduction of electrochemically active surface

area), dissolution of Pt particles into acidic operating environment and re-deposition during long term operation aggravate with increasing temperature.

3. ***Membrane degradation is accelerated*** under low humidity and high temperature conditions.
4. Since the proton conductivity is highly dependent on the presence of water, ***dehydration of the polymer electrolyte and consequent loss of proton conductivity*** is a major issue related to HT-PEMFC technology.
5. If ***high relative humidity is required for high proton conductivity at elevated temperatures***, a ***very high pressure*** is required which is technically and ***commercially not interesting***. Nevertheless a lot of research is going on for the development of polymer electrolyte systems utilizable under low humidity/anhydrous conditions which will be discussed later in this chapter.

#### ***1.4: Polymer Electrolyte Membranes (PEM)***

Historically, utilization of a proton conducting polymer electrolyte membrane as an electrolyte in the fuel cell was first demonstrated in the early 1960s by Williard Thomas Grubb and Leonard Niedrach of General Electric<sup>[3]</sup>. Since then, a variety of PEMs have been developed which will be discussed thoroughly later in this part.

The ***PEMs are usually based on thin ionomer (polymer functionalised with acidic function) films***. The main roles served by membrane are to ***separate the electrodes in order to avoid short circuit, to allow proton transportation from anode to cathode, to create a barrier against the passage of gases or fluids (e.g. methanol) and to provide mechanical strength to the assembly***. Nevertheless, the ionomer itself does not provide any appreciable conductivity and so must be swollen by small molecules (i.e. water) to ensure proton conductivity.

The basic/inherent properties of PEMs required for fuel cell application include high proton conductivity at low hydration levels, electro-chemical, chemical and mechanical stability, durability, low gas permeability and low cost. Moreover, gas-permeability properties, solubility of gases, good contact between polymer and catalyst are of great importance<sup>[33]</sup>. A good interfacial contact between the constituents of catalyst layer of the electrodes and the proton conducting membrane is of prime importance in order to achieve accelerated electrode reactions and hence high efficiency of the PEMFC as discussed previously. There are various key properties of a Polymer Electrolyte Membrane which have great influence on the performance of the PEMFC as listed below:

**Ion Exchange Capacity, Water Sorption and Proton Conductivity:** The Ion Exchange Capacity (IEC) of a polymer is defined as the reciprocal value of the equivalent weight (EW; dry mass equivalent per mole of acid groups, unit g/mol ( $H^+$ )). The *proton conductivity of ionomers is related to the (ion-exchange capacity) IEC* and it often increases abruptly at some specific IEC in relation with the ionomer structure and percolation limit. The IEC or the EW is often employed to characterize a polymer with protonic conduction or to compare various materials between them. However, the IEC, does not give any indication about the distribution of the sites of the acid functions through the thickness of the membrane, which is, however, of paramount importance so that the protons are transported all the way from anode to cathode. While the acid groups must dissociate so that the proton becomes mobile, the water content of the membrane will also have a strong influence on proton conductivity. Basically, the polymer electrolyte membrane is swollen by water due to high levels of hydration applied all across the membrane and the transport of proton takes place with the help of the water molecules present in the ionic domains of the polymer electrolyte membrane. The proton diffusion can occur by two mechanisms as shown in figure 3<sup>[34]</sup>: **Vehicular mechanism** involving migration of a proton with the help of a molecule such as water (hence forming hydronium ions) across the membrane and **Grotthuss mechanism** involving proton jumps from hydronium ions to adjacent water molecules by tunneling in a hydrogen bond and reorientation of the water molecule thus formed to acquire another proton. Obviously, the ability of a membrane to trap more molecules of water increases with the increase in the IEC due to the increase in polarity of membrane by higher concentration of acid functions.

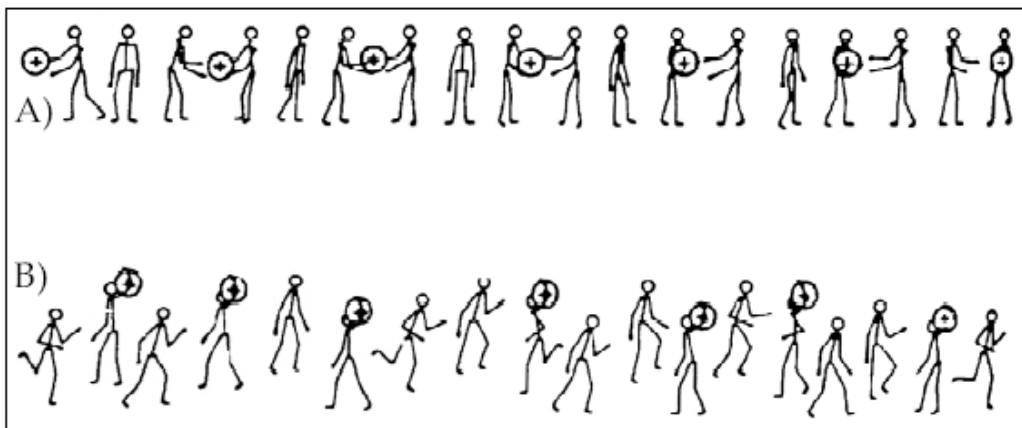


Figure 3: Types of conduction mechanisms (A): Grotthuss Mechanism; (B): Vehicular Mechanism

**Durability:** The maintenance of the *chemical and mechanical integrity of the membrane* is one of the key components of the durability of the PEMFC. The ageing of the membrane is associated with the loss of one or two functionalities of electrolyte and of separator. The loss of the acid functional

groups results in lower IEC which leads to the progressive reduction in the conductivity of membrane, while the loss of the mechanical integrity, by formation of hole, leads to the total failure of the cell by short circuit<sup>[35]</sup>. The ***membranes of PEMFC undergo chemical degradation by the scission of polymer chain, the loss of functional groups or the components (blocks, side chains, component of mixture), caused by the hydroxyl- and alkoxy- radicals***, which are formed in situ by H<sub>2</sub> and O<sub>2</sub> interaction with catalyst (Pt) of the anode and on the side of cathode<sup>[36]</sup>. In this context, the permeability of membrane to hydrogen and oxygen gases increases leading to an increase in the formation of radical species, hence accelerating the degradation of the membrane.

The mechanical properties of the membrane are also important. In addition to the breaking strength and the elongation with traction, ***dimensional stability during swelling, resistance to the crack and the propagation of a crack*** must also be considered. The creep of polymer is likely to occur because the membrane inflated by water is plasticized and the membrane is under a constant force of compressing in the cell. This can lead to a reduction in the thickness of the membrane, and formation of holes thereafter. An effect particularly related to swelling of polymer due to sorption of water is a phenomenon of fatigue, where the MEA is working with the periodic cycles of wetting and drying creating regular swelling and compression of the electrolyte membrane, can finish by the formation of the cracks in the membrane. This has been observed as one of the modes of failure of membrane<sup>[35]</sup>.

**Cost:** Reasonable cost is one of the most important features of a PEM for the commercialization of PEMFC technology. The “state of the art” ionomer employed today for PEMFCs are Perfluorosulfonic acid (PFSA) based membranes (*will be discussed in detail later in this section*) such as Nafion® (DuPont®), Flemion® (Asahi Glass®), Aciplex® (Asahi Kasei®) etc.. However, they have the ***disadvantage of being expensive because of the complicated and expensive fluorine chemistry utilized for their manufacturing***. Although the production of the membrane at industrial scale can reduce its price to great extent, the development of the alternative materials based on partially fluorinated or even non-fluorinated polymers is of great interest.

Initially, these PEM fuel cells were based on sulfonated Polystyrene<sup>[37]</sup>. However, these membranes were found to be not enough stable for the application due to the problem of their short life-time and stability. Since then, variety of ionomers have been developed and proposed for the application of Polymer Electrolyte Membrane (PEM) in PEMFCs which is elaborated thoroughly in the proceeding part of the section.

#### 1.4.1: Perfluorosulfonic acid (PFSA) based Membranes

Since the development of perfluorinated ionomer named Nafion<sup>®</sup> by Walter Grot from Dupont<sup>®</sup> in the 1960s, *perfluorinated ionomers have emerged as “state of the art” materials for low-temperature fuel cell applications* because of their high proton conductivity and their excellent chemical and thermal stability. Moreover, these ionomers provide the right medium for the electrode-electrolyte interface reactions due the fact that their terminal sulfonic acid groups do not adsorb on the surface of catalyst which results in high catalytic activity of the catalyst embedded in the carbon support for the oxygen reduction reaction (Approaches) & the solubility of O<sub>2</sub> and H<sub>2</sub> in these ionomers are quite high leading to fast electrode reaction kinetics<sup>[18]</sup>. *For decades, no other type of material has been found to be equally competitive, despite intense research and a number of severe limitations impeding an economical and wide-spread application of proton exchange membrane (PEM) fuel cells.*

Today, there are different perfluorinated ionomers available in the market commercially developed by different Companies. Some of these perfluorinated ionomers such as *Aciplex*<sup>®</sup> (Asahi Chemical Co Ltd.), *Flemion*<sup>®</sup> (Asahi Glass Co. Ltd.), *3 M membrane* (3 M Inc.) and *Gore*<sup>®</sup> *Select* (Gore and Associates Inc.) have chemical structure similar to Du Pont's *Nafion*<sup>®</sup> and all of them are with varying equivalent weight, thickness and processing method of membrane. Other type of perfluorinated ionomers also called Short Side Chain (SSC) membrane were first developed by Dow Chemical in early 80s with relatively lower equivalent weight (800-900) for chlorine production<sup>[38]</sup> but were soon tested for PEMFC application<sup>[39]</sup>. Presently, SSC ionomers such as *Hyflon*<sup>®</sup> *Ion*<sup>[40]</sup> (produced by Solvay Solexis Inc. with same structure as Dow's membrane but with simpler synthesis route<sup>[39]</sup>) and 3 M ionomers are available. The chemical structures of these ionomers are illustrated in figure 4. Lower EW values are known to generate an increase in proton conductivity up to a certain point due to an increase in the concentration of acid groups<sup>[41]</sup>. However, lower EW membranes have demonstrated inferior durability and mechanical stability due to increased swelling<sup>[42]</sup>.

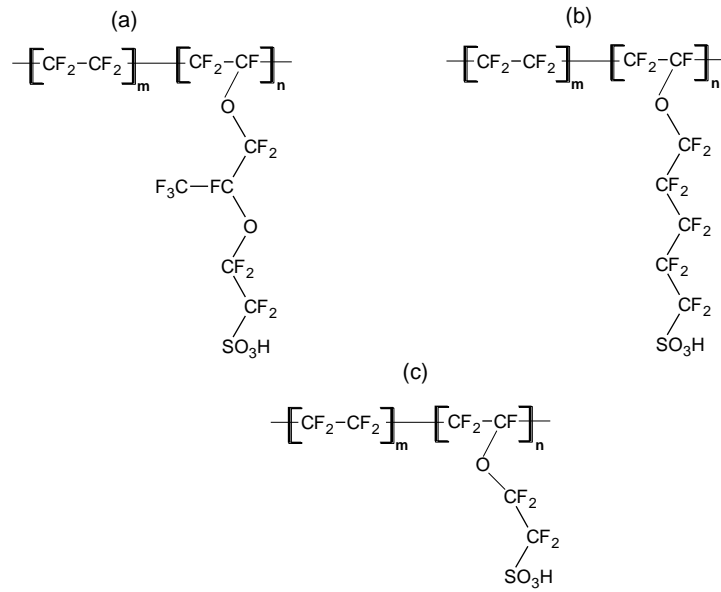


Figure 4: Chemical structures of different types of PFSA based membranes; (a): Nafion<sup>®</sup>; (b) 3M ionomer; (c) Dow Ionomer/Hyflon Ion

Table 2 shows the features of different perfluorinated ionomers available in the market.

Structure Parameter	Trade Name	Equivalent Weight	Thickness (μm)
$m=5-13.5$ ; $n=1$ $x=1$ ; $y=2$	Dupont		
	Nafion 120	1200	260
	Nafion 117	1100	175
	Nafion 115	1100	125
	Nafion 112	1100	80
$x=0,1$ ; $y=1-5$	Asahi Glass		
	Flemion-T	1000	120
	Flemion-S	1000	80
	Flemion-R	1000	50
$m=1.5-14$ ; $x=0$ ; $y=2-5$	Asahi Chemicals		
	Acidplex-S	1000-1200	25-100
$m=3.6-10$ ; $x=0$ ; $n=2$	Dow Chemical		
	Dow	800	125

Table 2: Features of different commercially available PFSA-based membranes <sup>[18]</sup>

Even though there are different perfluorinated ionomers developed with different names as discussed above, *most of the research has been concentrated primarily on Nafion<sup>®</sup> as a polymer electrolyte for*

*PEMFC application and a lot of work has been done to understand the relation between morphology and various interesting properties of these PFSA based polymers in dried as well as hydrated state.*

The morphology of Nafion<sup>®</sup> membrane has been extensively studied using primarily Wide Angle X-ray scattering (WAXS), Small angle X-ray and Neutron scattering (SAXS and SANS) and Ultra Small Angle X-ray scattering (USAXS). It has been proved that morphology has direct impact on the properties like the management of water and hydration degree of membrane at high temperatures, thermal and mechanical stability of a polymer electrolyte<sup>[43]</sup>. This is why a clear understanding of the morphology of a polymer electrolyte is considered very important.

Rubatat et al. have measured the scattering data of Nafion<sup>®</sup> over a wide range of scattering vector  $q$  using various scattering (WAXS, SAXS and USAXS) as shown in figure 5<sup>[44]</sup>. The main features of the scattering data include:

1. WAXS results show an amorphous peak superimposed with a crystalline peak at  $q=1.1 \text{ \AA}^{-1}$  and  $q=1.24 \text{ \AA}^{-1}$  respectively. These peaks are related to the organization in Nafion<sup>®</sup> at molecular level and more precisely related to the crystallinity of PTFE main-chain. The peak at  $q=1.1 \text{ \AA}^{-1}$  originates from the average distance between perfluorinated polymer chains in the amorphous phase. While the peak at  $q=1.24 \text{ \AA}^{-1}$  corresponds to the correlation distance between perfluorinated polymer chains in the crystalline zone. In addition, a crystalline peak around  $q=2.8 \text{ \AA}^{-1}$  corresponds to the inter-atomic correlation along the fluoro-carbon chain of Nafion<sup>®</sup>.
2. SANS results mainly cover the  $q$  range of  $0.01\text{--}0.2 \text{ \AA}^{-1}$  and show two peaks in this  $q$  range. The peak at  $0.15 \text{ \AA}^{-1}$  is referred as “ionomers peak” of Nafion<sup>®</sup> (in hydrated state). Another peak at  $0.05 \text{ \AA}^{-1}$  is often referred as “matrix knee”
3. USAXS results present the “ultra-small angle upturn (USAS upturn)” at very small  $q$  values. This upturn is related to the fluctuation in electronic density at large scale (certain Angstroms) are also observed.

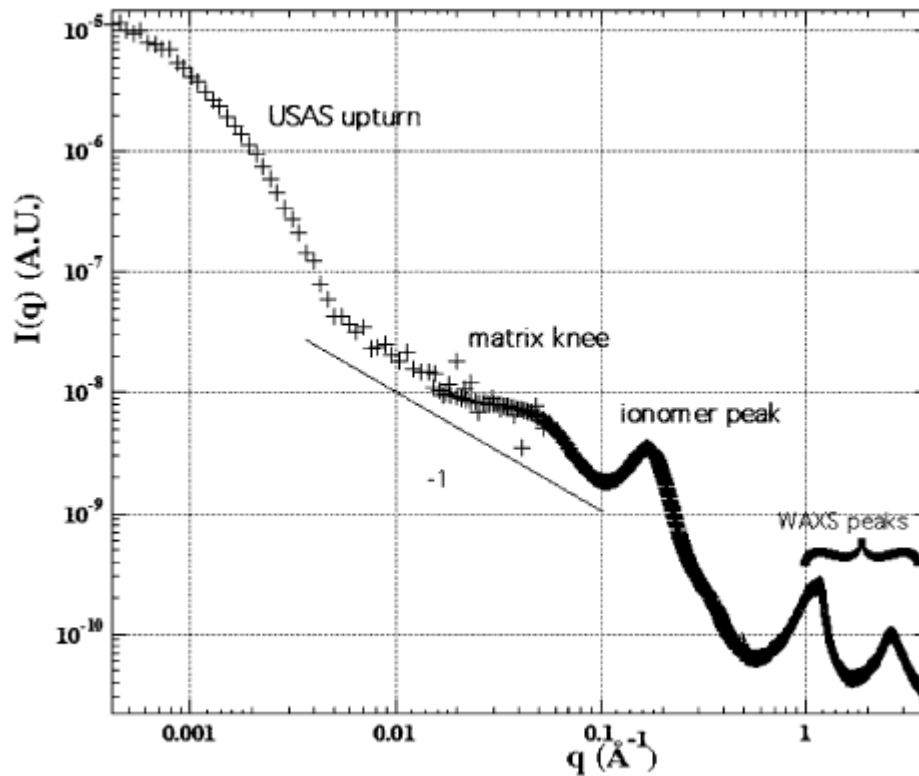


Figure 5: Scattering Spectra of Nafion® measured over wide range of diffusion vector  $q$  using various scattering & spectroscopic techniques<sup>(44)</sup>

Several models of Nafion® morphology have been proposed to fit this data over a period of almost 30 years. The important features of these models will be discussed briefly now.

One of the earliest models for Nafion® called the **“Cluster-Network Model”** was proposed by Gierke et al. using only the scattering data of ionomer peak<sup>(45)</sup>. This model considers the formation of periodically distributed ionic clusters of sulfonate ions (also described like reversed micelles) surrounded by the fluoro-carbon chains. The diameter of these ionic clusters is of the order of 3-5 nm inter-connected by 1nm wide narrow channels. The model is presented diagrammatically in figure 6. The cluster size and its water content were considered to change with changing degree of hydration. However, this model is considered **too simplistic** due to the assumption of periodic/continuous distribution of ionic clusters since  $q^{-1}$  variation of SAXS intensity at small  $q$  values is typically presented by elongated structures and not spherical clusters<sup>(46)</sup>. Moreover, **no account of crystalline fractions of the structure** was taken in this model. In addition, a **linear relation between the shift in the position of ionomers peak and amount of water absorbed** upon swelling has been observed which **cannot be explained** with this model<sup>(47)</sup>.



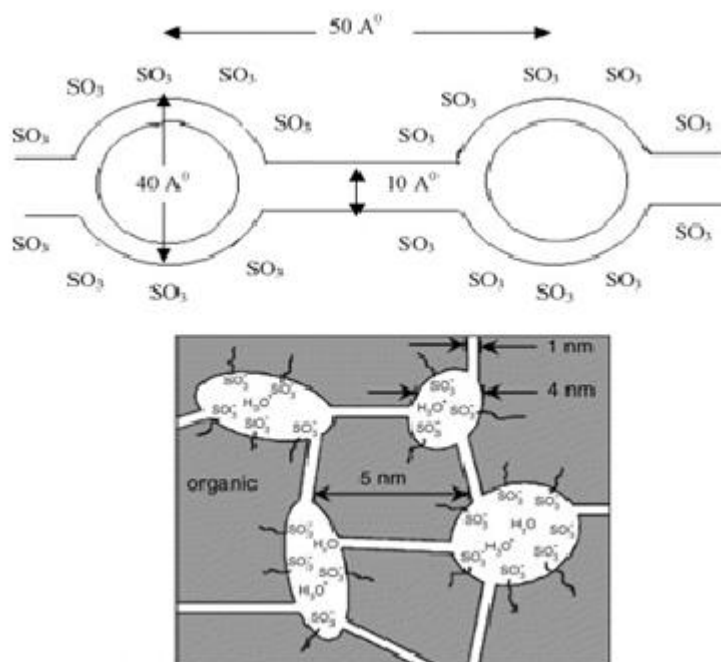


Figure 6: Schematic representation of model of ionic clusters proposed by Gierke et al. <sup>[48]</sup>

Litt et al. proposed a “**Lamellar Model**” of Nafion<sup>®</sup>. They considered the absorption of water by hydrophilic micelles which are separated by hydrophobic lamellae<sup>[49]</sup>. This model accounted for the basic information on the morphology *without profoundly dealing with the meso-scale structure of Nafion<sup>®</sup>*.

Gebel et al. have utilized the data of SAXS and SANS measurements to probe Nafion<sup>®</sup> structure and proposed the “**Polymer Ribbon Model**”. The model is schematically presented in figure 7. This model considers elongated polymer aggregates with a locally flat interface (ribbon) embedded in a continuous ionic medium. Parallel polymer ribbons form bundles of 50-100 nm in length and about 4 nm in diameter which are isotropically distributed in the absence of mechanical deformation<sup>[50-52]</sup>. This model has been considered one of the best in describing the full set of data obtained with Nafion<sup>®</sup> membranes.

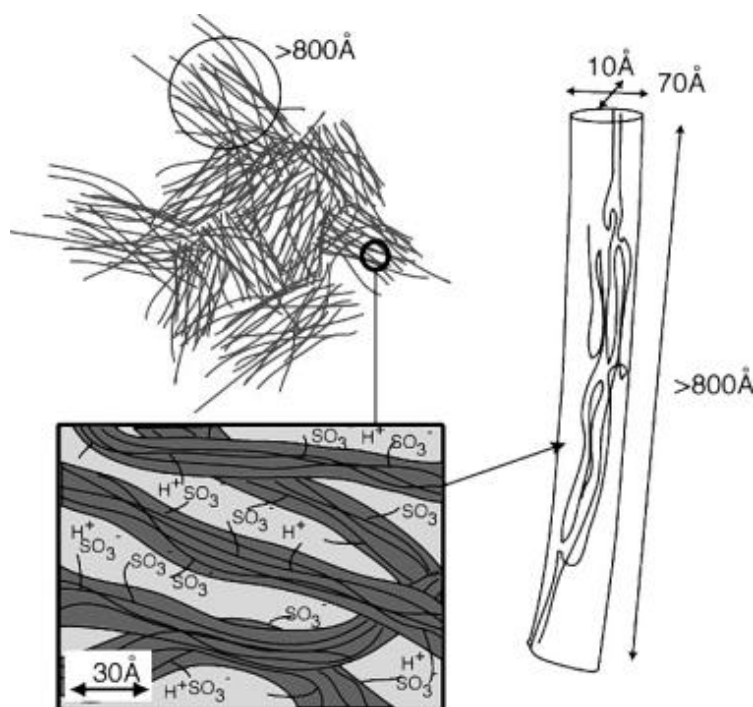


Figure 7: Schematic representation of model of elongated aggregates proposed by Gebel et al.

A competing model based on parallel cylindrical ionic domains (nano-channels) embedded in the perfluorinated matrix known as “**Parallel Water Channel Model**” has been proposed by Schmidt et al.<sup>[46]</sup>. The model is presented schematically in figure 8. According to this model, sulfonic acid groups auto-organize themselves in the form of the channels of diameter of  $\sim 2.4$  nm (at 20 volume% water) by which small ions can be easily transported. The hydrophobic chains organize in the form of crystallites ( $\sim 10$  volume %) of elongated structures of persistence length more than 20 nm in parallel to water channels and provide good mechanical stability.

Assuming some shape and size of the hydrophobic and ionic domains as well as polydispersity of the polymer, it is a hard task to differentiate between these two models. However, the high level of proton conductivity at very low water content<sup>[53]</sup>, the effect of confinement on water mobility<sup>[54]</sup>, the evolution of the SAXS and SANS spectra as a function of water content<sup>[50,55]</sup> and the very fast kinetic of swelling<sup>[56,57]</sup> favour the polymer ribbon model<sup>[58]</sup>.

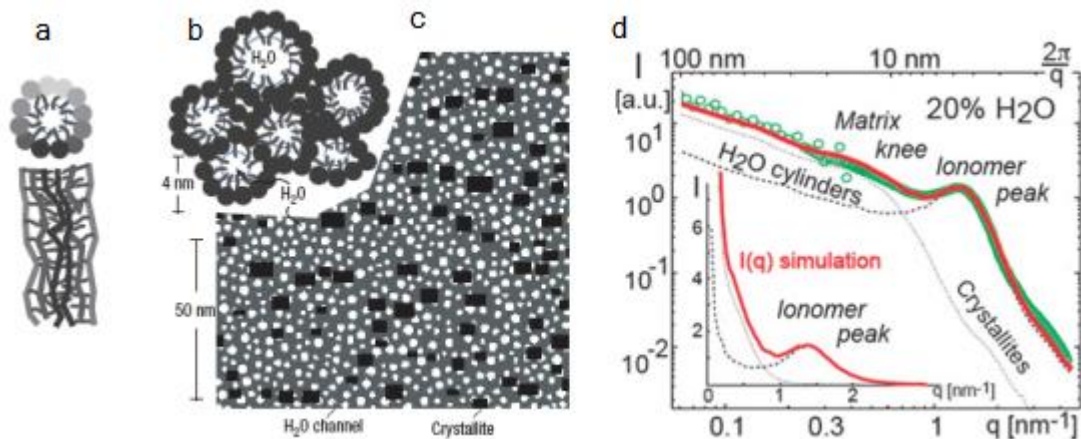


Figure 8: Illustration of the parallel water channel model of Nafion proposed by Rohr et al. (a) Cross-sectional and transverse views of an inverted micelle cylinder having hydrophobic main chain outside and hydrophilic acid groups on the inside surface of water channels. Darker shades represent features closer to the viewer; (b) Hexagonal packing of inverted micelle cylinders; (c) Cross-section of the simulated system showing water channels (white), Nafion crystallites (black) and amorphous Nafion matrix (dark grey); (d) Small Angle Scattering data  $I(q)$  as a function of scattering vector  $q$ . The Inset represents ionomer peak in a linear plot of  $I(q)$  by simulation. The experimental data of Rubatat et al.<sup>[50]</sup> are in green and the model curve is in red (solid line) for Nafion<sup>®</sup> with 20 vol% of water. The simulated curves from the water channels only (dashed) and crystallites only (dotted) are also shown.<sup>[46]</sup>

In summary, even if the shape and the size of the ionic domains in the Nafion<sup>®</sup> is still a matter of debate, some common features have emerged such as:

- 1) These polymers are a phase-separated system with a well-defined interface between a dense and hydrophobic perfluorinated phase and the ionic domains composed of sulfonic acid groups.
- 2) The hydrophobic/hydrophilic interface where sulfonic acid groups are located plays an important role in the performance of these membranes as PEMs in fuel cells. Thus, in the nano-structured membrane, the well-connected hydrophilic domain is responsible for the transport of protons; the hydrophobic domain provides morphological stability to the polymer and prevents the polymer from dissolution in water.

Now, considering the presence of water, the morphology and the functional properties (transport, thermo-mechanical, gas-permeation etc.) of Nafion<sup>®</sup> strongly depend on its water content. The water sorption behavior of Nafion<sup>®</sup> is presented in figure 9 at different temperatures and at different relative humidity values<sup>[59-61]</sup>.

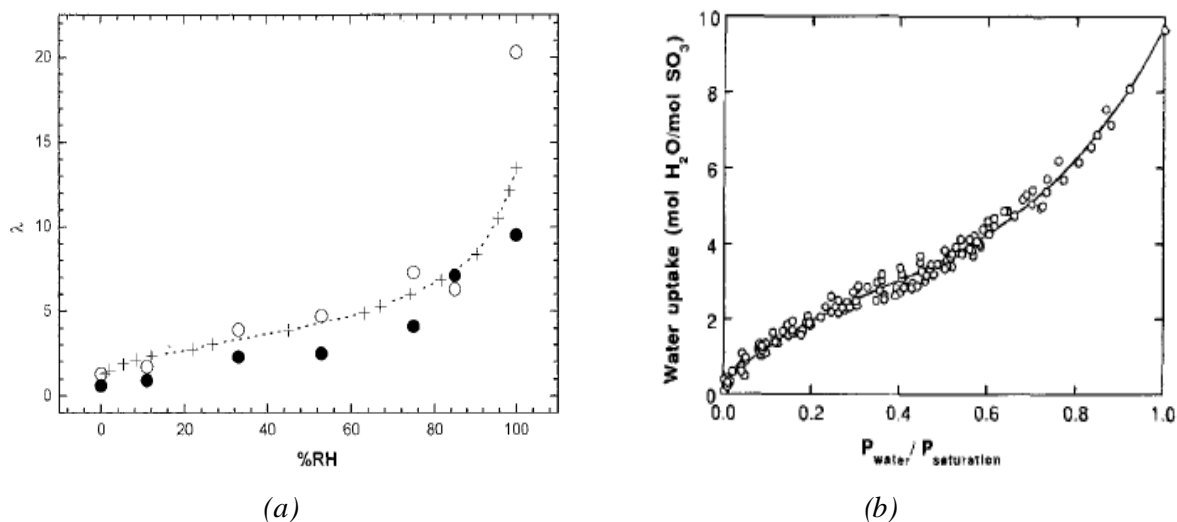


Figure 9: Water sorption isotherms (moles of water molecules per sulfonic acid groups in function of water activity) for Nafion® 117 membranes at different temperatures; a). 25°C<sup>(59,61)</sup>; b). 80°C<sup>(60)</sup>

The morphology of Nafion® in different hydrated states has been widely studied<sup>[45,46,50,51]</sup>. The evolution of SAXS spectra (in the nano-mesosopic length scale) for Nafion® membrane with different water contents has been demonstrated by their group (figure 10). It can be seen that the general shape of the scattering curves is similar whatever is the degree of membrane swelling which signifies swelling of the structure of Nafion® without any morphological reorganization of the material in the presence of water molecules. The ionomer peak and the matrix knee shift towards lower  $q$  value and their intensity increases on increasing water content of the system. According to the Polymer Ribbon model, the ionomer peak is the mean separation distance between the polymer ribbons and the matrix knee has been related to the long range crystallinity in Nafion®. The shift in the position of ionomer peak towards lower  $q$  value signifies swelling of the ionic domains and hence an increase in the mean separation distance between the polymer ribbons.

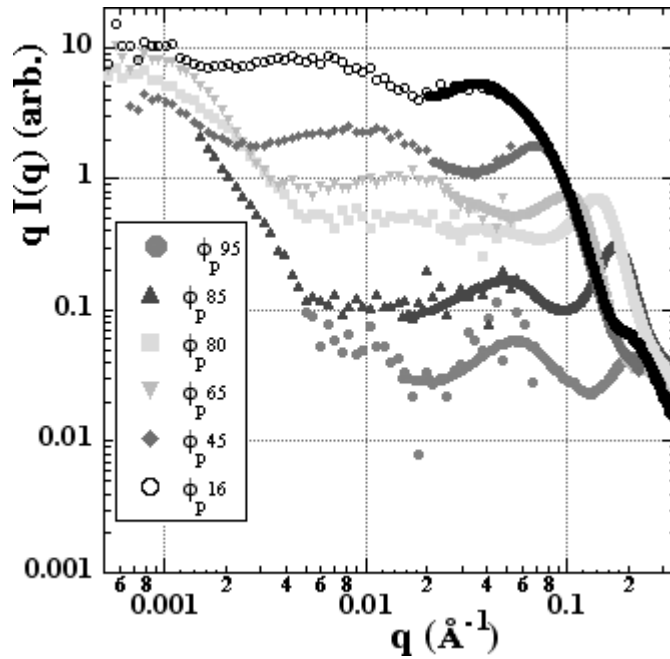


Figure 10: Evolution of SAXS spectra of Nafion® for different polymer fractions  $\phi_P \times$  (%), corresponding to weakly hydrated Nafion® 117 membrane to highly swollen Nafion® film <sup>[51]</sup>

The **proton conductivity of Nafion® strongly depends on its water content** as water is responsible for both the dissociation of the sulfonic acid protons which provides highly mobile hydrated protons and the proper percolation of these hydrophilic inclusions. Figure 11 which refers to experimental data measured on Nafion® give the temperature illustrates that the water content and the proton conductivity are directly related to the relative humidity<sup>[62]</sup>. In a fuel cell system, the fuels must thus be humidified so as to prevent the evaporation of the water from the membrane, in spite of the generation of great quantities of the water at cathode.

The proton conduction in the perfluorinated membranes is complex in nature and it has been proposed that there is a mixed mechanism (Grotthuss and Vehicular) involved for the migration of proton. When a vehicular mechanism is responsible for the transport of proton, for example in the form of  $H_3O^+$ , the migration of each proton is associated with at least one molecule of water.

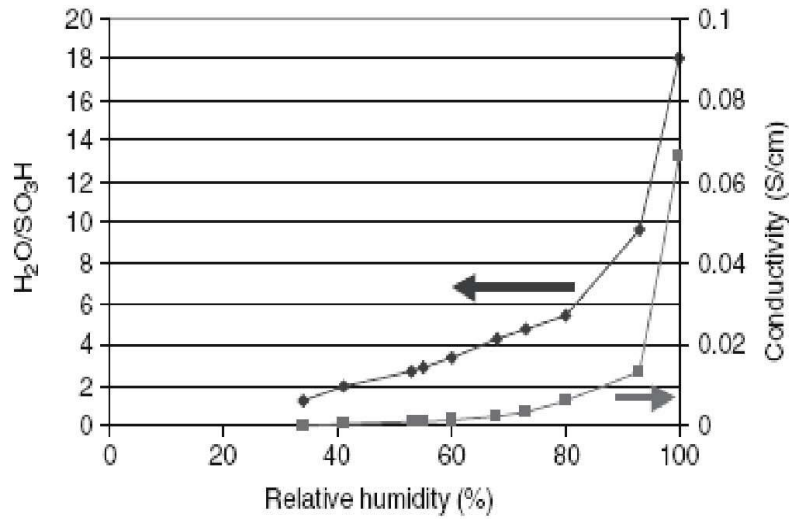


Figure 11: Dependence of water content and proton conductivity of Nafion® on relative humidity<sup>[62]</sup>

When PFSA based ionomers membranes are subjected to the temperatures ***above of 100°C under atmospheric pressure, a considerable reduction in conductivity is observed during the fuel cell working life due to dehydration and decay in proton conductivity*** has been found to be anisotropic in nature due to anisotropic deformation taking place under conditions of high temperature and certain relative humidity (shown in figure 12). This makes this family of the membranes not very suitable for temperatures higher than 100°C<sup>[63]</sup>.

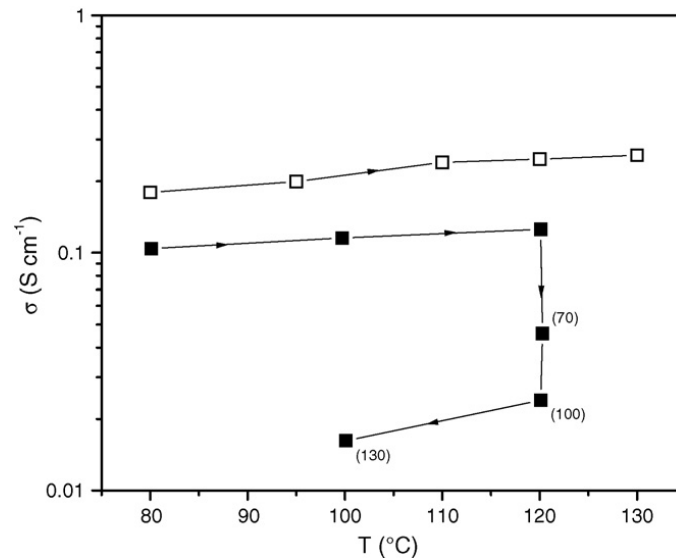


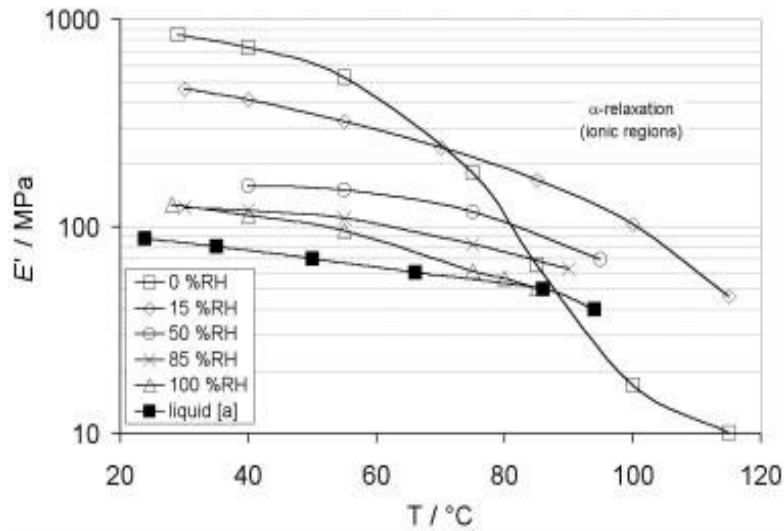
Figure 12: Normal conductivity (black coloured blocks) and tangential conductivity (white coloured blocks) as a function of temperature at 98% RH. Figures in the brackets represent number of hours elapsed before the beginning of decay in proton conductivity; arrows indicate the evolution of temperature change<sup>[63]</sup>

Thermo-mechanical properties of Nafion<sup>®</sup> have been widely studied due to the need of understanding the mechanical response of these membranes under humid conditions and elevated temperatures i.e. under fuel cell working conditions. The *dynamic mechanical relaxations of the Nafion<sup>®</sup> are strongly dependent on the strength of interactions between the side-chain terminals*. It is well-known that Nafion<sup>®</sup> in acidic form exhibits three kinds of relaxation giving a picture of multi-phase structure of Nafion<sup>®</sup><sup>[64-66]</sup> which are mentioned below (*however, their attribution is still a matter of debate*):

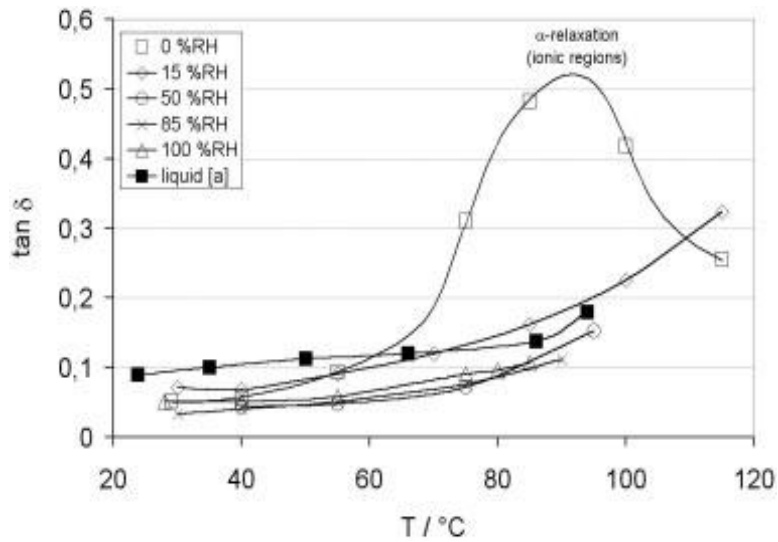
1.  $\gamma$  relaxation (-100°C) corresponding to vibrational and rotational movements of CF<sub>2</sub> groups placed at short distance from the ionic function
2.  $\beta$  relaxation (-20°C) corresponding to the movement of the hydrophobic PTFE main-chains and fluorinated ether side-chains
3.  $\alpha$  relaxation (100°C) corresponding to movement of ionic clusters (also usually referred as T<sub>g</sub> of the polymer)

The evolution of elastic modulus and mechanical loss tangent  $\tan\delta$  with temperature and relative humidity have been studied<sup>[67]</sup> and are presented in figure 13 (a) and (b) respectively.

A decrease in the *elastic modulus of Nafion<sup>®</sup> with increasing relative humidity and temperature occurs due to the plasticizing effect of water* creating a decrease in the stiffness of the polymer. Moreover, water acts a plasticizer at low temperatures but stiffens the membrane by stabilizing the network of ionic cluster at high temperatures. At very low humidity levels, an intermediate increase in mechanical strength is observed due to the formation of oligo-hydrates and enhancement of hydrogen-bonding among sulfonic acid groups. In addition, the maximum of  $\tan \delta$  profiles seem to move to higher temperatures with increase in relative humidity. An exchange of H<sup>+</sup> of sulfonic acid groups with bigger cations (such as Sodium, Potassium, Cesium etc.) causes a great improvement in the T<sub>g</sub> evidenced by the shift of  $\alpha$  relaxation from 100°C for H<sup>+</sup> form to more than 200°C for different cations due to stronger ionic interactions between vicinal sulfonic acid groups<sup>[68]</sup>.



(a)

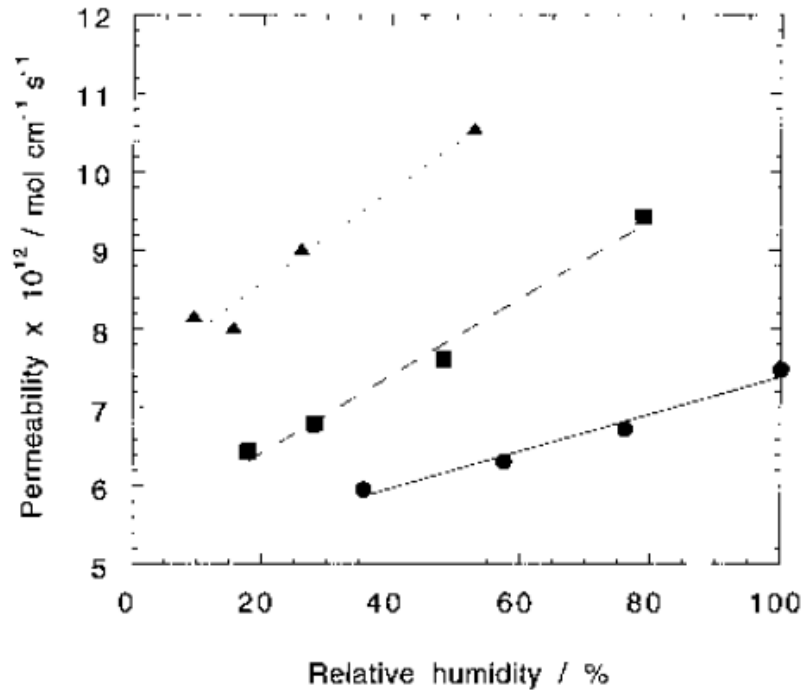


(b)

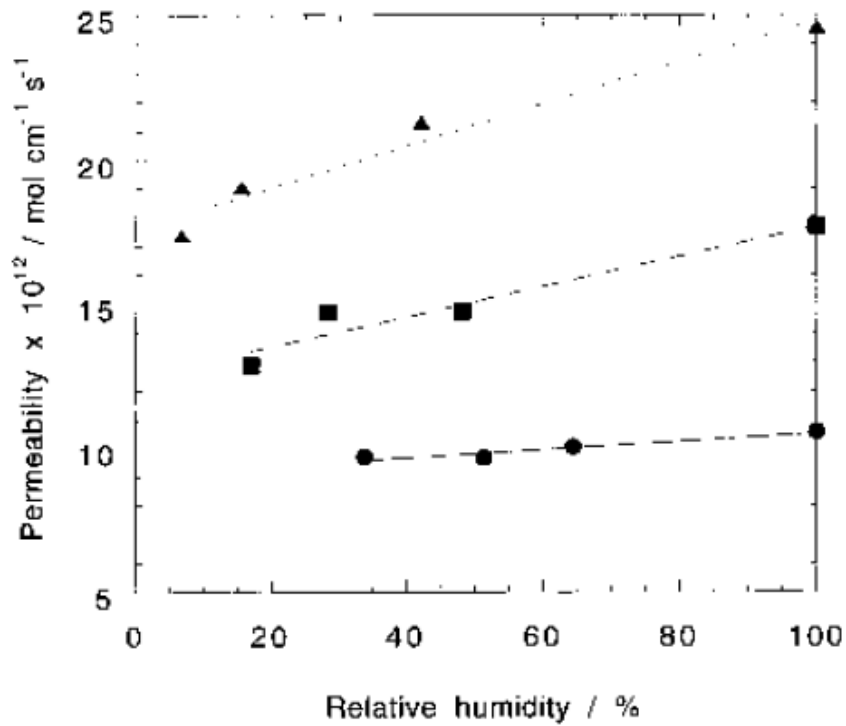
Figure 13: Evolution of (a) storage modulus (b)  $\tan \delta$  with temperature at different relative humidities; Liquid(a) represented by black motifs is Nafion in protonated form equilibrated in liquid water<sup>[67,69]</sup>

The gas-permeability through Nafion<sup>®</sup> membrane is another important property since the membrane serves the role of a gas barrier as well. The evolutions of oxygen and hydrogen permeability coefficients for Nafion<sup>®</sup> 117 membrane are presented in figure 14 (a) and (b) respectively<sup>[70]</sup>. It has been suggested in various works that the gas permeation in polymers containing hydrophobic and hydrophilic domains like Nafion<sup>®</sup> can take place mainly in the hydrophobic phase under anhydrous conditions<sup>[71,72]</sup>. However, under humid conditions, the hydrophilic as well as the hydrophobic phases contribute to the gas-permeation<sup>[70]</sup>.





(a)



(b)

Figure 14: Evolution of permeability coefficients at different temperatures and relative humidity values for Nafion® 117 membrane; a). Oxygen permeability coefficients; b). Hydrogen permeability coefficients; (tri) at 80°C, (square) at 60°C, (circle) at 40°C<sup>(70)</sup>

PEMFCs using the standard membranes of Nafion<sup>®</sup> have demonstrated a lifespan of more than 11,000 hours. However, *perfluorinated ionomer membranes are susceptible to various degradation phenomena such as mechanical degradation by creeping and thinning of membrane, chemical degradation by the attack of peroxy radicals formed at the electrodes during fuel cell operation*<sup>[73]</sup>.

Considering various drawbacks associated with PFSA based membranes, a lot of emphasis has been given to development of other polymer electrolytes as alternatives<sup>[74,75]</sup>. The *main disadvantages associated with PFSA based membranes* are listed briefly as follows:

1. High cost
2. Drop in conductivity with decreasing relative humidity and inability to work at high temperatures
3. Poor mechanical strength 100°C
4. Shrinkage and cracking under dehydrated conditions accelerating gas-crossover
5. Thermal and chemical degradation

Hence considering all these disadvantages associated with PFSA based membranes, the possibility of developing alternative polymers has garnered much attention. Other polymers studied as alternatives are basically either aromatic polymers or polymers containing inorganic elements such as Fluorine, Silicon etc. Different chemical routes (such as chemical modification of commercially available polymers/synthesis of block copolymers, etc.) have been exploited in order to fine tune the properties required for the PEMFC application. These will be discussed thoroughly in the proceeding section of this chapter.

#### **1.4.2: Partially Perfluorinated Polymers & Polysiloxanes**

The polymers containing inorganic elements such as Silicon and Fluorine (apart from PFSA based membranes) have been explored as alternatives to PFSA based membranes due to the high thermal stability attributed to high bond strengths of C-F (~485 kJ/mol) and Si-O (~445 kJ/mol) bonds<sup>[18]</sup>. The structures of these polymers are shown in figure 15.

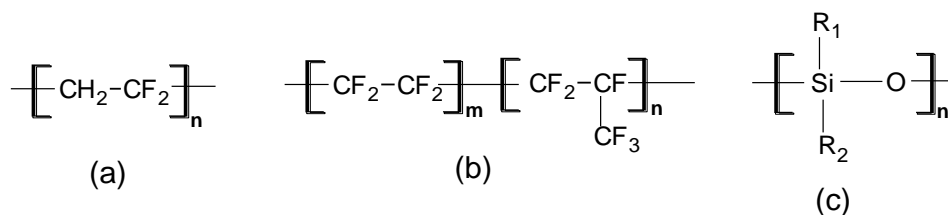


Figure 15: Chemical structure of different polymers containing inorganic elements; (a): Poly vinylidene fluoride; (b): Poly (tetrafluoroethylene-co-hexafluoropropylene); (c): Polysiloxane

#### a. Partially-perfluorinated polymers

Partially perfluorinated polymers such as Poly vinylidene fluoride (PVDF), Poly (tetrafluoroethylene-co-hexafluoropropylene) (FEP) have been proposed as alternatives to PFSA based membranes due to their **effective cost, melt processibility, availability and mechanical strength in addition to thermal properties**<sup>[76-86]</sup>. However, since these polymers are not ionomers, ionic function has to be introduced to their structures by chemical modifications or by blending them with Nafion®. In this regard, various possibilities have been explored by research groups and some of them will be briefly discussed here.

In the very beginning, Scherer et al. demonstrated membranes based on radiation grafting of polystyrene on FEP films followed by sulfonation<sup>[78]</sup>. These membranes were also crosslinked using divinylbenzene to see the effect of crosslinking on the swelling behavior and ionic conductivity. The membranes were found to be homogenously grafted up to 13% grafting degree. Higher swelling as well as lower specific resistivity was observed for non-crosslinked membranes compared to crosslinked membranes due to the fact that crosslinking induces lower water uptake and hence lower ionic conductivity.

Nasef et al. further studied these polystyrene grafted FEP membranes in detail. They reported that the degree of water uptake increased gradually and linearly with the degree of grafting<sup>[79]</sup>. A water uptake up to 80% was observed for membrane with 50% grafting level compared to 39% for standard Nafion® membrane under similar conditions. However, proton conductivity at room temperature increased sharply up to grafting degree of 16% showing proton conductivity of 0.02 S/cm and stabilized afterwards. This behavior was attributed to the homogeneous distribution of grafts at around 16% grafting level which could be enough to arrive at maximum proton conductivity for the system. In comparison, the value of proton conductivity for standard Nafion® 117 under same conditions was found to be 0.053S/cm.

Slade et al. explored the possibility of replacing FEP with PVDF as main-chain polymer and grafted it with styrene using electron beam irradiation and then sulfonated the polymer<sup>[80]</sup>. They reported a proton conductivity of 0.03 S/cm for membrane with 30% grafting degree at 23°C. These membranes were subjected to various other characterizations to evaluate their various properties in regard to PEMFC application. They were found to be thermally stable up to 370°C in inert atmosphere and up to 270°C under highly oxidizing atmosphere. Structural investigation on the system demonstrated a sharp decrease in the crystallinity of PVDF when subjected to grafting and sulfonation<sup>[81]</sup>. These membranes were also subjected to crosslinking using different crosslinking agents. The resulting membranes exhibited improved gas crossover and demonstrated good mechanical strength at even high degree of grafting<sup>[82]</sup>. These were also reported to show much higher water uptake compared to Nafion<sup>®</sup><sup>[83]</sup>. However, high degree of grafting inhibits the durability of the grafted PVDF membranes. Moreover, poor fuel cell performance compared to Nafion membrane due to poor contact between modified PVDF membrane and electrode had been observed in their work<sup>[84]</sup>.

A rather exotic approach involved inclusion of polystyrenesulfonic acid grafted silica particles into the inert matrix of poly (vinylidene fluoride-co-hexafluoropropylene) (PVDF-HFP) using solvent casting method<sup>[85]</sup>. A homogeneous distribution of the modified silica particles was obtained up to 30 wt% with conductivity of 15mS/cm at room temperature in water. Another exotic approach involves preparation of semi-interpenetrating polymer networks of Nafion<sup>®</sup> and PVDF through radiation crosslinking<sup>[86]</sup>. They reported tensile strength of the composite membranes in the range of 34-53 MPa compared to 23.9 MPa of Nafion<sup>®</sup> 212 and a proton conductivity of 0.337 mS/cm at 115°C.

#### ***b. Silicon containing polymers***

Another class of polymers containing silicon has been explored to some extent as an alternative to PFSA based membranes.

In this domain, Popall et al. developed an organic-inorganic proton conducting polymer electrolyte consisting of interpenetrated networks of inorganic oxide and organic components by using sol-gel method<sup>[87]</sup>. In their work, they synthesized alkylsulfone alkoxysilanes and condensed with polymerisable alkoxysilanes followed by cross-linking via UV-initiated and/or thermal polymerization. The ionic conductivity of this material was found to be dependent on -SO<sub>3</sub>H/Si ratio and the conductivity increased from 10<sup>-8</sup> S/cm to 5 mS/cm at room temperature under vacuum by changing this ratio from 0.2 to 0.6. The network was thermally stable upto 180°C.

Kuo et al. developed hybrid membranes based on crosslinked polysiloxanes (prepared by sol-gel process) and Nafion<sup>®</sup> by interaction between sulfonic acid groups of Nafion<sup>®</sup> and amine groups attached to polysiloxane<sup>[88]</sup>. Membranes were found to be much more hydrophilic compared to Nafion<sup>®</sup> at similar IEC value. This was attributed to the hydrophilic character of siloxane networks. A proton conductivity of 34 mS/cm at 30°C, ultralow methanol permeability of  $1.1 \times 10^{-8}$  cm<sup>2</sup>/s and adequate oxidative stability for the membrane containing 15 wt% polysiloxane have been reported.

Kalaw et al prepared Polysilsesquioxanes membranes comprising highly cross-linked Si-O backbone with organic side chains such as propylsulfonic acid and ethylphosphonic acid groups using sol-gel polymerization<sup>[89]</sup>. The membranes based on propylsulfonic acid groups showed high proton conductivity at high temperature and RH, while, membranes based on ethylphosphonic acid demonstrated high thermal stability.

Barreto et al. elaborated another inorganic-organic blend based on sulfonated hydrogenated styrene-butadiene copolymer and polysiloxanes using casting method with homogeneous distribution of the two phases<sup>[90]</sup>. The blends were found to be thermally stable up to 170°C along with enough good mechanical strength and water uptake. Moreover, hydrogen cross-over was found to be reduced with introduction of silane phase in the blend.

*Such kinds of polymers have shown promising results, but, the overall properties and performance required for PEMFC application are inferior to those of PFSA based membranes.*

### 1.4.3: Polymers based on Aromatic hydrocarbons

Apart from partially perfluorinated and silicon based polymers, *polymers based on aromatic hydrocarbons* have been widely investigated as an alternative to PFSA based membranes due to their *low cost, easy processibility and good oxidation resistance along with high thermal and mechanical stability*. Aromatic polymers such as poly(etheretherketone) (PEEK), poly(aryl etherketone) (PEK), poly(aryl ethersulfone) (PES), poly(benzimidazole) (PBI), polyimide (PI), poly(phenyl quinoxaline) (PPQ), poly phenylene oxide (PPO), polyphenylene sulfide (PPS) and polyphosphazenes (PPZ) have been explored for the purpose<sup>[18,48,91,92,93]</sup>.

Moreover, there are various acidic functions such as carboxylic acid, alkyl, aryl or perfluoro sulfonic acid, phosphoric acid and perfluorosulfonyl imide acid which can be easily attached to the aromatic backbone. The acidity and stability of carboxylic acid is not enough high for this kind of application and therefore will not be discussed here. Various research groups have investigated the possibility of substituting sulfonic acid and phosphonic acid functions on the aromatic main chain. However, *among*

*all the possible acidic functions, the sulfonic acid units have been by far the acidic moiety of choice.*

This is due to the wide range of reactants that are commercially available for sulfonation as well as ease in sulfonation reaction and also due to their enough high acidity and stability as well as much higher water uptake by sulfonated polymers compared to phosphonated polymers<sup>[93]</sup>.

Several methods have been used to prepare proton-conducting polymers from these aromatic polymers which include direct sulfonation/phosphonation of a commercially available aromatic polymer, grafting of an acidic ionic function (sulfonic/phosphonic acid terminated group) on to the polymer main chain, graft polymerization using high energy radiation followed by sulfonation of grafted component and synthesis of polymers from monomer units bearing acidic functions.

**a. Acidic function attached directly to the polymer main-chain and randomly distributed**

Direct sulfonation of polymers such as PBI, PPQ, PPO, PPS, PES, PEEK etc. has been carried out either using sulfuric acid, chlorosulfonic acid or sulfur trioxide as both solvent and sulfonating reagent by electrophilic substitution i.e. substitution of sulfonic acid function directed to electron-deficient ring of the repeat unit<sup>[18,91,94-104]</sup> (chemical structures represented in figure 16).

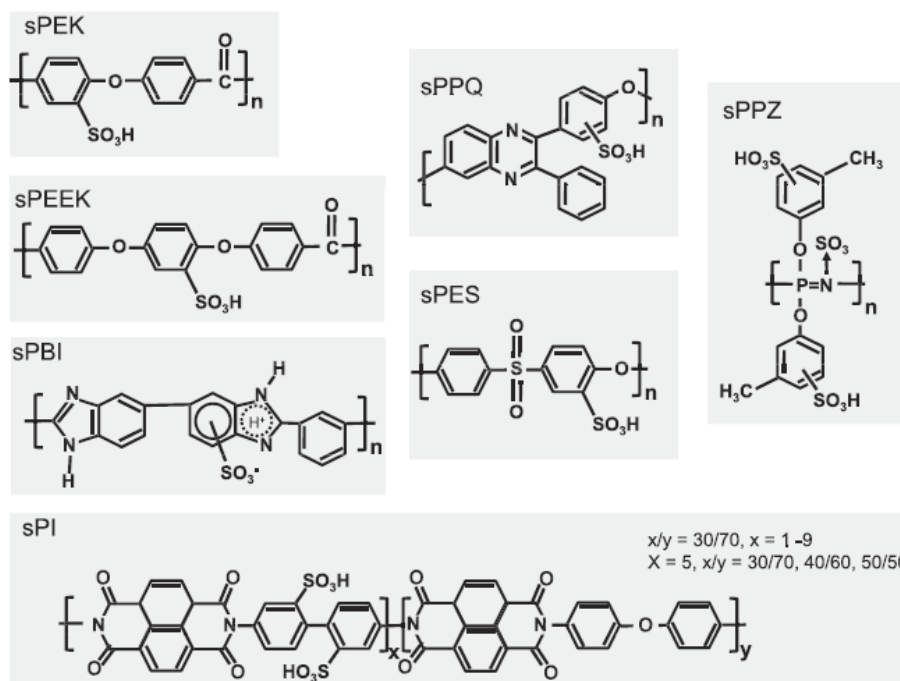


Figure 16: Chemical structure of different directly-sulfonated aromatic polymers

*Sulfonation using sulfuric acid or chlorosulfonic acid* can sometimes cause chemical degradation in some of these polymers which is why use of a mild sulfonating agent such as trimethylsilylchlorosulfonate is preferred<sup>[105]</sup>. *The degree of sulfonation (DS) depends on the molar ratio of sulfonating agent and polymer-repeating units and 30-100% DS can be reached depending on the reaction conditions*<sup>[106]</sup>. *Another method vastly explored is of metalation-sulfonation/phosphonation-oxidation*. It was developed by Kerres et al. for sulfonating polysulfones by aromatic nucleophilic substitution and is considered to provide higher stability towards desulfonation phenomenon<sup>[107]</sup>.

Some research groups synthesized *sulfonated aromatic random co-polymers by copolymerizing sulfonated monomers*. For eg., Wang et al. synthesised poly arylene ether sulfone based random copolymer by polycondensation of disodium 3,3-disulfonate-4,4-dichlorodiphenylsulfone (SDCDPS), 4,4-dichlorodiphenylsulfone (DCDPS) and 4,4-biphenol<sup>[94]</sup>. An increase in the content of sulfonated monomer significantly increased the amount of water uptake from 12% for 80/20 DSCPS-SDCDPS ratio to 148% for 40/60. The membranes prepared from the copolymer containing 60% sulfonated monomer content (IEC=2.42 meq/g) had shown conductivity of 0.17S/cm at 30<sup>0</sup>C in water compared to 0.12S/cm by Nafion 1135 (IEC=0.9 meq/g) under similar conditions. AFM study of this copolymer demonstrated an increase in the size of ionic domain from 10nm to 25nm and better continuity and connectivity of these ionic domains with the increase in the content of sulfonated monomer content. These membranes exhibited much higher water uptake, lower methanol permeability and much lower electro-osmotic drag coefficient compared to Nafion<sup>®</sup><sup>[108]</sup>. However, all the *random copolymers of sulfonated polyarylene sulfone do not show co-continuous phase separation* depending upon the structure of bi-phenol monomer units.

However, all the studies on *aromatic polymers with acidic function directly attached to the main chain*, either prepared by direct sulfonation of commercial polymer or by copolymerization of sulfonated monomers, *exhibited high proton conductivity only at high sulfonation degree and loss of mechanical properties due to dimensional swelling*. This renders them unsuitable for practical PEM applications.

Kreuer et al. investigated the morphology of sulfonated PEEK and tried to co-relate the mechanical collapse of PEMs based on aromatic polymers under working fuel cell conditions to their morphology. According to them, morphology of these directly sulfonated aromatic polymers is different from the PFSA based membranes<sup>[43]</sup> (shown in figure 17).

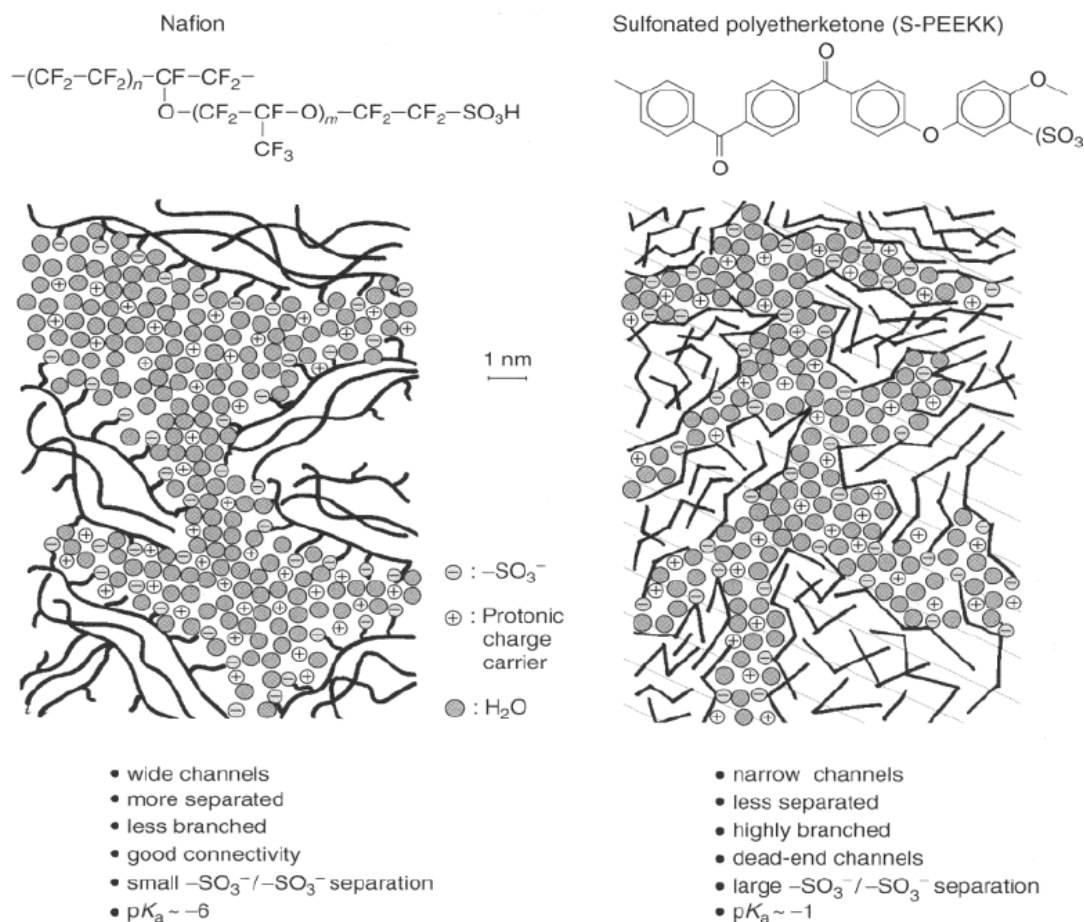


Figure 17: Difference in the morphology of Nafion<sup>®</sup> and sulfonated aromatic polymers such as sulfonated PEEK<sup>[43]</sup>

PFSA based membranes e.g. Nafion<sup>®</sup> possess defined nano-separation of hydrophobic and hydrophilic phase owing to highly hydrophobic backbone and highly hydrophilic/super acidic side-chain ionic functions. Hence, in the presence of water, there is formation of a very efficient network of ionic channels and consequently these membranes exhibit high proton conductivity due to high water uptake by hydrophilic phase and enough mechanical strength provided by hydrophobic domains under working conditions of a fuel cell.

However, in the case of *aromatic polymers e.g. sulfonated PEEK, the rigidity and lower hydrophobicity of aromatic backbone as well as lower acidity and polarity of terminal acidic function prevents the formation of continuous conducting channels in the membrane*. Consequently, the water molecules get completely dispersed in the morphology of these polymers resulting into poor mechanical strength of these polymers<sup>[109]</sup>.



Thus, various *strategies have been pursued to obtain efficient ionic networks* for enhancing the proton conductivity and mechanical stability of the membrane based on aromatic polymers which involve:

- (i) Cross-linking of the sulfonated-aromatic polymers
- (ii) Placement of highly ionic pendant groups carrying terminal acid moiety away from the main-chain
- (iii) Concentration of the ionic function on the specific chain segments in order to have nano-scale separation between hydrophobic and hydrophilic regions of the polymer (block copolymers)
- (iv) Use of polymer main chains containing highly hydrophobic fluorinated segments to improve hydrophobic- hydrophilic separation to achieve enough mechanical strength along with high proton conductivity.

***Cross-linking*** of the sulfonated-aromatic polymers such as PES, PEEK to acquire enough good dimensional stability has been explored by few research groups<sup>{110-113}</sup>. However, ***brittleness of the membrane due to covalent and weakening of ionic cross links at high temperature was observed along with lower proton conductivity due to usage of sulfonic acid functions for crosslinking sites. Hence, this approach will not be discussed further.***

#### **b. Polymers carrying acidic ionic function away from the backbone chain**

The approach of polymers bearing different side chains with terminal ionic function has garnered attention in the scientific community in order ***to facilitate/improve hydrophobic-hydrophilic separation***<sup>{114-118}</sup>. A few examples based on different aromatic backbone chains are shown in figure 18.

Jannasch et al. have concentrated their work on modification of commercially available polysulfones and studied various types of aromatic poly (arylene ether sulfone) (PES) ionomers functionalized with mono-, di- and tri- sulfonic acid groups isolated on different aromatic/aliphatic short side chains to enhance hydrophilic-hydrophobic separation with structure represented in figure 18 (a) to (e)<sup>{115,116}</sup>.

They studied the morphology of these membranes using SAXS which demonstrated that the concentration of the acidic groups to side chains promoted a high degree of phase separation and ionic clustering in the membranes. While comparing these sulfoalkylated PESs (as seen in the table 3), it can be seen that all these membranes swell up to limited extent at elevated temperature (80-100°C) except tsnb-PSU which swells extensively leading to membrane disintegration. Generally, it is

considered that dissociation of aryl sulfonic acids is probably higher than that of alkyl sulfonic acids. However, similar conductivities (table 3) have been reported for polymers bearing either a dangling alkyl sulfonic acid or an aryl sulfonic acid located on the main-chain of an ionomer.

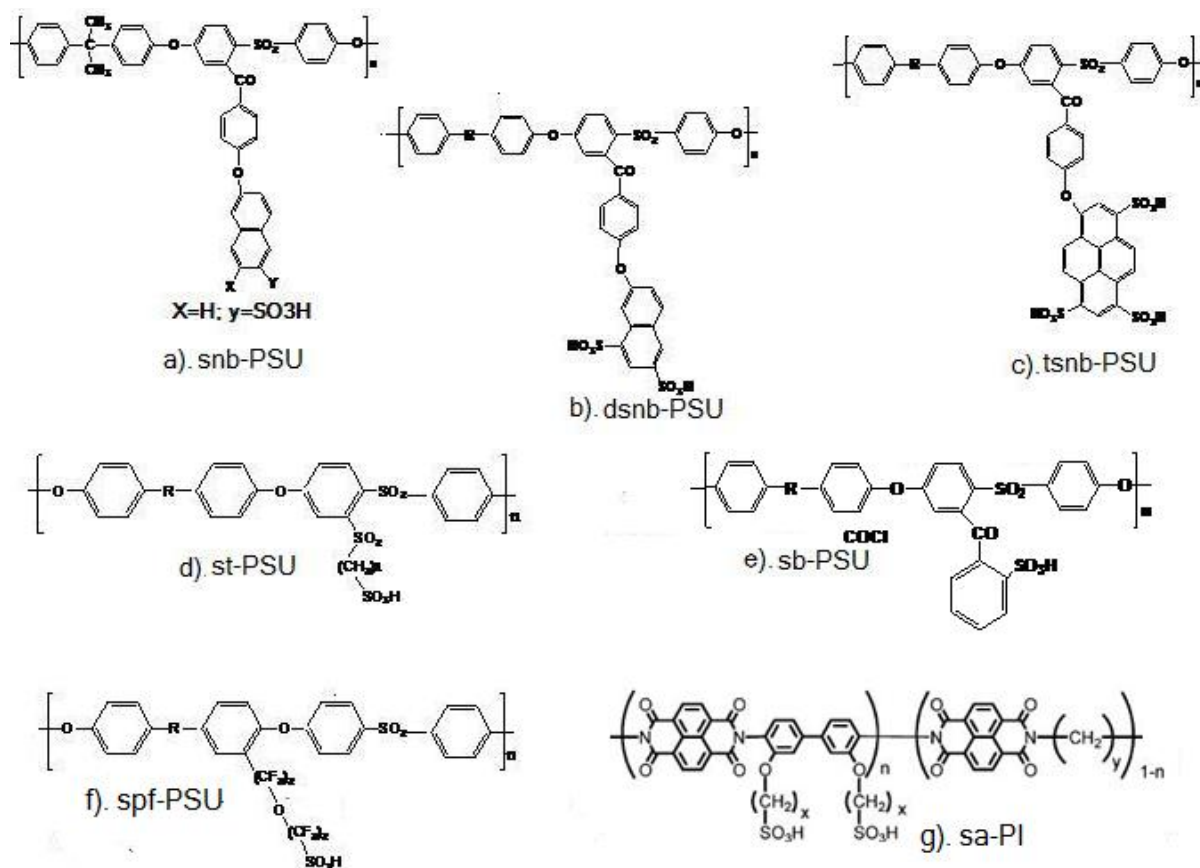


Figure 18: Different aromatic polymers carrying acidic ionic function away from the polymer backbone chain

Yoshimura et al. synthesized PES bearing a perfluorinated sulfonic acid function<sup>[117]</sup> (figure 18 (f):spf-PSU). The obtained polymer had an IEC of up to 1.58 meq/g with water uptake of 157% under immersed state and showed proton conductivity of up to 0.12 S/cm at 80 °C under 90% relative humidity. They also compared various characteristics of Nafion<sup>®</sup> and PES-PSA (IEC=1.34 meq/g) as both carry similar side-chains. It was observed with the help of SAXS measurements that the latter did not show any significant peak in dry state but formation of cluster channels took place in wet state (water content=38%; membrane was soaked in water at 80°C). However, the cluster size for PES-PSA (cluster size~3.7 nm, water content 38%) was smaller than that for Nafion<sup>®</sup>112 (cluster size~4.2 nm, water content 23%). This could be due to the rigid main-chain in PES-PSA preventing aggregation of the side-chain. The in-plane proton conductivity for PES-PSA (IEC=1.34meq/g, thickness=47μm) was 0.077S/cm at 80°C under 90% RH as compared to 0.089S/cm for Nafion<sup>®</sup> 112 under similar conditions. The through-plane proton conductivities of Nafion<sup>®</sup>112 and PES-PSA were 0.060 and 0.063 S/cm,

respectively. The difference in proton conductivity might account for ambiguous micro-phase separation/anisotropy in PES-PSA according to them.

<i>Membrane</i>	<i>IEC (meq/g)</i>	<i>% W<sub>water</sub><sup>1</sup></i>	<i>σ (S/cm)<sup>2</sup></i>	<i>T<sub>g</sub> (°C) in sodium form</i>	<i>T<sub>d</sub> (°C)<sup>3</sup> in sodium form; N<sub>2</sub> atm.</i>
<i>st-PSU</i>	<i>1,2</i>	<i>25</i>	<i>22x10<sup>-2</sup>*</i>	<i>na</i>	<i>340</i>
<i>sb-PSU</i>	<i>1,12</i>	<i>21</i>	<i>1x10<sup>-2</sup></i>	<i>173</i>	<i>310</i>
<i>snb-PSU</i>	<i>0,8</i>	<i>15</i>	<i>2,5x10<sup>-3</sup></i>	<i>309</i>	<i>431</i>
<i>dsnb-PSU</i>	<i>1,18</i>	<i>27</i>	<i>6x10<sup>-2</sup></i>	<i>194</i>	<i>442</i>
<i>tsnb-PSU</i>	<i>1,27</i>	<i>44</i>	<i>1x10<sup>-1</sup></i>	<i>199</i>	<i>431</i>

(<sup>\*</sup>): membranes humidified until equilibrium in liquid water and proton conductivity measured under humidifying conditions in an air-tight cell.

(<sup>1</sup>): %W<sub>water</sub> - % uptake water when immersed in water at room temperature;

$$\%W_{water} = [(W_{wet} - W_{dry}) / W_{dry}] * 100$$

(<sup>2</sup>): σ – Proton conductivity at 120°C with membranes fully immersed in water.

(<sup>3</sup>): The temperature at which polymer loses 5% of its original weight after the pre-dry at 150°C for 10 minutes.

*Table 3: Different characteristics of polymer electrolytes based on Polyarylene ether sulfone carrying different ionic function side chains*

Rikuwara et al. synthesized sulfonated polyphenylene polymer bearing a long side chain (-phenoxy benzoyl) separating main chain of the polymer from acidic ionic function<sup>[118]</sup>. This modified polymer presented good solubility in variety of solvents above 30% DS and a membrane with 65% sulfonation degree had a proton conductivity of ~10<sup>-2</sup> S/cm under 100% RH.

Another example has been demonstrated by Wantanabe et al.<sup>[120]</sup>. They synthesized **random copolymer based on sulfonated polyimide containing aliphatic groups** both in the main chain and pendant chain bearing sulfonic acid functions (figure 18 (g): sa-PI). The ionomer (IEC= 1.92 meq/g) presented proton conductivity value of 0.21 S/cm at 120°C under 100% RH and presented higher durability as well as stable proton conductivity for several hundred hours at high temperature and high RH compared to Nafion<sup>®</sup> under similar conditions. However, it exhibited inferior proton conductivity to Nafion<sup>®</sup> at low RH values at all the temperatures examined. This was attributed to the lack of ordered micro-phase separation compared to PFSA based ionomers and lower acidity of Aromatic-SO<sub>3</sub>H compared to CF<sub>2</sub>-SO<sub>3</sub>H group. **SAXS results corroborated these results as no peak was**

*observed for this ionomer under hydrated condition implying that ordered hydrophilic domains do not form in this hydrated ionomer and water rather gets distributed throughout the membrane.* However, it represented much lower hydrogen and oxygen permeability and compared to Nafion<sup>®</sup> 112 under any given condition tested (Temperature: 80°C & 120°C; RH: 0-90%) along with good hydrolytic and oxidative stability and mechanical properties.

**c. Copolymers based on separate hydrophilic-hydrophobic segments**

Additionally, various research groups have exploited *the synthesis of co-polymers from ionic/non-ionic monomers or/and hydrophobic/hydrophilic monomers*. This approach could allow a higher extent of separation between hydrophobic and hydrophilic domains in comparison to the chemical modification of commercial polymers results in which the functional groups are randomly distributed along the macromolecular backbone. As a result, this synthesis route should *restrict the swelling of the membrane to the hydrophilic domains and in turn improve both the dimensional stability and the tensile strength of the membranes*. Different architectures which can be employed are shown in figure 19.

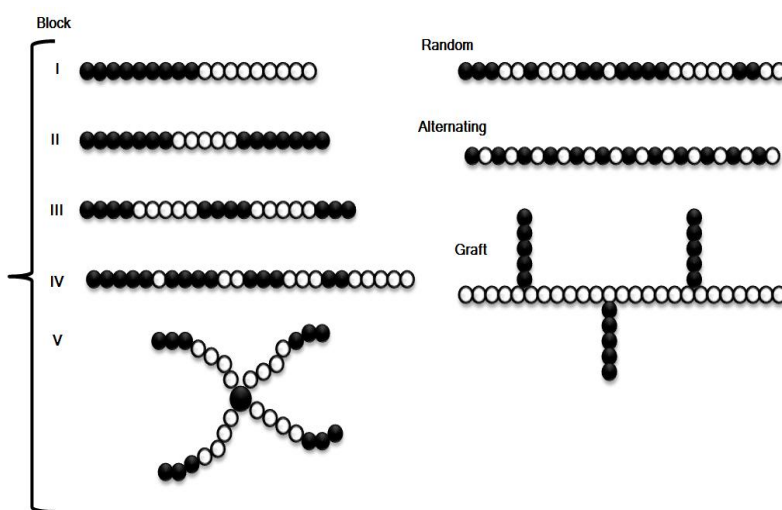


Figure 19: Different copolymer architectures; I: di-block; II: tri-block; III: multi-block; IV: graded block; V: four arm star block

Micro-phase separation of the different components in a copolymer depends on various factors such as compositional dissimilarity, molecular weight and crystallizability. Fine-tuning these parameters can result in variety of morphological structures such as spheres, lamellae, cylinders etc. which can result in continuous percolation of ionic and non-ionic domains required for high proton conductivity and mechanical strength, Moreover, by *differing the ratio of hydrophilic/hydrophobic monomer units*,

*not only morphology but also hydrophilicity of the copolymer can be modified* which in turn can help in *designing architectures according to the requirements*.

In this regard, Liang et al. have shown recently the *morphology differences between multi-block (MBC-PSU) and random (RC-PSU) copolymers based on sulfonated poly (arylene ether) sulfone (PSU) (figure 20 (a) & (b) respectively) using AFM as well as SAXS measurements*<sup>[119]</sup>. In addition, they studied the impact of the membrane morphology on their functional properties. At similar IECs, the water uptake and conductivity of the multi-block MBC-PSU membranes were higher than that of the random RD-PSU membranes.

For random sulfonated PSU copolymers, the sulfonic acid groups would be randomly distributed in the copolymer chain. Unlike random RD-PSU copolymers, the multi-block MBC-PSU copolymers had repeated hydrophilic and hydrophobic units. These (repeated units) were thought to be able to assemble into cluster like structures or spherical or cylindrical micelles as also confirmed by AFM and SAXS measurements. These kinds of structures made the hydrophilic domains well connected and tended to effectively keep more water in the membranes. By SAXS measurements they observed intense peaks at  $q$  values of approximately 1.64 and 4.30 nm<sup>-1</sup> for the Nafion<sup>®</sup> 117 and multi-block MBC-PSU3 membranes, respectively. These peaks were supposed to be caused by the clustering of the ionic groups in the polymer matrix. The Bragg spacing ( $d$ ) for the Nafion<sup>®</sup> 117 and multi-block MBC-PSU membranes were determined to be 3.8 and 1.5 nm, respectively. For the random RC-PSU membrane, no obvious peak was observed. These *SAXS investigations suggested that the multi-block MBC-PSU membrane had nano-scale clusters*.

Both the random and multi-block Polysulfone membranes showed lower methanol permeability and higher proton/methanol selectivity than the Nafion<sup>®</sup> 117 membrane. The multi-block PSU membrane showed slightly higher methanol permeability but quite higher proton/methanol selectivity than random RC-PSU membrane at similar IEC value due to the formation of ionic clusters in the former.

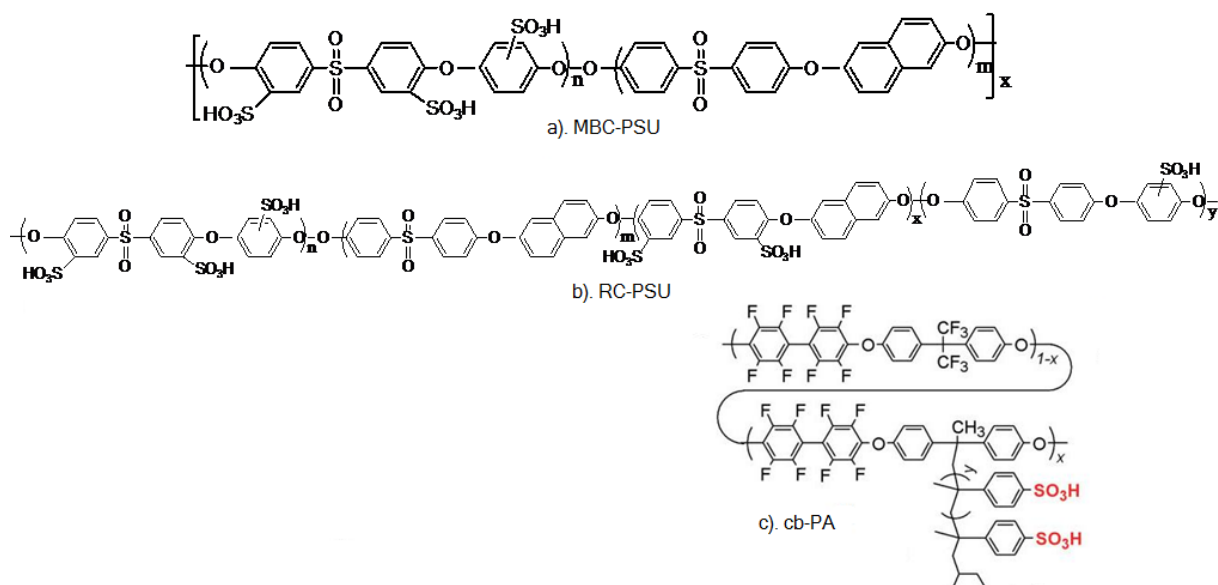


Figure 20: Different co-polymers based on aromatic hydrocarbons with enhanced hydrophobic-hydrophilic separation

Norsten et al. synthesized and investigated **highly fluorinated comb-shaped poly aromatic copolymer**<sup>[121]</sup>. The comb-shaped structure of the copolymer is based on highly fluorinated and rigid polyarylene ether backbone with and without long, flexible pendant poly ( $\alpha$ -methyl) styrene side-chains containing multiple sulfonic acid groups. The idea was to induce micro-phase separation due to high difference in the ionic character of the two repeating units of the copolymer (Figure 20 (c): cb-PA). The morphology of the membranes prepared from this copolymer was studied using SAXS and TEM analysis.

SAXS study revealed an increase in the value of scattering vector  $q$  corresponding to first-order scattering peaks with increasing ionic side-chain content. This signifies **narrower hydrophobic domains and hence ability to control the size of hydrophobic-hydrophilic domains by changing the ionic side-chain content**. TEM images represented distinct micro-phase separated morphologies with ionic domain connectivity. The copolymer was characterized by a monotonic increase in water uptake with increasing ionic side chain content although less significant than typical sulfonated aromatic polymer electrolytes as well as Nafion<sup>®</sup> for similar IEC value. This was attributed to its unique morphology with narrow hydrophilic domain and thicker alternating hydrophobic domains. The membrane with 38% ionic side chain (IEC=1.8 meq/g) represented a proton conductivity of 0.6 S/cm at 80°C under 100% RH. Furthermore, MEAs based on this comb-shaped copolymer exhibited similar fuel cell performance as Nafion based MEA at 30°C under humidified gases and ambient pressure.

The results obtained with different strategies for improving hydrophilic-hydrophobic separation (such as moving ionic function away from the main-chain or synthesizing block copolymers with hydrophobic and hydrophilic blocks) in aromatic polymer based ionomers seems very promising and great efforts are being put in these directions to find a suitable alternative to Nafion<sup>®</sup>.

*However, all the different ionomers discussed in this section have shown a strong dependence on high relative humidity for their good fuel cell performance which limits their utilization at temperature above 120°C under ambient pressure. Hence, various strategies have been proposed and investigated for the development of polymer electrolyte systems working at more than 120°C for the great interest to ensure good fuel cell performance as well as durability of the system for automotive applications. These strategies will be discussed in the next section of this chapter.*

### ***1.5: Polymer Electrolyte Membranes for High Temperature-PEMFCs***

PFSA based membranes and other groups of ionomers discussed in previous section have been modified to allow their functioning at low humidity and temperature higher than 80°C. These approaches include: Hygroscopic organic-inorganic composite membranes; Anhydrous proton conducting membranes; which will be discussed in detail in this section.

#### **1.5.1: Hygroscopic organic-inorganic composite membrane**

##### ***a. Addition of Hygroscopic particles***

Addition of hygroscopic oxides such as SiO<sub>2</sub>, TiO<sub>2</sub> etc. has been exploited by various research groups to improve water-retaining capacity of PFSA based membranes and other types of ionomers as well.

Wantanabe et al. presented thinner *Nafion<sup>®</sup> membranes blended with nano-crystallites of Platinum and hygroscopic materials such as SiO<sub>2</sub> and TiO<sub>2</sub>*<sup>{122}</sup>. The role of Platinum nano-crystallites was to suppress O<sub>2</sub> and H<sub>2</sub> crossover by promoting their catalytic combination to produce water within the membrane while the hygroscopic particles could trap these water molecules. They reported low resistance of these membranes under low humidification levels. Moreover, these membranes presented fuel cell performance at low humidity levels similar to that of unmodified Nafion<sup>®</sup> under fully humidified conditions<sup>{123}</sup>.

Mauritz et al. reported a new sol-gel technique for the first time to combine silica particles with Nafion<sup>®</sup> and demonstrated a nano-scale separation of the two phases present in the composite membrane<sup>{124}</sup>.

Similarly, Kim et al. investigated PEMs based on Nafion<sup>®</sup> and *binary oxides*  $\text{SiO}_2\text{-ZrO}_2$  for their application at temperature above 100°C<sup>{125}</sup>. They reported an increase in proton conductivity with increasing Zirconia content ratio upto 80°C but the effect of Zirconia is reversed at higher temperature due to the lack of liquid water in the system and a better performance of the membrane containing binary oxide has been obtained at 120°C.

Apart from these *inorganic compounds, zeolites such as Chabazite and Clinoptilolite* have been combined up to 40 volume percent with Nafion<sup>®</sup><sup>{126}</sup>. These composite membranes presented proton conductivity of an order of magnitude lower to recast Nafion<sup>®</sup> membranes. Another group combined Modernite power with Nafion<sup>®</sup> resin using hot pressing technique at 250°C under 6 bars<sup>{127}</sup>. They demonstrated that the proton conductivity increased with increasing content of Modernite above 90°C and was higher than that of Nafion<sup>®</sup> at such temperatures. Membrane containing 10% modernite showed best performance and this is attributed to water retention in the hygroscopic modernite at high temperatures.

#### ***b. Addition of Multi-functional particles***

Incorporation of multi-functional inorganic particles (such as treated silica particles, zirconium phosphate, heteropolyacids, metal hydrogen sulphates etc.), which are *both hygroscopic and proton conductor in nature*, into the ionomers has been investigated as well. These inorganic additives reduce chemical potential of water inside the membrane providing another pathway for proton conduction and increasing the number of water bonding sites in the membrane at the same time.

Yan et al. reported the elaboration of composite membranes based on Nafion<sup>®</sup> and bifunctional silica (i.e. *sulfonated phenethylsilica which is both hydrophilic and proton conducting*) by casting method<sup>{128}</sup>. They reported proton conductivities of Nafion<sup>®</sup> 117, Nafion<sup>®</sup> recast and Nafion<sup>®</sup> membrane containing 5% bifunctional silica in the order of 0.0308S/cm, 0.0235S/cm and 0.0774S/cm respectively at 80°C and 100% RH. The increase in proton conductivity was attributed to the increase in ion exchange capacity and hydrophilicity of the membrane upon addition of bifunctional silica.

*Composite membranes based on heteropolyacids and PFSA based polymers* have also been investigated due to high intrinsic conductivity of heteropolyacids. Savadogo et al. fabricated composite membranes based on Nafion<sup>®</sup> and *silicotungstic acid*-with/without thiopene<sup>{129}</sup>. They



reported water uptake of 60% for membrane containing 50% silicotungstic acid compared to 30% for Nafion<sup>®</sup> 117 at 25°C (membranes were equilibrated in boiling water for 24 hours followed by measurements of change in their weight at 25°C) and hence higher ionic conductivity in the former. They related this increase in water uptake and ionic conductivity to the increase in number of protonic sites in the membrane due to the presence of silicotungstic acid.

Similarly, Stimming et al. investigated composite membranes based on *molybdophosphoric acid* and Nafion<sup>®</sup> for DMFCs and compared the proton conductivity and methanol permeability of this system with pure and recast Nafion<sup>®</sup><sup>[130]</sup>. Staiti et al. demonstrated membranes based on silica particles impregnated with *phosphotungstic acid* (PWA) and silicotungstic acid (SWA) combined with Nafion<sup>®</sup> using casting method<sup>[131]</sup>. They reported a better performance of PWA based membranes compared to SWA based membranes as well as bare silica-Nafion<sup>®</sup> membranes in DMFC. However, the main disadvantage observed with systems based on heteropolyacids is their dissolution in water under fuel cell working conditions.

This approach has been extended to other polymer matrices such as (sulfonated PEEK, sulfonated PES and PBI etc.)<sup>[132]</sup>. These systems have presented similar/lower performances in comparison to Nafion<sup>®</sup> based composite membranes in general.

However, since the *performance of the systems discussed above involve proton conduction using water molecules, their performances deteriorate at high temperature* though less pronounced effect compared to pure Nafion<sup>®</sup>. *Replacement of water with low volatile solvents/heterocycles/proton conducting ionic liquids* to achieve proton conductivity at higher temperatures due to the rationale that other solvents can perform the function of water in the membrane has been investigated as an alternative approach.

### 1.5.2: Anhydrous Proton Conducting Membranes

The idea and possibility of acquiring high ionic conductivity in other dipolar solvent systems other than water opened gate for many different approaches for HT-PEMFC technology.

#### *a. Acid-Base Complexes*

Acid-base complexation has been considered as an effective method for the development of proton conducting membranes working in anhydrous environment. Basically, *a polymer bearing basic sites such as ether, alcohol, imine, amine, amide or imide groups can be combined with a strong or*

*medium strong acid to form a macromolecular ion pair* where the basic polymer acts as proton acceptor.

According to Kreuer et al., *amphoteric acids such as Phosphoric acid are particularly advantageous* for this purpose due to their high conductivity attributed to their ability to generate both proton donor and proton acceptor groups which can form dynamic hydrogen networks in which proton transfer can occur by hydrogen bond breaking and forming processes<sup>{133-135}</sup>. Phosphoric acid shows proton conductivity as high as 0.8 S/cm at 200°C. However, it is important to note that *the conductivity of phosphoric acid decreases on blending with a polymer matrix* and hence it is important to have relatively large quantities of phosphoric acid in the membrane to obtain good conductivity<sup>{136}</sup>.

Earlier investigations had been carried out on polymers such as Polyethyleneoxide, Polyarylamide, Polyethyleneimine, Poly (vinyl alcohol), Polyvinylpyridine etc. and phosphoric acid<sup>{137}</sup>. But most of these materials suffered from fundamental limitations such as insufficient chemical stability (e.g., hydrolysis of ethers or amides) or low mechanical stability, especially at higher temperatures and larger amounts of incorporated phosphoric acid.

However, a *highly promising performance had been demonstrated by the system based on polybenzimidazole (PBI)-phosphoric acid* developed by Savinell et al. which presented high proton conductivity at low relative humidity<sup>{138}</sup>. A conductivity of 0.04 S/cm with 500 mole percent of phosphoric acid (i.e. 5 phosphoric acid molecules per repeating unit of PBI) at 190°C at 10% RH is shown by this system. The proton conduction in this system occurs in the phosphoric acid domains and the mechanism depends on the acid doping level and presence of water molecules. At lower degree of acid doping, there is a co-operative motion of two protons along the polymer-anion chain. In contrary, at high doping levels, the conduction of proton is similar to pure phosphoric acid i.e. proton jump between two neighbouring phosphoric acid molecules. Nevertheless, in both cases, the mechanism of proton conduction is Grotthuss in nature. This system also represent good mechanical properties at medium doping levels<sup>{139}</sup> (330-660 mol % of phosphoric acid) and high thermal stability at temperatures even up to 200°C<sup>{140}</sup>.

Even though this system shows excellent properties required for a good fuel cell performance, there are *certain disadvantages which inhibit the possibility of its commercialization for High Temperature- PEMFC application*. These disadvantages include phosphoric acid leaching, slow kinetics of oxygen reduction due to adsorption of phosphates and impurities on the surface of electro-catalysts<sup>{141,142}</sup>, oligomerization of phosphoric acid under low RH and high temperature conditions leading to reduction in proton conductivity<sup>{143}</sup>.

### ***b. Heterocycles***

Another approach is aimed at *swelling ionomers (such as Nafion<sup>®</sup>, sulfonated PEK etc.) with heterocycles such as imidazole, pyrazole, benzimidazole, triazole* etc. to replace the role played by water<sup>{144,145}</sup>. These systems show conductivities between 150°C and 250°C similar to those of hydrated polymers and imidazole has shown particularly promising performance due to high degree of dissociation.

The mechanism of proton conduction in these types of systems (such as sulfonated PEK in combination with imidazole/pyrazole) has been studied by Kreuer et al.<sup>{144}</sup> It has been reported to be vehicular in nature i.e. diffusion of the protonated imidazole/pyrazole in these systems. However, at high concentrations of imidazole ( $\lambda=6$ ;  $\lambda$  is the number of molecules of imidazole per sulfonic acid function of the polymer), co-occurrence of Grotthuss (intermolecular proton transfer) as well as Vehicular mechanism is observed with former being more dominant. The contribution of Grotthuss mechanism decreases with decreasing concentration of imidazole and the conduction mechanism primarily becomes vehicular in nature at  $\lambda=2.3$ . ***Large contribution of vehicular type mechanism of proton conduction results in production of imidazole at the cathode and their eventual and overall volatility which limits their application in fuel cells***<sup>{19}</sup>.

As a solution, *immobilization of these heterocycles by tethering to small oligomers* (e.g. oligo-ethyleneoxide chains) was proposed. The idea was to suppress long range diffusion and provide high local mobility in order to promote Grotthuss type mechanism through the formation of short and elongated hydrogen bonds as well as solvent reorganization<sup>{146}</sup>. However, ***these systems represented fairly low proton conductivities***<sup>{147}</sup>.

Overall, the ***key problems*** associated with this approach include their adsorption on the platinum surface resulting in slow rate of oxygen reduction and electro-chemical stability as well as well accessible limit of proton conductivity up to  $10^{-3}$  S/cm which is too low for fuel cell application<sup>{135}</sup>.

Even though, these two alternative solvents discussed above possess certain disadvantages in regard of their application in PEMFC technology, an ***overview of their performance in comparison to water with the "state of the art- ionomer" Nafion<sup>®</sup>*** has been presented in the figure 21. It can be said that they demonstrate conductivities lower than that hydrated Nafion, however, proton conductivity at much higher temperature are accesible with these two alterantive solvent systems<sup>{147}</sup>.

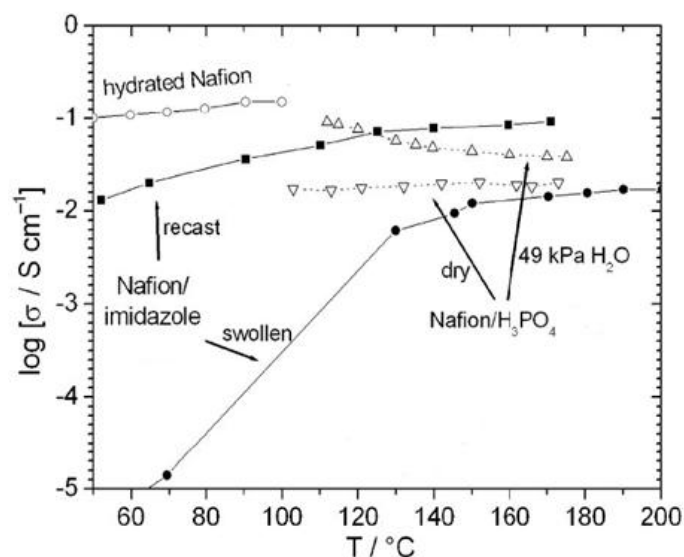


Figure 21: Comparison of different anhydrous membrane systems based on Nafion<sup>®</sup> membrane and dipolar solvent<sup>[147]</sup>

### c. Proton Conducting Ionic Liquids

Apart from mineral acids and heterocycles, utilization of **Proton Conducting Ionic Liquids (PCIL)** as *an alternative to water* has been considered as another *attractive approach for high temperature application of PEMFCs* owing to their various interesting properties such as *high ionic conductivity, immeasurably low vapor pressure, green nature, wide range of choice, high thermal and electro-chemical stability* to list a few<sup>[148,149]</sup>.

*The ionic liquids are basically molten salts having the melting point lower than 100°C* and they are composed of a cationic and an anionic moiety. Many ionic liquids are in liquid state at the room temperature and some of them even have a point of crystallization at very low temperatures. Obviously, the ionic liquids which are liquid at the room temperature offer more advantages compared to those which have the relatively high melting points. The ionic liquids are generally composed of an organic cations such as alkylphosphonium, alkylsulfonium, 1,3-dialkylimidazolium, alkylpyridinium, alkyltriazolium etc. (presented in figure 22). The anions utilized to prepare ionic liquids can be poly-nuclear like  $\text{Al}_2\text{Cl}_7^-$ ,  $\text{Fe}_2\text{Cl}_7^-$ ,  $\text{CuCl}_3^-$  etc. or mono-nuclear like  $\text{BF}_4^-$ ,  $\text{PF}_6^-$ ,  $\text{CF}_3\text{SO}_3^-$ ,  $\text{CH}_3\text{SO}_3^-$ ,  $(\text{CF}_3\text{SO}_2)_2\text{N}^-$ ,  $\text{CF}_3\text{CO}_2^-$  etc.

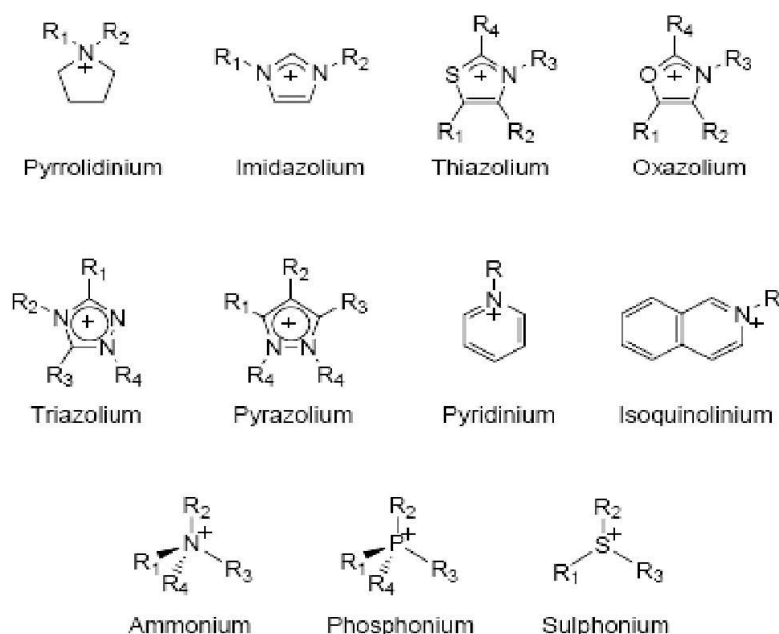


Figure 22: Various organic cations employed for the preparation of ionic liquids

***Ionic liquids are known to form large aggregates through dipole-dipole interactions or hydrogen-bonding and hence aggregation behavior depends primarily on the nature of cations and anions present chemically in the PCIL.*** For example, nitrate anion based ionic liquids show formation of large aggregates in contrary to lactate and formate anion based ionic liquids. Monoalkylammonium based ionic liquids exhibit formation of large aggregates irrespective of the alkyl length chain, while, di- and tri-alkylammonium based salts present lower tendency to the formation of stable aggregates due to higher steric hindrances and lower number of hydrogen present for hydrogen bonding. The tendency to form aggregates can lead to lower ionic conductivity<sup>[150]</sup>. The ***aggregates of ionic liquids have been largely assumed to be in the form of micelles or lamellae***<sup>[151]</sup>.

In order ***to be suitable for PEMFC application***, ionic liquid must act as solvent capable of conducting protons and it has been conferred that ***an ionic liquid has to be protic in nature*** in order to be capable of conducting protons in the neutral system.

Table 4 presents various characteristics of PCILs in regard of PEMFC application. Few research groups have thoroughly investigated various properties of PCILs based on different anionic and cationic species to evaluate their usefulness for PEMFC application.

In this regard, Wantanabe et al. synthesized PCILs based on different amines in combination with trifluoromethylsulfonyl imide<sup>[152,153]</sup>. They reported higher conductivities for neutral salts of pyrazine,

pyridine, pyrrolidine and triethylamine compared to imidazole as well as melting point close to room temperature for neutral salts of triethylamine, butyl-amine and 1,2,4-triazole. Later, they compared triflic acid (TF) based PCILs to TFSI based PCILs and the former was found to present higher open circuit potentials for O<sub>2</sub> reduction compared to the latter meaning more facile oxygen reduction. By comparing various features of all the PCILs they synthesized and studied, they accounted diethylmethyammonium triflate as the most promising PCIL with optimum properties for HT-PEMFC application.

Iojoiu et al. have also presented detailed studies on PCILs based on a large variety of cyclic and acyclic cations and three organic anionic species i.e. triflic acid (TF), pentafluorobenzene sulfonic acid (PF) and bis (trifluoromethylsulfonyl) imide (TFSI)<sup>(154)</sup>. The main characteristics of these PCILs are shown in table 4.

The T<sub>m</sub> of all the PCILs synthesized fall in the temperature range of -15 to 175°C depending on the constituent anionic and cationic species. On the basis of anionic constituent of the PCIL, the T<sub>m</sub> values are in the order: TFSI<PF<TF. Moreover, ***PCILs based on all these acids show lowest T<sub>m</sub> values in combination with tertiary amine (Triethylamine; TEA)***. Moreover, PCILs based on cyclic secondary amines represent higher T<sub>m</sub> compared to acyclic secondary and tertiary amines. The degradation temperature of all these PCILs fall in the range of 300-400°C depending on the constituent anions and cations, but it generally increases with increasing acidity of the acid moiety.

The ionic conductivity values for these PCILs are in the range of 0.1-6 (10<sup>-2</sup>S/cm) depending upon the constituent acid and base as well as the temperature. The general order of ionic conductivity on the basis of these anions is: TFSI>TF>PF. However, ***TF and TFSI based PCILs represent similar conductivities above their melting points***. Comparing the effect of different amines, TEA based PCILs exhibited higher ionic conductivity over a wide range of temperature compared to PCILs based on other amines. Moreover, it is assumed that ***alkyl amine based PCILs show more resistance to adsorption on the catalyst surface compared to imidazole based PCILs***.

Acid	Amine	T <sub>g</sub> ( <sup>0</sup> C)	T <sub>m</sub> ( <sup>0</sup> C)	T <sub>d</sub> ( <sup>0</sup> C)	σ <sup>*</sup>
<b>Bis(trifluoromethylsulfonyl) imide (TFSI)</b>	Pyrollidine	-	35	373	3.96
	Pyridine	-	60.3	314	3.04
	Pyrazine	-	53.6	229	3.38
	Butylamine	-	16.2	352	1.04
	Triethylamine	-	3.5	350	3.23
	Bis(methylethoxy)amine	-73	30	-	2.1 <sup>**</sup>
	Dimethylethylamine	-42	66	377	4.6 <sup>***</sup>
	Diethylmethylamine	-67	24	375	4.1 <sup>***</sup>
	Imidazole	-	73	379	2.7
	Piperazine	-	172.7	358	-
	Benzimidazole	-	101.9	368	1.3
	1,2,4-Triazole	-	22.8	287	2.2
<b>Triflic Acid (TF)</b>	Ethylamine	-	173	400	<sup>a</sup>
	Diethylamine	-	127	390	-
	Triethylamine	-58	36	380	3.1
	Dipropylamine	-	136	390	<sup>a</sup>
	Tripropylamine	-	160	380	<sup>a</sup>
	Dibutylamine	-	140	390	<sup>a</sup>
	Tributylamine	-	128	353	-
	Trihexylamine	-83	-1	361	0.2 <sup>***</sup>
	Dimethylethylamine	-117	41.6	360	5.6 <sup>***</sup>
	Diethylmethylamine	-	-13	360	4.3 <sup>***</sup>
	Bis(methylethoxy)amine	-	55	300	2.7
	Pyrollidine	-	157	395	<sup>a</sup>
	Methylpyrollidine	-	103	382	3
	Pyridine	-	145	390	<sup>a</sup>
	Methylpyridine	-	101	380	2.8
<b>Pentafluorobenzene sulfonic acid (PF)</b>	Trimethylamine	-	154	340	-
	Triethylamine	-59	26	350	-
	Dipropylamine	-	69	360	-
	Tripropylamine	-	69	350	-
	Bis(methylethoxy)amine	-55	37	300	-
	Butylpyridine	-	20	-	-

\*: Conductivity at 130<sup>o</sup>C (10<sup>-2</sup>S/cm); \*\*: Conductivity at 100<sup>o</sup>C (10<sup>-2</sup>S/cm); \*\*\*: Conductivity at 120<sup>o</sup>C (10<sup>-2</sup>S/cm)

<sup>a</sup>: Conductivity lower than 0.1(10<sup>-2</sup>S/cm)

Table 4: Different characteristics of Proton Conducting Ionic Liquids based on different anions and cations<sup>[152-154]</sup>

Iojoiu et al. also conducted studies on the study of conduction mechanism of various alkyl ammonium based PCILs using PFG-NMR technique<sup>[154]</sup>. It was observed that the *self diffusion coefficients of proton and alkyl ammonium moiety are similar and larger than anionic moiety indicating that the proton transfer occurs through the diffusion of ammonium species via vehicular mechanism*.

There have been few studies in which various PCILs have been combined with a polymer matrix (such as Nafion<sup>®</sup>, sulfonated aromatic polymers etc.) and performance of these systems have been evaluated for HT-PEMFC technology. The most common method employed for PCIL incorporation into the polymer matrix has been the “*swelling method*” which involves immersing the membrane in the PCIL at elevated temperatures.

Basically, the idea of combining a polymer matrix with a PCIL was first conceived by Fuller et al.<sup>[155]</sup>. They combined ionic liquids such as 1-ethyl, 3-methyl imidazolium (EMI) trifluoromethane sulfonate (triflate) and EMI tetrafluoroborate with poly(vinylidene fluoride)-hexafluoropropylene copolymer [PVdF(HFP)] for the application of secondary lithium batteries (polymer-in-salt).

However, Doyle et al. explored their possibility for HT-PEMFC application<sup>[156]</sup>. They studied the system based on Nafion<sup>®</sup> (in H<sup>+</sup> and Li<sup>+</sup> form) with 1-butyl, 3-methyl imidazolium triflate (BMITf) and BMI tetrafluoroborate (BMIBF<sub>4</sub>). They reported conductivities in the range of 0.06 S/cm to 0.11 S/cm (at 150 to 180°C) and claimed that there was no cation exchange between acidic sites of Nafion<sup>®</sup> and the ionic liquids. Moreover, they suggested that protons carry a significant fraction of current in these systems.

However, few groups reported later the possibility of *exchanging cations of PCIL with the acidic sites of Nafion<sup>®</sup>*. For instance, Crespo et al. explored the possibility of exchanging the cations of different ionic liquids with the protons of the sulfonic acid sites of Nafion<sup>®</sup><sup>[157]</sup>. They reported higher water retention at high temperatures. They also proposed that the conductivity of the membrane is dependent on the size of the cation of the ionic liquid used i.e. larger the cations, higher is the resistance of the membrane.

Another work, done by Ronghuan et al., involved elaboration of membranes based on Nafion<sup>®</sup> incorporated with ionic liquid cation 1-butyl-3-methylimidazolium (BMIm) and doped with phosphoric acid (PA)<sup>[158]</sup>. They reported proton conductivity of 10.9 mS cm<sup>-1</sup> and a tensile stress at break of 5.3 MPa for the composite membrane of Nafion/2.3BMIm/5.2PA in molar ratio at 160°C without humidification.



Benette et al. primarily focused on understanding the effect of these ionic liquids on the morphology of Nafion<sup>®</sup> 117 using SAXS and used the model proposed by Gierke et al. to discuss the effect<sup>[159]</sup>. They prepared membranes based on proton conducting ionic liquids such as 1-ethyl-3-methylimidazolium trifluoromethanesulfonate (EMI-Tf) and 1-ethyl-3-methylimidazolium bis(trifluoromethanesulfonyl)imide (EMI-Im) and Nafion<sup>®</sup> (in protonated form) by swelling method for the application of electromechanical transducers. ***They reported that EMI-Im, being hydrophobic in nature, disrupted the cluster morphology of Nafion<sup>®</sup> while addition of EMI-Tf led to an increase in the size of ionic clusters being excluded from the hydrophobic phase.***

Park et al. utilized the same ionic liquids used by Benette et al. and combined them with Nafion<sup>®</sup> and sulfonated poly aryl ether ketone (SPAEEK) (both in protonated form) by solution casting method<sup>[160]</sup>. They studied the morphology of these membranes by SAXS & TM-AFM. They ***reported a different evolution of SAXS spectra for EMI-Im combined with Nafion<sup>®</sup> and related this to the different method of elaboration.*** Moreover, they reported that the distance between hydrophobic and hydrophilic phase was lower in membranes containing hydrophilic ionic liquid than in those based on hydrophobic one. However, they suggested that the connectivity between ionic domains in EMI-Im based membrane was worse than EMI-Tf based membranes giving rise to lower conductivity in the former. They also reported that the SPAEEK based membranes didn't show any ionomer peak in SAXS spectrum despite the presence of ionic clusters due to poor phase separation.

Schmidt et al. concentrated their work on the study of the effect of ionic liquids (based on heterocyclic amines-organic/inorganic acids) on the mechanical and thermal properties of Nafion<sup>®</sup> 117 (in protonated form)<sup>[161]</sup>. They reported a ***plasticizing effect of the ionic liquids on Nafion<sup>®</sup>*** and suggested that ***higher hydrophobicity and voluminocity of the anion (of the ionic liquid) would stronger plasticizing effect on the Nafion<sup>®</sup> matrix.***

Choudhary et al. investigated rather an exotic approach. They combined an ionic liquid i.e. 1-butyl-3-methylimidazolium bis(trifluoromethylsulfonyl)imide (BMI-BTfSI) with Nafion<sup>®</sup> membrane (in acid form) reinforced with sulfonated-polyhedral oligomeric silsesquioxanes using layer by layer strategy<sup>[162]</sup>. They reported a proton conductivity of 5mS/cm at 150°C along with improvement in mechanical properties compared to Nafion-IL system.

Interestingly, Sanchez et al. reported the combination of PCILs based on tertiary alkyl ammonium with Nafion<sup>®</sup> in neutralized form for the first time<sup>[163,164]</sup>. ***Neutralization of the acidic sites in Nafion with the same base as used for the preparation of PCIL was done to avoid a cation exchange process between Nafion<sup>®</sup> and PCIL.*** In this kind of system, primarily dipole-dipole interactions exist between neutral PCIL molecules and dangling neutralized ionic sites in Nafion<sup>®</sup>. In their work, they

combined PCILs Triethylammonium neutralized Nafion<sup>®</sup> 117 membrane with PCILs such as ammonium methane sulfonate (MSTEA) and ammonium triflate (TFTEA) by swelling method. An *improvement in thermal properties of Nafion<sup>®</sup> has been reported due to neutralization of sulfonic acid sites*. Moreover, they reported an anhydrous conductivity of 10 mS/cm for TFTEA based membranes and 14mS/cm for MSTEA based membranes along with plasticization of membranes at high uptake of these PCILs. Moreover, they reported *an improvement in mechanical properties of Nafion<sup>®</sup> by neutralizing it with a diamine due to induction of physical crosslinking*. Later, they demonstrated better anhydrous conductivity of membranes imbibed with diamine based ionic liquids probably due to co-occurrence of Grotthuss and Vehicular conduction mechanism for proton transfer in these systems.

Vito di Noto et al. further studied the system developed by above authors in their collaboration and studied the system based on Nafion-TEA+TFTEA in detail by FTIR-Raman spectroscopy to understand the structure and interaction between different nano-phases present in this material<sup>[165]</sup>. A decrease in crystallinity of Nafion-hydrophobic phase was proposed owing to neutralization with amine and addition of ionic liquid. Raman study showed that *TF anions aggregate to form micelle like nano-clusters*. Furthermore, they utilized Broadband Dielectric Spectroscopy (BDS) to study the electrical properties and conduction mechanism for such systems<sup>[166]</sup>. According to Di Noto et al., *PCILS like TFTEA form anionic micelle-like nano-particles (referred to as MTAs) in the hydrophilic domains of Nafion<sup>®</sup> and proton migration occurs through hopping phenomenon between ammonium ions, sulfonate sites of the polymer and MTAs*. Also, the charge transfer largely depends on the segmental motion of the polymer chains and the molecular dimensions of the ionic liquid nanoaggregates in such systems.

Similarly, Wantanabe et al. have combined *sulfonated polyimide (neutralized with diethylmethylamine) with diethylmethylammonium triflate (DEMAT)* using solution casting method<sup>[167]</sup>. They reported a plasticizing effect of DEMAT on the polyimide matrix at high percentage content (>67wt%). An ionic conductivity of more than 10<sup>-3</sup>S/cm at 40<sup>0</sup>C has been reported for ionomers (IEC=2.15 and 1.41 meq/g) containing more than 67 wt % of DEMAT. In addition, they reported an increase in the hydrogen and oxygen gas permeability of the ionomers matrix on the incorporation of DEMAT. However, permeability coefficients were of same order as Nafion<sup>®</sup> in humidified state.

Recently, Segalman et al. exploited a slightly different idea and synthesized and combined a block copolymer i.e. poly (styrene-block-2 vinyl pyridine) with imidazolium bis(trifluoromethane)sulfonamide<sup>[168]</sup>. They characterized this system using SANS and DSC. They reported that the ionic liquids enter primarily poly (2-vinyl pyridine) domains for the polymer fraction

between 0.51 and 0.86. Furthermore, they proposed *a variety of morphologies such as lamellae, hexagonally packed polystyrene cylinders etc. depending on the ionic liquid content in the copolymer* by using SAXS measurements. A strong effect of morphology on the ionic conductivity was reported. Moreover, conductivity was shown to depend primarily on the ionic liquid volume fraction in this copolymer and hence copolymer with different content of the constituent blocks could be personalized to achieve a balance between mechanical strength and ionic conductivity.

### **Motivation of the thesis work:**

From the few studies based on Proton Conducting Ionic Liquid doped Ionomers discussed above, promising results have been demonstrated. However, most of the studies have been concentrated on imidazolium based PCILs (which generally show inferior properties such as lower conductivity, electro-chemical stability etc. compared to PCILs based on alkylammoniums). More importantly, a detailed study of the impact of the chemical structure/nature of the PCILs/functional polymers on the morphology (at different length scales) and various functional properties of the system has not been clearly demonstrated. Moreover, no detailed study has been presented on the study of transport properties (such as water sorption, gas-permeation) and degradation phenomena associated with such system which are equally important for its fuel cell application.

The understanding of the effect of PCIL addition on the morphology of an ionomer and its correlation with other properties such as electro-chemical, thermo-mechanical, transport etc. is very important in order to understand the behavior and performance of such system and also to be able to fine-tune the properties by choosing carefully an ionomer matrix and a PCIL for their optimum performance in the fuel cell.

*Thus, in this work, influence of the chemical structure/nature of PCILs (based on Triethylammonium and different perfluorinated anionic moieties) as well as functional polymers (Nafion® and Polysulfone based ionomer) on the evolution of morphology and consequent functional properties of the system will be deeply studied. Different characterization techniques will be utilized in order to study the response of such system at different length scales i.e. molecular, nanoscopic-mesoscopic and macroscopic scales.*

## ***References:***

1. Wolz, A.; Zils, S.; Michel, M.; Roth, C.; Journal of Power Sources **2010**, 195(24), 8162–8167.
2. Song, C.; Catalysis Today **2002**, 77, 17–49.
3. [www.fuelcells.si.edu](http://www.fuelcells.si.edu)
4. Dupuis, A.C.; Progress in Materials Science **2011**, 56, 289–327.
5. Peighambardoust, S.J.; Rowshanzamir, S.; Amjadi, M; International Journal of Hydrogen Energy **2010**, 35, 9349-9384.
6. Dyer, C.K.; Fuel Cells Bulletin No. 42
7. Hiesgen, R; Wehl, I.; Aleksandrova, E.; Roduner, E.; Bauder, A.; Andreas Friedrich, K.; International Journal of Energy Research **2010**, 34, 1223-1238.
8. Wolz, A.; Zils, S.; Michel, M.; Roth, C.; Journal of Power Sources **2010**, 195(24), 8162–8167.
9. O’Hayre, R.; Barnett, D.; Prinz, F.B.; Journal of the Electrochemical Society **2005**, 152(2), 439-444.
10. Chernyshov, S.F.; Journal of the Research Institute for Catalysis Hokkaido University **1982**, 30(3), 179-190.
11. Arico, A.S.; S. Srinivasan, S.; Antonucci, V; Fuel Cells **2001**, 1(2), 133-161.
12. Deluca, N.W.; Elabd, Y.A.; Journal of Polymer Science: Part B: Polymer Physics **2006**, 44, 2201–2225 (2006).
13. Wasmus, S.; Kuver, A.; Journal of Electroanalytical Chemistry 461 (1999) 14–31.
14. Heinzel, A.; Barragan, V.M.; Journal of Power Sources **1999**, 84, 70-74.
15. Neburchilov, V.; Martin, J.; Wang, H.; Zhang, J.; Journal of Power Sources **2007**, 169, 221–238.
16. Hamnett, A.; Catalysis Today **1997**, 39, 445-457.
17. Yun Wang, Y; Chen, K.S.; Mishler, J; Cho, S.C.; Adroher, X.C.; Applied Energy **2011**, 88, 981–1007.
18. Li, Q; He, R.; Jensen, J.O.; Bjerrum; N.O.; Chemistry of Materials **2003**, 15 (26), 4896-4915.
19. Yang, C.; Costamagna, P.; Srinivasan, S.; Benziger, J.; Bocarsly, A.B.; Journal of Power Sources **2001**, 103, 1-9.
20. Shao, Y.; Yin, G.; Wang, Z.; Gao, Y.; Journal of Power Sources **2007**, 167(2), 235-242.

21. Kreuer, K.D.; Paddison, S.J.; Spohr, E.; Schuster, M.; Chemical Reviews **2004**, 104, 4637-4678.
22. Boillat, P.; Kramer, D.; Seyfang, B.C.; Frei, G.; Lehmann, E.; Scherer, G.G.; Wokaun, A.; Ichikawa, Y.; Tasaki, Y.; Shinohara, K.; Electrochemical communication **2008**, 10(4), 546-550.
23. Oetjen, H.F.; Schmidt, V. M.; Stimming, U.; Trila, F.; Journal of Electrochemical Society **1996**, 143(12), 3838-3842.
24. Qi, Z.Q.; He, C.Z.; Kaufman, A.; Journal of Power Sources **2002**, 111, 239-247.
25. Zhang, J.L.; Xie, Z.; Zhang, J.J.; Tanga, Y.H.; Song, C.J.; Navessin, T.; Shi, Z.Q.; Song, D.T.; Wang, H.J.; Wilkinson, D.P.; Liu, Z.S.; Holdcroft, S.; Journal of Power Sources **2006**, 160, 872-891.
26. Parthasarathy, A.; Srinivasan, S.; Appleby, A.J.; Martin, C.R.; Journal of Electrochemical Society **1992**, 139(9), 2530-2537.
27. Zhang, L.; Zhang, J.J.; Wilkinson, D.P.; Wang, H.J.; Journal of Power Sources **2006**, 171(2), 558-566.
28. Wang, B.; Journal of Power Sources **2005**, 152, 1-15.
29. Hogarth, W.H.J.; Diniz da Costa, J.C.; Lu, G.Q.; Journal of Power Sources **2005**, 142(1-2), 223-237.
30. Knights, S.D.; Colbow, K.M.; St-Pierre, J.; Wilkinson, D.P.; Journal of Power Sources **2004**, 127(1-2), 127-134.
31. Collier, A.; Wang, H.J.; Yuan, X.Z.; Zhang, J.J.; Wilkinson, D.P.; International Journal of Hydrogen Energy **2006**, 31(13), 1838-1854.
32. Stevens, D.A.; Dahn, J.R.; Carbon **2005**, 43, 179-188.
33. Büchi, F.N.; Wakizoe, M.; Srinivasan, S.; The Journal of Electrochemistry **1996**, 143(3), 927-932.
34. Kreuer, K.D.; Cambridge University Press **1992**, 474-476.
35. Gubler, L.; Scherer, G.G.; Springer-Advances in polymer science **2008**, 215; 1-14.
36. Mittal, V.; Kunj, H.R.; Fenton, J.M.; Electrochemical Society Transaction **2006**, 3(1), 507-517.
37. Grubb, W. T.; "Fuel Cell United States" **1959**, Patent US2913511.
38. Ezzel, B. R.; Carl, W. P.; Mod, W. A.; United States **1982**, Patent US4358545.
39. Eisman, G. A.; Journal of Power Sources **1990**, 29(3-4), 389-398.
40. Ghielmi, A.; Vaccarone, P.; Troglia, C.; Arcella, V.; Journal of Power Sources **2005**, 145(2), 108-115.
41. Jalani, N.H.; Datta, R.; Journal of Membrane Science **2005**, 264(1-2), 167-175.

42. Garland, N.L.; Kopasz, J.P.; Journal of Power Sources **2007**, 172, 94–99.
43. Kreuer, K.D.; Journal of Membrane Science **2001**, 185, 29–39.
44. Van der Heijden, P.C.; Rubatat, L.; Diat, O.; Macromolecules **2004**, 37, 5327-5336.
45. Gierke, T. D.; Munn, G. E.; Wilson, F. C. Journal of Polymer Science-Polymer Physics **1981**, 19, 1687-1704.
46. Schmidt-Rohr K.; Chen Q.; Nature Materials **2008**, 7, 75–83.
47. Young, S.K.; Trevino, S.F.; Beck Tan, N.C.; Journal of Polymer Science: Part B: Polymer Physics **2002**, 40(4), 387-400.
48. Smitha, B.; Sridhar, S.; Khan, A.A.; Journal of Membrane Science **2005**, 259, 10-26.
49. Litt, M. H. PolymER Preparations **1997**, 38, 80–81.
50. Rubatat, L.; Rollet, A.-L., Gebel G.; Diat O. Macromolecules **2002**, 35, 4050–4055.
51. Gebel, G.; Diat, O.; Fuel Cells, **2005**, 5(2), 261–276.
52. Rubatat, L.; Gebel, G.; Diat, O.; Macromolecules, **2004**, 37(20), 7772-7783.
53. Sone, Y.; Ekdunge, P.; Simonsson, D. Journal of Electrochemical Society **1996**, 143, 1254-1259.
54. Perrin, J.C.; Lyonnard, S.; Volino, F., Journal of Physical Chemistry C, **2007**, 111(8), 3393-3404.
55. Gebel, G. Polymer, **2000**, 41, 5829-5838.
56. Gebel, G.; Lyonnard, S.; Mendil-Jakani, H.; Morin, A.; Journal of Phys. Condensed Matters **2011**, 23 234107.
57. Kusoglu, A.; Modestino; M. A.; Hexemer, A.; Segalman, R.A.; Weber, A.Z.; ACS Macromolecules Letters, **2012**, 1(1), 33-36.
58. Diat, O.; Gebel, G.; Nature Materials **2008**, 7, 13–14.
59. Morris, D. R.; Sun, X. Journal of Applied Polymer Science **1993**, 50(8), 1445-1452.
60. Hinatsu, J.T.; Mizuhata, M.; Takenaka, H; Journal of Electrochemical Society **1994**, 141(6), 1493-1498.
61. Krtíl, P.; Trojanek, A.; Samec, Z.; Heyrovsky, J.; Journal of Physical Chemistry B **2001**, 105(33), 7979-7983.
62. Ananataraman, A.V.; Gardner, C.L.; Journal of Electroanalytical Chemistry **1996**, 414, 115-120.

63. Casciola, M.; Alberti, G.; Sganappa, M.; Narducci, R.; Journal of Power Sources **2006**, 162 141-145.
64. Eisenberg, A.; Hodge, I.M.; Macromolecules **1978**, 11( 2), 289-293.
65. Kyu, T.; Hashiyama, M; Eisenberg, A.; Canadian Journal of Chemistry. 1983, 61, 680-687.
66. Di Noto, V.; Negro, E.; Sanchez, J-Y; Iojoiu, C.; Journal of American Chemical Society **2010**, 132, , 2183-2193.
67. Bauer, F.; Denneler, S.; Willert-Porada, M.; Journal of Polymer Science: Part B: Polymer Physics **2005**, 43(7), 786–795.
68. Page, K. A. ; Kevin, M. C.; Moore R. B. Macromolecules **2005**, 38, 6472-6484.
69. Uan-Zo-Li, J. T.; Master Thesis, Virginia Polytechnic Institute and State University, Blacksburg, VA, **2001**, page 130.
70. Broka, K.; Ekdunge, P.; Journal of Applied Electrochemistry **1992**, 27(2), 117-123.
71. Chiou, J.S; Paul, D.R.; Industrial and Engineering Chemical Research **1988**, 27; 2161-2164.
72. Ogumi, Z.; Kuroe, T.; Takehara, Z.; Journal of Electrochemical Society **1985**, 132, 2601-2605.
73. De Bruijn, F. A.; Dam, V.A.T.; Janssen; G. J. M.; Fuel Cells From Fundamentals to Systems **2008**, 8(1), 3-22.
74. Mathias, M.F.; Makharia, R.; Gasteiger, H.A.; Conley, J.J.; Fuller, T.J.; Gittleman, C.J.; Kocha, S.S.; Miller, D.P.; Mittelsteadt, C.K.; Xie, T.; Yan, S.G.; Yu, P.T.; The Electrochemical Society-Interface **2005**, 14, 24-35.
75. Hickner, M.A.; Ghassemi, H.; Kim, Y.S.; Einsla, B.R.; McGrath, J.E.; Chemical Reviews **2004**, 104, 4587-4612.
76. Rouilly, M.V.; Kotz, E.R.; Haas, O.; Scherer, G.G.; Chapiro, A.; Journal of Membrane Science **1993**, 81(1-2), 89-95.
77. Tsang, E.M.W.; Zhang, Z.; Shi, Z.; Soboleva, T.; Holdcroft, S.; Journal of American Chemical Society **2007**, 129(49), 15106-15107.
78. Gupta, B.; Buchi, F.N.; Scherer, G.G.; Chapiro, A.; Journal of Membrane Science **1996**, 118(2), 231-238.
79. Nasef, M.M.; Saidi, H.; Nor, H.M.; Foo, O.M.; Journal of Applied Polymer Science **2000**, 78, 2443-2453.
80. Hietala, S.; Koel, M.; Skou, E.; Elomaa, M.; Sundholm, F.; Journal of Material Chemistry **1998**, 8(5), 1127-1132.
81. Hietala, S.; Holmberg, S.; Karjalainen, M.; Näsman, J.; Paronen, M.; Serimaa, R.; Sundholm, F.; Vahvaselkä, S.; Journal of Material Chemistry **1997**, 7(5), 721-726.

82. Homberg, S.; Nasman, J.H.; Sundholm, F.; *Polymers for Advanced Technologies* **1998**, 9, 121-127.
83. Ostrovskii, D.I.; Torell, L.M.; Paronen, M.; Hietala, S.; Sundholm, F.; *Solid State Ionics* **1997**, 97, 315 -321.
84. Flint, S.D.; Slade, R.C.T.; *Solid State Ionics* **1997**, 97(1-4), 299-307.
85. Niepceron, F.; Lafitte, B.; Galiano, H.; Bigarre, J.; Nicol, E.; Tassin, J.F.; *Journal of Membrane Science* **2009**, 338, 100–110.
86. Zhou, B.; Pu, H.; Pan, H.; Wan, D.; *International journal of hydrogen energy* **2011**, 36, 6809-6816.
87. Depre, L.; Kappel, J.; Popall, M.; *Electrochimica Acta* **1998**, 43, 1301-1306.
88. Chen, W.F.; Kuo, P.L.; *Macromolecules* **2007**, 40, 1987-1994.
89. Kalaw, G.J.D.; Yang, Z.; Musselman, I.H.; Yang, D.J.; Balkus, K.J.; Ferraris, J.P.; *Separation Science and Technology* **2008**, 43(16), 3981-4008.
90. Monroy-Barreto, M.; Acosta, J.L.; del Rio, C.; Ojeda, M.C.; Munoz, M.; Aguilar, J.C.; Rodriguez de San Miguel, E.; de Gyves, J; *Journal of Power Sources* **2010**, 195, 8052-8060.
91. Roziere, J.; Jones, D.J.; *Annual Review of Material Research* **2003**, 33, 503-55.
92. Jannasch, P.; *Current Opinion in Colloid and Interface Science* **2003**, 8, 96-102.
93. Iojoiu, C.; Sood, R.; *Polysulfone-based ionomers, High Performance Polymers and Engineering Plastics* (ed. Mittal, V.) **2011**, John Wiley & Sons, Inc., Hoboken, NJ, USA.
94. Wang, F.; Hickner, M.; Kim, Y. S.; Zawodzinski, T. A.; McGrath, J. E.; *Journal of Membrane Science* **2002**, 197, 231–242.
95. Chikashige, Y.; Chikyu, Y.; Miyatake, K.; Watanabe, M.; *Macromolecules* **2005**, 38, 7121–7126.
96. Xing, P.; Robertson, G. P.; Guiver, M. D.; Mikhailenko, S. D.; Wang, K.; Kaliaguine, S.; *Journal of Membrane Science* **2004**, 229, 95-106.
97. Gil, M.; Ji, X.; Li, X.; Na, H.; Hampsey, J. E.; Lu, Y.; *Journal of Membrane Science* **2004**, 234, 75-81.
98. Shang, X.; Tian, S.; Kong, L.; Meng, Y.; *Journal of Membrane Science* **2005**, 266, 94-101.
99. Schuster, M.; Kreuer, K.-D.; Andersen, H. T.; Maier, J.; *Macromolecules* **2007**, 40, 598-607.
100. Bai, Z.; Dang, T. D.; *Macromolecules Rapid Communications* **2006**, 27, 1271–1277.
101. Genies, C.; Mercier, R.; Sillion, B.; Cornet, N.; Gebel, G.; Pineri, M.; *Polymer* **2001**, 42, 359-373.



102. Miyatake, K.; Zhou, H.; Matsuo, T.; Uchida, H.; Watanabe, M.; *Macromolecules* **2004**, 37, 4961-4966.
103. Kobayashi, T.; Rikukawa, M.; Sanui, K.; Ogata, N.; *Solid State Ionics* **1998**, 106, 219-225.
104. Fujimoto, C. H.; Hickner, M. A.; Cornelius, C. J.; Loy, D. A.; *Macromolecules* **2005**, 38, 5010-5016.
105. Iojoiu, C.; Marechal, M.; Chabert, F.; Sanchez, J.Y. *Fuel Cells (Weinheim, Germany)*, **2005**, 5, 344-354.
106. Iojoiu, C.; Genova-Dimitrova, P.; Marechal, M.; Sanchez, J.Y.; *Electrochimica Acta* **2006**, 51, 4789-4801.
107. Kerres, J.A.; Cui, W.; Reichle, S. J.; *Polymer Science Part A: Polymer Chemistry* **1996**, 34, 2421-2438.
108. Harrison, W.L.; Hickner, M.A.; Kim, Y.S.; Mc Grath, J.E.; *Fuel Cells* **2005**, 2, 201-212.
109. Rikukawa, M.; Sanui, K.; *Progress in Polymer Science* **2000**, 25, 1463-1502.
110. Kerres, J.; Zhang, W.; Cui, W.; *Journal of Polymer Science* **1998**, 36, 1441-1448.
111. Kerres, J.; Cui, W.; Junginger, M.; *Journal of Membrane Science* **1998**, 139, 227-241.
112. Kerres, J.; Ullrich, A.; Meier, F.; Häring, T.; *Solid State Ion* **1999**, 125, 243-249.
113. Soczka-Guth, T.; Baurmeister, J.; Frank, G; Knauf, R.; **1999**, International Patent No. 99/2976.
114. Glipa, X.; Haddad, M.E.; Jones, D.J.; Roziere, J.; *Solid State Ionics* 1997, 97, 323-331.
115. Jutemar, E.P.; Jannasch, P.; *Journal of Membrane Science* **2010**, 351, 87-95.
116. Karlsson, L.E.; Jannasch, P.; *Journal of Membrane Science* **2004**, 230, 61-70.
117. Yoshimura, K.; Iwasaki, K.; *Macromolecules* **2009**, 42, 9302-9306.
118. Ogata, N.; Rikukawa, M.; **1995**, US Patent No. 5403675.
119. Liang, C., Maruyama, T.; Ohmukai, Y.; Sotani, T.; Matsuyama, H.; *Journal of Applied Polymer Science* **2009**, 114, 1793-1802.
120. Asano, N.; Aoki, M.; Suzuki, S.; Miyatake, K.; Uchida, H.; Watanabe, M.; *Journal of American Chemical Society* **2006**, 128, 1762-1769.
121. Norsten, T.B.; Guiver, M.D.; Murphy, J.; Astill, T.; Navessin, T.; Holdcroft, S.; Frankamp, B.L.; Rotello, V.M.; Ding, J.; *Advanced Functional Materials* **2006**, 16, 1814-1822.
122. Watanabe, M.; Uchida, H.; Seki, Y.; Emori, M.; Stonehart, P.; *Journal of Electrochemical Society* **1996**, 143(12), 3847-3852.
123. Hagihara, H.; Uchida, H.; Watanabe, M.; *Electrochimica Acta* **2006**, 51, 3979-3985.

124. Mauritz, K.A.; Materials Science and Engineering **1998**, 6(2-3), 121-133.
125. Park, K.T.; Jung, U.H.; Choi, D.W.; Chun, k.; Lee, H.M.; Kim, S.H.; Journal of Power Sources **2008**, 177, 247-253.
126. Tricoli, V.; Nannetti, F.; Electrochimica Acta **2003**, 48, 2625-2633.
127. Kwak, S.H.; Yang, T.H.; Kim, C.S.; Yoon, K.H.; Electrochimica Acta **2004**, 50, 653-657.
128. Wang, H.; Holmberg, B.A.; Huang, L.; Wang, Z.; Mitra, A.; Norbeck, J.M.; Yan, Y.; Journal of Material Chemistry **2002**, 12, 834-837.
129. Tazi, B.; Savadogo, O.; Electrochimica Acta **2000**, 45, 4329-4339.
130. Dimitrova, P.; Friedrich, K.A.; Stimming, U.; Vogt, B.; Solid State Ionics **2002**, 150, 115-122.
131. Staiti, P.; Arico, A.S.; Baglio, V.; Lufrano, F.; Passalacqua, E.; Antonucci, V.; Solid State Ionics **2001**, 145, 101-107.
132. Herring, A.M.; Journal of Macromolecular Science Part C: Polymer Reviews **2006**, 46, 245-296.
133. Schuster, M.; Rager, T.; Noda, A.; Kreuer, K.D.; Maier, J.; Fuel Cells **2005**, 5, 355-365.
134. Paddison, S.J.; Kreuer K.D.; Maier, J.; Physical Chemistry Chemical Phys **2006**, 8, 4530-4542.
135. Steininger, H.; Schuster, M.; Kreuer, K.D.; Kaltbeitzel, A.; Bingol, B.; Meyer, W.H.; Schauff, S.; Brunklaus, G.; Maier, J.; Spiess, H.W.; Physical Chemistry Chemical Physics **2007**, 9, 1764-1773.
136. Schechter, A.; Savinell, R. F.; Solid State Ionics **2002**, 147(1-2), 181-187.
137. Asensio, J.A.; Sanchez, E.M.; Gomez-Romero, P.; Chemical Society Reviews **2010**, 39, 3210-3239.
138. Wainright, J.S.; Wang, J.T.; Weng, D.; Savinell, R.F.; Litt, M.; Journal of Electrochemical Society **1995**, 142(7),121-123.
139. Qingfeng, Li; Hjuler, H.A.; Bjerrum, N.J.; Journal of Applied electrochemistry **2001**, 31(7), 773-779.
140. Samms, S.R.; Wasmus, S.; Savinell, R.F.; Journal of Electrochemical Society **1996**, 143(4), 1225-1232.
141. Mamlouk, M.; Scott, K.; International Journal of Hydrogen Energy **2010**, 35(2), 784-793.
142. Oono, Y.; Sounai, A.; Hori, M.; Journal of Power Sources **2009**, 189(2), 943-949.
143. Ma, Y.L.; Wainright, J.S.; Litt, M.H.; Savinell, R.F.; Journal of the Electrochemical Society **2004**, 151(1), 8-16.

144. Kreuer, K.D. ; Fuchs, A. ; Ise, M. ; Spaeth, M.; Maier, J.; *Electrochimica Acta* **1998**, 43(10-11), 1281-1288.
145. Deng, W.Q.; Molinero, V.; Goddard, W.A.; *Journal of American Chemical Society* **2004**, 126, 15644-15645.
146. Schuster, M.; Meyer, W.H.; Wegner, G.; Herz, H.G.; Ise, M.; Schuster, M.; Kreuer, K.D.; Maier, J.; *Solid State Ionics* **2001**, 145, 85-92.
147. Schuster, M.F.H.; Meyer, W.H.; *Annual Reviews of Material Research* **2003**, 33, 233-261.
148. Belieres, J.P.; Angell, C.J.; *Journal of Physical Chemistry B* **2007**, 111, 4926-4937.
149. Greaves, T.L.; Drummond, C.J.; *Chemical Reviews* **2008**, 108, 206-237.
150. Kennedy, D.F.; Drummond, C.J.; *The Journal of Physical Chemistry B Letters* **2009**, 113, 5690-5693.
151. Greaves, T.L.; Drummond, C.J.; *Chemical Society Reviews* **2008**, 37, 1709-1726.
152. Susan, M.A.B.H.; Noda, A.; Mitsushima, S.; Watanabe, M.; *Chemical Communications* **2003**, 938-939.
153. Nakamoto, H.; Watanabe, M.; *Chemical Communications* **2007**, 2539-2541.
154. Iojoiu, C.; Judeinstein, P.; Sanchez, J.Y.; *Electrochimica Acta* **2007**, 53, .1395–1403.
155. Fuller, J.; Breda, A. C.; Carlin, R.T.; *Journal of the Electrochemical Society* **1997**, 144, 67-70.
156. Doyle, M.; Choi, S.K.; Proulx, G.; *Journal of The Electrochemical Society* **2000**, 147 (1), 34-37.
157. Neves, L.A.; Benavente, J.; Coelho, I.M.; Crespo, J.G.; *Journal of Membrane Science* **2010**, 347, 42-52.
158. Yang, J.; Che, Q.; Zhou, L.; He, R.; Savinell, R.F.; *Electrochimica Acta* **2011**, 56, 5940-5946.
159. Bennett, M.D.; Leo, D.J.; Wilkes, G.L.; Beyer, F.L.; Pechar, T.W.; *Polymer* **2006**, 47, 6782-6796.
160. Cho, E.K.; Park, J.S.; Sekhon, S. S.; Park, G.G.; Yang, T.H.; Lee, W.Y.; Kim, C.S.; Park, S.B.; *Journal of The Electrochemical Society* **2009**, 156(2), 197-202.
161. Schmidt, C.; Gluck, T.; Schmidt-Nake, G.; *Chemical Engineering and Technology* **2008**, 31(1), 13-22.
162. Subianto, S.; Mistry, M.K.; Choudhury, N.R.; Dutta, N.K.; Knott, R.; *Applied Materials and Interfaces* **2009**, 1(6), 1173-1182.
163. Iojoiu, C.; Hana, M.; Molmeret, Y.; Martinez, M.; Cointeaux, L.; Kissi, N.E.; Teles, J.; Lepretre, J.C.; Judeinstein, P.; Sanchez, J. Y.; *Fuel Cells* **2010**, 10(5), 778–789.

164. Iojoiu, C.; Martinez, M.; Hanna, M.; Molmeret, Y.; Cointeaux, L.; Lepretre, J.C.; Kissi, N.E.; Guindet, J. ; Judeinstein, P.; Sanchez, J. Y.; *Polymer for Advanced Technologies* **2008**, 19, 1406–1414.
165. Di Noto, V.; Negro, E.; Sanchez, J-Y; Iojoiu, C. *J. Am. Chem. Soc.*, **2010**, 132, , 2183-2193.
166. Di Noto, V.; Piga, M.; Giffin, G. A.; Lavina, S.; Smotkin, E. S.; Sanchez, J-Y.; Iojoiu, C. *J. Phys. Chem. C* **2012**, 116(1), 1370-1379.
167. Lee, S.Y.; Ogawa, A.; Kanno, M.; Nakamoto, H.; Yasuda, T.; Watanabe, M.; *Journal of American Chemical Society* **2010**, 132, 9764-9773.
168. Hoarfrost, M.L.; Segalman, R.A.; *Macromolecules* **2011**, 44, 5281–5288.

## 2. Triethylammonium Triflate (TFTEA) doped Nafion<sup>®</sup> membranes based on the swelling method

Nano-structuration of a polymer electrolyte is the key to its optimum performance in the working conditions of fuel cells. Hence, considering the system of Ionomer-Proton Conducting Ionic Liquid, it is very important to underline the effect of addition of Proton Conducting Ionic Liquid (PCIL) on the nano-structuration of the ionomer and consequent functional properties. A good understanding of:

- effect of type/concentration of the PCIL on the nano-structuration of the polymer electrolyte
- co-relation between different properties such as electro-chemical, thermo-mechanical and transport properties with evolving nano-structuration of the membrane

can greatly help in fine-tuning the properties of the doped membrane for its application at high temperature.

Hence, this chapter is focused on the characterization of doped membranes based on neutralized Nafion<sup>®</sup>117 containing different concentrations of a highly conducting PCIL, Triethylammonium Triflate (TFTEA) elaborated by *swelling method*. The chemical structures of Nafion<sup>®</sup>117 (neutralized form) and TFTEA are shown in figure 1.

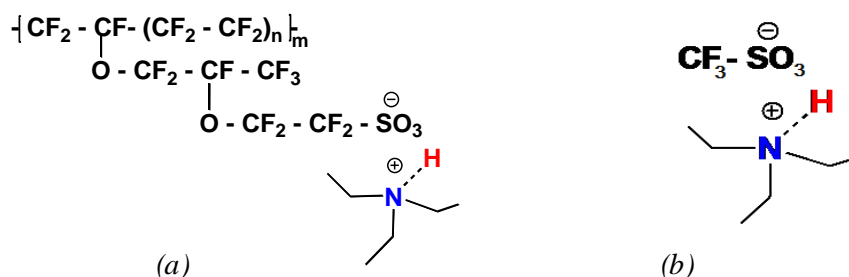


Figure 1: Chemical structures of: a). Nafion-TEA; b). TFTEA

These were chosen as the components of this study since:

- ❖ Nafion<sup>®</sup> is well known for its nano-structured morphology and performance as well as stability. It has been utilized in neutralized form (neutralized with the same amine utilized for the PCIL

preparation) to facilitate the compatibility with the PCIL, avoid cation-exchange with the PCIL and improve the thermal stability of doped membranes<sup>(1,2)</sup>.

- ❖ PCILs based on alkyl ammonium seem to be more adapted due to higher proton activities and lesser absorption on the electrode's surface in comparison to PCILs based on imidazolium<sup>(3)</sup>. Moreover, Triflate and bis(trifluoromethane)sulfonimide (TFSI) based PCILs show similar conductivities at above their melting temperatures though TFSI is more expensive than triflic acid<sup>(4)</sup>. Keeping these points in mind, TFTEA was considered to be appropriate for this study. The important characteristics of TFTEA are shown in table 1.

<i>Important characteristics of TFTEA</i>	
<i><math>\sigma \times 10^2</math> (S/cm) at 110°C</i>	1.89
<i><math>T_m(^{\circ}\text{C})</math></i>	34
<i><math>T_d(^{\circ}\text{C})</math></i>	376

*Table 1: Various characteristics of TFTEA*

Though some results on the thermal, thermo-mechanical, electro-chemical and dielectric properties have already been published on TFTEA doped neutralized Nafion membranes<sup>{1,2,5-7}</sup>, impact of the concentration of TFTEA on the properties of the system has never been thoroughly discussed. Additionally, the study of the morphology, gas permeability, water sorption and influence of presence of water on the properties of this system will be discussed profoundly for the first time in this chapter.

*A part of these results have been published in the Journal of Physical Chemistry C (J. Phys. Chem. C 2012, 116, 24413-24423).*

The aim of this chapter is to demonstrate the impact of TFTEA concentration on the morphology of neutralized Nafion<sup>®</sup> and implicitly on its intrinsic properties (such as conductivity, thermo-mechanical properties, gas-permeability and water sorption properties). As the goal is to evaluate/pinpoint the influence of TFTEA, all the membranes characterized were in anhydrous state. Moreover, since the presence of water is practically inevitable in working conditions of a PEMFC, the water sorption behavior of TFTEA doped Nafion<sup>®</sup> based membranes has been analyzed. Since an evolution of water sorption with TFTEA concentration in the doped Nafion-TEA membrane was observed, the influence of presence of water on their morphology and conductivity has been investigated afterwards.

This chapter has been divided into three parts such as:

- ❖ In the first part of this chapter, neutralized Nafion<sup>®</sup> (referred as *Nafion-TEA*) has been characterized and compared with Nafion<sup>®</sup>117 in acidic form (denoted as Nafion-H<sup>+</sup>) since Nafion-TEA serves as the reference membrane of the TFTEA doped membranes.
- ❖ In the second part, the effect of TFTEA addition/concentration on morphology and functional properties of Nafion-TEA will be discussed in detail.
- ❖ The third part of this chapter concentrates on the evolution of morphology and conductivity of the TFTEA doped Nafion-TEA membranes under relatively humid conditions at different temperatures.

### ***2.1: Polymer matrix: effect of neutralization***

The neutralization process involved three steps:

1. ***Reactivation of the ionic functions of Nafion<sup>®</sup>117 membrane*** by treating the membranes in refluxing 2M nitric acid aqueous solution (to reactivate all the ionic sites) followed by washing with deionized water up to neutral pH. This membrane is denoted as *Nafion-H<sup>+</sup>*.
2. ***Neutralization of sulfonic acid groups of Nafion-H<sup>+</sup> by mildly stirring the membrane in 1M triethylamine (TEA) in water/ethanol solution (50:50 v/v) under mild stirring at room temperature overnight followed by washing the membrane to neutral pH. The neutralized Nafion<sup>®</sup> membrane is referred as Nafion-TEA.***
3. ***Drying of Nafion-TEA*** at 80°C under vacuum for 48 hours. The dried membrane is stored in glove box under argon atmosphere.

The impact of neutralization process on the following characteristics of Nafion<sup>®</sup> will be presented in this section:

- a. *Morphology*
- b. *Thermo-mechanical properties*
- c. *Conductivity*
- d. *Gas-permeability*
- e. *Water sorption properties*

### *a. Morphology*

It is well known that the nano-structured morphology of Nafion<sup>®</sup> is responsible for its high performance in PEMFCs<sup>[8]</sup>. In the case of Nafion-TEA, the small sized and hydrophilic proton is replaced by a comparatively more bulky and hydrophobic ammonium. Thus, we studied firstly the *influence of this bulky cation on the nano-structuration of Nafion<sup>®</sup>* in the length scale of 20-500 Å. In this study, *Small Angle Neutron Scattering (SANS)* was performed on dried Nafion-TEA and compared with dried Nafion<sup>®</sup> membrane (Nafion-H<sup>+</sup>-dry) as well as low water content Nafion<sup>®</sup> membrane (Nafion-H<sup>+</sup>-4H<sub>2</sub>O). Both the membranes i.e. Nafion-H<sup>+</sup>-dry and Nafion-TEA were dried at 80°C under vacuum for 48 hours while Nafion-H<sup>+</sup>-4H<sub>2</sub>O was obtained by equilibrating the membrane several days under a relative humidity of 22% (adjusted by a saturated salt solution of CH<sub>3</sub>COO<sup>-</sup> K<sup>+</sup>) in a specially designed neutron cell prior to scattering measurements. The corresponding membrane hydration was quantified by the  $\lambda$  parameter which is the number of water molecules per ionic group<sup>[9]</sup>. At 22% RH,  $\lambda$  is equal to 4 at equilibrium

The SANS spectrum of Nafion<sup>®</sup> generally exhibits the following peaks:

1. A correlation peak called *ionomer peak* is observed in the  $q$  range of 0.1-0.2 Å<sup>-1</sup>. This peak is usually considered as a fingerprint of the nano-structure of the ionomer membrane<sup>[10]</sup>. It arises from the hydrophobic-hydrophilic phase separation at nano-metric scale. Its position  $q^*$  is related to a characteristic distance  $d=2\pi/q^*$  which has been frequently interpreted as the mean separation distance between inter-connected ionic domains.
2. A second scattering maximum, often referred to as “*matrix knee*” in the literature<sup>[10]</sup>, appears in the  $q$  range of 0.01-0.1 Å<sup>-1</sup>. This rather large bump is attributed to correlations between crystalline domains on typical scales of a tenth of nanometres.

The SANS spectra of all the samples described before did not present any significant differences concerning “matrix knee”. Hence, the discussion will be focussed only on the ionomer peak in this section. The SANS spectra of Nafion-TEA in comparison to the well-known SANS spectra obtained for dry and low water content-acidic Nafion<sup>®</sup> 117 are presented in figure 2 focussing on ionomer peak.



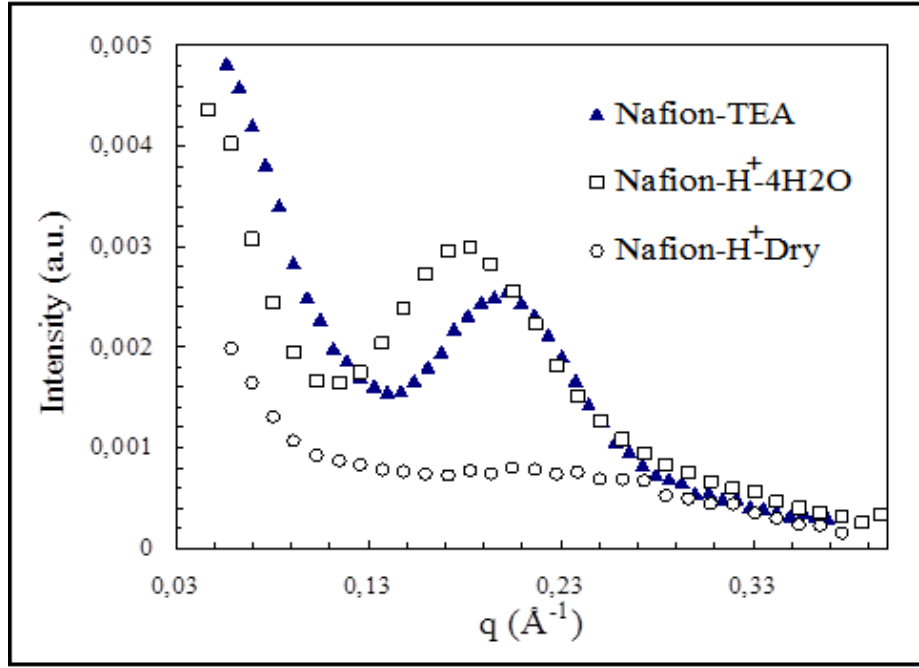


Figure 2: SANS spectra of neutralized Nafion-TEA membrane (▲), compared to acidic Nafion® in dry state (○) and at low water content ( $[H_2O]/[SO_3^-] = 4$ , □), extracted from Ref [31].

As seen from Figure 2, a broad ionomer peak is measured in the hydrated acidic Nafion® at position  $q^* = 0.183 \text{ \AA}^{-1}$  ( $d = 34.3 \text{ \AA}$ ) while it is hardly distinguishable in the dried sample (position around  $0.23 \text{ \AA}^{-1}$ ,  $d \sim 27.3 \text{ \AA}$ ). Under the presented drying conditions, “dry” Nafion® can be considered to contain around one water molecule per ionic site ( $\lambda=1$ ), which is not sufficient to produce a significant contrast to generate a well-marked peak. It is thus not possible to experimentally determine the value of  $d$  in a completely anhydrous acidic Nafion®. However, a **limit value of  $d$  at zero  $\lambda$ , called  $d_0$** , can be extrapolated from the dilution law, *i.e.* the peak position variation plotted as a function of water content.  $d_0$  is the mean correlation distance in the absence of water, and is thus directly related to the mean width of hydrophobic aggregates. A value of  $d_0=27 \text{ \AA}$  has been found in **acidic Nafion®117**. A schematic representation of the local polymer organization is given in Figure 3 (a)-(b) for ideally dry and low water content Nafion® membranes. Sulfonic acid head groups are located at the hydrophobic/hydrophilic interface, protons and water molecules in the ionic phase. A lamellar local geometry has been chosen for the purpose of representing  $d$  and  $d_0$ .

Now comparing the SANS spectra of acidic Nafion® membranes under different hydration states with that of Nafion-TEA, following observations can be made:

1. The SANS spectrum of **dry Nafion-TEA** is similar to the one obtained with the acidic Nafion®117 at low hydration indicating that the highly protonated counter-ion behaves as water

molecules from the scattering point of view. A *well-defined and pretty intense scattering peak* is thus measured as a consequence of a *high contrast between the hydrophobic phase and TEA ions*.

2. The ionomer peak position ( $q^* = 0.202 \text{ \AA}^{-1}$ ) for Nafion-TEA is in between the values obtained for the dry and  $\lambda=4$  acidic Nafion<sup>®</sup> membranes. The associated *separation distance  $d_{\text{TEA}}$  has been found equal to  $31 \text{ \AA}$* .
3. The sharpness of the peak in the case of Nafion-TEA with respect to the acidic Nafion indicates *a better ordering at the nanometric scale*. Interestingly, the difference between  $d_0$  and  $d_{\text{TEA}}$  is  $4 \text{ \AA}$  which corresponds to the size of one TEA cation<sup>(11)</sup>, suggesting a *string-like organisation of TEA ions at the hydrophobic/hydrophilic interface*.

Figure 3 (c) shows a schematic picture of this optimized packing and organisation resulting from this single-layer structure. As a TEA ion contains 16 protons, the corresponding  $\lambda$  of anhydrous Nafion-TEA should be  $\sim 8$ . However, the volume of a bulky triethyl ammonium cation is rather comparable to an aqueous cluster of 3-4 water molecules. This is consistent with the observed SANS spectra where the ionomer peak of Nafion-TEA is observed at slightly higher  $q$  values than that of a  $\lambda=4$  acidic Nafion<sup>®</sup> one.

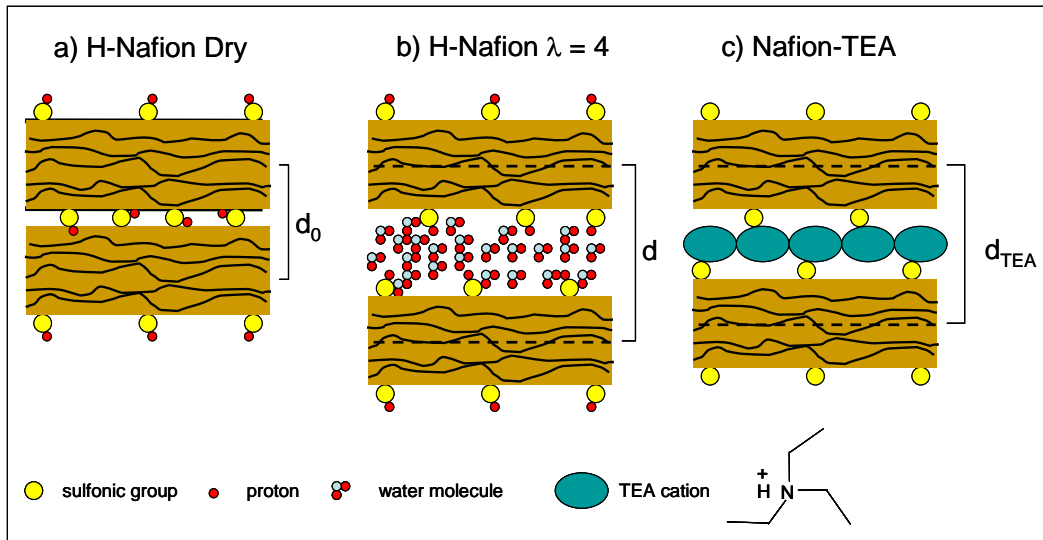


Figure 3: Schematic representation of the hydrophobic/hydrophilic interface in acidic Nafion<sup>®</sup> and Nafion-TEA.

Assuming a lamellar structure with an average thickness of 27 Å for the acidic form, the average distance between two sulfonic groups can be easily calculated. Taking into account the equivalent weight of Nafion<sup>®</sup> 117 (EW=1100 g/eq) and the matrix polymer density ( $d=2.1 \text{ g/cm}^3$ ), the average fluorinated volume per sulfonic group is  $V_s = 913.7 \text{ Å}^3$ . The average surface of interface per sulfonic group in lamellar geometry can thus be deduced. Considering that the 27 Å thick polymer membrane has a sulfonic group on each side, we found an area of  $67.6 \text{ Å}^2$  per sulfonic group and consequently an average distance between two sulfonate groups at the polymer interface of 8.2 Å. Therefore, it is necessary to *pack two TEA counter ions with a 4 Å diameter to fill the ionic interface*. It follows that the *TEA cations have the exact size to produce the structure depicted on Figure 3 (c)*. We can predict that increasing the size of the ammonium counter ion, the  $d_{\text{counterion}}$  spacing will increase and the width of the ionomer peak will be affected because of a less favourable counter-ion packing, except when doubling the ammonium size.

From these experimental observations, following *conclusions* can be drawn:

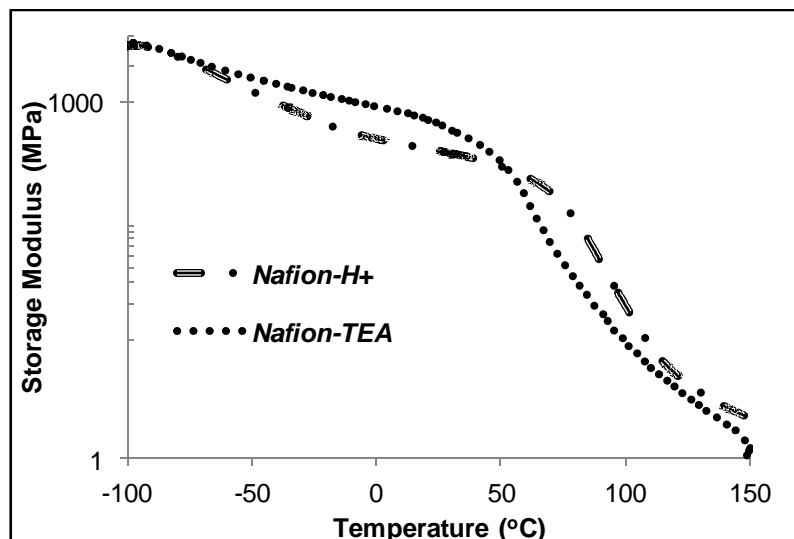
- Neutralization of acidic sites with triethylamine in Nafion<sup>®</sup> membranes does not significantly affect its nano-structuration and in fact seems to improve ordering at nanometric scale.
- It is proposed from these results that Nafion-TEA exhibits a string-like organisation of TEA ions at the hydrophobic/hydrophilic interface with mean nano-phase separation of 31 Å.

#### **b. Thermo-mechanical properties**

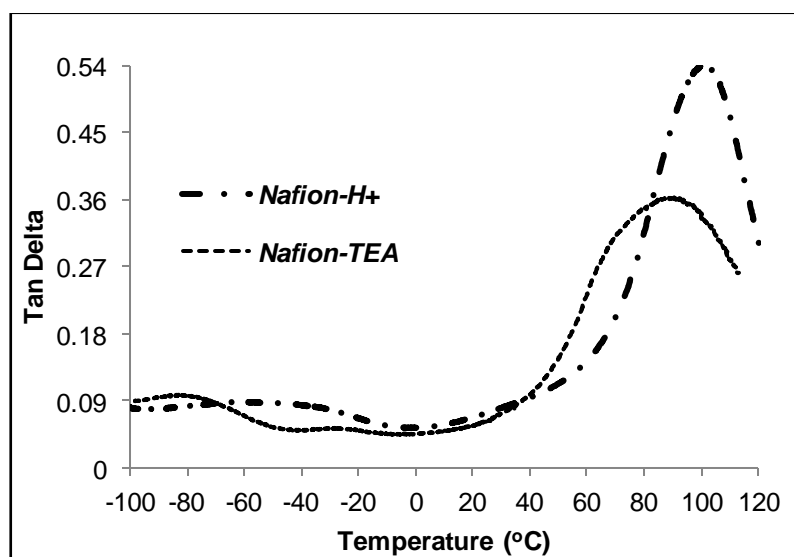
The impact of neutralization process on thermo-mechanical behavior of Nafion<sup>®</sup> 117 has been investigated by DMA. The measurements were carried out on Nafion-TEA in comparison to the data obtained with Nafion-H<sup>+</sup> in terms of storage modulus and  $\tan\delta$  in function of temperature (figure 4 (a) and (b) respectively).

#### **Storage Modulus versus Temperature**

The storage modulus versus temperature profiles of Nafion-TEA and Nafion-H<sup>+</sup> (Figure 4 (a)) show *similar response*. However, Nafion-TEA indicate a slight enhancement of  $E'$  between -100°C and 50°C in comparison to Nafion-H<sup>+</sup> that can be ascribed to the strong steric hindrance between neutralized side-groups of Nafion-TEA.



(a)



(b)

Figure 4: DMA of Nafion- $H^+$  and Nafion-TEA; a) storage modulus vs temperature;  
b)  $\tan \delta$  vs temperature

### Tan $\delta$ versus Temperature

The dynamic mechanical relaxations of the Nafion<sup>®</sup> strongly depend on the strengths of interactions between the terminal side chains. It is well-known that Nafion<sup>®</sup> in acidic form exhibits three kinds of relaxation<sup>[2,7,12,13]</sup>. However, the attribution of the origin of these relaxations is a matter of debate. These relaxations are:

1.  **$\gamma$ -relaxation** ( $\sim 100^\circ\text{C}$ ) attributed to vibrational and rotational movements of  $\text{CF}_2$  groups located at short distance from the ionic function
2.  **$\beta$ -relaxation** ( $-20^\circ\text{C}$ ) corresponding to the movement of the hydrophobic PTFE main-chain and the fluorinated ether side-chain
3.  **$\alpha$ -relaxation** ( $100^\circ\text{C}$ ) related to the physical crosslinks associated with the ionic groups

Now considering *tan $\delta$  profiles of Nafion-TEA in comparison to Nafion- $\text{H}^+$* , following differences can be observed (Figure 4 (b)):

1. It is difficult to interpret the appearance of  $\gamma$ -relaxation since the temperature window for DMA measurements was in the range of  $-100$  to  $150^\circ\text{C}$  for Nafion- $\text{H}^+$ . But, it seems that it appears at lower temperature for Nafion- $\text{H}^+$  in comparison to Nafion-TEA (for Nafion-TEA, it appears around  $-80^\circ\text{C}$ ).
2. Concerning  $\beta$ -relaxation, the  $T_\beta$  relaxation is slightly higher and the relaxation peak is less pronounced for Nafion-TEA. The higher  $T_\beta$  can be explained through the specific morphology acquired by particular organisation of TEA cations at the hydrophobic/hydrophilic interface as suggested from the SANS results (Figure 3). This organisation along with ***bulky cation (TEA) should restrict the local mobility of chains***. Thus, it results in higher temperature at which PTFE side chains and fluorinated side-chains become mobile. Moreover, it yields a relatively lower population that are capable of activated motions at low temperatures ( $\sim T_\alpha$ ).
3. The  $\alpha$ -relaxation is much broader and the value of  $T_\alpha$  is slightly lower in Nafion-TEA than in Nafion- $\text{H}^+$ . The lower value of  $T_\alpha$  can be explained by the ***replacement of hydrogen bonding networks formed by the strong dipole-dipole interactions of Nafion- $\text{H}^+$  with weak van der Waals interactions between triethylammonium end-group of side chains*** along with more hindered steric interferences.

Finally, the thermo-mechanical properties of Nafion-TEA, in agreement with the previously published results<sup>[2,7]</sup>, are very different from those of Nafion neutralized with tetraethyl ammonium<sup>[14]</sup> where much higher  $T_\alpha$  and  $T_\beta$  were obtained probably due to the cation dissymmetry enhancement, electrostatic interactions and specific organization.

From these experimental observations on temperature dependent storage modulus and  $\tan\delta$  profiles of Nafion-TEA membrane, following **conclusions** can be drawn:

- Neutralization of acidic sites of Nafion<sup>®</sup> with TEA does not profoundly change its storage modulus.
- Neutralization with TEA results in slightly lower  $T_\alpha$  but slightly higher  $T_\beta$  in Nafion<sup>®</sup> membrane.

### c. Conductivity

Since, the doped membranes have to be characterized in anhydrous state and Nafion-TEA serves as the reference membrane, it is important to measure the proton conductivity of Nafion-TEA too in anhydrous state. Therefore, Nafion-TEA was dried at 80°C under vacuum and in order to compare the effect of neutralization of acidic sites on the conductivity, Nafion-H<sup>+</sup> was also dried under similar conditions. ***Prior to conductivity measurements, the water content of the dried membranes was evaluated using NMR technique since even a very small amount of water can play an important role in the proton conductivity.*** The water content of the membranes was determined by quantitative measurement of the NMR signal and it was found about 1.5 moles of water /moles of SO<sub>3</sub><sup>-</sup> in the Nafion-H<sup>+</sup> and 0.9 moles of water/ moles of TEA neutralized SO<sub>3</sub><sup>-</sup> in the Nafion-TEA. While the measurement is rather precise in the case of Nafion-H<sup>+</sup> because most of the protons belong to water molecules, the measurement is obviously more difficult and less precise in the case Nafion-TEA.

Afterwards, conductivity measurements were performed in a closed Swagelog cell. The plots of conductivity for Nafion-H<sup>+</sup> and Nafion-TEA are shown in figure 5. The ***higher conductivity of Nafion-H<sup>+</sup>, at temperature lower than 120°C, compared to that of Nafion TEA*** can be explained by proton (cation) conduction mechanism. Thus, we assume in Nafion-H<sup>+</sup> with  $\lambda=1.5$ , jump like motion of the H<sup>+</sup> between neighbouring SO<sub>3</sub><sup>-</sup> groups is possible in percolated ionic domains. While for Nafion-TEA, a reorganisation of triethylammonium is required before a proton (cation) jumps from an anion to another. Moreover, Nafion-H<sup>+</sup> contains higher amount of water in comparison to Nafion-TEA, this could also be one of the reasons for higher conductivity of Nafion- H<sup>+</sup>. However, ***the conductivity of Nafion-TEA becomes comparable to that of Nafion-H<sup>+</sup> at temperatures higher than 100°C.*** This can be attributed to the high chain mobility allowing easier motion and jump of TEA cations leading to an increase in the conductivity in Nafion-TEA while a decrease in the conductivity due to the evaporation of residual water molecules as well as sulfonic anhydride<sup>(15)</sup> formation at high temperatures is observed in Nafion-H<sup>+</sup>.

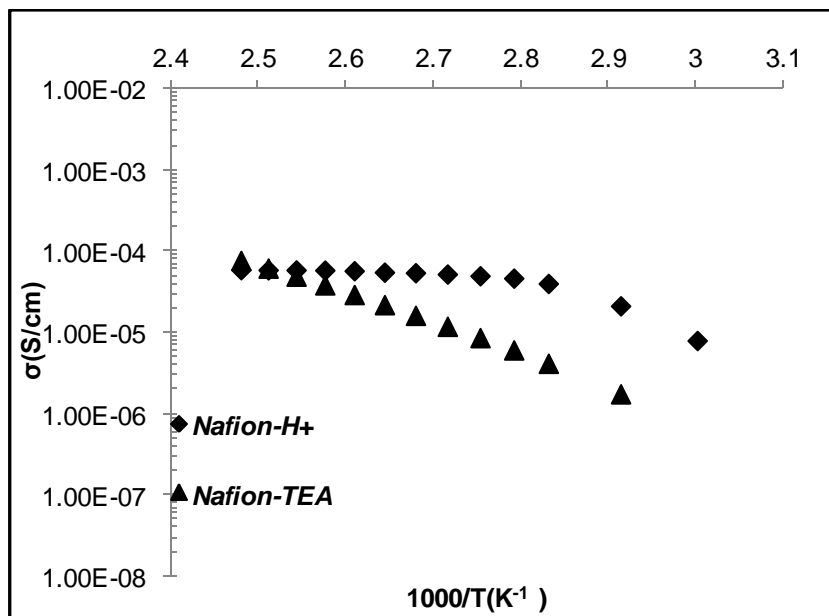


Figure 5: Conductivity vs temperature of Nafion- $H^+$  and Nafion-TEA in anhydrous conditions

#### d. Gas permeability properties

In addition to the ionic conduction and the mechanical properties, the gas permeation is a key property for fuel cell application. The hydrogen and oxygen permeability coefficients measured under anhydrous conditions with Nafion- $H^+$  (5.5 barrer and 0.9 barrer, respectively) are in good agreement with those generally reported in the literature<sup>[16-18]</sup>. The membrane **neutralization by TEA cations induces a significant increase of the membrane permeability** with 10.2 barrer and 2.5 barrer as permeability coefficients for hydrogen and oxygen, respectively. This increase points towards an increase in the contribution by ionic phase towards permeability of gases as neutralization step does not affect the hydrophobic phase (as evidenced by SANS). Hence, this **result could appear as in contradiction with different published works** which suggest that the gas permeation in polymers containing hydrophobic and hydrophilic domains like Nafion® can take place mainly in the hydrophobic phase under anhydrous conditions<sup>[17,19]</sup>. However, the ionic character of ionic clusters in Nafion-TEA is much weaker than ionic clusters of Nafion- $H^+$  and the resulting gas permeation through ionic clusters can then affect the global permeability. Another point has to be taken into account, namely the chain mobility. The effect of membrane neutralization by  $Cs^+$  and  $Pt^{2+}$  has been studied in the previous works and a decrease in the gas permeability coefficients has been observed<sup>[20]</sup>. The decrease in gas permeability has been attributed to an enhancement in chain stiffness due to stronger ionic interactions when  $H^+$  is exchanged by  $Cs^+$  or  $Pt^{2+}$ . The **increase in gas permeability observed on Nafion-TEA can be related to the replacement of the strong ionic interactions by weak dipole-dipole forces between polymer chains** as evidenced from DMA results, in addition to the

*increase in free volume of the percolated ionic domains by the presence of the bulky alkyl moieties of TEA amine.*

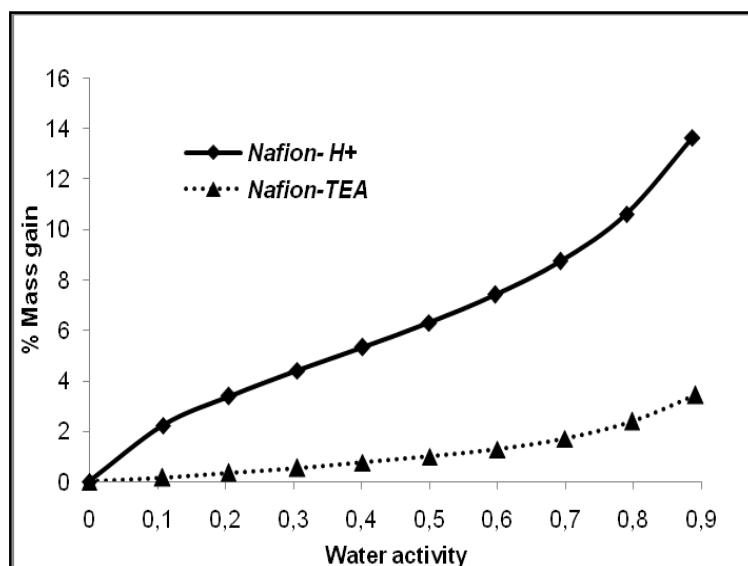
*e. Water Sorption*

Because during the PEMFC operation, water is formed at the cathode, the ability of the membrane to uptake water is an important asset to be discussed. Thus the sorption isotherm and the evolution of the square root of half sorption time as a function of the water activity of Nafion-TEA have been studied at 25°C and compared to the data obtained on Nafion-H<sup>+</sup>. Moreover, number of water molecules gained per ionic site for each water activity was calculated using water sorption isotherms in order to discuss the role of the ionic sites on the water sorption mechanism.

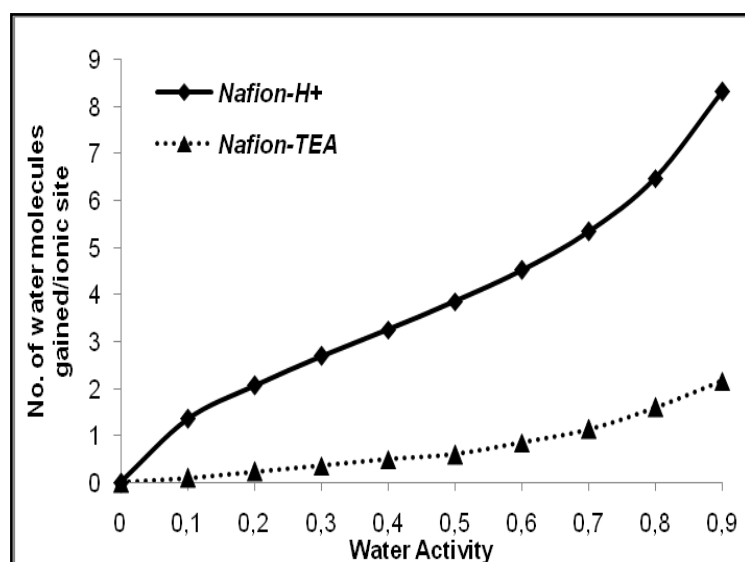
The water sorption isotherm of *Nafion-H<sup>+</sup>* underlines the hydrophilic character of this polymer, with a ***water uptake of about 14 wt% near a water activity of 0.9*** (Figure 6(a)) which corresponds to approximately 8 molecules of water per ionic *site* (Figure 6(b)). The isotherm has a sigmoidal shape corresponding to ***B.E.T. II type*** isotherm in the Brunauer-Emmett-Teller classification. The data are in good agreement with the results generally reported for Nafion<sup>®</sup> in the literature<sup>{15,16,21}</sup>. This type of curve is characteristic of the water sorption mechanisms generally involved in ionomers discussed as follows:

- ❖ ***At low water activity***, the B.E.T. II isotherm presents a concave form, which is usually analyzed as the sorption step corresponding to the formation of the primary hydration sphere of the sulfonic acid groups. Indeed, it is considered that the ionic groups act as Langmuir sites.
- ❖ ***At middle water activity***, the isotherm becomes linear in agreement with a Henry type behaviour
- ❖ ***At high water activity***, the isotherm presents a convex form, which can be explained by the formation of water clusters around the first sorbed water molecules.





(a)



(b)

Figure 6: Water uptake behaviour of Nafion- $H^+$  and Nafion-TEA; a) Water sorption Isotherm vs water activity; b) Number of water molecules present per ionic site vs water activity

The Nafion-TEA represents a significantly *different shape of the sorption isotherm* corresponding to a *B.E.T. III type*. i.e., linear at low activity and increasing slightly at high water activity (Figure 5(a)). The main features include:

- ❖ The linear part at *low activity* is associated to a Henry sorption mode with a uniform distribution of the water molecules.

- ❖ The positive deviation of the water uptake observed at **high activity** is associated to a water clustering phenomenon.

On comparing the water sorption isotherm of Nafion-H<sup>+</sup> and Nafion-TEA (figure 6(a)-(b)), certain differences can be seen accounted such as:

1. The water uptake for Nafion-H<sup>+</sup> is much higher than for Nafion-TEA in all the range of water activity and especially **at low activity**, where the concave part of the curve corresponding to the *Langmuir sites is no more observed in Nafion-TEA*.
2. *Nafion-TEA exhibits water uptake of approximately 3.5% at 0.9 water activity corresponding to only 2 molecules of water per ionic site compared to 8 molecules of water per ionic site for Nafion-H<sup>+</sup>*. This behavior can be attributed to the fact that the sulfonic acid site have been neutralized in Nafion-TEA and can thereby no more act as Langmuir sites, limiting the membrane hydrophilicity. Moreover, the clustering phenomenon is limited in Nafion-TEA at high water activity due to its hydrophobic nature evident from the great difference in the number of water molecules present per ionic site especially at high water activity.

The differences between Nafion-TEA and Nafion-H<sup>+</sup> can also be clearly observed from the kinetic of water sorption expressed as the half sorption time,  $t_{1/2}$  in function of water activity (figure 7). The interpretation of the kinetic data obtained from the sorption experiments in terms of diffusion coefficient is subject to controversies as it generally leads to very low D values in comparison to the diffusion coefficient determined by pulse field gradient NMR (lower by two orders of magnitude)<sup>{22}</sup>. However, the comparative analysis of the  $t_{1/2}$  experimental values obtained under the same experimental conditions on Nafion-H<sup>+</sup> and Nafion-TEA can be performed.

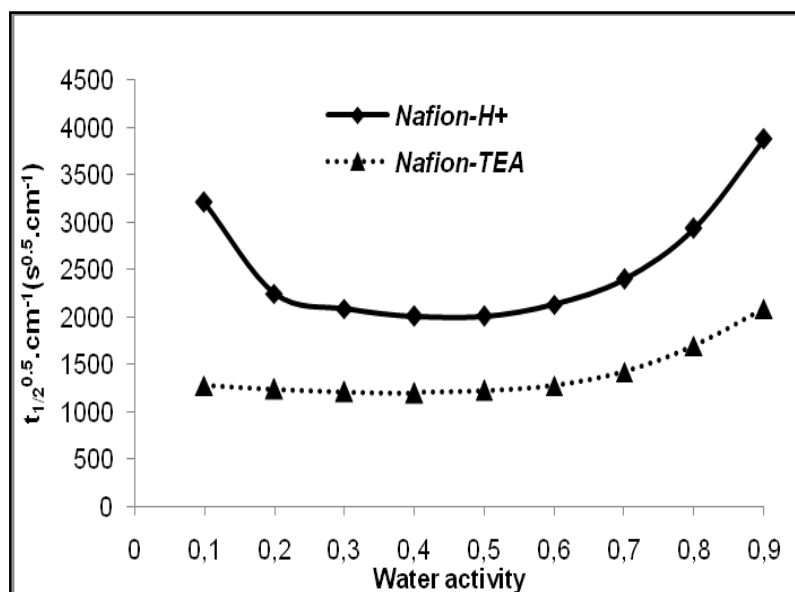


Figure 7: Water Sorption Kinetics of Nafion® in acidic form and Nafion-TEA

Different conclusions can be drawn from these data and especially from the combined analysis of the evolution of the water uptakes and half sorption times as a function of the water vapour activity. It can be noticed that the *variation of  $t_{1/2}$  as a function of the activity is not monotonous for any of the membranes*. In agreement with the previously discussed sorption mechanism, three domains can be distinguished for Nafion-H<sup>+</sup> discussed as follows:

1. In the first domain corresponding to low activity (*below 0.3*), a decrease of  $t_{1/2}$  is observed. In this activity range, *water is bound to specific polymer sites (sulfonic acid sites) leading to a plasticization effect* and to a decrease of the half sorption time.
2. For intermediate  $a_w$  ( $0.3 < a_w < 0.7$ ), *no significant variations of  $t_{1/2}$*  are noticed.
3. At high activity ( $a_w > 0.7$ ), an increase of  $t_{1/2}$  is observed. The trend observed in the last domain can be related to the high increase of water uptake and to the *formation of large water aggregates whose size makes diffusion more difficult*.
4. The rather constant value of  $t_{1/2}$  observed in the intermediate activity range can be related to the opposite effect of plasticization one hand and water clustering on the other hand.

For Nafion-TEA, the curve evolves as follows:

1. The value of  $t_{1/2}$  remains *constant below the water activity of 0.7* and then *increases at higher activity*. This evolution is *consistent with the water isotherm shape* previously discussed for

this film. ***Below the water activity of 0.7***, the linear shape of the isotherm is representative of a Henry type sorption that is characterized by ***a constant value of the solubility and diffusion coefficients***, respectively.

2. ***At high activity***, as observed for Nafion- $H^+$  also, the increase of water uptake associated with ***water clustering phenomenon leads to an increase of the half sorption time***.

On comparing Nafion-TEA with Nafion- $H^+$ , it can be observed that:

1. The ***water diffusion rate is always higher in Nafion-TEA than in Nafion- $H^+$*** .
2. In Nafion  $H^+$ , the strong interactions involved at the beginning of the sorption process between water and the acid sulfonic sites make the water molecules much less mobile than in Nafion-TEA in which weaker polymer-water interactions are involved in the water sorption mechanism at low activity.
3. The limited clustering phenomenon observed in Nafion-TEA at high activity results also in higher mobility of water molecules in this range of activity.

In a nutshell, it can be concluded that ***Nafion-TEA is more hydrophobic in nature compared to Nafion- $H^+$*** .

## **Conclusion**

In summary, impact of neutralization process on the morphology as well as functional properties of virgin Nafion<sup>®</sup> membrane has been demonstrated in this section. Taking into account the conductivity and the thermal stability<sup>[2]</sup> ( $T_D$  of Nafion- $H^+$ : 170-250°C;  $T_D$  of Nafion-TEA: 380°C) for the HT-PEMFC applications, the Nafion-TEA can be recommended as a better alternative to Nafion- $H^+$  for high temperature applications. In order to further understand the evolution and correlation of different properties with morphology of Nafion-TEA membranes under different conditions, it would be very interesting to characterize the membranes under different conditions such as different water vapour pressure, temperatures etc.

## 2.2: TFTEA doped Nafion-TEA membranes

Membranes based on Nafion-TEA and TFTEA were elaborated by swelling method at 80°C under argon atmosphere. The characteristics of doped Nafion-TEA membranes with different TFTEA concentrations are shown in table 2.

<i>Sample</i>	<i>% TFTEA (by weight)</i>	<i>% TFTEA (by volume)</i>	<i>Moles TFTEA/ moles SO<sub>3</sub><sup>-</sup>HN(C<sub>2</sub>H<sub>5</sub>)<sub>3</sub> of Nafion (<math>\lambda</math>)</i>
<i>Nafion-TEA+5%TFTEA</i>	<i>5</i>	<i>5.2</i>	<i>0.25</i>
<i>Nafion-TEA+8%TFTEA</i>	<i>8</i>	<i>10.3</i>	<i>0.42</i>
<i>Nafion-TEA+12%TFTEA</i>	<i>12</i>	<i>15.2</i>	<i>0.65</i>
<i>Nafion-TEA+14%TFTEA</i>	<i>14</i>	<i>17.7</i>	<i>0.78</i>
<i>Nafion-TEA+17%TFTEA</i>	<i>17</i>	<i>21.3</i>	<i>0.98</i>
<i>Nafion-TEA+18%TFTEA</i>	<i>18</i>	<i>22.5</i>	<i>1.1</i>
<i>Nafion-TEA+20%TFTEA</i>	<i>20</i>	<i>24.8</i>	<i>1.12</i>
<i>Nafion-TEA+24%TFTEA</i>	<i>24</i>	<i>29.5</i>	<i>1.51</i>
<i>Nafion-TEA+29%TFTEA</i>	<i>29</i>	<i>35.1</i>	<i>1.96</i>

Table 2: TFTEA mass and volume concentration as well as  $\lambda$  values for different Nafion-TEA+x%TFTEA membranes (Density of Nafion-TEA: 1.85g/cm<sup>3</sup>; Density of TFTEA: 1.4g/cm<sup>3</sup>)

In this section, evolution of the nano-structuration of Nafion-TEA with addition/concentration of TFTEA will be discussed. Afterwards, co-relation of the evolution of their properties with nano-structuration will be investigated.

Before starting the characterization, a study on the stability of these doped membranes against leaching phenomenon under different conditions was carried out and will be discussed briefly in this section.

### *a. Membrane Stability*

Firstly, it is very interesting to know the stability of these membranes towards leaching of TFTEA at ambient temperatures with time since the swelling of the membranes was carried out at 80°C. Hence,

in order to evaluate the stability of these doped membranes, the doped membrane with highest weight percent content of TFTEA obtained at 80°C i.e. 24% was utilized. Membrane with such high weight percent content was chosen since it had shown the formation of a passive layer of TFTEA on its surface with time. Membranes with lower concentrations of TFTEA did not show such phenomenon.

The stability towards leaching was studied at room temperature under argon atmosphere as well as ambient atmosphere. It has been observed that *atmosphere has not a significant impact on the leaching phenomenon of TFTEA*. For high doping level, the leaching of TFTEA starts after 2-3 days. Moreover, the process is pretty slow and 40 days are necessary to obtain a stable weight. Whatever is the initial doping, *the stabilization weight was found to be close to 21wt%* content of TFTEA.

The leaching phenomenon could occur due to the following reason: Swelling of the membranes with ionic liquid is done at elevated temperature leading to an increase in the free volume of the polymer. Thus, it is possible that the polymer could accommodate excess of ionic liquid molecules which are not in strong interaction with it. However, later when the surrounding temperature is close to ambient conditions, these ionic liquid molecules could exude itself due to the contraction of free volume in the membrane.

Taking into account these results, for most of the characterization techniques and procedures, membranes doped up to 20% TFTEA weight percent were utilized in order to avoid device contamination and experimental errors. However, some experiments (such as morphology study, thermo-mechanical properties, conductivity) have been performed with higher doping levels (>21wt%) in order to have more information on the distribution and/or organization of the PCIL in the structure of Nafion-TEA. But, this was done using only freshly prepared samples since samples are stable up to 2-3 days against leaching phenomenon.

### ***b. Morphology***

The impact of TFTEA addition as well as its concentration on the nano-structure of Nafion-TEA membrane was studied by SANS. The SANS spectra of Nafion-TEA + xwt% TFTEA composite membranes are presented on Figure 8 on a log-log scale. The q-range of the spectra has been extended with respect to Figure 2. An offset has been applied along the intensity scale for clarity after subtraction of a constant background due to hydrogen incoherent scattering.

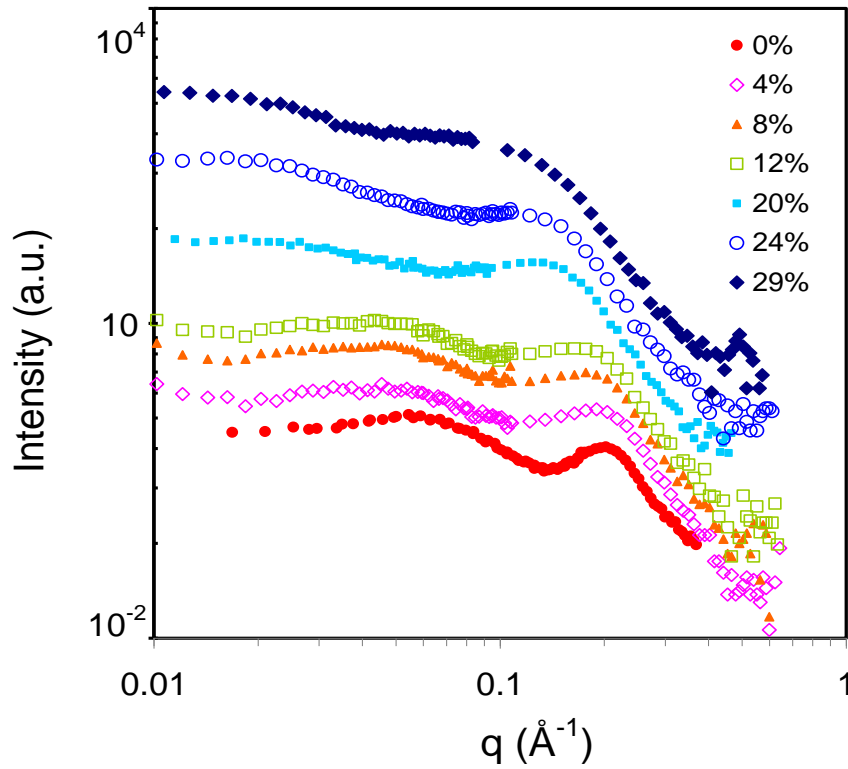


Figure 8: SANS spectra of neutralized Nafion with different percentage of TFTEA (Nafion-TEA+x%TFTEA)

From the spectra in figure 8, following observations can be made:

1. The *nano-structuration of Nafion-TEA is clearly maintained upon doping with TFTEA* as revealed by the observation of the *typical ionomer peak* and a second scattering maximum i.e. *matrix knee* up to the maximum doping level (29wt%).
2. The effect of *increasing the amount of TFTEA* within the membrane induces *a continuous shift of both the ionomer peak and the matrix knee towards smaller angles* similarly to the previously observed effect of water sorption on the structure of Nafion<sup>®</sup><sup>{23-25}</sup>.
3. A  $q^{-4}$  behaviour (Porod's law) is observed at high  $q$  values, even if data are scattered, which is the signature of a sharp interface at sub-nanometre scale, as observed in water-swollen acidic Nafion<sup>®</sup>. The *composite membrane is thus a phase-separated system with a well-defined interface between a dense and hydrophobic perfluorinated phase and the ionic domains containing the ionic liquid in addition to the TEA counter-ions*.

4. Overall, the observed behaviour is similar to an acidic membrane swollen with a polar solvent such as water.
5. Swelling a Nafion-TEA membrane with TFTEA thus does not profoundly modify the polymeric architecture.

Concerning the evolution of both the peaks in the spectra with TFTEA addition and/or concentration, following comments can be made:

1. The shifting and broadening of *matrix knee* towards lower  $q$  values point towards change in the local crystalline order of Nafion-TEA on TFTEA addition.
2. Now considering the swelling behaviour of ionic domains of Nafion-TEA, the position and shape of *ionomer peak* has to be analysed thoroughly. The ionomer peak position varies from  $q=0.202 \text{ \AA}^{-1}$  (free of PCIL) to  $0.105 \text{ \AA}^{-1}$  (maximum loading 29wt%), corresponding to characteristic distances increasing from an initial separation of  $31 \text{ \AA}$  in Nafion-TEA to a final value of  $59 \text{ \AA}$ . It can be clearly observed in Figure 8 that the ionic liquid insertion induces a significant broadening of the ionomer peak even at the minimum of the doping level (4wt%). This effect results from the insertion of the bulky ionic liquid molecules which disrupts the particular organization of TEA cations on the interface in Nafion-TEA. Moreover, the bulky TFTEA molecules cannot homogeneously swell the structure of Nafion-TEA at very low doping levels corresponding to one TFTEA molecule for 4 sulfonate groups (Table 3) and hence *the distribution in size induces the broadening of the ionomer peak*.

The swelling behaviour of ionic domains can be analysed more deeply through the variation of the characteristic distance  $d$  obtained from the ionomer peak position, as a function of TFTEA content of the membrane. The *swelling state of a membrane can be characterized either by a local parameter  $\lambda$  defined as the number of doping molecules per sulfonic group or by a macroscopic parameter such as the polymer or solvent volume fractions  $\phi_p$  and  $\phi_w$  respectively*. Figure 9 shows a plot of  $\log(d)$  as a function of  $\log(\phi_p)$ , a representation that is useful to compare the behaviour of different membranes under different swelling conditions and solvents.  $\log(d)$  presents a linear variation with  $\log(\phi_p)$  as previously observed for Nafion<sup>®</sup><sup>[24]</sup>. At  $\phi_p=1$ , one finds a  $4 \text{ \AA}$  difference between Nafion-H<sup>+</sup> in acid form and Nafion-TEA discussed in the previous section, corresponding to the single-layer packing of TEA counter-ions at the interface. Then, *as TFTEA is introduced into Nafion-TEA matrix*, the *nanometric swelling follows a very similar trend as acidic Nafion<sup>®</sup>*, with a slope equal to 1.33. It is worth noting that determination of the peak position for the membranes with high PCIL content is very difficult as the peak has been strongly enlarged due to high PCIL content. Notably, the value obtained at 29wt% displays important error bars. *In this composite, the average separation distance appears to*



be 59 Å while it is 41 Å in hydrated acidic Nafion® at the same volume fraction of polymer. The peak enlargement can result from much more heterogeneous distribution of TFTEA in the ionic domains of Nafion-TEA than that of water molecules in acidic Nafion®. As suggested by a recent paper<sup>[2,30]</sup>, the TFTEA molecules are likely to form micelles of typical size of 16 Å within Nafion®. When swelling with TFTEA, the morphology of Nafion-TEA undergoes distortions to accommodate the presence of these micelles.

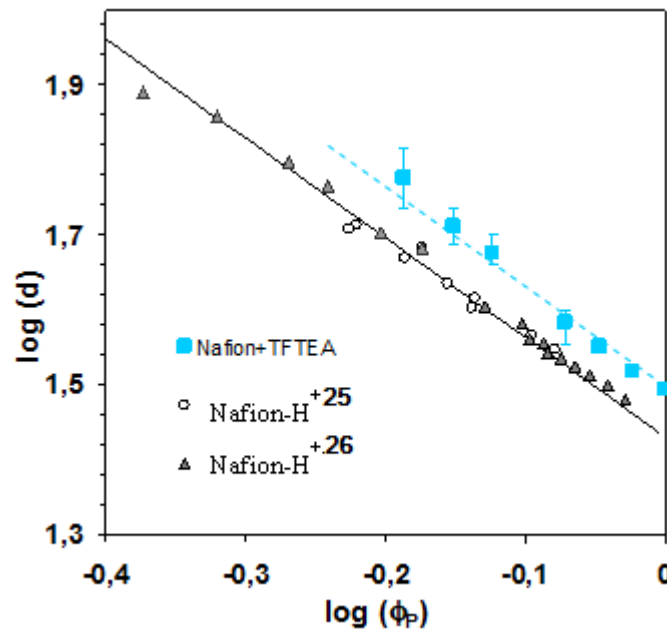


Figure 9: Dilution law  $\log(d)=f(\log\phi_p)$  of NafionTEA+TFTEA (■),  $d$  being the characteristic correlation distance obtained as  $2\pi/q^*$  with  $q^*$  the ionomer peak position, and  $\phi_p$  the polymer volume fraction. Data measured in acidic Nafion swelled with water [25,26] (○, ▲) are also reported for comparison. The lines are a guide for the eyes.

In a nutshell, the **key points concerning TFTEA addition in Nafion-TEA** from morphological point of view can be listed as:

- The nano-structuration of Nafion-TEA remains intact even when TFTEA is added in high concentration.
- Swelling behaviour of TFTEA doped membranes is quite similar to that of water swollen ones.
- However, there is inhomogeneous increase in the size of the ionic domains probably due to heterogeneous distribution of TFTEA.

#### *c. Differential Scanning Calorimetry*

In order to have further information on the distribution and/or organization of the PCIL within the polymer matrix, DSC measurements were carried out.

The modulated-DSC measurements were carried out in the temperature range of  $-50^{\circ}\text{C}$  to  $150^{\circ}\text{C}$  with  $5^{\circ}\text{C}$  per minute of heating rate using modulation of  $0.6^{\circ}\text{C}$  every 60 seconds under argon atmosphere on all the doped membranes studied in this work.

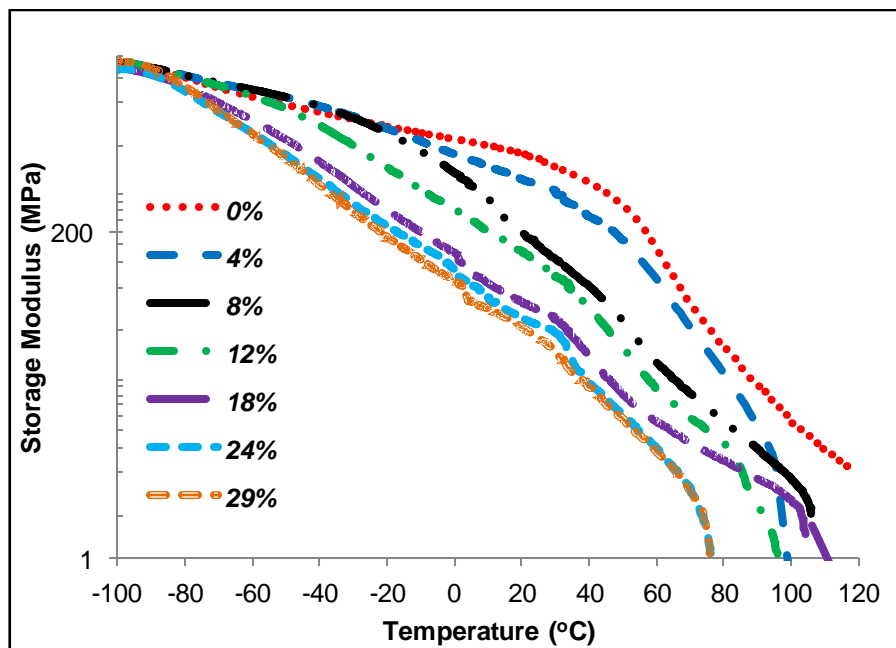
No melting temperature corresponding to pure TFTEA or TFTEA aggregates has been observed for all the doped membranes. This signifies complete dispersion of the PCIL into the matrix of Nafion-TEA. However, presence of nano-aggregates/micelles which are in interaction with Nafion-TEA cannot be excluded since it is possible that the fraction of PCIL molecules, which form aggregates, do not crystallize within the polymer matrix due to their small size.

#### *d. Thermo-mechanical properties*

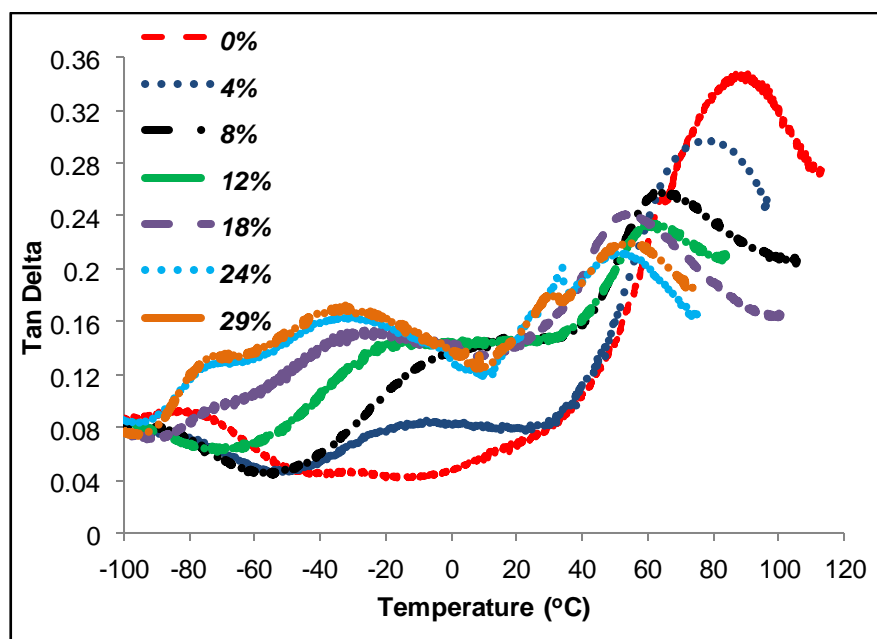
The effect of the concentration of ionic liquid on the dynamical mechanical properties of doped membranes has been investigated by measuring the evolution of storage modulus and  $\tan\delta$  vs temperature and comparison with Nafion-TEA (figure 10 (a) and (b) respectively).

#### *Storage Modulus versus Temperature*

A *decrease in mechanical stability* (storage modulus) has been observed *with the increase of TFTEA concentration*, due to the *plasticizing effect of the ionic liquid* (figure 10 (a)). The monotonic decrease of storage modulus with increasing the doping level (from  $-80^{\circ}\text{C}$  to  $60^{\circ}\text{C}$  or higher) indicates that TFTEA acts like plasticizer even at very low temperatures which underlines the *complete dispersion of TFTEA at the interface between hydrophobic and hydrophilic domains of the doped membrane*. These results are in agreement with the DSC measurements where no melting temperature corresponding to pure TFTEA or TFTEA aggregates has been observed for all the doped membranes.



(a)



(b)

Figure 10: DMA of TFTEA doped Nafion-TEA membranes; a) storage modulus vs temperature; b):  $\tan \delta$  vs temperature

### Tanδ versus Temperature

The tanδ versus temperature plots for doped Nafion-TEA membranes containing different concentrations of TFTEA are presented in figure 10 (b). The main features are discussed as follows:

1. The *γ-relaxation* for Nafion-TEA observed at -80°C shifts to lower value upon adding TFTEA in small quantity i.e. 4 wt%. Afterwards, the relaxation peak does not shift on further increasing the TFTEA content in the membrane.
2. In the temperature range of -80°C to 20°C, an increase in amplitude and a broadening of *β-relaxation* with increasing TFTEA content signifying an easier *relaxation of the perfluorinated main-chains and side-chains because of decreasing ion-ordering in the ionic domains and inter-chain interactions*. Apart from β-relaxation, a second peak appears around -77°C from 18wt% TFTEA content onwards. It can be assumed that this second relaxation is associated to the presence of TFTEA-enriched zones within the membrane (in agreement with the assumption of a heterogeneous distribution at high TFTEA concentration proposed by SANS results).
3. The energy dissipated for the *α-relaxation* is higher for Nafion-TEA compared to the doped membranes and the *T<sub>α</sub> value decreases with the increase of TFTEA concentration*. The polar side-groups of Nafion, SO<sub>3</sub><sup>-</sup>N(C<sub>2</sub>H<sub>5</sub>)<sub>3</sub>H<sup>+</sup> are solvated and plasticized by TFTEA resulting in the reduction of the strength of the electrostatic interactions within the ionic domains of the membranes. However for the *doped membranes containing more than 18wt% TFTEA*, a *second peak is observed in temperature range of 28-35°C* and the temperature of appearance for this relaxation decrease with the increase in TFTEA loading. This small peak could be attributed to the *α-relaxation of TFTEA rich-phase* in the polymer matrix due to concentration gradient of TFTEA at high percentage content (as proposed in the case of β-relaxation) or could be *associated to conformational relaxation modes of the fluorocarbon backbone chains of PTFE domain specifically, a 13<sub>6</sub>→15<sub>7</sub> conformational transition for α and an order-disorder conformational transition for α'* which could be more visible in the presence of high concentration of TFTEA<sup>{27,28}</sup>.

In summary, following important points can be noted:

- ✓ TFTEA has a plasticizing effect on the mechanical properties of Nafion-TEA matrix.
- ✓ DMA results have also pointed towards the heterogeneous distribution of TFTEA in Nafion-TEA similarly as SANS results. More precisely, the appearance of extra relaxation peaks more

particularly evident from 18wt% content of TFTEA ( $\lambda > 1$ ) could correspond to domains with richer TFTEA concentrations meaning heterogeneous distribution of TFTEA. This allows us to confirm the previously reported literature which proposed that the ionic liquid molecules auto-organize above certain concentration in the ionic domains of Nafion-TEA resulting in their heterogeneous distribution within the nano-structure of Nafion-TEA<sup>[2.5]</sup>.

#### e. Conductivity

The effect of TFTEA addition and its concentration has been investigated through the conductivity measurements as well. In order to evidence the effect of concentration and avoid the major effect of small amounts of water on the conductivity, the cells were prepared in argon environment and the *ionic conductivities were recorded under anhydrous atmosphere*.

*A significant increase in the conductivity of Nafion-TEA with subsequent introduction of TFTEA in the polymer matrix* as well as a decrease in the temperature dependence was observed with increasing TFTEA content (Figure 11).

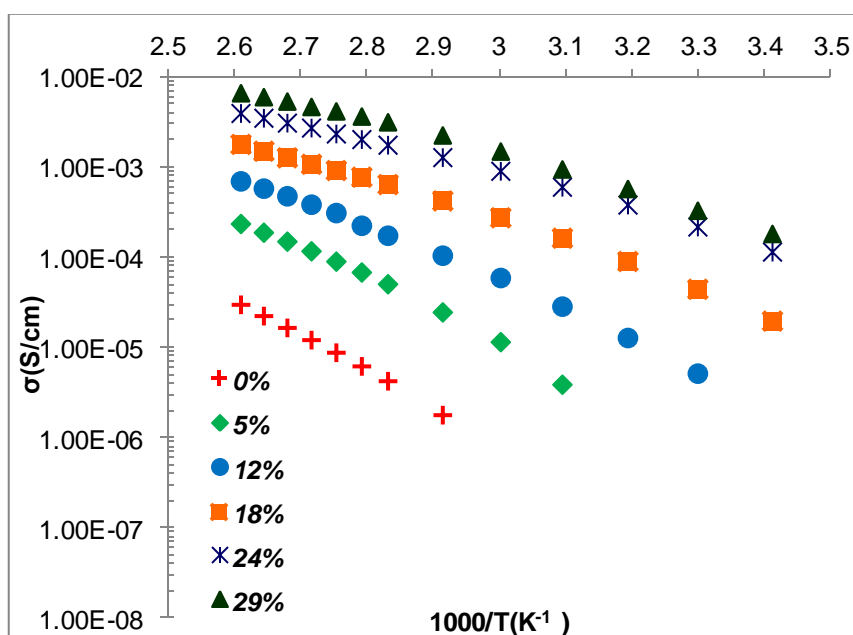


Figure 11: Ionic conductivity of neutralized Nafion with different percentage of TFTEA (Nafion-TEA+xwt%TFTEA)

The doped membrane with 29wt% TFTEA content shows anhydrous conductivity of around 6.5mS/cm at 110°C. It is interesting to note that the conductivities of membranes containing 24wt% and 29wt% are very close. This could be due to the possibility that TFTEA could form nano-

aggregates/micelles (heterogeneous distribution of TFTEA as proposed from SANS and DMA results) at high doping levels which would result in limited impact of presence of TFTEA on the conductivity. However, due to plasticizing effect of TFTEA, creeping phenomenon was exhibited by the doped membranes during the conductivity measurements. That is why the conductivity measurements were conducted only up to 110°C.

#### *f. Gas permeability*

The influence of TFTEA concentration on hydrogen and oxygen permeability coefficients are reported in Table 3 for the Nafion-TEA+xwt% TFTEA membranes containing up to 20wt% of TFTEA.

<i>TFTEA weight fraction (%)</i>	<i>H<sub>2</sub> (barrer)</i>	<i>O<sub>2</sub> (barrer)</i>
<i>0</i>	<i>10,2</i>	<i>2,5</i>
<i>5</i>	<i>10,4</i>	<i>2,3</i>
<i>8</i>	<i>9,6</i>	<i>2,4</i>
<i>12</i>	<i>9,7</i>	<i>2,6</i>
<i>20</i>	<i>7,1</i>	<i>2,7</i>

*Table 3: Permeability coefficients of H<sub>2</sub> and O<sub>2</sub> gases measured on Nafion-TEA membranes doped with xwt% of TFTEA (The uncertainty is estimated to be ±5%)*

Surprisingly, *the introduction of TFTEA within neutralized Nafion<sup>®</sup> membranes has a negligible effect on their gas permeation properties*. The gas permeation coefficients are found to be more or less constant whatever the doping level is, despite the significant swelling of the nano-structure as evidenced by SANS. This result can be considered as a confirmation of the already percolated structure of the Nafion-TEA and it suggests that the free volumes are mainly located at the interface between the percolated ionic domains and the hydrophobic phase, thus limiting the influence of the TFTEA content at least for the small sized diffusing molecules utilized for the study. Moreover, it can also be proposed that the gas permeability in the ionic domains of Nafion-TEA+TFTEA is close to that in the ionic domains of Nafion-TEA. This hypothesis seems logical keeping in mind the similar chemical nature of ionic functions of TFTEA and Nafion-TEA.

#### *g. Water Sorption*

Even if the PCIL doped polymer membranes are envisioned for their anhydrous application in PEMFCs i.e. without humidification of reactant gases, water will still be present in the MEA

due to its production at the cathode. Hence, it is indeed very important to investigate the water sorption behavior of these doped membranes. Like the study of gas permeability properties, water sorption studies were also carried on to samples containing less than 21 wt% of TFTEA at 25°C.

Firstly, in order to *check the stability of the membranes upon water vapor exposure, two consecutive cycles of sorption and desorption were performed on each sample*. Figure 12 represents the two consecutive cycles for Nafion-TEA membrane containing 12 wt% TFTEA. Similar behavior was demonstrated by all the doped membranes towards the consecutive cycles of sorption-desorption.

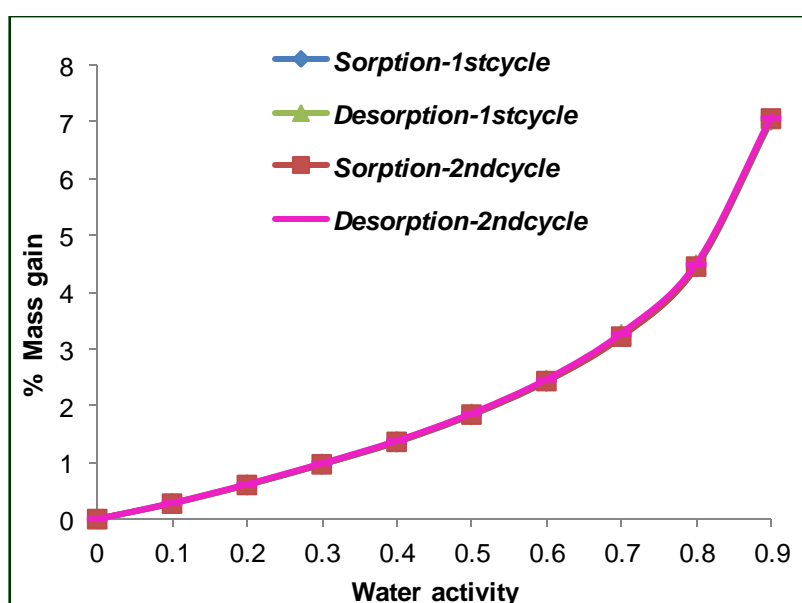


Figure 12: Water sorption isotherms representing consecutive sorption and desorption cycles for Nafion-TEA containing 12 wt% TFTEA

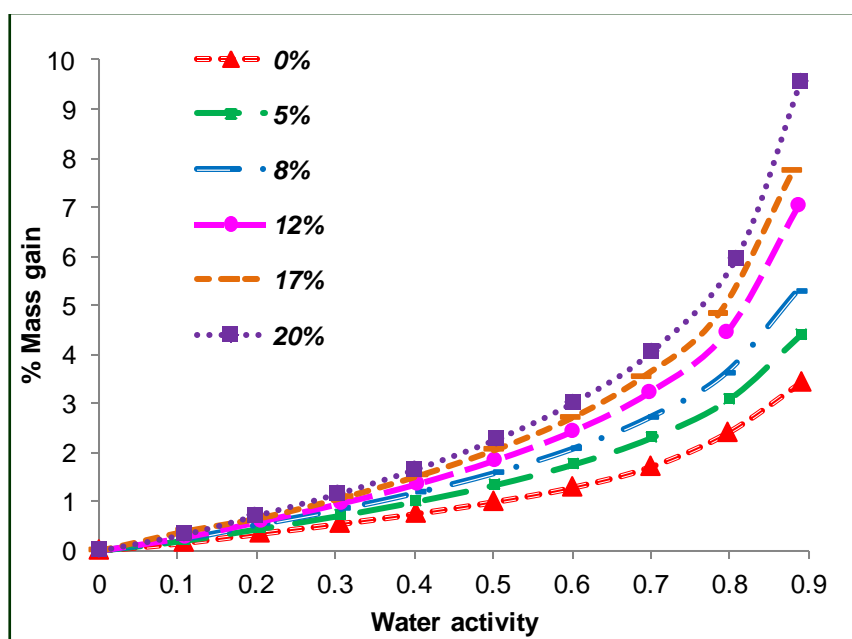
From figure 12, it can be concluded that:

1. The experiments were perfectly *reproducible*.
2. The sorption and desorption equilibrium data defining a single isotherm curve for each sample indicates that *the TFTEA doped Nafion-TEA membranes do not present any sorption hysteresis phenomenon*.

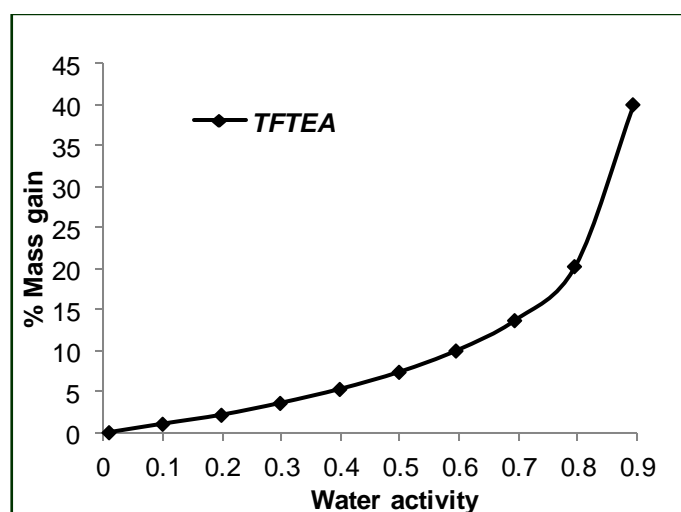
The *water sorption isotherms* of Nafion-TEA membranes containing increasing amounts of ionic liquid are represented in Figure 13 (a). In order to better understand the water sorption properties of

Nafion-TEA+x wt% TFTEA films, the water sorption isotherm characteristic of the ionic liquid was also determined as shown in Figure 13 (b).

*All the isotherms are of BET III type.* TFTEA exhibits a higher water uptake than Nafion-TEA, especially at water activities above 0.7 where a high increase of the water uptake is observed. As expected, *the water uptake measured on Nafion-TEA/TFTEA membranes increases with the content of ionic liquid contained in the membranes.*



(a)



(b)

Figure 12: Water sorption isotherm; a) TFTEA doped Nafion-TEA membranes; b) TFTEA



Moreover, *average number of water molecules per ionic site as a function of water activity* (considering all the  $-\text{SO}_3^- - \text{H}^+\text{N}-(\text{C}_2\text{H}_5)_3$  sites as “ionic site” present in the Nafion-TEA and TFTEA) for virgin Nafion-TEA, doped membranes and TFTEA were determined (Figure 14). In order to calculate the average number of water molecules gained by each ionic site of all the samples, their water sorption isotherms were utilized. The number of ionic sites has been calculated by taking into account the ionic functions of Nafion-TEA and TFTEA for the doped membranes. It can be clearly observed that the number of water molecules gained per ionic site is pretty close for lower water activity values i.e. up to 0.7 for the membranes with and without TFTEA. At higher water activity, there is a steady increase in the number of water molecules gained with increasing TFTEA content and highest for TFTEA alone. This result points towards *an improvement in the overall hydrophilicity of the system with increasing TFTEA concentration*.

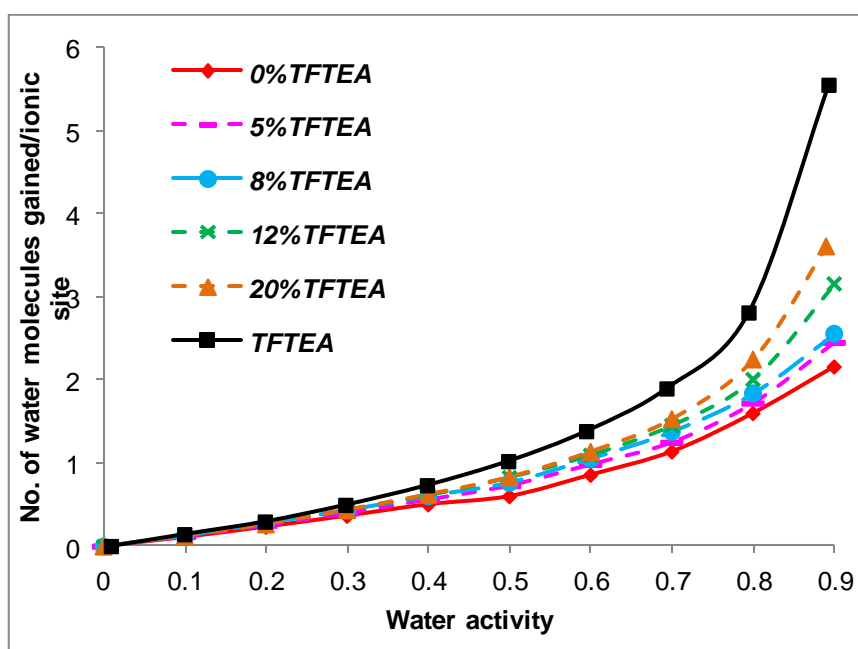


Figure 14: Number of water molecules gained per ionic site vs water activity ratio for Nafion-TEA, doped membranes & TFTEA

In addition, the “experimental isotherms” relative to Nafion-TEA+xwt% TFTEA have been compared with the “calculated isotherms”. These calculated isotherms have been obtained on the basis of an additive contribution of the water uptakes of each component i.e. Nafion-TEA and TFTEA to the water sorption mechanism of the composite system. Figure 15 allows the comparison between calculated and experimental isotherm of Nafion-TEA doped with 20 wt % of TFTEA. It illustrates the trend which is observed whatever the membrane composition is. At low water activity (below 0.7), the experimental and calculated water uptakes values are very close. However, for higher water activity,

the experimental data are lower than those calculated and the difference is emphasized as the water activity increases. This behavior confirms *the hindering effect of the polymer matrix that limits the water sorption capacity of the TFTEA molecules within the membrane*.

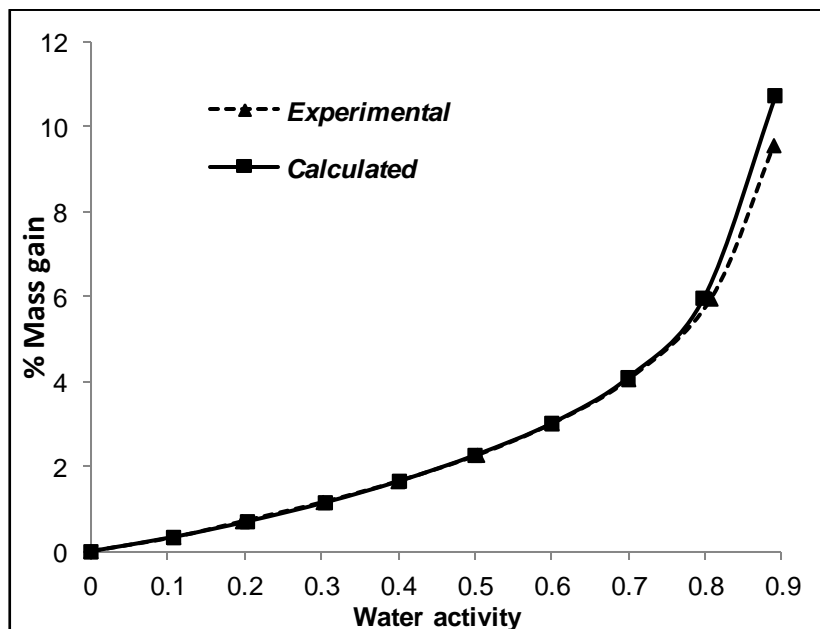


Figure 15: Comparison of experimental & calculated Water Sorption Isotherms for TFTEA doped Nafion-TEA membranes

**Guggenheim Anderson de Boer model (GAB)** was used to go deeper in the analysis of the water sorption mechanism. GAB equation has already been used to model BET type III isotherms with good accuracy<sup>[29]</sup>. The equation of GAB model is expressed as:

$$M = M_m \frac{C_G \cdot K \cdot a_s}{(1 - K \cdot a_s)(1 + (C_G - 1) K \cdot a_s)}$$

In this modelling approach, the three parameters,  $M_m$ ,  $C_G$ , and  $K$ , have a physical meaning.  $M_m$  characterizes the availability of membrane ionic sites for the first sorbed water molecules as it represents the saturation of all primary adsorption sites by one water molecule (formerly called the monolayer in BET theory).  $C_G$  which is the Guggenheim constant is indicative of the binding strength of water to the primary binding sites.  $K$  is a correcting factor lower than 1, for the properties of the multilayer molecules with respect to the bulk liquid. The curve fitting efficiency was estimated from the mean relative percentage deviation modulus (MRD) which is defined by:

$$MRD = \frac{100}{N} \sum_{i=1}^N \frac{|m_i - m_{pi}|}{m_i}$$

where  $m_i$  is the experimental value,  $m_{pi}$  is the predicted value, and  $N$  is the number of experimental data. A modulus value below 10% is indicative of an accurate fit of the experimental isotherm curve by the model. We calculated the values of GAB parameters for each film by fitting the isotherm curve according to the software Tablecurve 2D. Determination of  $M_m$ ,  $C_G$  and  $K$  values was also performed for neat TFTEA. The value of MRD and GAB parameters are shown in table 4.

<b><i>TFTEA weight fraction (%)</i></b>	<b><i>M<sub>m</sub></i></b>	<b><i>C<sub>G</sub></i></b>	<b><i>K</i></b>	<b><i>MRD (%)</i></b>
<b><i>0</i></b>	<i>0.009</i>	<i>2.28</i>	<i>0.853</i>	<i>1.7</i>
<b><i>5</i></b>	<i>0.0128</i>	<i>2.14</i>	<i>0.830</i>	<i>1.8</i>
<b><i>8</i></b>	<i>0.0140</i>	<i>2.40</i>	<i>0.848</i>	<i>2.5</i>
<b><i>12</i></b>	<i>0.0147</i>	<i>2.54</i>	<i>0.899</i>	<i>3.6</i>
<b><i>20</i></b>	<i>0.0187</i>	<i>2.16</i>	<i>0.914</i>	<i>2.4</i>
<b><i>100</i></b>	<i>0.0491</i>	<i>2.81</i>	<i>0.981</i>	<i>6.6</i>

Table 4: Values of MRD & GAB parameters for neutralized Nafion with different percentage of TFTEA (Nafion-TEA+x%TFTEA)

Certain points which could be noted on looking at the table 4 are mentioned as follows:

1. From the calculated MRD values for the membranes and the ionic liquid, it can be concluded that *the GAB model can appropriately describe the water sorption isotherms*.
2. All the *GAB parameters tend to increase with increasing the TFTEA content* revealing an increase of the membrane hydrophilicity.
3. In particular, *the linear increase of M<sub>m</sub> value as a function of TFTEA content* in the concentration range from 0 to 100wt% *confirms the validity of the additivity law on water uptake for low activities* (Figure 16).

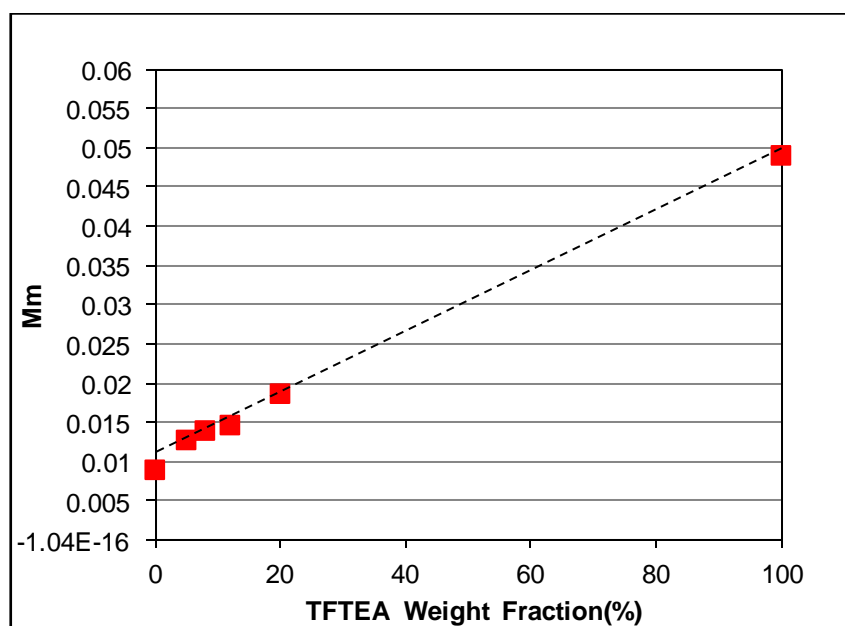


Figure 16: Evolution of  $M_m$  values determined from GAB modelling as a function of the TFTEA weight fraction

The **water sorption kinetics** was also studied for all the doped membranes and the square root of half sorption time ( $t_{1/2}$ ) was plotted as a function of the water activity in figure 17. The results of pure Nafion-TEA have been reported in figure 17 as reference and the results of Nafion- $H^+$  have also been included in figure 17 for comparison.

The values of  $t_{1/2}$  characteristic of the water diffusion in Nafion-TEA+x% TFTEA films are all lying between the curves representative of Nafion- $H^+$  on one hand and Nafion-TEA on the other hand. The global trends that are defined by the experimental points are, for all doped membranes, a constant value of  $t_{1/2}$  in the activity range below 0.3, followed by a slight increase of  $t_{1/2}$  values up to an activity of 0.7 and finally a larger increase of the half sorption time at high water activity. This **trend is here again consistent with the BET III type sorption mechanism** that had been previously discussed for pure Nafion-TEA. We can remark that the **presence of a small amount of ionic liquid with Nafion-TEA film leads to a global decrease of the diffusion rate, especially at high water activity**. This trend is observed up to 12 wt% content of TFTEA. In contrast, membrane with 20 wt% TFTEA content presents a curve quite close to that obtained with membrane containing 5wt% content of TFTEA. This could seem rather surprising. However, these measurements have been made on two samples which gave similar results. For this ionic liquid content, a heterogeneous distribution of TFTEA is suspected (i.e. TFTEA aggregates/micelles begin to get formed). This specific organization of the ionic liquid

molecules could lead to a decrease of the interactions towards water molecules, favoring then water diffusion.

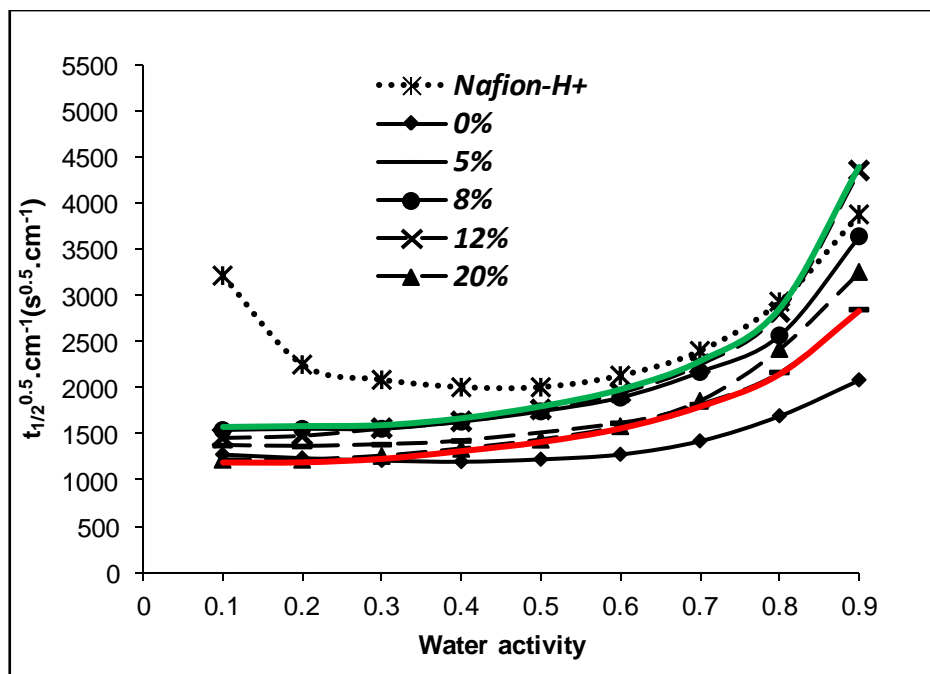


Figure 17: Water Sorption kinetics of Nafion- $H^+$  and Nafion-TEA doped with different percentages of HTFTEA; Red and green curves present the lower and upper limits of the  $t_{1/2}$  for the TFTEA doped membranes

Hence, it is clear from the water sorption experiments that *doped membranes are more hydrophilic in nature compared to virgin Nafion-TEA membrane* and the water uptake is related to the TFTEA content as well as water activity.

### Conclusion

In summary, the evolution of morphology and functional properties of TFTEA doped membranes has been demonstrated. It can be concluded from this study that the morphology and consequently the functional properties of the PCIL doped membranes are dependent on the concentration of the PCIL. With increasing TFTEA content in the Nafion-TEA membrane, the conductivity and the hydrophilicity of the doped membranes improve while its thermo-mechanical properties deteriorate.

### ***2.3: TFTEA doped Nafion-TEA membranes in the presence of water***

The presence of water can greatly influence both the morphology as well as conductivity of polymer electrolytes<sup>{1,7,24}</sup>. As water sorption experiments clearly show an evolution of water sorption behavior of doped membranes with TFTEA content, it is very interesting to study the influence of presence of water on various properties of the TFTEA doped membranes. Few results have also been published on the impact of presence of water on the properties of pure PCILs (such as conductivity, diffusion coefficients of ionic species and viscosity) and significant effect of water presence have been illustrated<sup>{1,32,33}</sup>. Thus, we assume that water presence would affect the properties of the PCIL doped ionomers as well.

Hence, in this section, following will be discussed:

- a. The impact of presence of water on the morphology of TFTEA doped membrane(20wt%) at ambient temperature*
- b. Conductivity measurements on doped membranes with different TFTEA concentrations at different water activities as well as temperatures*

Since it has been observed from water sorption study that the sorption -desorption cycles for the doped membranes are perfectly reversible at ambient temperature, stability of the samples in the presence of water is not in question at least under ambient conditions.

#### ***a. Morphology***

In order to determine the effect of water on morphology of TFTEA doped membranes, SANS technique was utilized. For this study, two equally doped membranes; one without water and another with amount of water added additionally on the surface of the membrane (amount of water corresponding to water uptake at 0.9 water activity at room temperature for the membrane with particular percentage of TFTEA); were utilized. For this experiment, Nafion-TEA membrane containing 20 % wt TFTEA prepared by swelling method was utilized because the amount of water to be added would be calculable and precise compared to membranes with lower percentage of TFTEA which absorb much lesser amount of water (as seen in their water sorption isotherms). Thus, the amount of water added on the surface of the second membrane was 10% of total weight of the membrane, evident from water sorption experiment, 24 hours prior to SANS measurement and the cell was closed immediately. The other cell with the doped membrane in dry state was prepared and closed in the glove box under argon atmosphere. Figure 18 present SANS spectra (focussed in the  $q$  range of  $0.05\text{-}0.5 \text{ \AA}^{-1}$ ) of the two membranes.

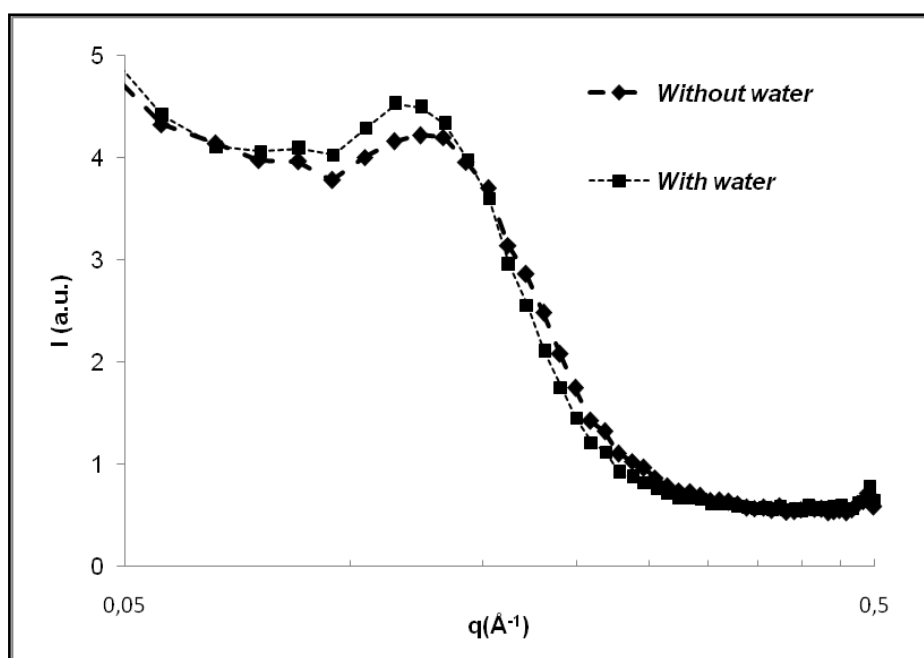


Figure 18: SANS spectra for Nafion-TEA+20%TFTEA with & without water

From figure 18, it can be seen that the *ionomer peak* shifts towards lower  $q$  value and becomes a little sharper for the membrane containing water compared to the membrane containing no water. This observation shows that the ionic domains in the doped membrane swell slightly more in the presence of water. The sharper ionomer peak could either be due to better *separation between hydrophobic and hydrophilic part in the presence of water along with the ionic liquid or could also be due to better contrast of the system owing to the protons of water in the system*. Water molecules must be principally in interaction with the  $-\text{SO}_3^- - ^+\text{HN}(\text{C}_2\text{H}_5)_3$  entity of both the polymer and the PCIL.

#### **b. Conductivity**

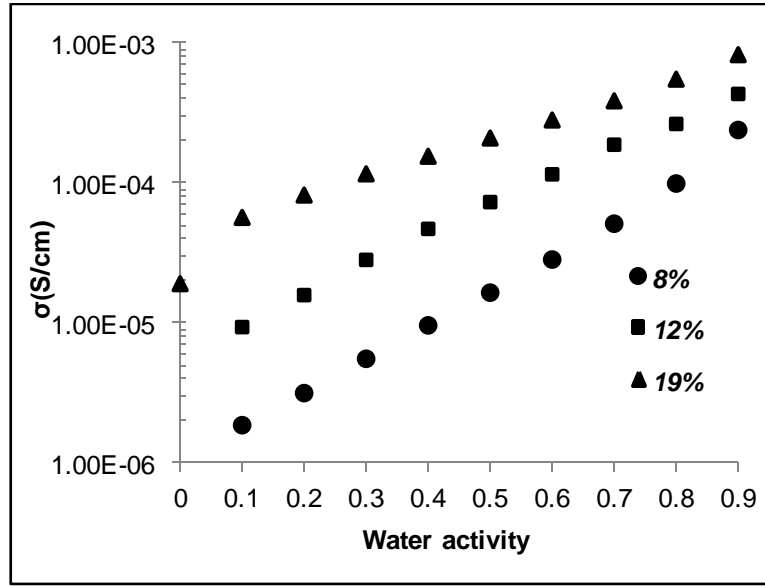
For Nafion- $\text{H}^+$ , the presence of water in the membrane is very important as the proton conduction is assured by water molecules. Thus, at  $25^\circ\text{C}$ , an increase of more than 200 times is observed between the conductivity at 10 % RH and 90% RH ( $3.7 \cdot 10^{-5} \text{ S.cm}^{-1}$  at 10% RH and  $7.72 \cdot 10^{-3} \text{ S.cm}^{-1}$  at 90% RH respectively)<sup>[34]</sup>. Similarly, previously reported investigations on the influence of water on the PCILs properties show that viscosity sharply decreases in presence of water, while conductivity and diffusion coefficients significantly increase<sup>[1]</sup>. In addition, it was evidenced that water intrinsically contributes to the conductivity enhancement, through a Grotthuss-like mechanism. Hence, it is very interesting to analyze the impact of presence of water on the conductivity of the hybrid system of Nafion-TEA and PCILs. Figure 19 (a) presents the conductivity of TFTEA doped Nafion-TEA membranes at  $25^\circ\text{C}$  at

different water vapour pressures. The conductivities were measured at each water activity value every hour for 12 times (before going to higher water activity value) in order to obtain a saturated value for that water activity. It was observed that the conductivity values saturated after 7-8 hours (i.e. conductivity measurements between 8<sup>th</sup> and 12<sup>th</sup> time gave same values). Moreover, the ratio of conductivities of these doped membranes at various RH values to the conductivity at 10% RH have also been calculated (figure 19 (b)).

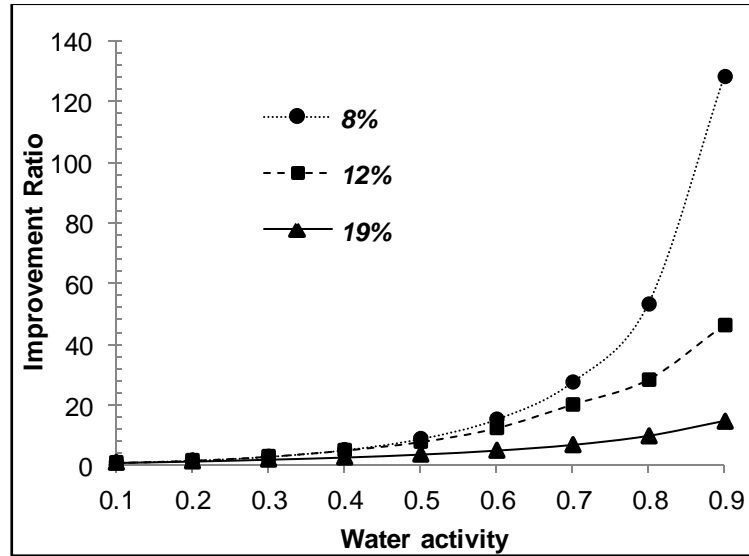
From both these figures (19 (a) and (b)), it can be observed that:

1. The *membrane containing lower percentage of TFTEA exhibits more pronounced effect of water on the conductivity* compared to membrane containing higher amount of TFTEA although the former absorbs lower amount of water than the latter (as seen in water sorption study).
2. Hence, an enhancement of the conductivity with a factor of 130 is obtained for Nafion-TEA+8% TFTEA membrane while the difference is only of 14 times for the Nafion-TEA+20% TFTEA membrane between 10% and 90% RH.
3. On comparing the conductivity values for Nafion-TEA+20% TFTEA under anhydrous condition and 10% RH, a 3 times increase is observed at 25°C. This means that *presence of water can significantly affect the ion conduction in the doped membrane even at ambient temperature*.
4. For membranes with lower TFTEA percentage, conductivity at 25°C under anhydrous conditions could not be measured unlike under even slightly humid conditions (say 10% RH). This observation points out that *presence of water even in minute quantities can result in measurable conductivities for the PCIL doped membranes (with low PCIL content) at ambient temperature*.





(a)



(b)

Figure 19: Conductivity trends of Nafion-TEA containing different percentage of TFTEA as a function of water activity at 25°C; a). Ionic conductivities; (b). Improvement factor of conductivity at 25°C calculated by the ratio of conductivity at each RH value to the conductivity at 10%RH

In general, the conductivity enhancement can be explained by the following properties of water:

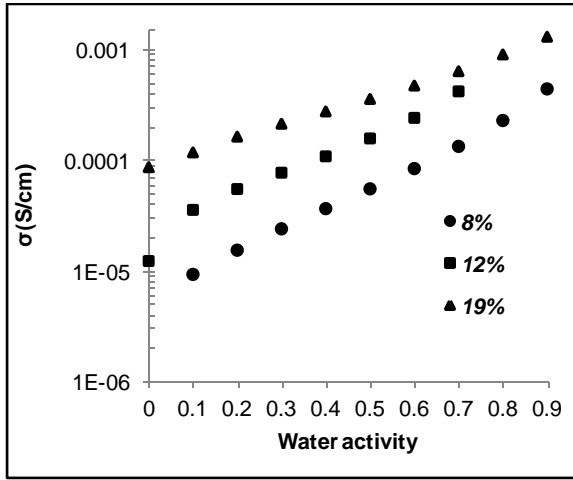
- 1). High dielectric constant that favours ion-pair dissociation,

- 2). High solvating ability reflected by its Donor Number (DN=18) and its high Acceptor Number (AN=54.8)
- 3). Ability to contribute to proton mobility
- 4). Very low viscosity

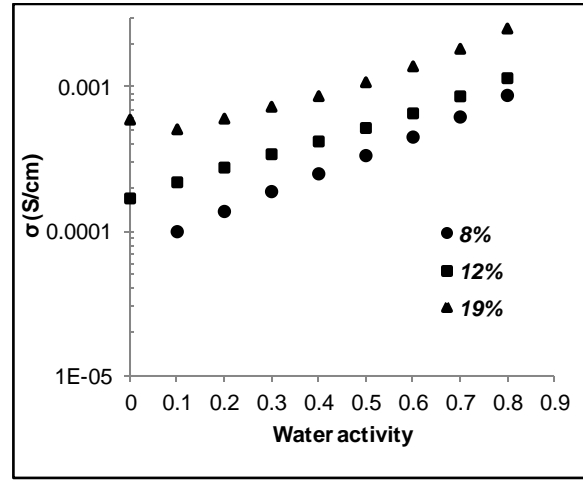
Considering the effect of presence of water on the morphology of membrane with high TFTEA content, it can be assumed that the addition of water to the doped membrane with low percentage of TFTEA improves much more significantly not only *the mobility of ionic species* (by reducing overall viscosity of the system) but also *the percolation of ionic domains* in the doped membrane. Hence a comparatively higher increase in conductivity is observed in the latter in contrast to the former in which the percolation of ionic domains as well as the mobility of ionic species is already enough good due to high concentration of ionic liquid.

Furthermore, *at higher temperatures* i.e. 40°C and 80°C (figure 20 (a) and (b) respectively), the trend of *change in ionic conductivity of these membranes was found to be similar to the trend at 25°C under various RH*. At these temperatures also, the conductivities were measured at each water activity value every hour for 12 times (before going to higher water activity value) and the conductivity values saturated after 7-8 hours (i.e. conductivity measurements between 8<sup>th</sup> and 12<sup>th</sup> time gave same values). The impact of increasing water activity on the conductivity is still more pronounced for lower percentage of TFTEA compared to membrane with higher percentage of TFTEA though the difference in their improvement factor becomes lesser significant with increasing temperature. There is an improvement of the conductivity with a factor of 47 for Nafion-TEA+8% TFTEA and a factor of 11 for the membrane Nafion-TEA+20% TFTEA between 10% and 90% RH at 40°C figure (21 (a)). The improvement further drop to 9 times for Nafion-TEA+8% TFTEA membranes and 5 times for Nafion-TEA+20% TFTEA membrane between 10% and 80% RH at 80°C (figure 21 (b)). This drop in improvement factor with increasing temperature is apparently related to the reduced viscosity of the system at high temperatures and hence improved mobility of the ionic species as well polymer segments whatever the PCIL content is.

Clearly, this drop in the improvement factor with increasing temperature is much less drastic in the case of membrane containing 20% TFTEA compared 8% TFTEA based membrane. This could be due to the fact that the membrane with high percentage of TFTEA is enough plasticized by TFTEA providing better mobility of ionic species and also contribution of TFTEA in ionic conductivity is more important than water. However, the membrane with low percentage of TFTEA is less plasticized i.e. restricted mobility in the system and hence addition of water greatly influences the ionic conductivity and influence diminishes at higher temperature when the system gains higher mobility.

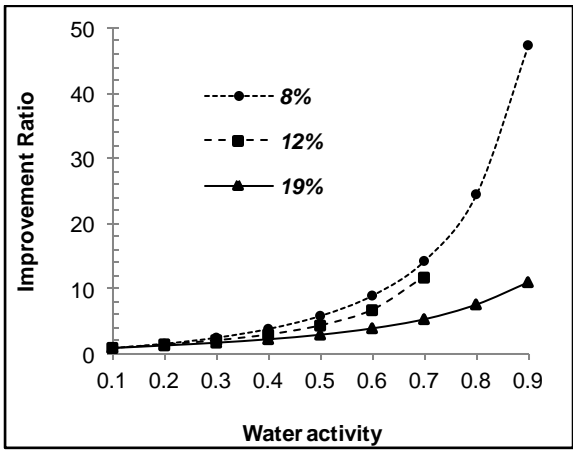


(a)

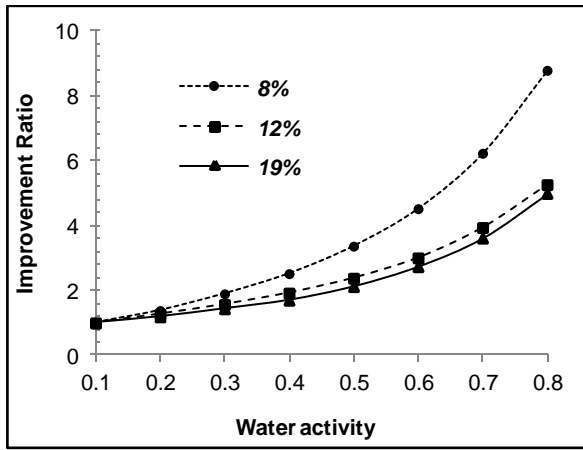


(b)

Figure 20: Ionic conductivity of neutralized Nafion with different percentage of TFTEA (Nafion-TEA+x%TFTEA) vs water activity; (a) 40°C; (b) 80°C



(a)



(b)

Figure 21: Improvement factor of conductivity of neutralized Nafion with different percentage of TFTEA (Nafion-TEA+x%TFTEA) vs water activity; (a) 40°C; (b) 80°C

## Conclusion

In this section, it has been clearly evidenced that presence of water has positive impact on the evolution of both morphology and conductivities of PCIL doped Nafion-TEA membranes. However, it will be interesting to better understand and quantify the impact of presence of water at higher temperatures by performing following experiments at higher temperatures:

- ✚ SANS measurements at different temperatures and water vapour pressures
- ✚ Diffusion coefficient measurements on the doped membranes in the presence of water molecules
- ✚ Gas permeability measurements at different temperatures and different water vapour pressures
- ✚ Water sorption study: stability towards cycles of sorption-desorption at elevated temperatures

## 2.4: General Conclusion

SANS measurements of anhydrous Nafion-TEA suggest a specific arrangement of the TEA counterions. The difference between the characteristic distance, extracted from the ionomer peak of a dry acidic Nafion<sup>®</sup>,  $d_0$  and a *Nafion-TEA*  $d_{TEA}$  **corresponds to the size of TEA cation (4 Å) suggesting a single layer organization of interdigitated TEA cations at the hydrophobic-hydrophilic interface**. For the doped membranes, the *evolution of nano-structure of Nafion-TEA with TFTEA concentration is very similar to that of acidic Nafion<sup>®</sup> swollen by water*. However, the broader peaks at high TFTEA content indicate a more heterogeneous distribution of TFTEA in Nafion-TEA probably due to the micellar organization of TFTEA in the membrane.

It has been shown by DMA measurements that the *ionic liquid solvates and plasticizes the Nafion-TEA side group* reducing the dipolar interactions in the ionic domains inducing more facile mobility of the main fluorocarbon backbone chains. This phenomenon amplifies with the increase of TFTEA concentration.

The introduction of *ionic liquid within the Nafion<sup>®</sup> membranes significantly boosts the ionic conductivity under anhydrous conditions*.

The gas permeability of doped membranes is very close to that of the polymer matrix i.e. Nafion-TEA whatever is the doping level. The water sorption of Nafion TEA is not predominated by the presence of specific sites of sorption as demonstrated by BET III isotherms and pretty low water uptakes are obtained. However, addition of *ionic liquid improves water sorption capacity of Nafion-TEA*.

The present study demonstrates that the presence of *water greatly affects the ionic conductivity of doped membranes*. In addition, presence of water molecules seems to result in higher swelling of ionic domains and better nano-phase hydrophilic-hydrophobic separation in TFTEA doped membranes.

## **References:**

1. Iojoiu, C.; Hana, M.; Molmeret, Y.; Martinez, M.; Cointeaux, L.; Kissi, N.E.; Teles, J.; Lepretre, J.C.; Judeinstein, P.; Sanchez, J. Y.; *Fuel Cells* **2010**, 10(5), 778–789.
2. Di Noto, V.; Negro, E.; Sanchez, J-Y; Iojoiu, C.; *Journal of American Chemical Society* **2010**, 132, , 2183-2193.
3. Nakamoto, H. ; Watanabe, M.; *Chemical Communications* **2007**, 2539–2541
4. Iojoiu, C.; Judeinstein, P.; Sanchez, J. Y.; *Electrochimica Acta* **2007**, 53, 1395–1403
5. Di Noto, V.; Piga, M.; Giffin, G. A.; Lavina, S.; Smotkin, E. S.; Sanchez, J-Y.; Iojoiu, C.; *Journal of Physical Chemistry C* **2012**, 116(1), 1370-1379.
6. Iojoiu, C.; Martinez, M.; Hanna, M.; Molmeret, Y.; Cointeaux, L.; Lepretre, J.C.; Kissi, N.E.; Guindet, J. ; Judeinstein, P.; Sanchez, J. Y.; *Polymer for Advanced Technologies* **2008**, 19, 1406–1414.
7. Martinez, M.; Molmeret, Y.; Cointeaux, L.; Iojoiu, C.; Lepretre, J.C.; Kissi, N.E.; Judeinstein, P.; Sanchez, J. Y.; *Journal of Power Sources* **2010**, 195, 5829–5839.
8. Pathapati, P R; Xue, X; Tang, J.; *Renewable Energy* **2005**, 30 1-22.
9. Springer, T.E.; Zawodzinski, T.A.; Gottesfeld, S.; *Journal of the Electrochemical Society* **1991**, 138(8), 2334-2342.
10. Gebel, G.; Diat, O.; *Fuel Cells* **2005**, 5(2); 261-276.
11. Ue, M.; Murakami, A.; Nakamurab, S.; *Journal of the Electrochemical Society* **2002**, 149(10), A1385-A1388.
12. Eisenberg, A.; Hodge, I.M.; *Macromolecules* **1978**, 11(2), 289-293.
13. Kyu, T.; Hashiyama, M; Eisenberg, A.; *Canadian Journal of Chemistry* **1983**, 61, 680-687.
14. Page, K. A. ; Kevin, M. C.; Moore R. B. *Macromolecules* **2005**, 38, 6472-6484.
15. Collette, F.M.; Lorentz, C.; Gebel, G.; ThomINETTE, F.; *Journal of Membrane Science* **2009**, 330(1-2), 21–29.
16. Hamdy, H.F.M.; Ito, H.; Kobayashi, Y. ; Takimoto, N.; Takeota, Y.; Ohira, A.; *Polymer* **2008**, 49; 3091-3097
17. Chiou, J.S; Paul, D.R.; *Industrial and Engineering Chemical Research* **1988**, 27; 2161-2164.
18. Broka, K.; Ekdunge P.; *Journal of Applied Electrochemistry* **1997**, 27(2); 117-123.
19. Ogumi, Z.; Kuroe, T.; Takehara, Z.; *Journal of the Electrochemical Society* **1985**, 132, 2601-2605.
20. Hamdy, F.M.M.; Kobayashi, Y.; Kuroda, C.S.; Ohira, A.; *Journal of Physics* **2010**, Conference series 225, 012038.
21. Zawodzinski, T.A., Derouin, C.; Radzinski, S.; Sherman, R.J.; Smith, V.T.; Springer, T.E.; *Journal of the Electrochemical Society* **1993**, 140, 1041-1047.
22. Majsztrik, .W; Satterfield, M.B.; Bocarsly, A.B.; Benziger, J.B.; *Journal of Membrane Science* **2007**, 301, 93-106.

23. Rubatat, L.; Gebel, G.; Diat, O.; *Macromolecules* **2004**, 37(20), 7772-7783.
24. Gebel, G.; *Polymer*, **2000**, 41, 5829-5838.
25. *Kreuer, K. D.; Paddison, S. J.; Spohr, E.; Schuster, M.; Chemical Reviews* **2004**, 104, 4637-4678
26. Gebel, G.; Lyonnard, S.; Mendil-Jakani, H.; Morin, A.; *Journal of Physics: Condensed Matter* **2011**, 23 234107.
27. Di Noto, V.; Piga, M.; Lavina, S.; Negro, E.; Yoshida, K.; Ito, R.; Furukawa, T.; *Electrochimica Acta* **2010**, 55 (4), 1431-1444.
28. Di Noto, V.; Gliubizzi, R.; Negro, E.; Pace, G.; *Journal of Physical Chemistry B* **2006**, 110 (49), 24972-24986.
29. Dolmaire, N. ; Espuche, E.; Méchin, F.; Pascault, J.P.; *Journal of Polymer Science Part B: Polymer Physics*, **2004**, 42, 473-449.
30. Greaves, T.L.; Drummond, C.J.; *Chemical Society Review*, **2008**, 37, 1709–1726.
31. Perrin, J.C.; Lyonnard, S.; Volino, F.; *Journal of Physical Chemistry C*, **2007**, 111(8), 3393-3404.
32. Cammarata, L.; Kazarian, S. G.; Salter, P. A.; Welton, T.; *Physical Chemistry-Chemistry Physics* 2001, 3, 5192-5200.
33. Seddon, K. R.; Stark, A.; Torres, M.J.; *Pure Applied Chemistry* **2000**, 72 (12), 2275–2287.
34. Marechal, M.; Doctoral Thesis. Polyelectrolytes for fuel cells: tools and methods of characterization. Internationale Polytechnique de Grenoble (Grenoble-INP), **2004**.

### 3. Elaboration of Triethylammonium Triflate (TFTEA) doped Nafion membranes: Swelling and Casting

This chapter aims to evaluate the impact of elaboration method i.e. swelling and casting on the morphology and resulting functional properties of the doped membranes. Indeed, the swelling method involved imbibing a PCIL in a pre-structured morphology of Nafion-TEA while the casting method involves preparing suspension of Nafion-TEA in combination with a PCIL in a polar solvent followed by organization and formation of the hybrid membrane in one step during solvent evaporation. The key differences between these two methods are depicted in figure 1.

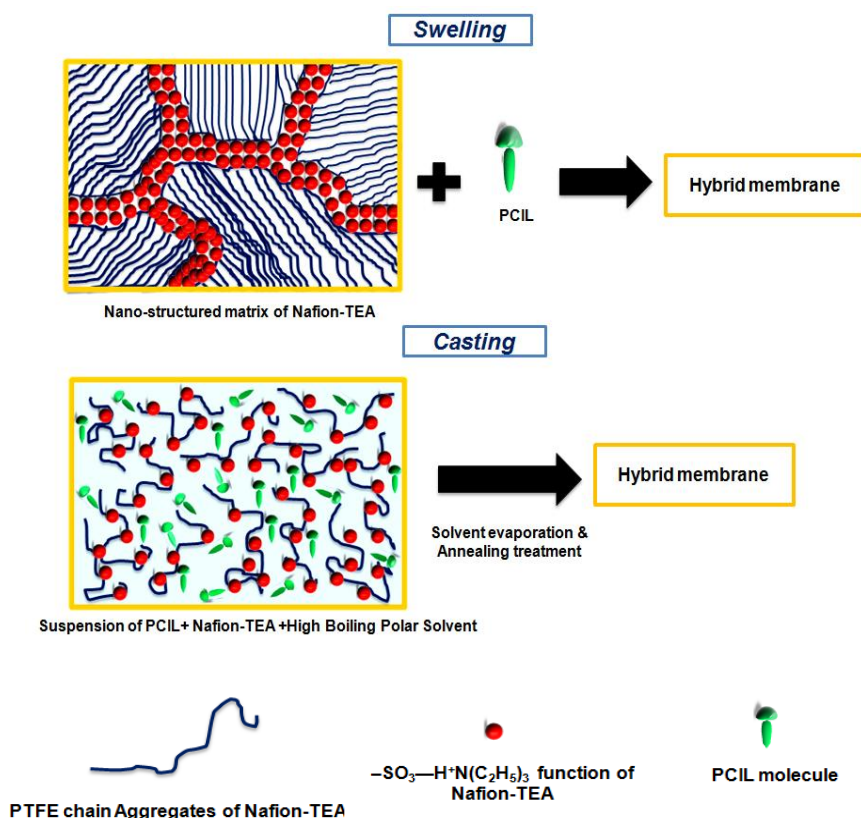


Figure 1: Comparison of different elaboration methods for PCIL doped Nafion-TEA membranes

This chapter has been divided into three parts such as:

- ❖ In the first section of this chapter, various properties of Nafion-TEA prepared by casting method (referred as *Nafion-TEA-casting*) will be compared with that of Nafion-TEA prepared from

commercially available-extruded Nafion membrane (referred as *Nafion-TEA-extruded*) since Nafion-TEA serves as the reference membrane for the doped membranes.

- ❖ In the second part, PCIL doped Nafion-TEA membranes prepared by casting and swelling methods will be discussed in detail.
- ❖ In the third part, fuel cell performance of TFTEA doped membrane (casting based) and degradation phenomena associated with the system based on TFTEA and Nafion-TEA in the presence of peroxy radicals have been investigated.

### ***3.1: Nafion-TEA by casting method***

The casting method employed for the elaboration of Nafion-TEA membrane involves dissolution of polymer in a high boiling polar solvent i.e. Dimethylacetamide (boiling point:156<sup>0</sup>C) followed by solvent evaporation at medium temperature (60<sup>0</sup>C) and thermal/annealing treatment afterwards at 150<sup>0</sup>C for one hour and finally vacuum drying at 80<sup>0</sup>C for 48 hours. The impact of elaboration method on the following will be presented in this section:

- a. *Morphology*: In the previous chapter, morphology of Nafion-TEA based membranes was discussed thoroughly at nano-mesoscopic scale. In this chapter, we will take into consideration the morphology of Nafion-TEA based membranes at molecular length scale as well.
- b. *Thermo-mechanical properties*
- c. *Conductivity*
- d. *Gas-permeability*
- e. *Water sorption properties*

#### ***a. Morphology***

The multi-scale organization of Nafion<sup>®</sup> has been explained in detail in the bibliographic chapter. In short, the morphology of Nafion<sup>®</sup> membrane can be described at different length scales namely:

- 1). *Molecular scale* signifying the extent of crystallinity of the PTFE chains (crystalline peaks)
- 2). *Nanoscope scale* signifying hydrophobic-hydrophilic nano-separation (ionomer peak)
- 3). *Mesoscope scale* signifying long range order of crystallinity (matrix knee)

It has been demonstrated in previous works that the method of elaboration can have significant impact on the different scales of morphology of Nafion<sup>®</sup>. The annealing treatment is particularly important for



the resulting morphology of the recast Nafion<sup>®</sup> membranes<sup>{1-3}</sup>. Recast-Nafion<sup>®</sup> membrane prepared by solvent evaporation at room temperature and without any annealing treatment suffers from poor mechanical properties, brittleness as well as solubility in organic polar solvents at room temperature, unlike extruded membranes. This occurs due to the formation of poorly crystallized and/or small sized crystallites along with the amorphous regions and absence of long range order between lamellar crystallites which are randomly distributed in the amorphous phase<sup>{2}</sup>. However, utilization of high boiling solvents such as dimethylsulfoxide, dimethylacetamide etc. for dissolution of the polymer and application of annealing treatment afterwards provides enough thermal energy for the morphological redevelopment resulting in formation of large lamellar crystallites and long range crystalline order (of order of 200Å; (evidenced by co-relation of position and/or shape of Matrix knee with the crystalline peaks)<sup>{2,3}</sup>. Moreover, increase in annealing temperature results in improved crystalline order and a simultaneous increase in mean separation distance at the hydrophilic-hydrophobic interface (evidenced by shifting of ionomer peak towards lower q value) in the recast Nafion<sup>®</sup> membranes. This is why we also employed annealing treatment for our membranes at 150°C for one hour after solvent evaporation at 60°C. Therefore, considering the multi-scale organization of Nafion<sup>®</sup>, it is important to characterize Nafion-TEA membranes based on commercial as well as casting method at different scales to see differences in their morphology if any.

### **Molecular scale**

Wide Angle X-ray Scattering (WAXS) measurements have been employed in order to compare the morphology of both the membranes at the molecular length scale. The membranes utilized for the WAXS measurements were dried before at 80°C under vacuum for 48 hours but were kept under ambient conditions while the measurements were carried out in transmission mode and hence membranes might have absorbed small amounts of water during the measurements. The WAXS profiles (Intensity vs q) of both types of Nafion-TEA membranes along with Nafion 117<sup>®</sup> in acidic form (Nafion-H<sup>+</sup>) as reference are shown in figure 2. Generally, the WAXS profile of Nafion-H<sup>+</sup> shows ensemble of two peaks<sup>{4}</sup>:

- A correlation peak at  $q=2.8 \text{ Å}^{-1}$  ( $d=2.24 \text{ Å}$ ) which corresponds to inter-atomic correlation along the perfluorinated chain i.e. distance between two consecutive  $-CF_2$  moieties along the helix.
- An amorphous peak ( $q=1.1 \text{ Å}^{-1}$ ;  $d=5.7 \text{ Å}$ ) superimposed with a weak crystalline peak ( $q=1.24 \text{ Å}^{-1}$ ;  $d=5.1 \text{ Å}$ ) corresponding to the organization/crystalline feature or packing of the perfluorinated chains. In order to separate the crystalline peak from the amorphous peak and calculate the degree of crystallinity of these perfluorinated chains, the WAXS spectra are fitted with two lorentzian functions after subtracting a linear baseline. Once the integrated intensity of each contribution is obtained, one can quantify the degree of crystallinity of Nafion<sup>®</sup> membrane.

From figure 2, concerning Nafion- $H^+$ , it can be clearly observed that a broad peak at  $q=1.14\text{\AA}^{-1}$  is observed along with another correlation peak at  $q=2.75\text{\AA}^{-1}$ . The superimposition of crystalline-amorphous peaks in the  $q$  range of  $1.1\text{--}1.25\text{\AA}^{-1}$  is not clearly visible. This is consistent with the existing results in literature according to which extruded-Nafion<sup>®</sup> membranes do not show very clearly the superimposition of the amorphous and crystalline peak in this  $q$  range<sup>{1}</sup>.

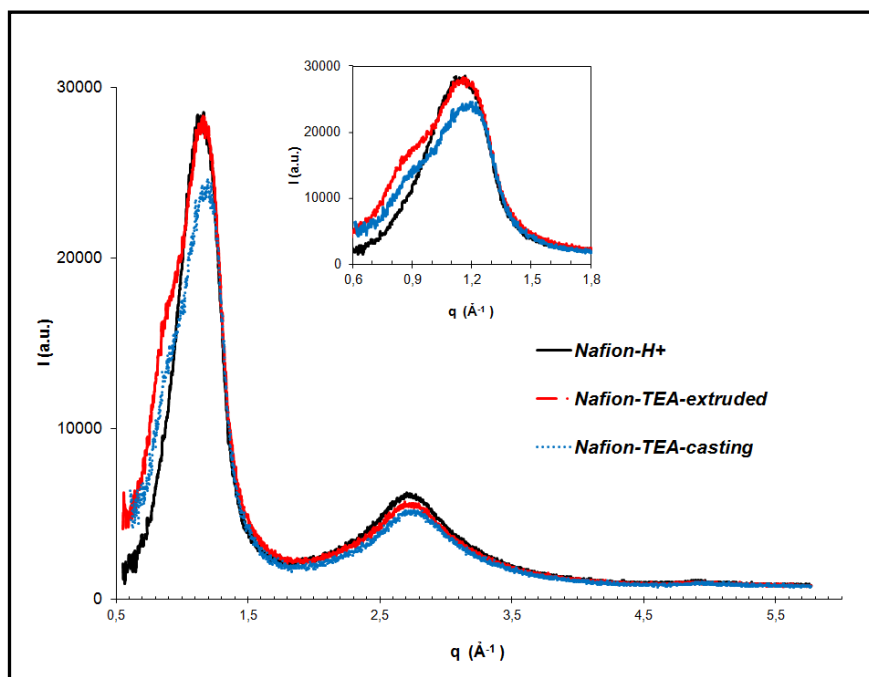


Figure 2: WAXS profiles of different types of Nafion<sup>®</sup> membranes

Now concerning both the types of Nafion-TEA membranes, three features have been observed (figure 2):

1. The correlation peak at  $q=2.75\text{\AA}^{-1}$  remains at similar position for both the types of Nafion-TEA membranes similarly as Nafion- $H^+$ . This underlines *no change in the distance between two consecutive  $-CF_2$  moieties along the helix.*
2. The broad peak at  $q=1.14\text{\AA}^{-1}$  ( $d=5.51\text{\AA}$ ) is observed for Nafion-TEA-extruded similarly as Nafion- $H^+$  while this peak shifts to slightly higher  $q$  value ( $q=1.18\text{\AA}^{-1}$ ;  $d=5.32\text{\AA}$ ) for Nafion-TEA-casting. This points towards *better local packing of perfluorinated chains in Nafion-TEA-casting.*

3. In addition, a *supplementary peak/halo* is observed at lower  $q$  value ( $q = 0.75-0.85 \text{ \AA}^{-1}$ ) for both the TEA-neutralized membranes unlike Nafion<sup>®</sup> in acidic form. Hence, this supplementary peak must be a *contribution from triethylammonium (TEA)* present at the hydrophobic-hydrophilic interface. This  $q$  value corresponds to a distance of  $8 \text{ \AA}$ . In the previous chapter, it was suggested that the presence of Triethylammonium at the interface adds  $4 \text{ \AA}$  to the size of the ionic domain and there is a string like packing of triethylammonium at the hydrophobic-hydrophilic interface in Nafion-TEA-extruded in dried state. Here, a peak corresponding to Triethylammonium with a characteristic distance of  $8 \text{ \AA}$  is observed. But important point to note is that the membrane is not in anhydrous state and presence of water molecules can change the string like organization of TEA at the interface.

From these experimental observations, following *conclusions* can be drawn:

- Neutralization of Nafion<sup>®</sup> with Triethylamine does not change the intra-atomic co-relation along the PTFE chain for both recast as well as extruded Nafion-TEA membranes.
- The local packing of the hydrophobic chains/PTFE chains does not get affected when commercial Nafion<sup>®</sup> 117 membrane is neutralized by Triethylamine but improves when the Nafion-TEA membrane is elaborated by casting method.

Unfortunately, the appearance of supplementary peak at  $q \sim 0.80 \text{ \AA}^{-1}$  makes it difficult to fit the lorentzian functions and thus not possible to quantify the degree of crystallinity of these neutralized membranes with present tools. In order to further understand certain features of neutralized membranes such as effect of neutralization on the crystallinity of Nafion-TEA, possible arrangements of TEA at the interface, and quantification as well as comparison of the crystallinity of both the types of Nafion-TEA, it would be interesting to perform the WAXS experiment on neutralized membranes under anhydrous conditions as well as different relative humidities. It could be also interesting to study the impact of degree of neutralization.

### *Nanosopic-Mesosopic scale*

In order to further understand the impact of elaboration method on the morphology of Nafion-TEA at larger scale ( $\sim 20-500 \text{ \AA}$ ), Small Angle Neutron Scattering (SANS) measurements have been carried out. The membranes utilized were dried before at  $80^\circ\text{C}$  under vacuum for 48 hours and the measurement cells were prepared and closed in anhydrous conditions prior to the measurements. The SANS profiles of the two types of neutralized membranes are compared in figure 3.

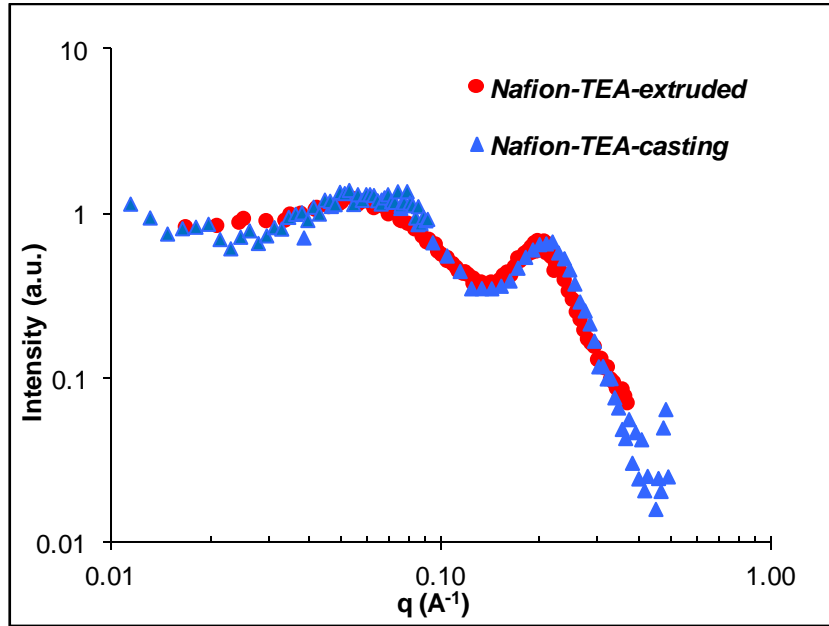


Figure 3: SANS spectra of neutralized Nafion-TEA membrane elaborated by two different methods

From the figure 3, it can be observed that both show the same features discussed as follows:

1. The **ionomer peak** related to Nafion-TEA-casting is present at  $q=0.21 \text{ Å}^{-1}$  ( $d=30 \text{ Å}$ ) in comparison to the one for Nafion-TEA-extruded at  $q=0.202 \text{ Å}^{-1}$  ( $d=31.1 \text{ Å}$ ). Thus, the **characteristic size of nano-phase separation is unaffected by the elaboration method**. In the literature, few studies have been concentrated on the comparison of extruded as well as recast Nafion® in acidic form. Sacca et al. have compared SAXS spectra of recast and thermally annealed-Nafion® with extruded-Nafion® sample (both in acidic form) under ambient humid conditions (since it is difficult to compare the position/shape of ionomer peak in anhydrous state due to the lack of electronic contrast between poorly solvated ionic domains and hydrophobic domains)<sup>[5]</sup>. They reported a higher mean separation distance for recast and annealed Nafion® ( $d=37 \text{ Å}$ ) than for commercial Nafion® ( $d=30 \text{ Å}$ ). This increase in characteristic nano-phase distance is related to the annealing temperature and it evolves with increasing the temperature of annealing treatment<sup>[1]</sup>. Moreover, Mauritz et al. used electrical impedance studies and suggested that recast and annealed Nafion® membrane experiences a more disordered packing of side chains and hence more disruption of order in the ionic phase along with stronger structural cohesion in the matrix/hydrophobic phase<sup>[3]</sup>. This could explain the higher mean separation distance in recast and annealed Nafion® membranes in acidic form. But concerning the TEA neutralized-Nafion® membranes, the contrary results could be explained due to the fact that particular “string-like” organization/packing of cations (Triethylammonium) in the ionic

domains of Nafion-TEA is energetically the most feasible for this system and hence no change in the morphology is observed even if elaboration conditions are changed.

2. The *matrix knee* appears to be slightly more pronounced in the case of casting based Nafion-TEA though present at same position as in the case of Nafion-TEA-extruded. This observation of a *more pronounced matrix knee in the case of Nafion-TEA-casting* is consistent with the existing results on the recast and extruded Nafion® in acidic form<sup>[5]</sup>. This result points towards ***improvement in the long range crystalline order of the membrane when elaborated by casting method***<sup>(1,6)</sup>.

From these experimental observations, following *conclusions* can be drawn:

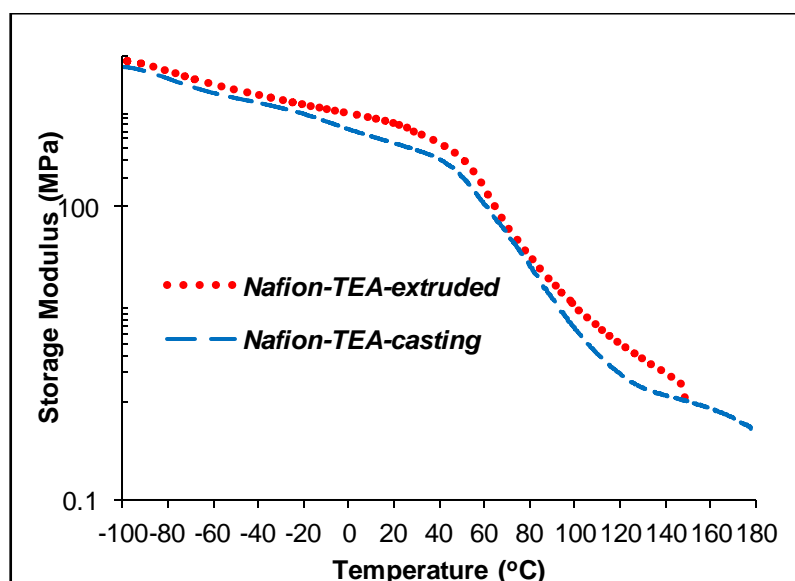
- Elaboration method does not significantly affect the mean-separation distance between inter-connected ionic domains in Nafion-TEA membrane.
- Size and/or long range crystalline order of lamellar crystallites could improve when Nafion-TEA membrane is elaborated by casting method.

In summary, the impact of casting method on the morphology of Nafion-TEA is different at different length scales accounted as follows:

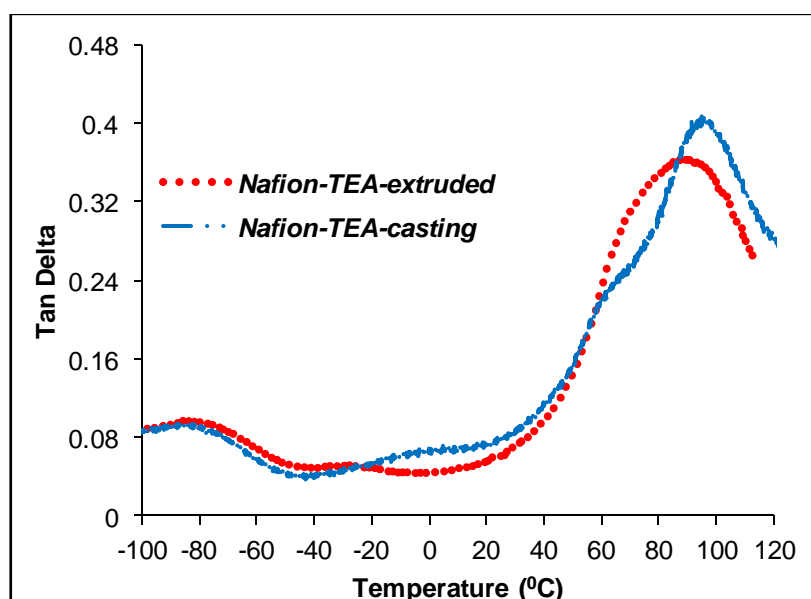
- ✓ At crystallographic scale, the local packing of the hydrophobic chains/PTFE chains gets improved.
- ✓ At nanoscopic scale, negligible effect is observed. Thus, it can be suggested that the ionic domains of Nafion-TEA-casting are arranged in pretty similar fashion as in Nafion-TEA-extruded.
- ✓ At mesoscopic scale, the crystallites in PTFE backbone chain could be better organized and/or larger in size in the casting based Nafion-TEA.

#### ***b. Thermo-mechanical properties***

The thermo-mechanical responses of both the types of Nafion-TEA membranes were compared by DMA measurements. The plots of storage modulus and  $\tan\delta$  versus temperature are shown in figure 4(a) and figure 4(b) respectively.



(a)



(b)

Figure 4: (a): DMA of Nafion-TEA elaborated by two methods; a) storage modulus vs temperature;  
b)  $\tan \delta$  vs temperature

### Storage Modulus versus Temperature

The thermal response of storage modulus of these two types of membranes is almost similar in nature (figure 4(a)). However, the *casting based membrane retains better mechanical properties at temperature above 150°C*. It maintains a storage modulus of about 1MPa in the temperature range of 150- 190°C while Nafion-TEA-extruded collapses at 150°C. Indeed the storage modulus of casting

based membrane above 150°C is not enough for the PEMFC application, but still more promising compared to the other one. This relative improvement in the thermo-mechanical response could be due to higher chain entanglements and better long range crystalline order/larger crystallites in the hydrophobic domains. Although WAXS data did not provide significant information on the degree of crystallinity of these neutralized membranes, still more pronounced matrix knee could be an indication of higher ordering at large scales (~100 Å).

### **Tanδ versus Temperature**

Concerning the dynamic relaxations associated with these two types of membranes (figure 4 (b)), important features are discussed as follows:

1. The ***γ-relaxation*** of both casting based and extrusion based Nafion-TEA membranes have been observed at -80°C. This observation underlines that there is ***no significant change in the vibrational and rotational movements of CF<sub>2</sub> groups*** located at short distance from the ionic function of Nafion-TEA on changing the elaboration conditions.
2. The ***β-relaxation*** appears to be in much broader temperature range for Nafion-TEA-casting in comparison to that of Nafion-TEA-extruded. The temperature window of this relaxation seems to be in the range of -50 to 0°C for Nafion-TEA-extruded while it seems to fall in the range of -40 to 60°C for Nafion-TEA-casting. This shift of temperature window to higher temperature could be due to the ***improved order of crystallites/denser packing of PTFE main-chains*** and hence more restricted low temperature-local mobility of the hydrophobic main-chains as well as side-chains in casting based Nafion-TEA membrane.
3. Concerning ***α-relaxation***, the value of T<sub>α</sub> is slightly higher and the relaxation peak is sharper in Nafion-TEA-casting compared to that of Nafion-TEA-extruded. The slightly higher value of T<sub>α</sub> could be due to ***more dense packing of ionic domains in Nafion-TEA-casting***. In addition, sharpness of the relaxation peak corresponds to the fact that larger population of chains is relaxing at the same time at a particular temperature. This could mean that ***ionic domains are more homogeneously organized in Nafion-TEA-casting*** compared to Nafion-TEA-extruded.
4. In addition to α-relaxation at ~100°C, ***another overlapped relaxation peak*** in the temperature range of 50-60°C is observed for the casting based membrane. The appearance of this additional peak could be due to following possibilities:

- a) Since ***β-relaxation*** peak seems be very broad (appears in the temperature range of -40 to 60°C), it could superimpose with ***α-relaxation***. On deconvolution of these two peaks, one could find the area corresponding to the overlapping responses of both these peaks. This common area could generate a hump alongside ***α-relaxation***.
- b) It could also be associated to conformational relaxation modes of the polymer chains in the hydrophobic PTFE domain (discussed in the previous chapter). These ***conformational relaxation modes of fluorocarbon backbone chain could be more clearly visible in the case of casting based membrane*** due to the reorganization of chains during casting process and annealing treatment.

Moore et al. observed similar dynamic response for the recast and annealed Nafion<sup>®</sup> membranes neutralized with tetrabutylammonium (TBA) in the temperature range of 50-120°C. They reported two overlapping relaxations in the temperature range of 70-120°C (first one at 78°C and second at 118°C) in place of one  $\alpha$ -relaxation but no  $\beta$ -relaxation in the temperature range of -50 to 0°C<sup>(7,8)</sup>. The interesting point to note is that they observed similar  $\tan\delta$  profiles for TBA neutralized recast as well as extruded Nafion<sup>®</sup> membrane, unlike in the case of Nafion-TEA. In order to understand the behavior of TBA neutralized membranes and verify the assignment for the molecular origins of the relaxations, Moore et al. characterized recast membranes with mixed counter ions (i.e. Sodium and TBA) having different compositions. Sodium-only neutralized membrane exhibited a strong  $\alpha$ -relaxation at 244°C and a weak  $\beta$  relaxation at 160°C and these two relaxations moved towards lower temperature in uniform fashion exhibiting decreasing magnitude of  $\alpha$ -relaxation and increasing magnitude of  $\beta$ -relaxation with increasing TBA content. Hence, in the case of TBA-only neutralized Nafion<sup>®</sup>, the first one (at 78°C) was assigned as  $\beta$ -relaxation and second one as  $\alpha$ -relaxation (at 118°C) by them.

From these experimental observations on temperature dependent storage modulus and  $\tan\delta$  profiles of both the types of Nafion-TEA membranes, following ***conclusions*** can be drawn:

- When Nafion-TEA membrane is elaborated by casting method, an improvement in the long range crystalline order and/or size of lamellar crystallites could occur.
- Moreover, casting method could result in more homogeneously and densely organized ionic domains in Nafion-TEA membrane.



- Both the above mentioned phenomena could have additional effect on the mobility of side-chains of Nafion-TEA. This reduced mobility of side-chains in Nafion-TEA could be another reason for the appearance of  *$\beta$ -relaxation* at higher temperatures for casting based membrane.
- This could probably result in better thermo-mechanical properties at temperatures above 150°C. Hence, the scenario could be: when the polymer chains start to slide pass each other above  $T_{\alpha}$ , the crystallites (in the PTFE backbone) which are better organized and/or larger in size prevent the membrane from flowing completely thereby help in retaining a storage modulus of around 1 MPa up to 180°C.

### c. Conductivity

The Arrhenius plots of conductivity for Nafion-TEA-extruded and Nafion-TEA-casting in anhydrous conditions are shown in figure 5. The ionic conductivity for Nafion-TEA-casting is relatively lower compared to Nafion-TEA-extruded up to 100°C. *Above 100°C, both the membranes demonstrate similar conductivities.* It is interesting to note that the proton of ionic liquids based on perfluorinated anion and triethylammonium is carried by the amine through ammonium cation in anhydrous conditions (discussed in the bibliographical chapter). In the case of Nafion-TEA membranes, the conductivity should be similar and involve conduction of proton primarily through diffusion/migration of ammonium species in the ionic domains. These ionic domains are packed in a peculiar “string-like” fashion. Hence ammonium being a bulky group is not so mobile already to diffuse easily through the ionic zone. Moreover, it has been proposed in the previous parts of this section that casting based membrane:

- acquires more densely packed PTFE backbone chains at nanoscale (evidenced by WAXS).
- exhibits improved long range crystalline order and/or larger crystallites of perfluorinated chains (proposed on the basis of SANS and DMA results).
- consists of more densely packed and homogeneously organized ionic domains (proposed on the basis of DMA results).

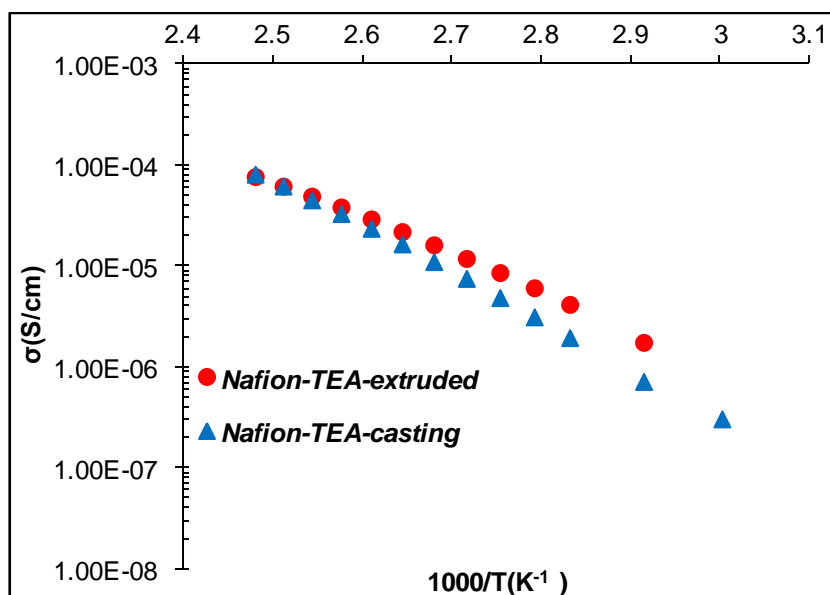


Figure 5: Conductivity vs temperature of Nafion-TEA elaborated by two different methods

These factors would definitely result in lower mobility and higher rigidity of side-chains carrying ionic functions. Hence, the diffusion of ammonium species would be even more difficult in Nafion-TEA-casting compared to Nafion-TEA-extruded especially at temperatures lower than  $T_g$ . Thus, it can be said that conductivity results are consistent with the results on morphology and DMA analysis.

#### d. Gas permeability

The  $H_2$  and  $O_2$  permeability coefficients measured on extruded as well as casting based Nafion-TEA membrane are presented in table 1. It has been discussed in the previous chapter that the permeation of dry gases occurred through the hydrophobic phase of Nafion- $H^+$ . However, an additional contribution of the ionic domains to the permeation mechanism should also be considered in the case of Nafion-TEA-extruded. This additional contribution is probably due to the presence of a bulky alkyl ammonium and consequent existence of weak dipole-dipole interactions in the ionic phase of Nafion-TEA in place of strong hydrogen bonding networks of Nafion- $H^+$ . On comparing the results of table 1, it can be observed that **going from Nafion-TEA-extruded to Nafion-TEA-casting leads to an overall decrease in the permeability coefficients** by a factor in the range of 1.1-1.4 depending on the gas. This decrease further supports the hypothesis derived from the results of other characterizations discussed before in this section:

- An improvement in the polymer chain packing and/or long range order as well as larger size of lamellar crystallites in the membrane (based on results of WAXS, SANS and DMA) in casting based membrane
- Better packing and organization of ionic domains (based on results of DMA) in Nafion-TEA-casting

These two effects would collectively result in reduced free volume and hence lower permeability coefficients for Nafion-TEA-casting. Various previous works have also reported lower permeability coefficients of oxygen, hydrogen and neutral compounds like glucose, hydroquinone, trimethylammonium-substituted ferrocene etc. for recast and annealed Nafion-H<sup>+</sup> membrane in comparison to extruded Nafion-H<sup>+</sup> membrane<sup>[9,10]</sup>.

<i>Sample</i>	<i>H<sub>2</sub> (barrer)</i>	<i>O<sub>2</sub> (barrer)</i>
<i>Nafion-TEA-extruded</i>	<i>10.2</i>	<i>2.5</i>
<i>Nafion-TEA-casting</i>	<i>9.3</i>	<i>1.8</i>

*Table 1: Permeability coefficients value of different gases for Nafion-TEA elaborated by two different methods (The uncertainty is estimated to be ±5%).*

#### *e. Water Sorption*

Apart from different properties discussed above, water sorption behavior of these membranes has also been studied. In this regard, water sorption isotherms (percent mass gain versus water activity) and kinetics (the half sorption time “t<sub>1/2</sub>” versus water activity) have been compared as shown in figure 6 and figure 7 respectively.

From Figure 6, it can be clearly seen that the water sorption isotherms of both the type of membranes *exhibit B.E.T. III shape* at 25°C. Moreover, *Nafion-TEA-casting is characterized by a slightly higher water uptake compared to Nafion-TEA-extruded* in the middle range of water activity and almost similar amounts of water at low water activity (below 0.2) on one hand and at high water activity (above 0.8) on the other hand. Small differences in water uptakes for recast-annealed Nafion-H<sup>+</sup> membrane compared to extruded one have also been observed in the literature<sup>[5,11,12]</sup>. However, the more hydrophilic membrane was either the recast membrane or the extruded one, depending on the authors and on the conditions of preparation.

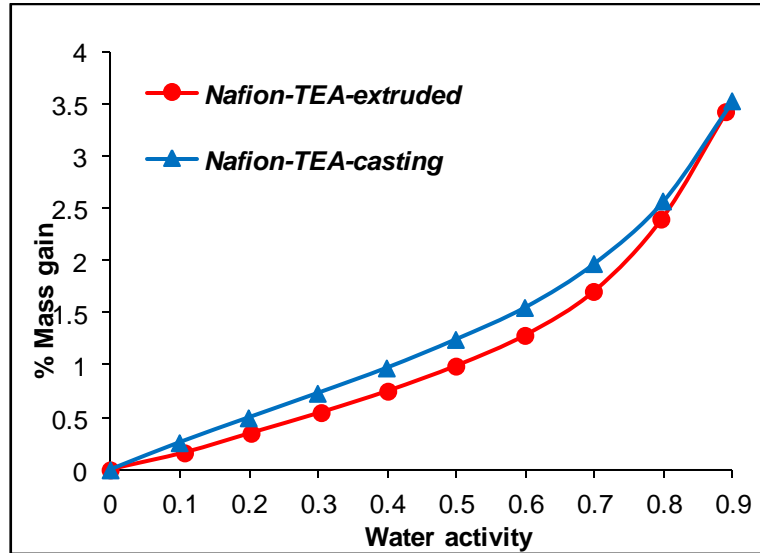


Figure 6: Water sorption isotherm of the Nafion-TEA membranes elaborated by two methods

In order to go deeper in the water sorption analysis, modeling of the isotherms by GAB equation was performed. According to the GAB parameters reported in Table 2, it seems that:

1.  $M_m$  and  $K$  are very similar for both the types of Nafion-TEA membranes. This result indicates that the *available sorption sites are similar in both membranes*, being consistent with the similar chemical composition of the membranes. Moreover, the water molecules involved in the water aggregates present a similar behavior in both types of membranes.
2. However,  $C_g$  value is significantly higher for the Nafion-TEA-casting in comparison with Nafion-TEA-extruded. This result indicates that water sorption on the first sorbed water molecules is favored in Nafion-TEA-casting.

<i>Sample</i>	<i><math>M_m</math></i>	<i><math>C_g</math></i>	<i><math>K</math></i>
<i>Nafion-TEA-extruded</i>	<i>0.009</i>	<i>2.28</i>	<i>0.853</i>
<i>Nafion-TEA-casting</i>	<i>0.01</i>	<i>3.63</i>	<i>0.819</i>

Table 2: GAB parameters for the two types of Nafion-TEA membranes

The small differences in the water uptake of Nafion-TEA-casting and Nafion-TEA-extruded only observed at middle water activity should be related to the hypothesis (proposed from the results of DMA) that Nafion-TEA-casting exhibits homogeneous organization of ionic domains. This organization should allow to accommodate a slightly higher equilibrium water uptake at middle activity without modifying the water uptake at low activity, which is essentially governed by the

chemical composition of the membrane and the water uptake at high activity which is defined by the global swelling ability of the membrane.

The kinetics of water sorption expressed as the half sorption time,  $t_{1/2}$  versus water activity for both the types of membranes are presented in figure 7. First of all, it can be clearly seen that the two membranes exhibit the same shape of kinetics curve. Two domains are clearly distinguished in agreement with the BET III sorption mechanism: the first domain up to water activity of 0.7 is characterized by a constant value of  $t_{1/2}$  and the second domain at high activity in which water clustering takes place shows an increase of  $t_{1/2}$  value. However, values of  $t_{1/2}$  obtained for Nafion-TEA-casting are much higher compared to Nafion-TEA-extruded in all the range of water activity. The *slowdown in water diffusion rate observed in Nafion-TEA-casting membrane* is in agreement with the various hypotheses made with the previous results especially the increase in the long range order and/or size of lamellar crystallites collectively resulting in increase of rigidity of the membrane thereby lowering the rate of diffusion of water molecules.

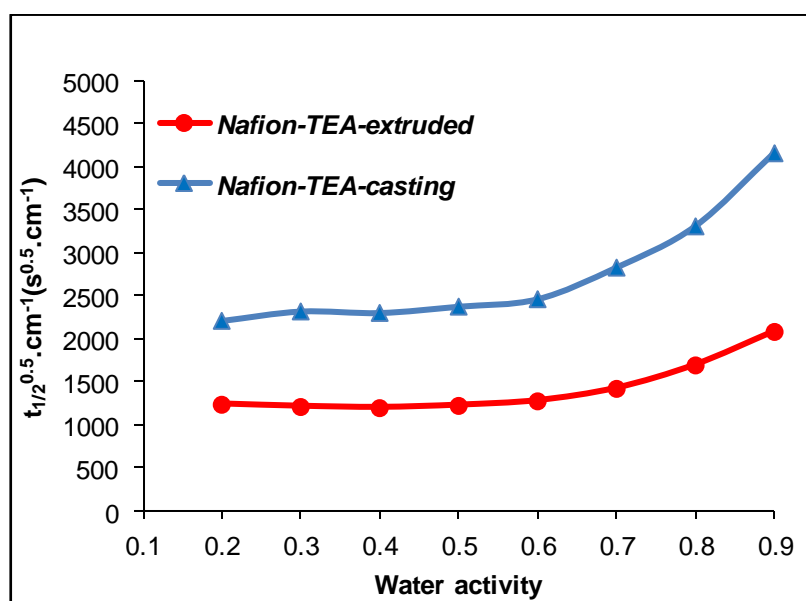


Figure 7: Water sorption kinetics ( $t_{1/2}$  versus water activity) of the Nafion-TEA membranes elaborated by two methods

## Conclusion

In summary, correlation of morphology and functional properties of Nafion-TEA membrane based on different elaboration methods have been attempted in this section. However, special attention should be paid to the fact that different characterizations were carried out under different sets of variable parameters namely measurement conditions, temperature and presence of water to list a few.

### 3.2: TFTEA doped Nafion-TEA membranes: Comparison of properties based on elaboration method

In this section of the chapter, the impact of TFTEA-doping level as well as preparation methods (casting and swelling) on various properties of doped membranes has been discussed. Casting based TFTEA doped Nafion-TEA membranes were elaborated by similar method as employed for Nafion-TEA-casting. The different concentrations obtained and related  $\lambda$  values are shown in table 3. The membranes were cast with up to 20 wt % of TFTEA and they were found to be stable against leaching phenomenon. However, the membrane with 20 wt% TFTEA was not transparent but translucent.

<i>Sample</i>	<i>% TFTEA (by weight)</i>	<i>% TFTEA (by volume)</i>	<i>Moles TFTEA/ moles <math>SO_3^-</math>- <math>^+HN(C_2H_5)_3</math> of Nafion-TEA  (<math>\lambda</math>)</i>
<i>Nafion-TEA+5%TFTEA</i>	<i>5</i>	<i>6.3</i>	<i>0.25</i>
<i>Nafion-TEA+10%TFTEA</i>	<i>10</i>	<i>12.8</i>	<i>0.53</i>
<i>Nafion-TEA+15%TFTEA</i>	<i>15</i>	<i>18,4</i>	<i>0.85</i>
<i>Nafion-TEA+20%TFTEA</i>	<i>20</i>	<i>24.2</i>	<i>1.12</i>

Table 3: Concentration and  $\lambda$  values for different casting based Nafion-TEA+xwt% TFTEA membranes (Density of Nafion-TEA-casting:  $1.79\text{g/cm}^3$ ; Density of TFTEA:  $1.4\text{g/cm}^3$ )

The results will be presented and discussed in similar manner in this section as presented in the previous section of this chapter.

#### a. Morphology

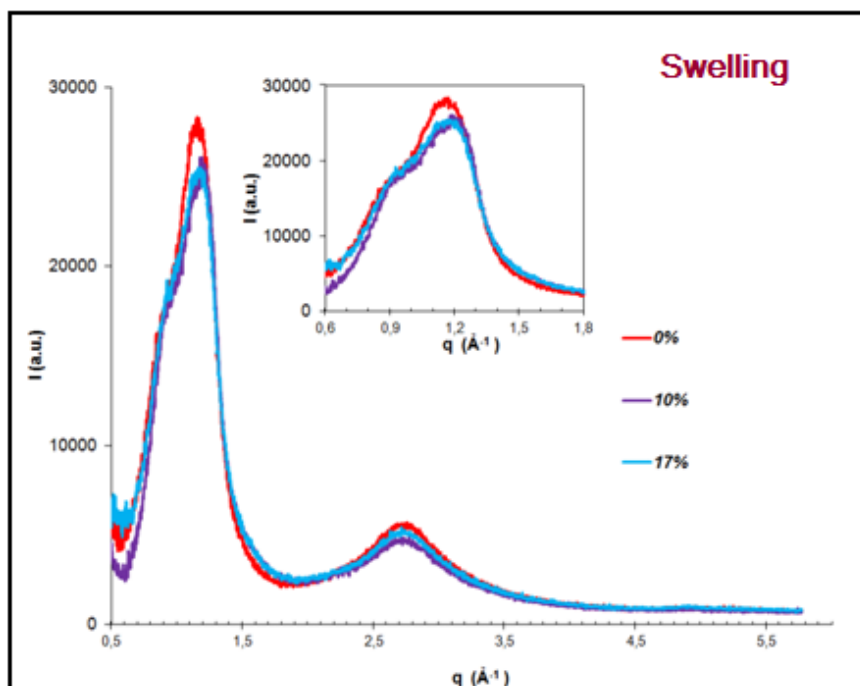
The morphology of TFTEA doped membranes prepared by both the methods were compared by using WAXS and SANS in similar fashion as in the previous section. Both the sample preparation and the measurements were carried out under same conditions. Two effects have been studied here:

- ❖ Impact of TFTEA addition and its concentration on the morphology of Nafion-TEA.
- ❖ Impact of elaboration method

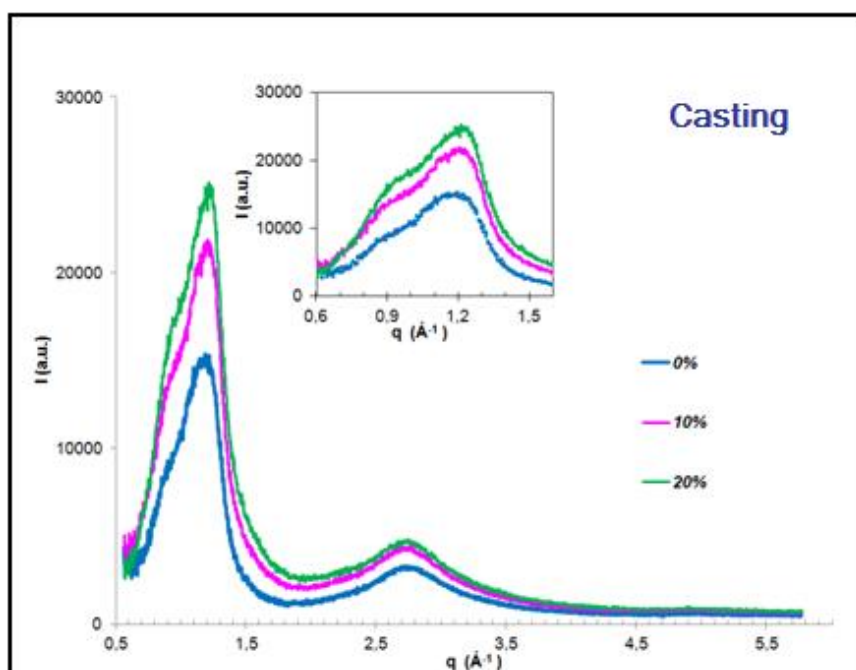
### Molecular scale

WAXS measurements were carried out on the both types of TFTEA doped membranes. The WAXS profiles of swelling based and casting based doped membranes are shown in figure 8 (a) and (b) respectively. From the WAXS profiles of both the types of doped, it can be seen that:

1. In the case of swelling based doped membranes, the tip of the superimposed crystalline-amorphous peak (observed at  $q = 1.14 \text{ \AA}^{-1}$ ;  $d = 5.51 \text{ \AA}$  for Nafion-TEA-extruded) shifts very slightly towards higher  $q$  value ( $q \sim 1.17 \text{ \AA}^{-1}$ ;  $d = 5.36 \text{ \AA}$ ) on TFTEA addition. Concerning casting based doped membranes, this broad peak (observed at  $q = 1.18 \text{ \AA}^{-1}$ ;  $d = 5.32 \text{ \AA}$  for Nafion-TEA-casting) shifts to higher  $q$  value ( $q \sim 1.21 \text{ \AA}^{-1}$ ;  $d = 5.19 \text{ \AA}$ ) like in the case of swelling based membranes but the shift is more significant for casting ones. This peak corresponds to the packing of hydrophobic PTFE chains. The change in its position towards higher  $q$  value underlines the fact that presence of TFTEA promotes *more compact packing of the hydrophobic chains of Nafion-TEA in the doped-hybrid membrane*. Interestingly, the *effect is more significant when the membrane is elaborated by casting method*. Moreover, the wt% content of TFTEA present in the system seems to have negligible effect on the shift of this peak in both the types of doped membranes i.e. the shift in the position of the peak is similar for different contents of TFTEA in the membrane studied in this work.
2. The halo at  $q \sim 0.80 \text{ \AA}^{-1}$  and the crystalline peak at  $q = 2.75 \text{ \AA}^{-1}$  do not get changed on TFTEA addition in both the kinds of doped Nafion-TEA membranes.



(a)



(b)

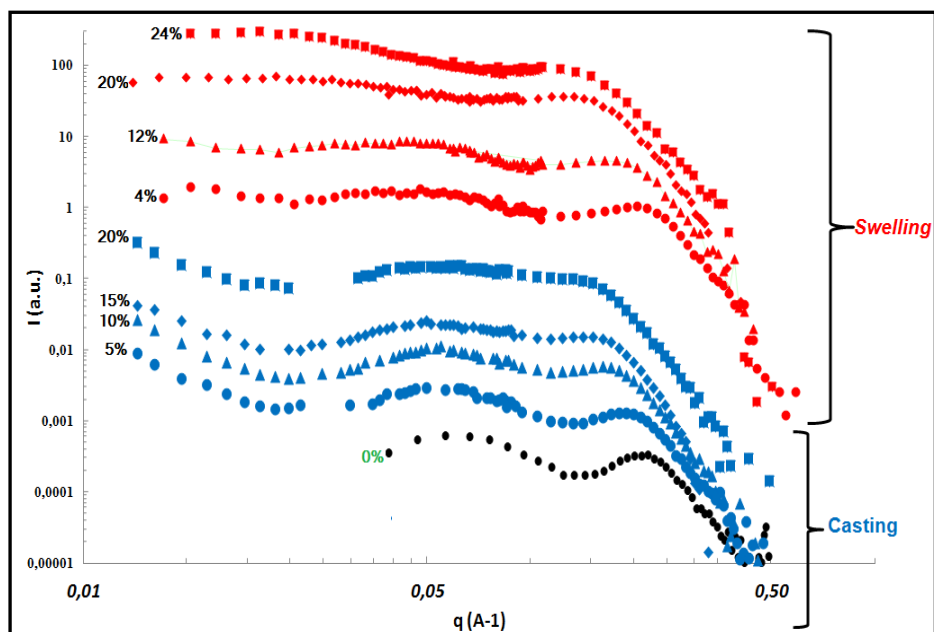
Figure 8: WAXS profiles of TFTEA doped Nafion-TEA membranes elaborated by (a). Swelling;  
(b). Casting



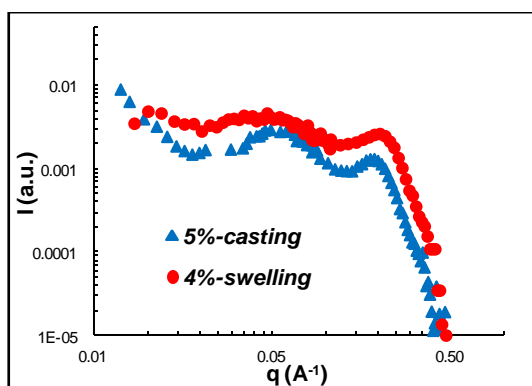
### Nanoscopic-mesoscopic scale

In addition, the morphologies of these two types of TFTEA doped membranes were compared at a larger length scale using SANS measurements. The conditions of the sample preparation and measurements were similar to those described in the previous section. The SANS profiles of casting and swelling based Nafion-TEA + x% TFTEA doped membranes are presented in figure 9 (a) on a log-log scale. Moreover, a comparison of both kinds of membranes for different weight percentages has been shown in figure 9(b)-(d). An offset has been applied along the intensity scale for clarity after subtraction of a constant background due to hydrogen incoherent scattering. After the first glance at the spectra, few similarities can be accounted such as:

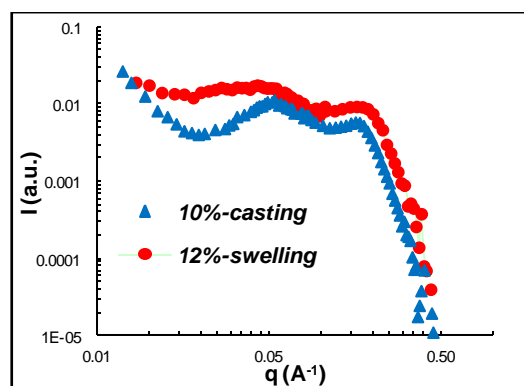
1. The evolution of the spectra for casting based doped membrane is similar to swelling based doped membranes.
2. Since both the peaks (ionomer peak and matrix knee) are observed, it means that the membranes *keep their nano-structuration* on TFTEA addition.
3. Moreover, these peaks broaden and shift towards lower value of wave vector  $q$  with increasing TFTEA content. This means that there is *an increase in the characteristic size of nano-phase separation upon TFTEA addition*.
4. In addition, all the membranes demonstrate  $q^{-4}$  behaviour (Porod's law) at high  $q$  values pointing toward sharp interface at sub-nanometric level and hence *a well phase-separated system*, as also observed in water-swollen acidic Nafion<sup>®</sup>.



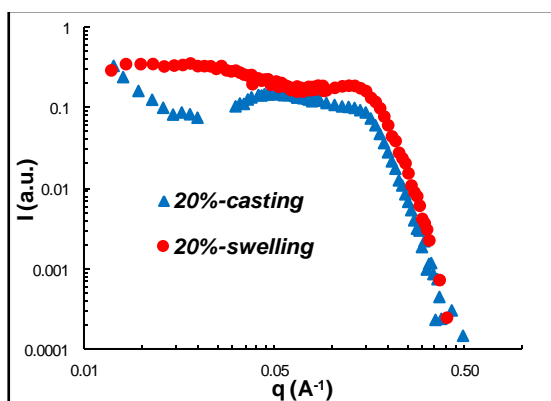
(a)



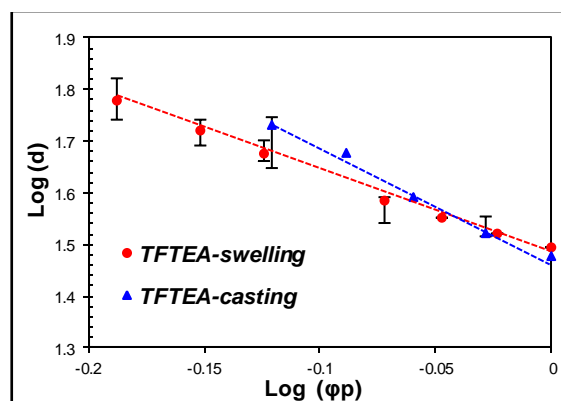
(b)



(c)



(d)



(e)

Figure 9: (a). SANS profiles of casting and swelling based TFTEA doped membranes; (b)-(d). Comparison of SANS profiles of casting and swelling based membranes doped with similar TFTEA

content; (e): Dilution law  $\log(d)=f(\log\phi_p)$  of casting and swelling based Nafion-TEA+x wt%TFTEA membrane,  $d$  being the characteristic correlation distance obtained as  $2\pi/q^*$  with  $q^*$  the ionomer peak position, and  $\phi_p$  the polymer volume fraction

However considering the position and shape of the two peaks for different concentrations of TFTEA in both the types of doped membranes, few differences can be observed which are:

1. Concerning **ionomer peak**, it seems that the shift as well as the broadening of this peak is similar for both the types of doped membranes at low TFTEA contents (figure 9(b)-(c)). However, the shift seems to be larger in the case of casting based membranes compared to swelling based membranes for high TFTEA content (figure 9(d)). Additionally, the ionomer peak seems to start broadening at lower concentrations of TFTEA for the casting membranes in comparison to swelling based ones. This could be explained by a more heterogeneous distribution of TFTEA in the ionic domains from lower TFTEA concentrations in the former.

Hence, in order to better understand and quantify the increase in the size of ionic domains with TFTEA addition, the evolution of the mean separation distance between inter-connected ionic domains with increasing TFTEA content was analysed for both the types of membranes. This was done by using the characteristic distance “ $d$ ” (calculated from the ionomer peak’s position  $q^*$  using the formula  $d=2\pi/q^*$ ) as a function of PCIL content. Figure 9(e) presents the plot of  $\log(d)$  as a function of  $\log(\phi_p)$  ( $\phi_p$ : volume fraction of Nafion-TEA) for both types of doped membranes. This plot is also known as “dilution law”. The  $q$  value of ionomer peak utilized to calculate “ $d$ ” for each TFTEA wt% was obtained by visual observation (by taking the  $q$  value at which the intensity was maximum) as well as different curve fitting methods. The differences in those values have been presented by error bars shown on the figure 9(e). From figure 9(e), it seems that the dilution law is very similar for both the types of doped membranes at low TFTEA concentration. However, a higher deviation is observed for casting ones compared to swelling ones from 15 wt% TFTEA content. This underlines higher mean separation distance between inter-connected ionic domains implying **a greater characteristic size of ionic domains in casting based membranes**. For instance, at 20 wt% TFTEA content, the characteristic mean separation distance is 54 Å for casting based membrane in comparison to 47 Å for swelling based membrane. However, one must pay attention to the difficulty of extracting a peak position from the spectra because of overlapping of ionomer peak with the matrix knee especially at high PCIL content.

Similar evolution of morphology of the recast Nafion<sup>®</sup> membrane (acidic form) in the presence of water molecules has been reported by Sacca et al<sup>[5]</sup>. The recast Nafion<sup>®</sup> membrane presented much larger size of ionic domains (mean separation distance of 53 Å) than extruded Nafion<sup>®</sup> membrane (mean separation distance of 43 Å) after swelling both the membranes up to saturation by dipping in water.

2. Now, regarding the *matrix knee*, it can be clearly observed that it shifts and broadens to lesser extent in casting based membrane compared to swelling based membrane when TFTEA is content is small i.e. 5wt% (figure 9(b)). On further increasing the content of TFTEA, the matrix knee neither shifts nor broadens extensively in the casting based membrane unlike swelling based membranes (figure 9(c)-(d)). This result points towards much *less significant effect of TFTEA addition on the long range crystalline order of Nafion-TEA when elaborated by casting method* compared to the swelling method. Moreover, *hydrophobic domain seems to be organized more homogeneously in casting based ones* due to lower broadening of the matrix knee. Sacca et al. reported similar evolution of matrix knee for recast Nafion<sup>®</sup> membrane (acidic form) in the presence of water molecules<sup>[5]</sup>.

In a nutshell, the *main differences observed between casting based and swelling based doped membranes* from morphological point of view can be listed as:

- The PTFE backbone chains are more densely packed in casting based TFTEA doped membranes.
- There is more prominent and/or inhomogeneous increase in the size of the ionic domains in the casting based membranes compared to swelling based membranes at high concentration of TFTEA.
- There seems to be less significant effect of TFTEA addition on the crystalline order of Nafion-TEA in the casting ones compared to swelling ones. Moreover, crystallites in the hydrophobic domain seem to be organized more homogeneously in casting based ones.

These peculiar results on the morphology of casting based membranes can be attributed to the fact that these membranes are elaborated in the presence of a polar solvent and the system is in solution form in the beginning, unlike in the case of swelling based membranes where the ionic liquid is made to enter into a pre-developed morphology of commercial membrane.

On the basis of these results, it would be very interesting to ponder over the type of distribution as well as organization of TFTEA in the Nafion-TEA matrix in the casting based membranes. The probable scenarios of the development of the morphology of these casting based doped membranes will be discussed now.

The polymer and the ionic liquid are dissolved in a solvent in the beginning and this solvent is evaporated afterwards. During gradual evaporation of the solvent, there are two possibilities for the types of organization as well as distribution of the ionic liquid molecules within the membrane morphology such as:

1. The ionic liquid molecules could distribute themselves *homogeneously in the ionic domains of Nafion-TEA* and hence increasing the mean separation distance of the membrane. In this case the ionic liquids are in strong interaction with the ionic function of Nafion-TEA.
2. The ionic liquid molecules could prefer to auto-organise to form TFTEA aggregates/ *micelles* ( $\text{SO}_3$  as the head of the micelle)/*reverse micelles* ( $\text{CF}_3$  as the head of the micelle) during the solvent evaporation process. Auto-organization of ionic liquids has been reported in the literature<sup>(13)</sup>. This type of organization of TFTEA molecules would result in *heterogeneous distribution of TFTEA in the Nafion-TEA matrix*. The few possibilities about the location of these micelles in the matrix of Nafion-TEA are:
  - a) TFTEA aggregates/micelles could be located in the ionic domains close to the hydrophobic-hydrophilic interface and hence well-separated from hydrophobic domains of Nafion-TEA. In this case, it would affect less the local crystalline order of Nafion-TEA. Additionally, the presence of TFTEA aggregates could decrease the plasticizing effect of TFTEA on ionic domains due to lesser interactions between TFTEA and ionic functions of Nafion-TEA.
  - b) TFTEA aggregates/micelles could be located at the hydrophobic-hydrophilic interface of Nafion-TEA. But it has been previously discussed that these doped membranes exhibit porod's law meaning a sharp interface at sub-nanometric scale and hence a well separated interface. Hence, this option of the distribution of TFTEA aggregates is not feasible as this would lead to disruption of the sharp hydrophobic-hydrophilic interface of the system. However, if it organizes itself at the hydrophobic-hydrophilic interface in such a manner that the hydrophobic part of the aggregate is in interaction with the hydrophobic main-chains of Nafion-TEA while hydrophilic is in interaction with the

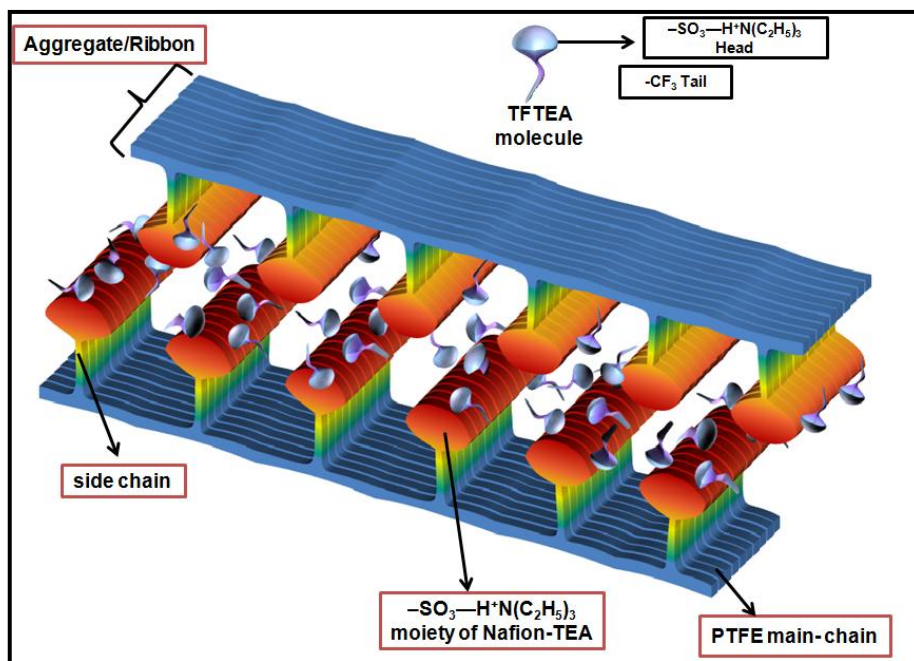
ionic side-groups of Nafion-TEA and hence no disruption of the interface, then it could be feasible.

- c) There is another possibility that the ionic liquid molecules can form reverse micelles during solvent evaporation process and gets trapped in the hydrophobic domains of the polymer. However this possibility is kinetically/energetically less probable and no significant evidence has been found from these results on morphology supporting this hypothesis.

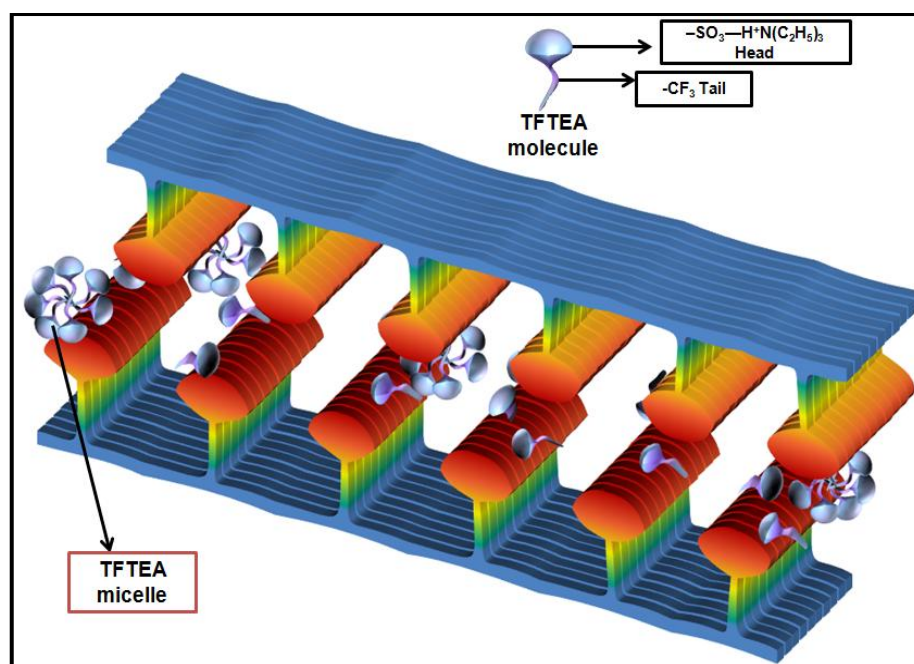
Hence, from all the possibilities discussed above, we propose that:

- ❖ The ionic liquid is homogeneously distributed in the ionic domains of Nafion-TEA by dipole-dipole interactions between the TFTEA and ionic function of Nafion-TEA (presented in figure 10 (a)). This case more probable for low concentration of TFTEA.
- ❖ During the solvent evaporation, the ionic liquid molecules auto-organise (TFTEA aggregates/micelles) in the ionic domains of Nafion-TEA consequently leading to an inhomogeneous distribution of TFTEA (presented in figure 10 (b)). This case is more probable for the membranes with high TFTEA concentration.

*(Note: The ionic entity “ $-SO_3-H^+N(C_2H_5)_3$ ” of the PCIL is shown smaller in size compared to that of Nafion-TEA in the picture for clarity; The organization of the anionic entity of the ionic liquid is mainly focused in the schematic representations of figure 10.)*



(a)



(b)

Figure 10: Types of distribution of TFTEA moieties in the ionic domains of Nafion-TEA: a). Homogenous distribution; b). Inhomogeneous distribution due to formation of micelles of TFTEA (The ionic entity " $-\text{SO}_3-\text{H}^+\text{N}(\text{C}_2\text{H}_5)_3$ " of the PCIL is shown smaller in size compared to that of Nafion-TEA in the picture for clarity.)

### **b. Differential Scanning Calorimetry**

DSC measurements were also carried out in order to gain further information on the distribution and/or organization of the PCIL within the polymer matrix if possible. *No melting peak corresponding to pure TFTEA or TFTEA aggregates had been observed for the casting method doped membranes similarly as for swelling based membranes* from these measurements. This signifies complete dispersion of the PCIL into the ionic domains of Nafion-TEA. Even if some TFTEA aggregates are formed, their critical size might not be enough high to crystallize and hence not detected by DSC measurements.

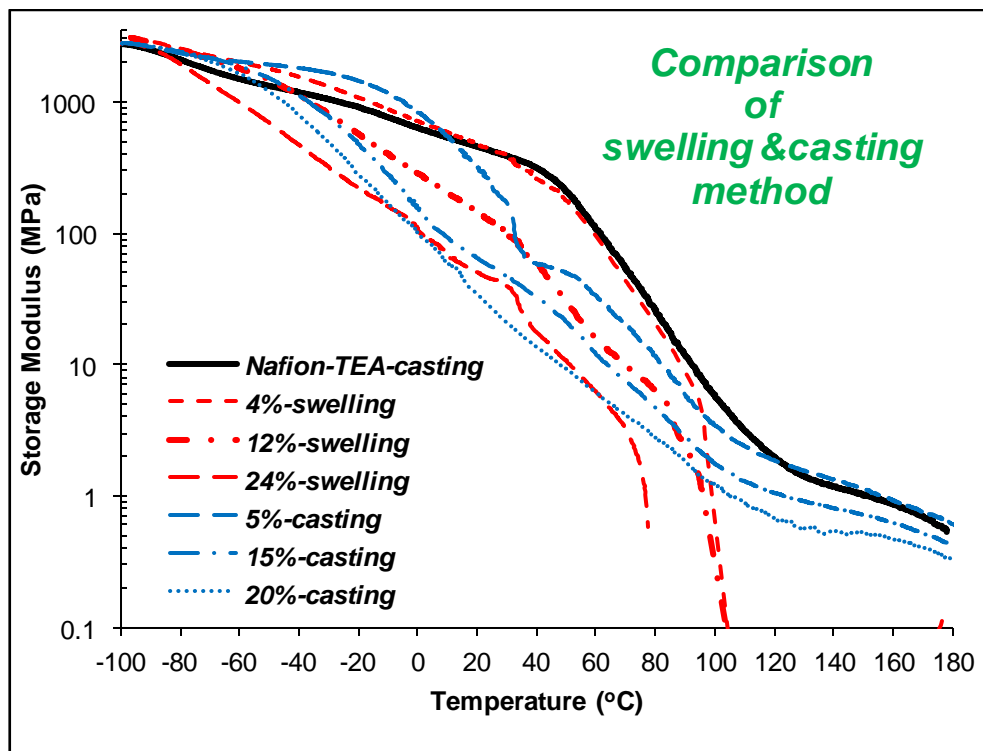
### **c. Thermo-mechanical properties**

The evolution of thermo-mechanical properties in the case of casting based membranes was evaluated and compared with swelling based membranes. Figure 11 (a) and (b) present the storage modulus and  $\tan\delta$  as a function of temperature respectively for both the kinds of doped membranes.

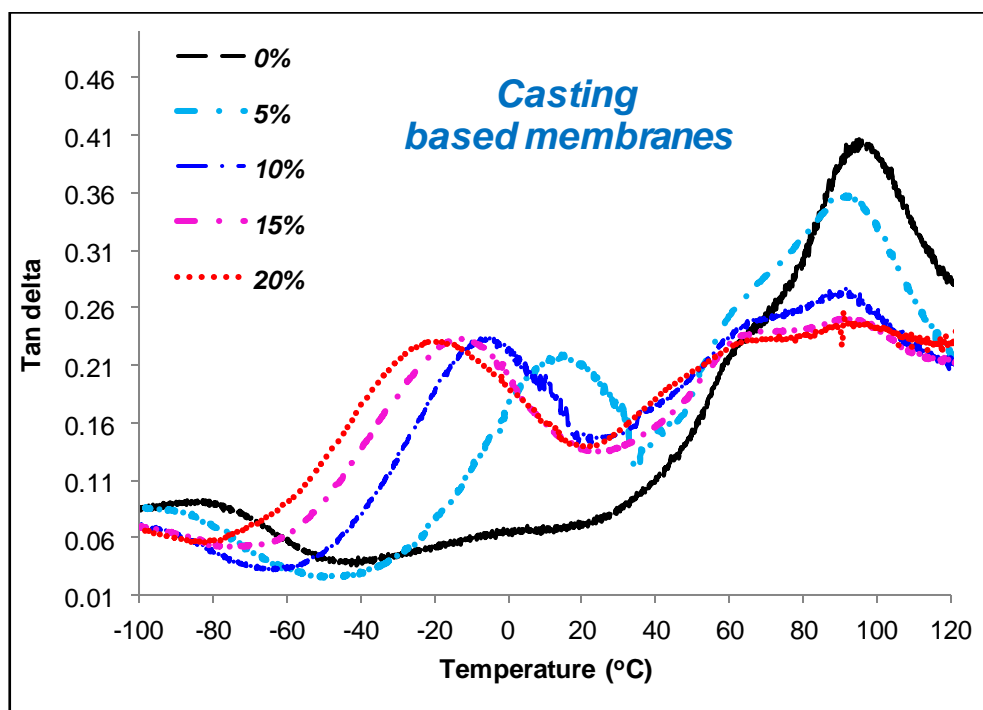
#### **Storage Modulus versus Temperature**

From figure 11 (a), *similar effect of TFTEA addition on the mechanical stability for both types of doped membranes can be observed up to 100°C*. A decrease of storage modulus with increasing TFTEA content in the range of -80°C to 60°C is observed for all the casting based membranes, similarly as in the case of swelling based membranes. This indicates the complete dispersion of TFTEA in the ionic domains of Nafion-TEA membrane (no phase separation between Nafion and TFTEA). These results are in agreement with the *DSC measurements where no melting temperature corresponding to pure TFTEA* has been observed for all the casting based doped membranes. However, above 100°C, the casting based membranes do not collapse and retain a storage modulus of 1-2 MPa in the range of 100-180°C, unlike swelling based membranes which collapse at temperatures close to 100°C depending upon the TFTEA content. This underlines relatively *better thermo-mechanical properties of casting based membranes* at high temperatures. This result could be explained with the same hypothesis that casting based membranes exhibit better organization/efficient packing of hydrophobic chains having *more significant long range crystalline order*. Also we suppose by casting method a better chain entanglements is obtained. The higher chain entanglement density along with long range crystalline order could prevent the chain slipping before the melting of the crystallites.

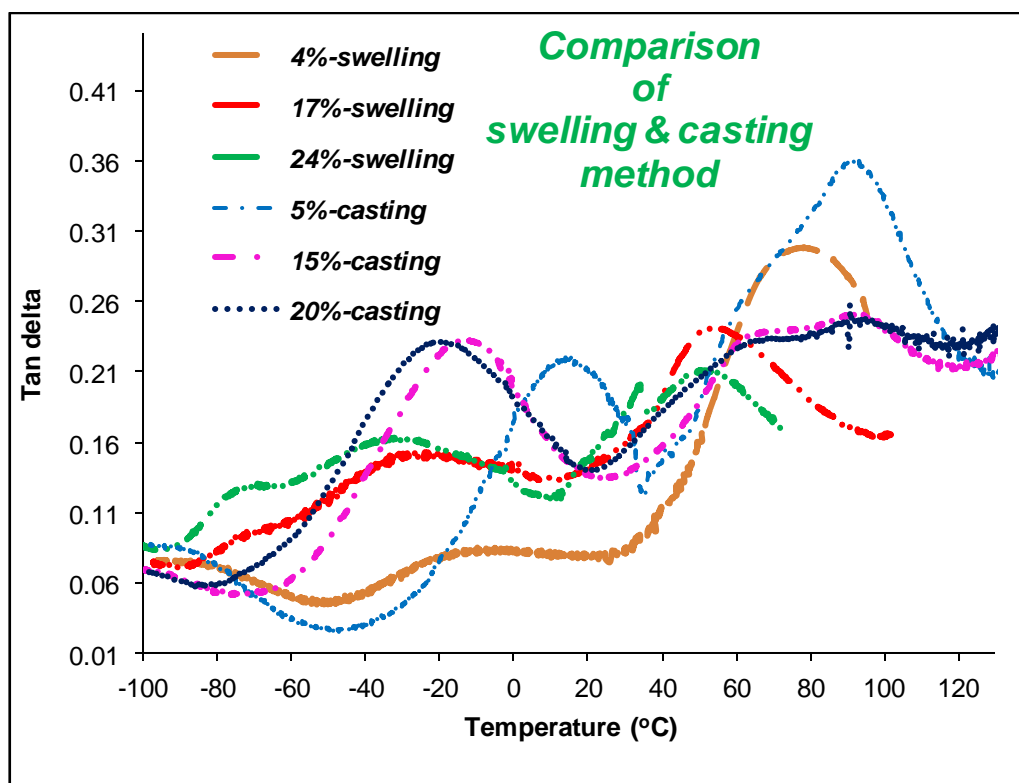




(a)



(b)



(c)

Figure 11: DMA profiles of TFTEA doped Nafion-TEA membranes elaborated by two methods; a). comparison of Storage modulus vs Temperature profiles; b).  $\tan \delta$  vs Temperature profiles of membranes based on casting method; c). comparison of  $\tan \delta$  vs Temperature profiles

### Tan $\delta$ versus Temperature

The  $\tan \delta$  versus temperature plots for casting based membranes is presented in figure 11 (b). The comparison of these profiles for swelling and casting based doped membranes is illustrated figure 11 (c). The main features are discussed as follows:

1. Practically, no difference in the appearance of  $\gamma$ -relaxations was observed for both the kinds of pure Nafion-TEA membranes. In the case of both the kinds of doped membranes, it seems that the relaxation peak shifts to lower values in the beginning upon adding TFTEA into the polymer matrix (up to ~10 wt% TFTEA content in casting based membranes; up to ~5 wt% TFTEA content in swelling based membranes). Afterwards, no further shift in the relaxation peak is observed on further increasing the TFTEA concentration for both types.
2. Concerning  $\beta$ -relaxation related to the movements of hydrophobic main- chains as well as side-chains of Nafion-TEA, a very intense and large relaxation emerges in the temperature range of - 80 to 40°C for the casting based doped membranes (depending upon TFTEA concentration).

Moreover, it shifts towards lower temperatures with increasing TFTEA content. It can be noted that this relaxation peak was much less intense for virgin Nafion-TEA-casting. The stronger relaxation observed in the doped membranes in comparison to virgin membranes can be explained by the fact that the presence of TFTEA inside the matrix of Nafion-TEA could cause a reduction in the dipolar interaction crosslinks between the polyether side groups and consequently, could increase the number density of Nafion-TEA side chains involved in the  $\beta$ -mechanical relaxations.

Now we compare swelling and casting based membranes. It can be seen that it appears at higher temperatures and are much more *prominent in casting based membranes* compared to that of swelling based membranes. The increase in the temperature of its appearance for casting based membranes further corroborates the results from WAXS and SANS. Thus, it supports the hypothesis done for casting based membranes i.e. perfluorinated chains are more densely packed and TFTEA influences the local crystalline order of crystallites to much lower extent in casting based doped membranes. The stronger intensity of the relaxation in casting based doped membranes signifies higher mechanical energy dissipated during the  $\beta$ -relaxation. This could be explained due to the fact that larger population of species relaxes at similar time (at similar temperature) due to their similar organization. This means that the perfluorinated chains are more homogeneously organized in casting based doped membranes (supporting the SANS results).

3. Concerning  *$\alpha$ -relaxation*, a slight shift with increasing TFTEA content has been evidenced for the casting based doped membranes. However, the peak intensity decreases significantly and peaks become broader with increasing TFTEA content. This result is in contrast with swelling based doped membranes where an important shift in temperature and a decrease in intensity have been observed. The slight shift in the case of casting ones could be due to *limited plasticization effect of TFTEA in casting based membranes probably due to its stronger and more prominent intra-micellar interactions (aggregation/micellar formation) in comparison to interactions with the ionic function of Nafion-TEA*. The broadening of the relaxation peak with increasing TFTEA content could be due to the different responses of domains of Nafion-TEA exhibiting different degrees of TFTEA's plasticization effect. Thus, the dipole-dipole interactions among some of the Nafion-TEA's ionic side-groups might not get much affected and consequently the relaxation is observed at the same position. However, decrease in its intensity with increasing TFTEA content could be due to diminishing population of ionic functions of Nafion-TEA showing close dipole-dipole interactions as virgin Nafion-TEA.

4. Moreover, the hump observed alongside  ***$\alpha$ -relaxation*** does not shift significantly as well on addition of TFTEA and/or increase in its concentration in the casting based membranes. This could be due to the following possibilities:
  - a) Let us first consider the assumption that this hump appears due to the convulsion of large  ***$\beta$ -relaxation*** with  ***$\alpha$ -relaxation***. In this case, the population of PTFE main-chains and side-chains 1.better organized or 2.associated with the un-plasticized ionic functions of Nafion-TEA could give the mechanical response of  ***$\beta$ -relaxation*** at the same temperature as that of pure membrane. Hence, the hump could remain at the same temperature.
  - b) Now, we assume that this hump is related to the conformational relaxation modes of the polymer chains in the hydrophobic PTFE domain. In this case, these ***conformational relaxation modes of fluorocarbon backbone chain could be still visible in the case of doped membranes as well*** due to the method of elaboration.

By collectively considering the results from WAXS, SANS and DMA measurements on casting based doped Nafion-TEA membranes, we propose that ionic liquid molecules organize and/or distribute in the following ways:

- 1). TFTEA molecules distribute themselves homogeneously in the ionic domains of Nafion-TEA by interacting with the ionic functions of Nafion-TEA when present in low concentration.
- 2). At higher concentration, we suppose that TFTEA molecules self-organize to some degree either in the form of aggregates/micelles and get distributed in the ionic domains of Nafion-TEA or at the interface. Indeed, the size of aggregates should to be nanometric while any melting point specific to pure ionic liquids have been measured. This phenomenon has been observed in the both kind of membranes but it appears at comparatively higher TFTEA concentration for the swelling based membranes ( $\lambda > 1$ ). Moreover in the case of membranes elaborated by casting, TFTEA does not change much the electro-static interactions between some of the ionic functions of Nafion-TEA.

In order to further understand how the structure of an ionic liquid influences:

- 1). ionic liquid's interactions with the host matrix;
- 2). the morphology of Nafion-TEA;
- 3). ionic liquid's distribution and organization in the Nafion-TEA matrix;

when elaborated by casting method, investigations on the systems based on Nafion-TEA and ionic liquids containing perfluorinated anions of different chain lengths will be discussed in Chapter 4.

#### d. Conductivity

The electro-chemical performance of these two types of doped membranes was also compared as shown in figure 12. The conductivity cells were prepared and closed in argon atmosphere as before to avoid any absorption of water. **Both the systems give conductivities of similar order.** However, no significant increase in conductivity is observed on further increasing TFTEA content above 15wt % TFTEA content i.e. the conductivities of the recast membranes with 15 and 20 wt% content of TFTEA content are similar. This could be related to the structuration of TFTEA in the ionic domain and the formation of larger or more aggregates at higher TFTEA concentration (20wt%) (as described in the previous sections). This structuration of TFTEA molecules could result in increase the viscosity/reduces mobility of TFTEA molecules and hence could limit increase in the conductivity at high TFTEA concentrations. This trend has been observed for swelling based membranes for 20 wt% and 24 wt% doping levels of TFTEA. This result further supports the idea that the heterogeneous distribution of TFTEA starts at lower TFTEA concentration for casting based membranes.

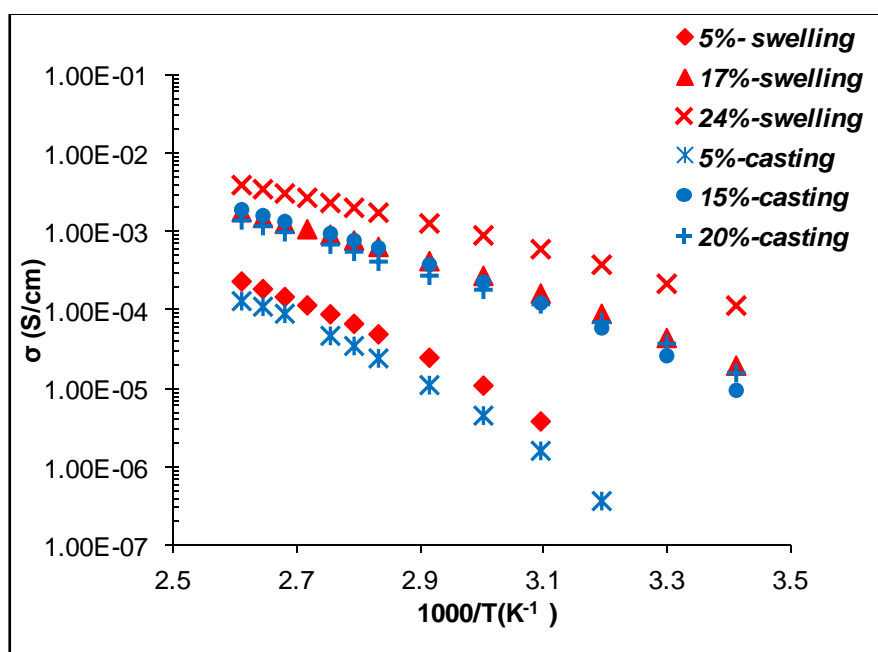


Figure 12: Ionic conductivities of TFTEA doped Nafion-TEA membranes elaborated by two different methods

***e. Gas permeability***

The gas permeability study and analysis performed on H<sub>2</sub> and O<sub>2</sub> on both the kinds of membranes demonstrate that ***casting based doped membranes show overall lower permeability coefficients compared to swelling based doped membranes*** for both the gases (table 4).

As for swelling based membranes, the variations of the gas permeability values as a function of TFTEA content remain small in casting based membranes too. The important point to note here is that despite the fact that casting based doped membranes exhibit either higher and/or heterogeneous swelling of the ionic domains (evident from SANS results) than swelling based membranes, the overall permeability of gases is lower for the former. These results further intensify the hypothesis that the chains in hydrophobic region of Nafion-TEA are better organized in the case of casting based doped membranes thereby limiting the gas-diffusion.

<i>Sample (wt%)</i>	<i>H<sub>2</sub> (Barrer)</i>	<i>O<sub>2</sub> (Barrer)</i>
<b><i>Nafion-TEA-extruded (0%)</i></b>	<i>10.2</i>	<i>2.5</i>
<b><i>5%-swelling</i></b>	<i>10.4</i>	<i>2.3</i>
<b><i>8%-swelling</i></b>	<i>9.6</i>	<i>2.4</i>
<b><i>12%-swelling</i></b>	<i>9.7</i>	<i>2.6</i>
<b><i>20%-swelling</i></b>	<i>7.1</i>	<i>2.7</i>
<b><i>Nafion-TEA-casting (0%)</i></b>	<i>9.3</i>	<i>1.8</i>
<b><i>5%-casting</i></b>	<i>9.6</i>	<i>2.04</i>
<b><i>10%-casting</i></b>	<i>8.8</i>	<i>1.92</i>
<b><i>15%-casting</i></b>	<i>6.2</i>	<i>1.7</i>
<b><i>20%-casting</i></b>	<i>6.5</i>	<i>1.92</i>

*Table 4: Permeability coefficients of different gases for Nafion-TEA+*x*wt%TFTEA membranes elaborated by two methods*

***f. Water Sorption***

The water sorption behavior was also analyzed for both the types of membranes at 25<sup>0</sup>C. All the casting based membranes were made to undergo a consecutive cycle of sorption and desorption in order to check their stability towards exposure to water vapor. Furthermore, no hysteresis phenomenon was observed as for the swelling based doped membranes. The water sorption isotherms for the two types of doped membranes are shown in figure 13. It can be observed that the isotherms for both the kinds of membranes are of ***B.E.T. III type with an expected increase of the water uptake as the TFTEA content increases in the membrane***. It is important to note that the recast membranes containing 15 and 20 wt% TFTEA show quite similar uptake of water. This could be related to more

prominent micellar formation of TFTEA molecules in 20wt% membrane which further limits the water sorption capacity of TFTEA in the Nafion-TEA matrix.

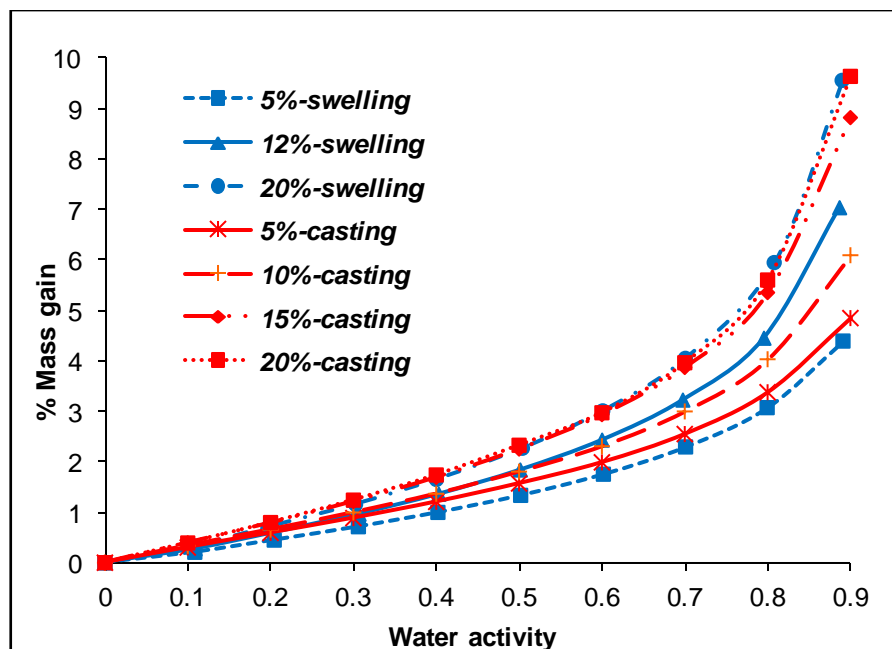


Figure 13: Water sorption isotherm of TFTEA doped Nafion-TEA membranes elaborated by two different methods

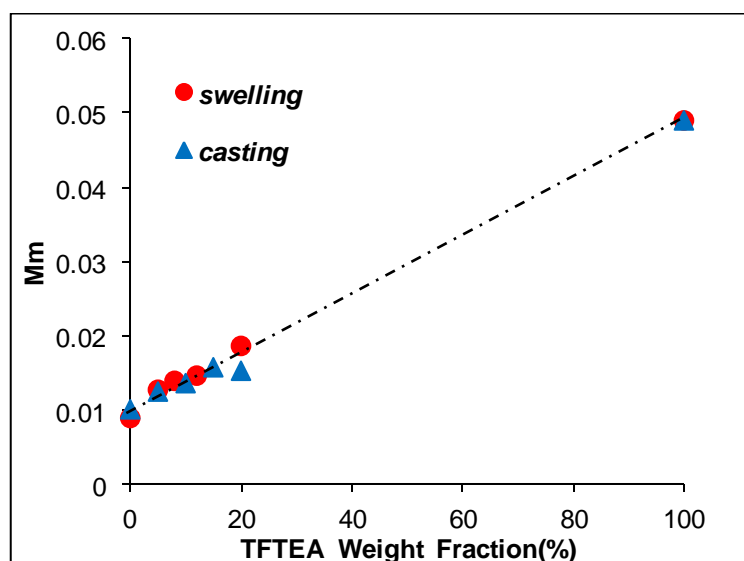
The isotherms of casting based doped membranes have also been analyzed by GAB model as was discussed for swelling based membranes for further analysis of water sorption phenomenon. GAB parameters i.e.  $M_m$ ,  $C_G$  and  $K$  have been calculated using the curve isotherm fitting and the efficiency of curve fitting was also determined by calculating MRD (discussed thoroughly in the previous chapter).

The evolution of the GAB parameters values as a function of the TFTEA weight content regarding casting based doped membranes are shown in figures 14 (a) to (c).  $M_m$ ,  $C_G$  and  $K$  values determined on the swelling based membranes have also been reported for comparison on the same figures. On comparison, following trends are observed:

1. The evolution of  $M_m$  with TFTEA concentration (figure 14 (a)) is similar for swelling as well as casting based membranes i.e. linear in nature except for the membrane with 20 wt% content elaborated by casting method. Thus, both the kinds of doped membranes show *the additive contribution of ionic sites of Nafion-TEA and TFTEA towards the sorption of water molecules*. For the casting based membrane (20 wt% TFTEA content) with anomalous

behaviour, it seems that there is actually lesser number of accessible ionic sites for water sorption compared to the calculated additive contribution of Nafion-TEA and TFTEA which could be related to the different type of organization/distribution of TFTEA in the membrane supported by the previous results (DMA, conductivity).

2. Concerning  $C_G$  (figure 14 (b)), its value does not evolve significantly with increasing TFTEA content in casting based membranes like swelling based membranes. However, the doped membranes based on casting present higher value of  $C_G$  parameter compared to swelling based doped membranes over the entire range of TFTEA concentration studied. Thus it seems that the *morphology developed by casting method is more favourable for the sorption of water molecules* at middle range activity for all the membrane compositions studied.
3. The  $K$  parameter (figure 14 (c)) evolves in similar fashion for both the kinds of doped membranes i.e. increasing slightly with increasing TFTEA content. This signifies *similar interactions between ionic sites and bulk water molecules* in both the types of doped membranes.



(a)



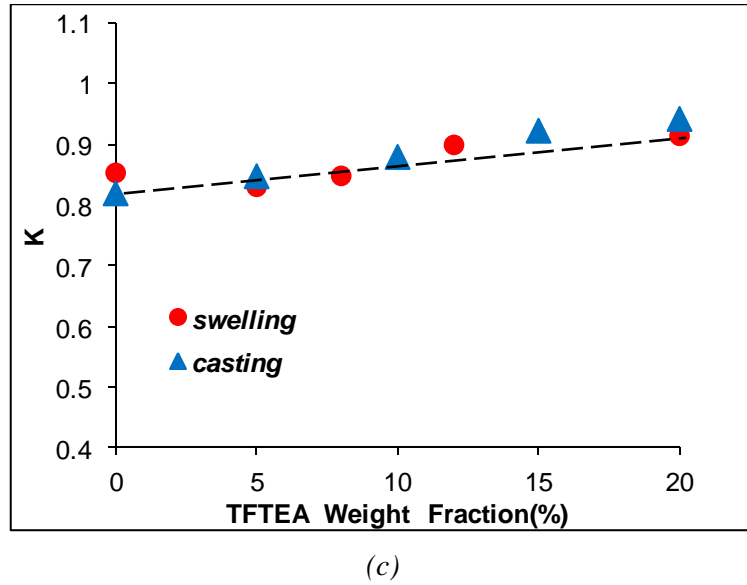
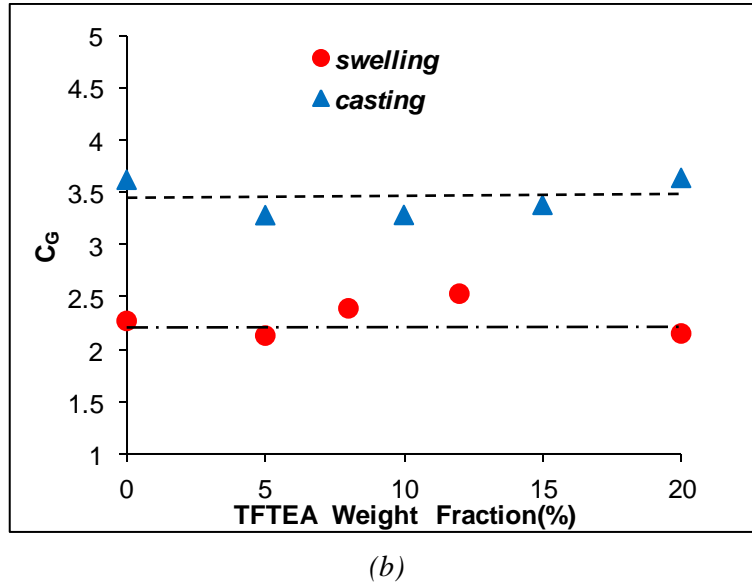


Figure 14: Evolution of GAB parameters determined from GAB modelling as a function of the TFTEA weight fraction for both the kinds of doped Nafion-TEA membranes; (a)  $M_m$ ; (b)  $C_G$ ; (c)  $K$

In short, the water sorption behavior of both the types of doped membranes is quite similar in nature. Moreover, it seems that auto-organization of TFTEA molecules within the structure of Nafion-TEA limits water retaining capacity of the system and this phenomenon is evident at lower TFTEA concentrations in casting based membranes.

### Conclusion

In summary, the morphology and function properties of casting as well as swelling based membranes have been studied and discussed. After comparing two methods, clues of different types of

structurations of TFTEA molecules in the structure of Nafion-TEA have been found. In order to better understand the types of distribution and organization of TFTEA molecules in the Nafion-TEA structure (when elaborated by casting method) and develop more the correlations between morphology and functional properties, various other studies would be very interesting such as:

- ✚ Elaboration of membranes using different solvent systems and annealing treatments
- ✚ SANS and WAXS measurements at different temperatures
- ✚ Water sorption study at different temperatures
- ✚ Gas permeability measurements at different temperatures and varying water vapour pressures

### ***3.3: Fuel cell performance and Degradation study***

In this section, the feasibility of a PCIL based membrane in a fuel cell will be explored. Afterwards, various studies on the possible degradation phenomena associated with this type of system will be discussed.

#### ***a. Fuel Cell Performance***

The casting based doped membranes have been utilized to evaluate the fuel cell performance of PCIL based system because of the following reasons:

1. Casting based TFTEA doped membranes presented better performance in comparison to swelling based doped membranes mainly in terms of thermo-mechanical properties above 100°C.
2. Moreover, a membrane with 5cmx5cm dimensions is required which is easier to be obtained by casting method.

Concerning casting based doped membranes, membranes with 15 and 20 wt% contents of TFTEA show similar thermo-mechanical properties as well as ionic conductivities. However, taking into account the fact that liquid water would also be formed at the cathode which could elute a part of the ionic liquid from the membrane, we preferred to use the membrane with maximum TFTEA concentration. Hence, the membrane with 20wt% was chosen for the study.

The Membrane Electrode Assembly (MEA) based on this doped membrane was prepared by using the protocol of Paxitech<sup>®</sup> Company (described in experimental section). The ionic conduction in the active layer of the MEA is assured by a PFSA ionomer.

Firstly, the fuel cell tests were carried out under anhydrous conditions as well as low relative humidity values at 100°C. But, very low Open Circuit Voltage (OCV) and performance had been observed in

such conditions. This is probably due to the presence of Nafion<sup>®</sup> in the active layer of MEA which needs water for the conduction of protons. Thus, the performance of TFTEA doped membrane was evaluated at 100°C using 100% humidified gases and 1atm relative pressure.

An increase in the relative humidity to 100% gave an OCV value of approximately 0.95 V for TFTEA doped membrane. This OCV value is close to the one obtained for Nafion-H<sup>+</sup> at 80°C and 100% RH (OCV~1,06V). Afterwards, the system was stabilized at 0.6 V to acquire a constant value of drawn electric current. The drawn electric current increased slowly and it took 12 hours to reach a constant value. Then, the MEA was subjected to a round cycle of voltage in the range 0.9-0.3V and drawn electric current was registered. The duration of the each cycle of the applied voltage was 3 hours. This cycle was repeated several times. The performance of the membrane improved with increasing number of cycles up to the 6<sup>th</sup> cycle. The fuel cell polarization curves obtained for 6<sup>th</sup> cycle (voltage as a function of current density) for the TFTEA doped Nafion-TEA membrane is presented in figure 15 and compared with that of Nafion-H<sup>+</sup> and Nafion-TEA.

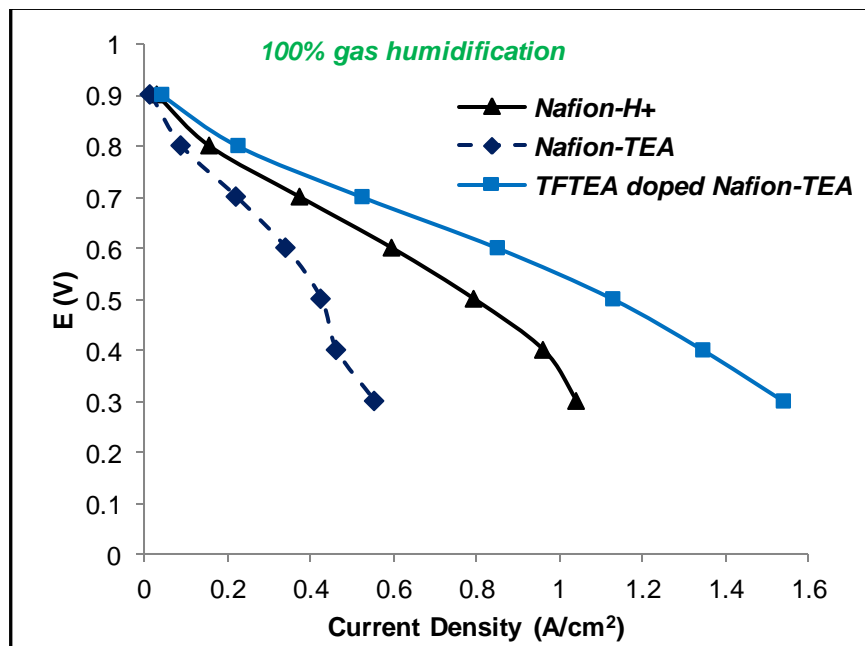


Figure15: Polarization curves of: Nafion-H<sup>+</sup> at 80°C and 100% RH; Nafion-TEA and Nafion-TEA +20wt% TFTEA membrane at 100°C and 100% RH

It can be seen from figure 15 that:

1. Addition of TFTEA in Nafion-TEA drastically improves the fuel cell performance of Nafion-TEA.

2. ***TFTEA doped membrane gives a better performance (current density=0.85 A/cm<sup>2</sup> at 0.6 V) in comparison to the best performance obtained for Nafion-H<sup>+</sup> (current density=0.79 A/cm<sup>2</sup> at 0.6 V; 80°C and 100% RH).***

The doped membrane presented the performance illustrated up to 3 days. Afterwards, a gradual loss in its performance with increasing number of voltage cycles was observed (more than 20% of performance in 2 days).

This gradual loss of performance of this TFTEA doped membranes could be because of the following reasons:

- a. ***Elution of TFTEA by water molecules:*** The PCIL could be washed off from the membrane by the water molecules from the humidified gases or produced at the cathode during the working of fuel cell. In order to verify this phenomenon, the water from the out-let in the fuel cell test was collected and analyzed using NMR technique. The amount of TFTEA detected by NMR after the lyophilization of effluent water was found to be very low (~10mg). Thus, the loss of such small amount of TFTEA cannot solely explain the loss in the fuel cell performance of the doped membrane
- b. ***Degradation of the electro-catalyst:*** There are two possibilities for the degradation of the electro-catalyst:
1. In PCIL based systems, it has been proposed that the proton conduction occurs through the diffusion of ammonium species. Once the reaction at the cathode occurs, amine is liberated that could adsorb on the surface of the catalyst at the cathode side. This adsorption could significantly reduce the activity of the catalyst resulting in a decline of the fuel cell performance of the system. However, this phenomenon has not been evidenced on similar PCILs<sup>[14]</sup>.
  2. The degradation of the carbon support in the active layer results in agglomeration of the electro-catalyst<sup>[15,16]</sup>. This agglomeration of the catalyst results in lower active surface area thereby affects the fuel cell performance.

It will be interesting to analyze the active surface of the catalyst after the conclusion of fuel cell tests on the PCIL based system. However, it was not possible to perform this analysis with the present system.

- c. ***Creeping of the membrane resulting in mechanical degradation:*** Due to the plasticizing effect of TFTEA on Nafion-TEA as well as the gas pressure in the system, the doped

membrane could exhibit mechanical degradation which would result in poor fuel cell performance. After the tests were finished, the MEA was inspected and creeping of the membrane was observed which points towards loss of mechanical properties of the membrane during the fuel cell test.

- d. *Attack of peroxy radicals:*** It is well-known that the peroxy radicals are formed in the working conditions of the fuel cells. These peroxy radicals are known to attack the polymer electrolyte membrane. The consequent degradation of the membrane very significantly adds to the factors which result in the inferior fuel cell performance of the system.

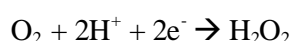
Hence, in order to evaluate the impact of peroxy radicals on the chemical stability of the PCIL doped membrane, a degradation study was done. This will be discussed in the succeeding section.

**b. *Degradation in the presence of peroxy radicals***

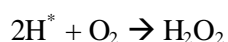
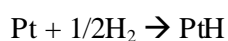
A preliminary study on the degradation phenomena associated with the PCIL doped membranes has been illustrated in this part.

Apart from physical, mechanical degradations such as membrane thinning and pinhole formations, free radical attack has been considered one of the most important reasons for the degradation of fuel cell membranes. The presence of free radical in the system occurs due to the formation of hydrogen peroxide. Hydrogen peroxide has been proposed to be formed in two ways<sup>{17,18}</sup> such as:

1. Oxygen gets reduced at the cathode according to the following reaction and hence hydrogen peroxide is formed.



2. Oxygen crossover from cathode to anode takes place or air-bleed on the anode side occurs resulting in oxygen at the anode side and consequent reaction with protons to form hydrogen peroxide according to the following reaction.



Once formed in the system, it generates peroxy and hydroperoxy radicals which attack and degrade the membrane. Thus, a lot of research has been focused on the effect of hydrogen peroxide's presence on the degradation of Nafion<sup>®</sup> (acidic form). The studies have been carried out under different conditions by varying temperature, relative humidity, counter-ions, electro-catalysts, accelerating degradation conditions using metallic ions to list a few<sup>{19-25}</sup>. The studies have

demonstrated that the degradation of Nafion<sup>®</sup> can occur in two ways<sup>25</sup>: main-chain unzipping process and side-chain scission process (as discussed in the chapter 1). The degradation is initiated by abstraction of Hydrogen from the residual carboxylic acid ionic functions. This abstraction initiates a consecutive oxidation process producing carbon dioxide and hydrogen fluoride detected in the effluent water. The peroxy radical could also attack the side-chains carrying sulfonic acid functions and produce trifluoro acetic acid as a degradation product. However, no study has been reported on the impact of peroxy radicals on an amine-neutralized Nafion<sup>®</sup> as well as a PCIL doped Nafion<sup>®</sup> membrane in the literature. Hence, the idea is to understand:

- degradation phenomena associated with a PCIL doped membrane
- impact of amine neutralization on the degradation phenomena associated with Nafion<sup>®</sup>

Thus, a study of degradation phenomenon in the presence of peroxy radicals has been carried out on the different components of PCIL doped Nafion-TEA membranes i.e.

1).**PCIL**: The study has been done on TFTEA in the presence of different quantities of hydrogen peroxide solution at elevated temperatures and observing the changes using NMR technique (<sup>1</sup>H; <sup>19</sup>F)..

2).**Nafion-TEA membrane**: Evolution of FTIR-spectra (ATR and transmission mode) of Nafion-TEA membranes on exposure to hydrogen peroxide solution at 80°C in a closed system was studied.

3). **Nafion-TEA+xwt%TFTEA membranes**: The doped membranes based on TFTEA were studied in similar manner as pure Nafion-TEA membrane mentioned above.

It is important to keep in mind that accelerated conditions have been utilized in this work which means that the concentration of hydrogen peroxide and of peroxy radicals utilized in these tests is much higher compared to their concentration in an operating fuel cell.

### PCIL

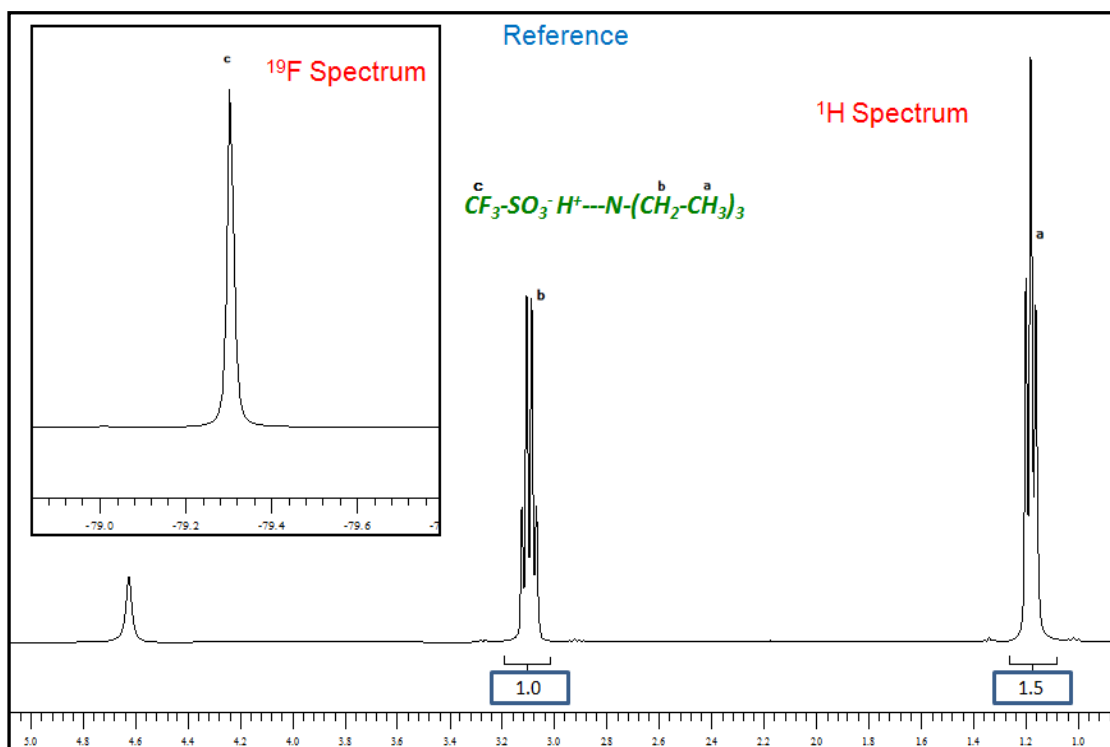
The chemical stability of TFTEA against different concentrations of hydrogen peroxide at 110°C has been evaluated by NMR spectroscopy.

It has been observed that there is *no change in the NMR spectra of TFTEA on exposure to different concentrations of hydrogen peroxide which can be observed from the NMR spectra (<sup>1</sup>H; <sup>19</sup>F) of TFTEA before and after the exposure to the maximum concentration of hydrogen peroxide* shown in figure 16 (a) and (b) respectively (Note: The chemical shifts of peaks associated with a triethylammonium are different from those associated with a triethylamine; i.e. if there was any triethylamine present in the system, it should have had given out peaks in the proton spectrum at

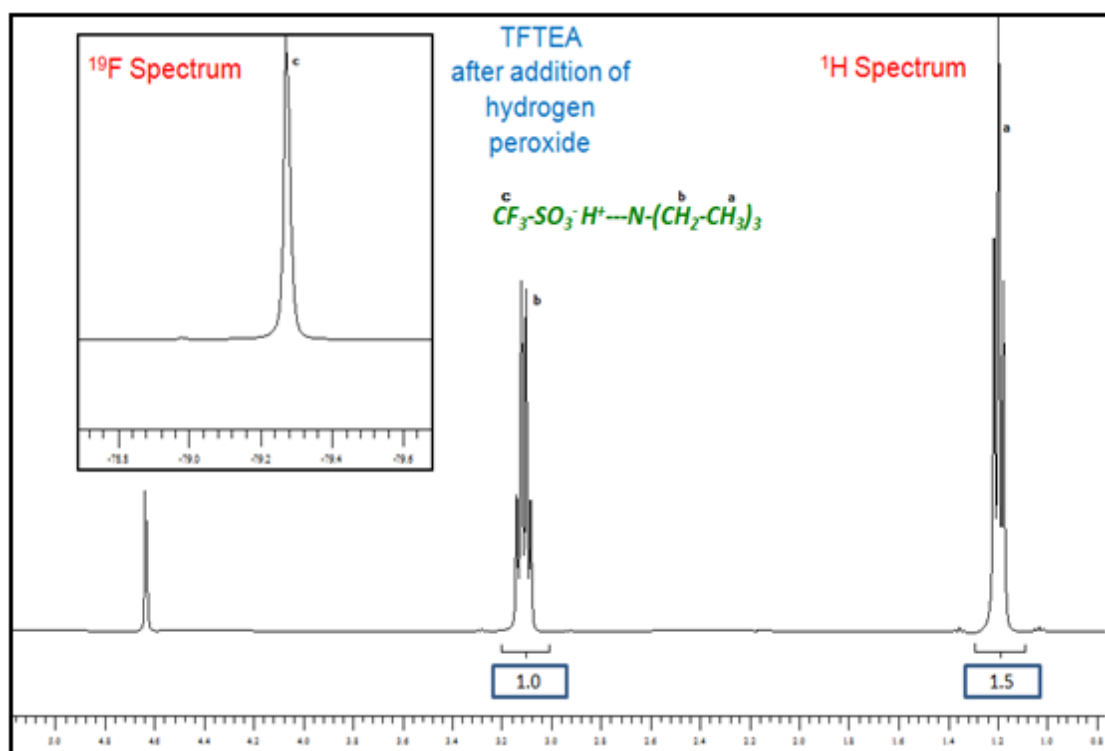
different chemical shifts). Thus, it is clear from these results that there is no product from the degradation of TFTEA present in the solution.

Now, the question appears if there is any product from the degradation phenomenon which could either precipitate or evaporate during the study. This evaporation/precipitation of such product could change the concentration of TFTEA in the solution. Hence, in order to verify if the concentration of TFTEA remains equal or not before and after exposure to hydrogen peroxide, equal quantities of solutions of TFTEA before and after the study were analyzed in the presence of a known amount of internal reference (trifluoro ethanol). The molar ratio between the peaks of internal reference and the peaks of TFTEA (in  $^1\text{H}$  and  $^{19}\text{F}$  spectra) were found to be equal in both the cases. This signifies that no evaporation or precipitation of products of degradation occurred in the case of TFTEA exposed to hydrogen peroxide.

It is known that *triethylamine is easily oxidised in the presence of peroxy radical attack* forming various products<sup>(26)</sup> such as alkylamine-N-oxide, alkyl imine etc. However, *in the case of TFTEA, it seems that the ionic liquid demonstrates good chemical resistance against peroxy radicals*. The stability of TFTEA in contrast to triethylamine could be due to the fact that amine is in protonated form in TFTEA and protonation of the amine could possibly prevent its oxidation by the peroxy radicals.



(a)



(b)

Figure 16: NMR spectra of TFTEA ( $^1\text{H}$ ;  $^{19}\text{F}$ ); a).Reference; b).After fourth step of hydrogen peroxide addition

### Nafion-TEA

The evolution of chemical stability of the neutralized membrane in the presence of peroxy radicals was studied by using FTIR spectroscopy.

Figure 17 presents the ATR-FTIR spectrum of virgin Nafion-TEA before exposure to peroxy radicals and the main bands are attributed in the range of 800-1500  $\text{cm}^{-1}$ <sup>[27]</sup>.



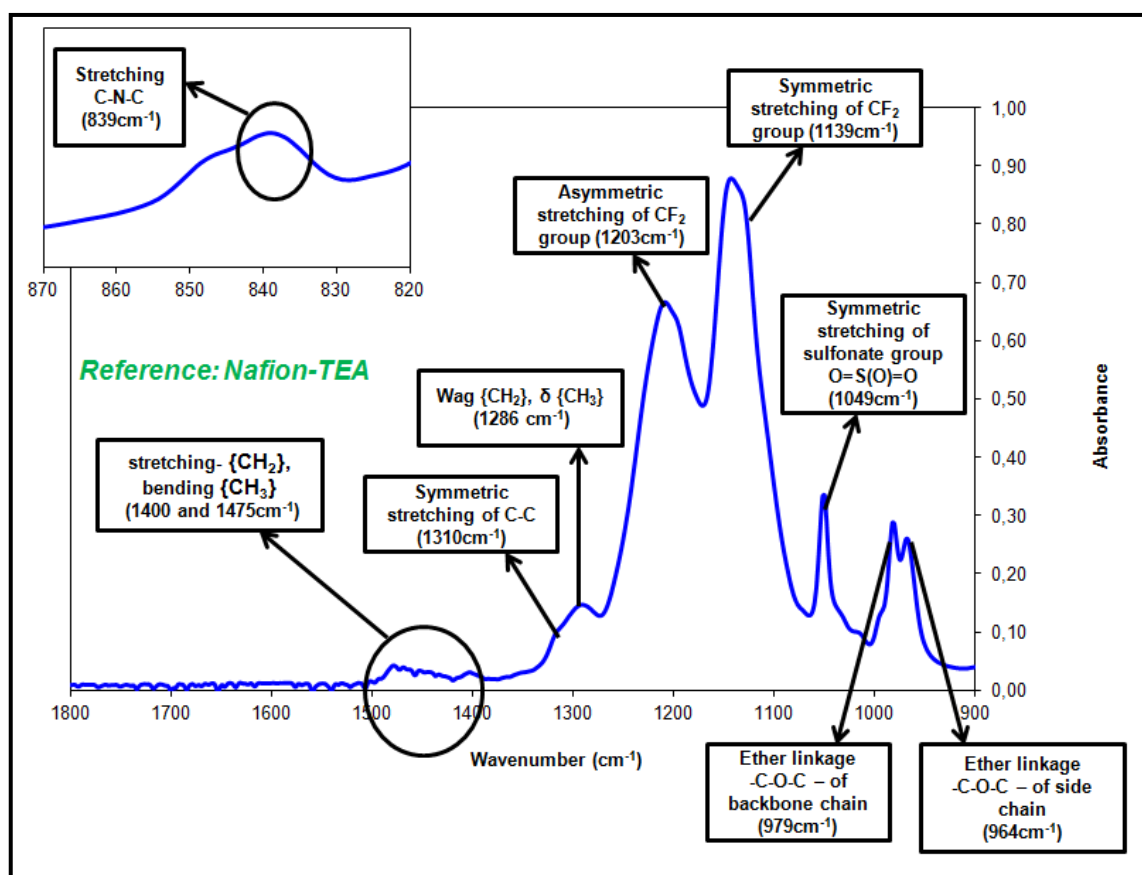


Figure 17: ATR-FTIR spectrum of Nafion-TEA with attributed bands

Figure 18 presents the evolution of the ATR-FTIR spectrum of Nafion-TEA in function of time of exposure to the peroxide rich atmosphere.

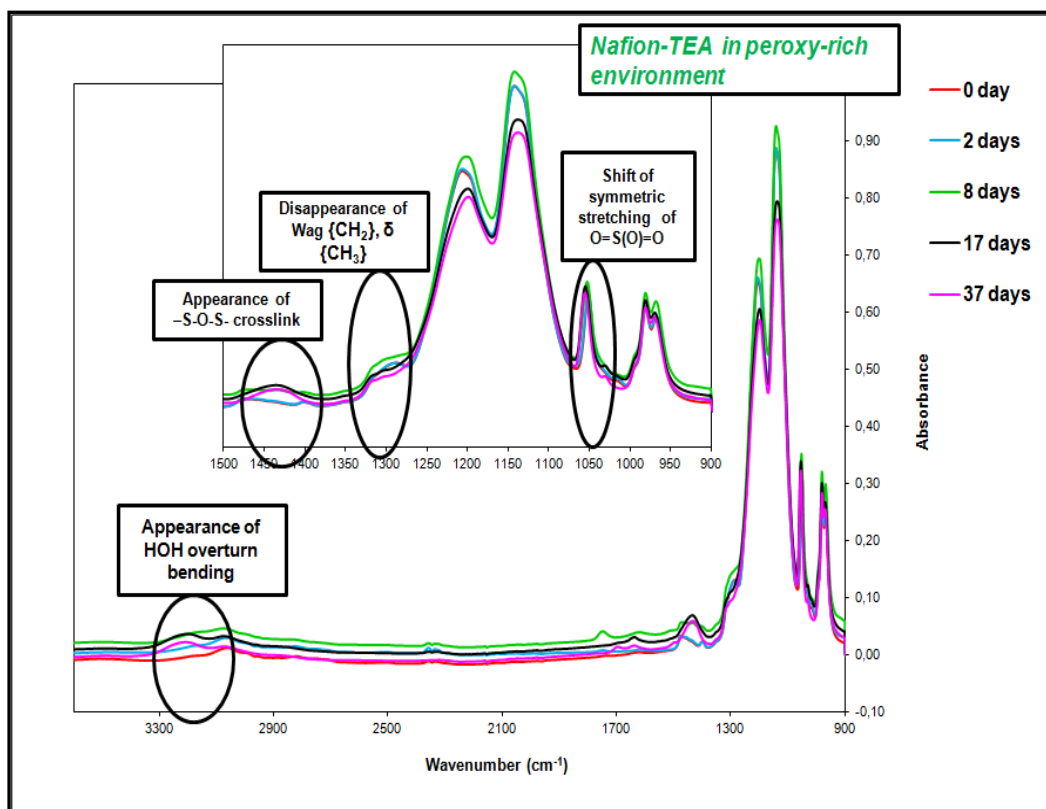


Figure 18: Evolution of ATR-FTIR spectrum of Nafion-TEA with time under peroxy rich environment at 80°C

The main changes in the spectra (Figure 18) on exposure to peroxy-rich environment and their interpretations are listed as follows:

1. A disappearance of band at  $1286\text{ cm}^{-1}$  corresponding to the  $\text{CH}_2\text{CH}_3$  stretchings (originating from triethylammonium) after few days of exposure to peroxide rich environment is seen. The band seems disappeared from the spectrum of 8<sup>th</sup> day of the exposure. This result is surprising because ionic liquid didn't present any degradation in the presence of peroxy radicals.
2. The band associated with the sulfonate group ( $\text{O}=\text{S}(\text{O})=\text{O}$  stretching) shifts to slightly higher wavenumber (from  $1049\text{ cm}^{-1}$  to  $1060\text{ cm}^{-1}$ ) from the 8<sup>th</sup> day of exposure to the experimental conditions. This signifies that the sulfonate group of Nafion<sup>®</sup> transforms from triethylamine neutralized form to acidic form.
3. There is gradual appearance of new band at  $1430\text{ cm}^{-1}$  on exposure to peroxy radical-rich atmosphere. This band starts to appear from the 17<sup>th</sup> day of the study. Okada et al. has

attributed this absorption band to the *S-O-S links* between the side groups of Nafion® due to the formation of sulfonic anhydride.

4. In addition, there is *appearance of a new band at 3230 cm<sup>-1</sup>* on exposure to experimental conditions from the 17<sup>th</sup> day. This band has been attributed to the HOH bending overtone associated with the water molecules present in less hydrophilic domains of Nafion® after exposure to peroxy radical for certain period of time (reduction in sulfonic acid density due to the formation of sulfonic anhydride by oxidative effect of hydrogen peroxide) <sup>(19)</sup>. It is interesting to note that the presence of water molecules which are in interaction with sulfonic anhydride in the membrane do not show a significant band at 1734cm<sup>-1</sup>.

From all these observations, it seems that *Triethylammonium moiety associated with the sulfonate group of Nafion-TEA disappears from the system and formation of sulfonic anhydride takes place on exposure to these conditions.*

(Note: The bands associated with Triethylammonium moiety at 1400cm<sup>-1</sup> and 1475cm<sup>-1</sup> could not be observed due to the appearance of the band associated to S-O-S cross link at 1430 cm<sup>-1</sup> and the band at 839 cm<sup>-1</sup> could not be observed properly either in this experiment).

Now, concentrating on the disappearance of Triethylammonium moiety from Nafion-TEA membrane, there could be two possibilities. Its disappearance could be:

- a. either due to elution of triethylammonium moieties of Nafion-TEA because of the presence of water in the system.
- b. or due to the presence of peroxy radicals in the system during the experiment.

Hence, in order *to answer to this dilemma, another study was conducted on Nafion-TEA membranes.* In this study, Nafion-TEA membranes were exposed to *pure water instead of hydrogen peroxide solution* at 80°C in similar fashion as in the previous study and the evolution of the ATR-FTIR spectrum was studied in function of time of exposure to the conditions. The evolution of ATR-FTIR spectrum of Nafion-TEA with increasing time of exposure to water (both vapor and liquid form) is shown in figure 19. It can be clearly seen that *any evolution of FTIR spectra is observed with increasing time of exposure to the peroxy-free experimental conditions.*

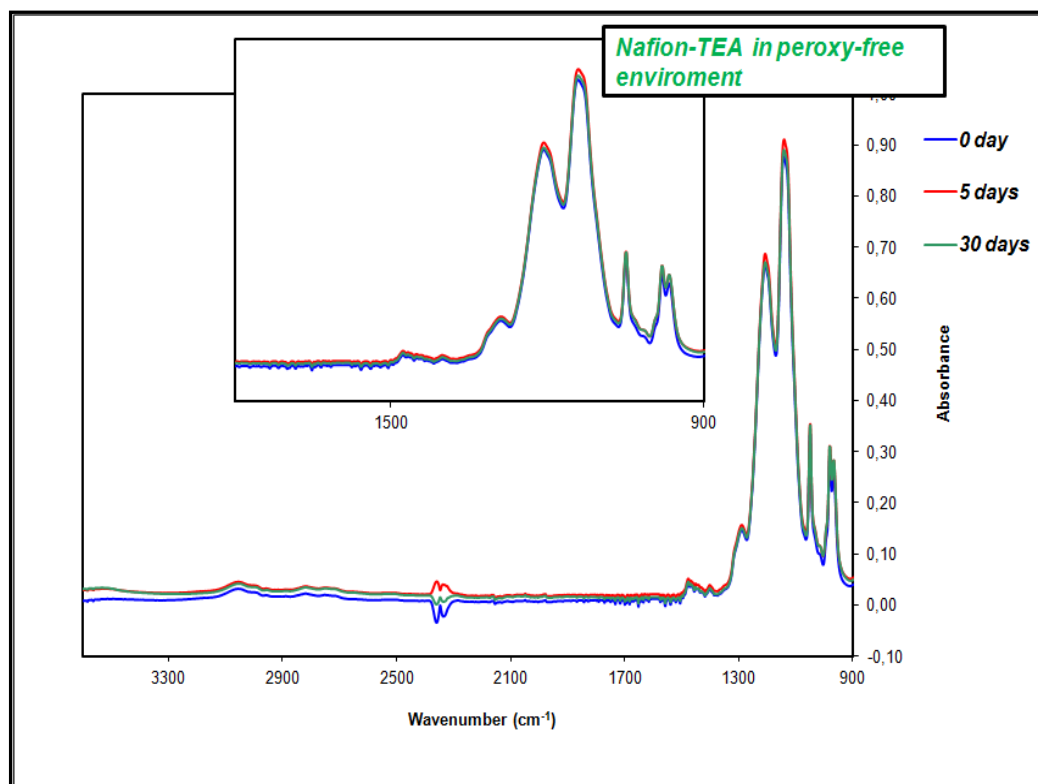


Figure 19: Evolution of ATR-FTIR spectrum of Nafion-TEA with time in peroxy-free environment at 80°C

***From all the studies discussed above on Nafion-TEA, it can be asserted that:***

1. Nafion-TEA is completely stable in the presence of water at elevated temperatures.
2. Triethylammonium entity associated with sulfonate group of Nafion-TEA gets eliminated on exposure to peroxy-rich environment.
3. The membrane exhibits the formation of sulfonic anhydride in peroxy-rich atmosphere.

Now, in order to compare the rate of formation of sulfonic anhydride in Nafion-TEA to that in Nafion-H<sup>+</sup>, the behavior of Nafion-H<sup>+</sup> membranes were evaluated in the same experimental conditions as employed for Nafion-TEA membranes. The evolution of ATR-FTIR spectra of Nafion-H<sup>+</sup> in function of time of exposure to peroxy-rich atmosphere is shown in figure 20.

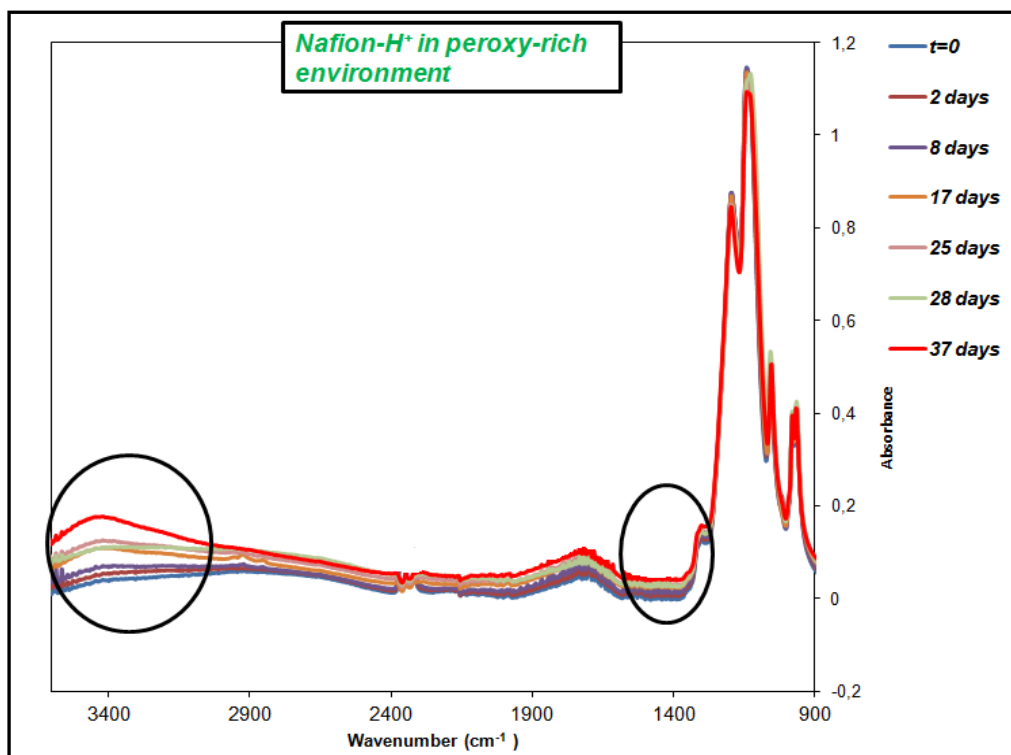


Figure 20: Evolution of ATR-FTIR spectrum of Nafion- $H^+$  with time under peroxy-rich environment at 80°C (same experimental conditions as employed for Nafion-TEA)

It can be observed from figure 20 that:

1. Nafion- $H^+$  does not present any absorption band at  $1440\text{cm}^{-1}$  in contrast to Nafion-TEA under same conditions.
2. Nafion- $H^+$  membranes show a broad absorption band in the range of  $2900\text{-}3500\text{cm}^{-1}$ . The intensity of this large band increases with increasing time of exposure to the experimental conditions. However, the presence of HOH bending overtone of water molecules observed at  $3320\text{cm}^{-1}$  cannot be pointed. In contrary, Nafion-TEA clearly shows an absorption band at  $3320\text{cm}^{-1}$  corresponding to HOH bending overtone of water molecules from 17<sup>th</sup> day of the study.

Both these observations signify that *Nafion-TEA exhibits much higher degree of the formation of sulfonic anhydride in comparison to Nafion- $H^+$*  under similar conditions. This means that the peroxy radicals have stronger oxidative effect on the sulfonic acid functions of Triethylammonium neutralized Nafion® in comparison to that of Nafion® in acidic form. The interesting thing to note is that the formation of anhydride is observed only after the disappearance of triethylammonium moiety from the

system. Now, the question appears why the neutralized membranes exhibit faster degradation even if it changes to acidic form in few days on exposure to the experimental conditions. It could be possibly related to:

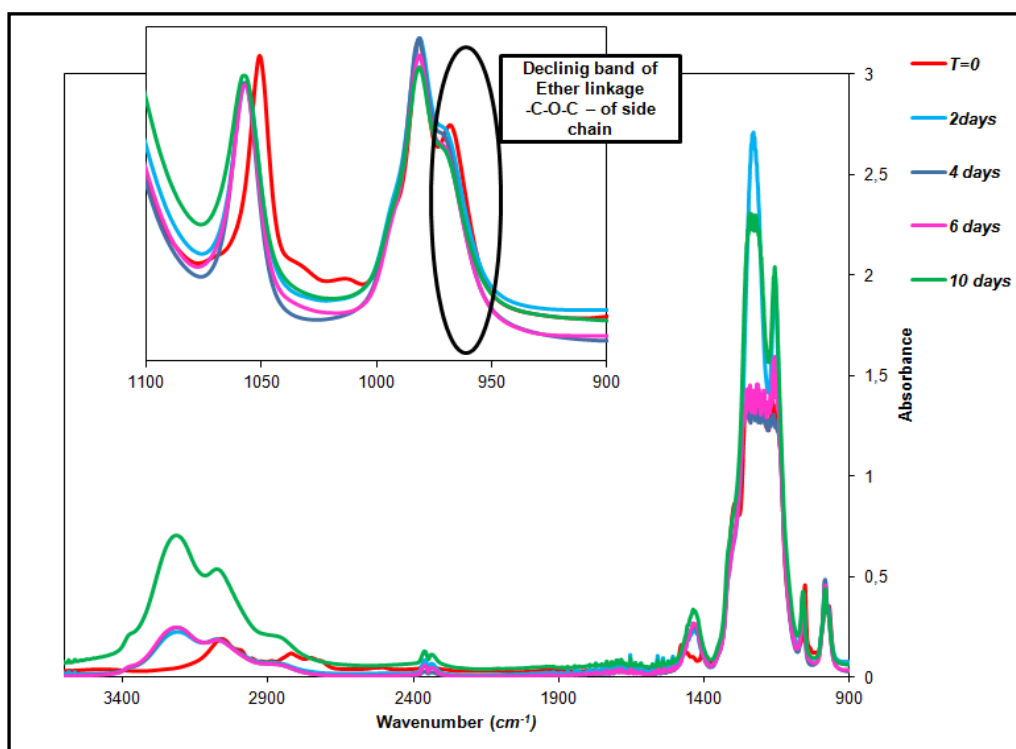
- the dissociation of sulfonic acid function in neutralized form which could eventually amplify the oxidative action of peroxy radicals.
- the triethylamine eluted from the membrane might cause a change in the pH of the system consequently accelerating the formation of sulfonic anhydride.

However, it is interesting to note that we did not observe these phenomena in TFTEA even though its chemical structure is similar to that of Nafion-TEA. The degradation is observed in the case of Nafion-TEA and not in the case of TFTEA could be because of the following reasons:

- In the case of Nafion-TEA, the tests are done in the vapor phase. Thus, once triethylamine or any other product liberated the membrane, it would be either washed off by the water molecules condensed on the surface of the membrane or it would simply evaporate from the system. However, in the case of TFTEA, the tests were done in the solution form in a closed system. So, if the degradation process is reversible in liquid water, we would not observe any change on NMR spectrum.
- The Triethylammonium sulfonate moieties are confined in the matrix of Nafion-TEA which could favor the formation of sulfonic anhydride.

Now, we concentrate on the triethylammonium moiety which is no more detected/found in the chemical structure of Nafion-TEA on exposure to peroxy-rich environment. It could be possible that ***only those TEA moieties which are present at the surface of the membrane disappear and not necessarily all of them present throughout the thickness of the membrane.*** The probability of this possibility comes from the fact that the studies discussed before are based on ATR-FTIR technique for which the surface penetration length is only up to 5  $\mu\text{m}$ . Using FTIR technique in transmission mode could answer this doubt. However, in order to be able to do this, very thin membranes (with thickness of the order of 10-20  $\mu\text{m}$ ) would be required otherwise FTIR spectra would not be useful because saturated.

Thus, ***another study was carried out on very thin films of Nafion-TEA (20-25  $\mu\text{m}$ ) in hydrogen peroxide environment.*** This study was carried out over a period of 10 days in more vigorous conditions (20% w/w hydrogen peroxide solution) to accelerate the degradation phenomena. The evolution of FTIR spectra of thin Nafion-TEA films on exposure to peroxy radicals over a period of 10 days are shown in figure 21 (a)-(b). (Note: The bands associated with  $-\text{CF}_2$  groups of Nafion-TEA are saturated in some cases while all the other bands are very sharp.)



(a)

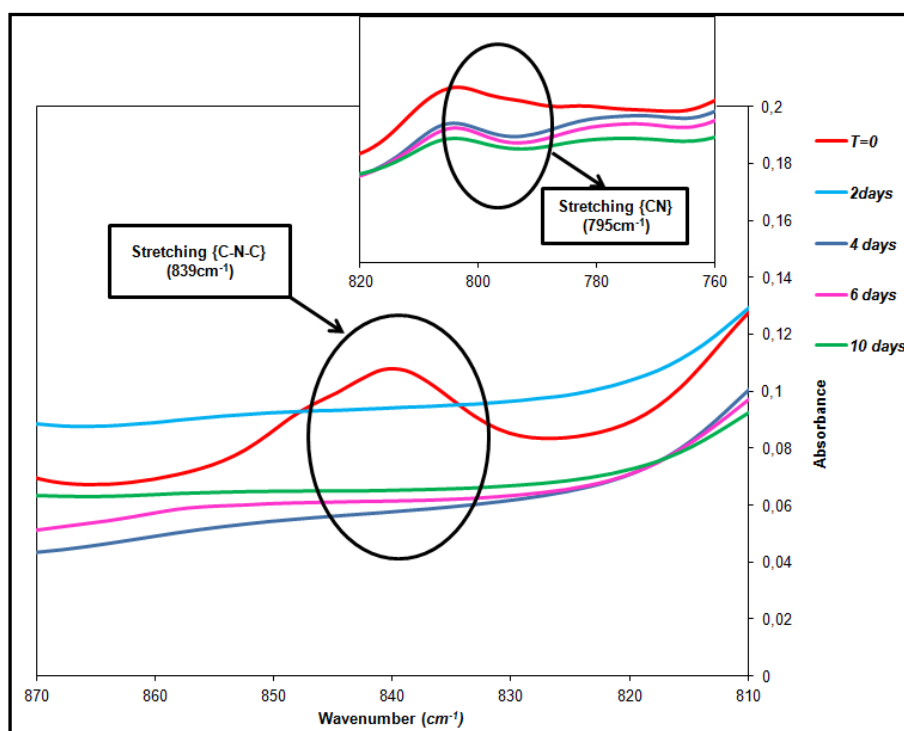


Figure 21: Evolution of ATR-FTIR spectrum of thin Nafion-TEA film with time under peroxy-rich environment in the range of: a).  $900\text{-}3400\text{cm}^{-1}$ ; b).  $800\text{-}900\text{cm}^{-1}$

From figure 21, it can be seen that all the **gradual changes** which were observed in the spectra from the first study on Nafion-TEA are still observed. However, all the bands are clearer and pronounced in

the FTIR spectra (transmission mode) in comparison to the ATR-FTIR spectra. Moreover, in this study, all the changes are observed right from the second day which must be due to higher concentration of hydrogen peroxide used in this study. In brief, the mains changes observed are:

1. ***Disappearance of bands related to triethylammnium:*** In addition to the disappearance of bands at  $1286\text{cm}^{-1}$ , ***disappearance of other bands associated with Triethylammonium could be clearly observed in this study (figure 21 (b)).***
2. ***Shifting of band associated with the sulfonate of Nafion-TEA***
3. ***Appearance of band related -S-O-S- cross-links***
4. ***Formation of a large peak around  $3230\text{ cm}^{-1}$***
5. In addition, another phenomenon is clearly visible i.e. ***significant decrease in the intensity of the band associated with the ether linkage in the side-chain of Nafion<sup>®</sup>.*** This signifies that the side-chain of Nafion-TEA exhibits ***side-chain scission on exposure to peroxy rich environment.***

Particularly, the absorption bands associated with anhydride formation and with HOH bending overtone of water poorly attached to the ionic functions of Nafion<sup>®</sup> are:

- very intense (probably due to observation of these phenomenon throughout the thickness of the membrane).
- evolve with increasing time of exposure to peroxy-rich environment throughout the mass of the membrane.

Hence, it is clear that Nafion-TEA exhibits the elimination of triethylammonium moiety followed by the formation of sulfonic anhydride throughout its thickness under these experimental conditions.

### **Nafion-TEA + TFTEA**

In the case of TFTEA doped Nafion-TEA membrane, the TFTEA molecules interact mainly with the triethylammonium sulfonate entity of Nafion-TEA. This interaction of TFTEA molecules could delay the degradation phenomena associated with the Triethylammonium sulfonate entity of Nafion-TEA. However, it should be noted that there could be the problem of PCIL elution due to the condensation of water molecules on the surface of the membrane since the temperature of degradation studies is less than  $100^{\circ}\text{C}$ .



Thus, in order to understand the impact of the presence of TFTEA on the degradation behavior of Nafion-TEA membrane, experiments were carried out in similar manner as for the thin Nafion-TEA membrane and studied with FTIR spectroscopy in transmission mode.

Figure 22 shows the FTIR spectrum (transmission mode) of Nafion-TEA membrane doped with 20wt% TFTEA with the attributed bands<sup>[27]</sup>. It is important to note that the absorption bands at  $1400\text{cm}^{-1}$ ,  $1475\text{cm}^{-1}$ ,  $839\text{cm}^{-1}$  and  $795\text{cm}^{-1}$  associated with Triethylammonium (apart from the band at  $1284\text{cm}^{-1}$ ) are clearly visible in the transmission mode-FTIR spectrum of TFTEA doped membrane.

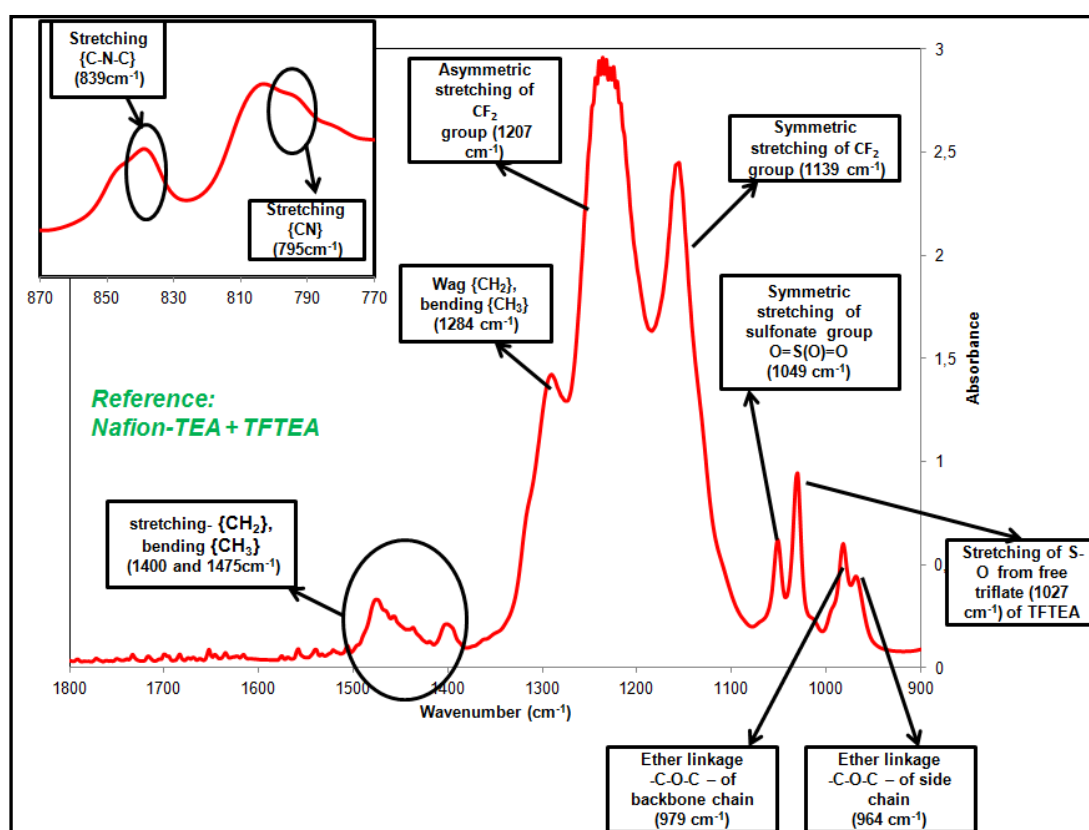
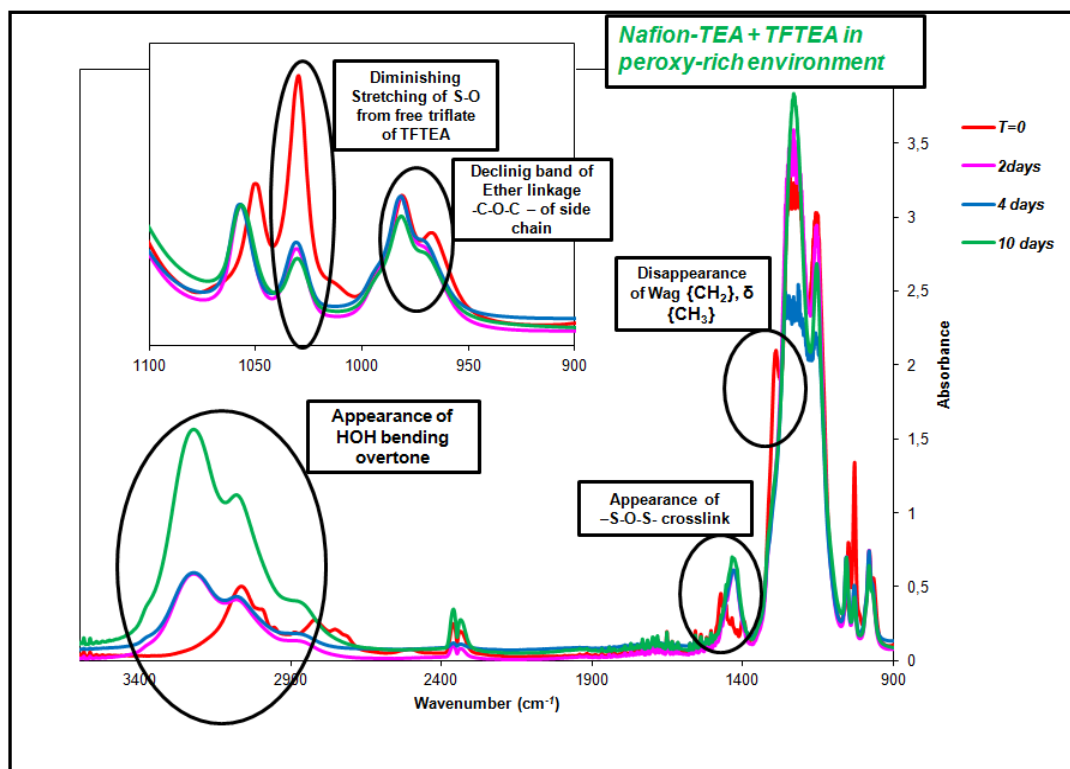
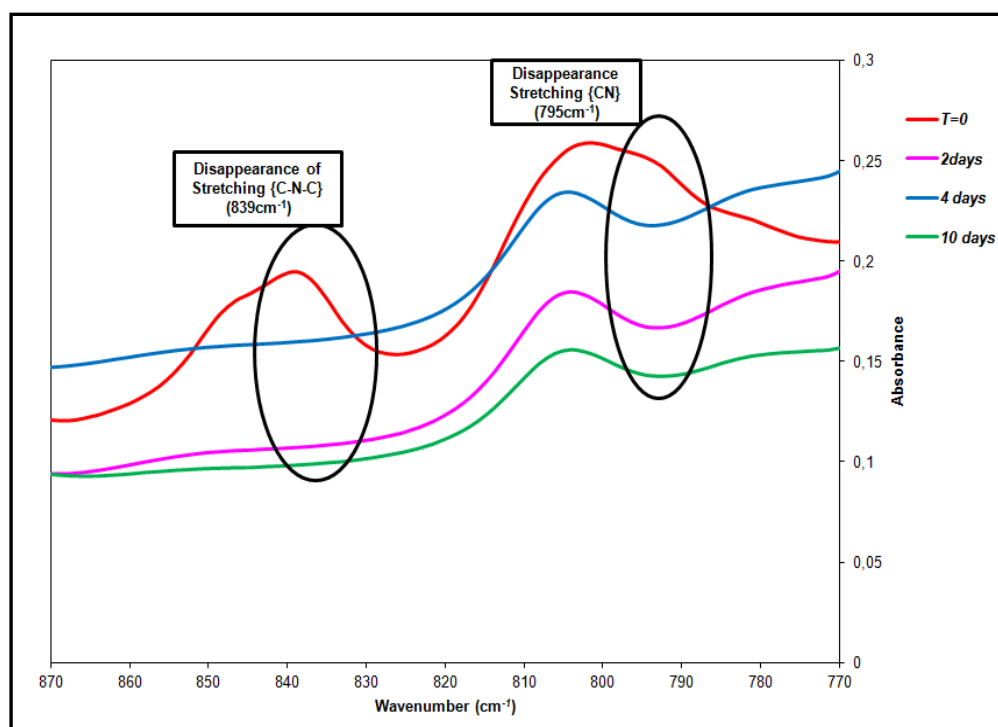


Figure 22: Reference FTIR spectrum (Transmission mode) of thin film of Nafion-TEA+20wt%TFTEA with labeled bands at time  $t=0$

The evolution of the FTIR spectrum (transmission mode) of the doped membrane with increasing time of exposure to hydrogen peroxide solution is shown in figure 23 (a) and 23 (b).



(a)



(b)

Figure 23: Evolution of FTIR spectrum (Transmission mode) of thin film of Nafion-TEA+20wt%TFTEA with time under peroxy-rich environment at 80°C in the range of: a). 900-3400cm<sup>-1</sup>; b). 770-870cm<sup>-1</sup>

From these spectra (figure 23 (a)-(b)), it can be seen that:

1. *The evolution of the spectra on exposure to peroxy radicals with the passage of time for TFTEA doped Nafion-TEA membrane is same as that of Nafion-TEA membrane.*

*a).* The triethylammonium moiety associated with the sulfonate group of Nafion-TEA disappears gradually from the system right after 2 days of exposure to these conditions. This is apparent from the disappearance of the bands at and  $795\text{cm}^{-1}$ ,  $839\text{cm}^{-1}$ ,  $1284\text{cm}^{-1}$  and  $1475\text{cm}^{-1}$  associated with the Triethylammonium entity. However, disappearance of the absorption band at  $1400\text{cm}^{-1}$  is not clear. Subsequently, the band associated with sulfonate of Nafion-TEA ( $1049\text{cm}^{-1}$ ) shifts to higher value ( $1060\text{cm}^{-1}$ ) signifying a change in its form from neutralized form to acidic form.

*b).* The formation of sulfonic anhydride evolves with increasing time of exposure to hydrogen peroxide solution (as the intensity of band at  $1430\text{cm}^{-1}$  corresponding to S-O-S cross link HOH bending overtone at  $3230\text{cm}^{-1}$  increases with time of exposure to the experimental conditions)

*c).* A significant decrease in the intensity of the bands associated with the ether linkage in the main-chains and side-chains of Nafion<sup>®</sup> is also observed signifying scission of main-chains and side-chains of Nafion<sup>®</sup> in the presence of peroxy radicals.

2. *In addition, in the case of TFTEA doped membrane, there is an evolution of sulfonate groups of TFTEA (at  $1027\text{cm}^{-1}$ ).*

*a).* The intensity of the band associated with the S-O stretching of TFTEA decreases drastically after 2 days of exposure to the experimental conditions. But, still, the absorption band is observed though reduced intensities even up to 10<sup>th</sup> day of the experiment and its intensity varies very slightly between 2<sup>nd</sup> and 10<sup>th</sup> day of the study.

*b).* Surprisingly, bands associated with the Triethylammonium associated with TFTEA are not detected (as all the bands associated with Triethylammonium are no more observed).

These changes in the bands associated with TFTEA in the membrane could be due to the following reasons:

- Triflate could be no more attached to Triethylammonium but since, no shift in the S-O stretching of Triflate is observed, this possibility can be negated since Triflic acid shows S-O stretching at  $1033\text{cm}^{-1}$ <sup>[28]</sup>.
- Triflate could have dissociated from Triethylammonium and form trifluoromethane sulfonic anhydride. But this possibility has to be negated because trifluoromethane sulfonic anhydride shows S-O stretching at  $\sim 1120\text{cm}^{-1}$  which is not observed in our case<sup>[29]</sup>.

Thus, we assume that TFTEA is present intact within the membrane (though in small quantity). However, due to its small quantity, the sharp band of S-O stretching of Triflate could be observed while the broad bands associated with triethylammonium of TFTEA could not be detected.

The disappearance of bands associated with Triethylammonium entity of Nafion-TEA has been already accounted in the previous section. However, disappearance of band associated with TFTEA could either mean degradation of TFTEA in the presence of the peroxy radicals in the system (which would be surprising as pure TFTEA has been found to be stable against peroxy radical attack) or elution of TFTEA from the Nafion-TEA membrane due to the condensation of water on the surface of the membrane. Thus, in order to verify this, TFTEA doped membrane was study in the presence of pure water at  $80^{\circ}\text{C}$  in similar fashion as in the case of Nafion-TEA (discussed in the precious section).

Unfortunately, this study was done only by using ATR-FTIR. Moreover, the doped membrane used in this study has lower doping level compared the doped membrane studied in the presence of peroxy radicals.

The evolution of ATR-FTIR spectrum of Nafion-TEA+14wt%TFTEA under these conditions is shown in figure 24.

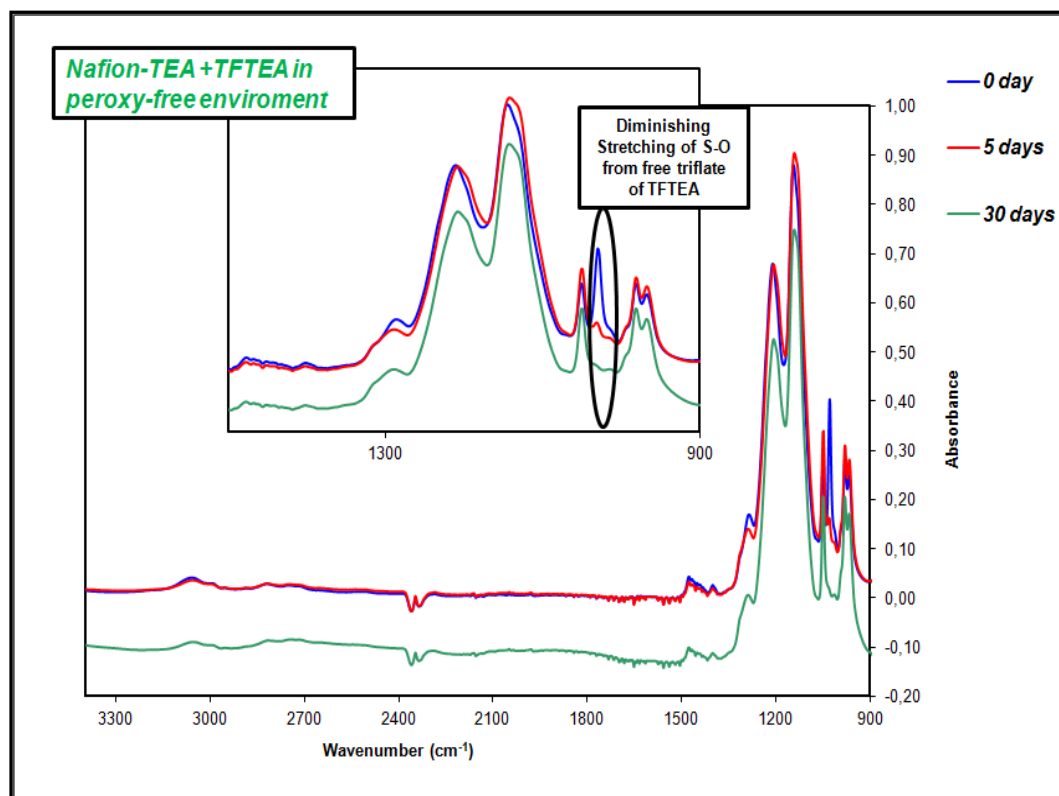


Figure 24: Evolution of ATR-FTIR spectra of Nafion-TEA+14wt%TFTEA with time at 80°C under humid environment

From figure 24, it can be clearly seen that:

1. The *peaks associated with triethylammonium and sulfonate groups of Nafion-TEA do not get affected* at all.
2. However, the *peak associated with triflate of TFTEA disappears* with passage time during the experiment.

From both the studies on the TFTEA doped membrane, two *important points* can be asserted:

1. TFTEA mainly elutes from the membrane due to the condensation of water on the surface of the membrane.
2. Presence of ionic liquid in the membrane does not have any significant impact on the degradation phenomena associated with Nafion-TEA.

## **Conclusion**

The fuel cell tests have shown that TFTEA doped Nafion-TEA membrane gives better performance in comparison to the optimum performance of Nafion-H<sup>+</sup> in the beginning. However, a loss of performance is observed after a functioning time of 3 days. The main reasons behind the loss in the performance of the doped membrane are likely to be:

1. ***Mechanical degradation due to insufficient mechanical strength of the doped membrane at elevated temperatures:*** The membranes exhibited the phenomenon of creeping during the fuel cell tests. Moreover, the results of DMA demonstrated low storage modulus at high temperatures for this type of doped membranes. Hence, it would be interesting to investigate TFTEA doped membranes based on other high-performance polymers such as Polysulfones in order to see if any improvement in thermo-mechanical properties is observed (Chapter 5).
2. ***Chemical degradation due to the attack of peroxy radicals on the system:*** It has been observed that the Nafion-TEA membrane is susceptible to degradation in the presence of peroxy radicals. However, in order to better understand the degradation phenomena associated with an amine-neutralized Nafion<sup>®</sup> membrane, it will be interesting to study the impact of chemical structure of amines as well as different temperatures. The evolution of degradation phenomenon in the case of Nafion-H<sup>+</sup> will be evaluated by FTIR-transmission mode under same experimental conditions in order to compare the rate of formation of sulfonic anhydride in Nafion-H<sup>+</sup> to that in Nafion-TEA membrane.
3. ***Elution of at least a part of TFTEA during fuel cell functioning:*** This has been evidenced by the traces of TFTEA detected in the effluent stream of water.
4. ***Degradation of the electro-catalyst:*** This phenomenon has been largely associated with the loss in the fuel cell performance of an MEA in the literature. Thus, it will be interesting to study the active surface of the catalyst in the MEA (based on a PCIL doped membrane) after fuel cell tests in the future.

## **3.4: General conclusion**

In this chapter, the impact of elaboration method on the morphology and various properties such as thermo-mechanical, electro-chemical and transport properties of PCIL doped Nafion-TEA membranes has been demonstrated.

In the first section of this chapter, Nafion-TEA membrane elaborated by casting has been characterized and compared with Nafion-TEA elaborated by neutralization of extruded commercial Nafion117 membrane.

WAXS results have demonstrated that the *perfluorinated chains of Nafion-TEA are more densely packed when elaborated by casting method*. Furthermore, SANS profile of *casting based Nafion-TEA has demonstrated a more pronounced matrix knee* in comparison to extruded Nafion-TEA. This could be due to better and more homogeneously organized crystalline domains of PTFE main chains in casting based Nafion-TEA.

DMA study has shown that *recast Nafion-TEA presents better thermo-mechanical properties above 150°C* and sustains a storage modulus of approximately 1 MPa in the temperature range of 150-190°C while extruded Nafion-TEA collapses completely above 150°C. Tan $\delta$  profiles have given clues about more homogeneously and densely packed ionic domains in Nafion-TEA-casting.

Conductivity of recast Nafion-TEA is comparatively lower than that of extruded Nafion-TEA below 100°C and similar afterwards probably due to denser packing of ionic functions and lower mobility of the side chains in the former up to  $T_g$ .

Gas permeability coefficients of gases have been found lower for casting based membrane compared to the extruded one.

Concerning water sorption properties of these membranes, casting based membrane present relatively higher water uptake compared to extruded one in the water activity range of 0.1-0.8 and similar at activity ratio of 0.9. However, the *water diffusion rate is much slower in casting based membrane*. All these results are in agreement with the hypothesis that the casting based membranes exhibits better long range crystalline order and/or larger size of crystallites, better packing of ionic domains and reduced free volume of the system.

In the second part of this chapter, casting based TFTEA doped Nafion-TEA membranes were discussed and compared with the swelling based TFTEA doped Nafion-TEA membranes.

WAXS results on these hybrid membranes suggested that presence of *TFTEA promotes more compact packing of perfluorinated chains and the effect is more prominent in casting based membranes*.

SANS results have demonstrated that *casting based membranes exhibit higher and/or more heterogeneous swelling of ionic domains of Nafion-TEA on TFTEA* compared to swelling based doped membranes with increasing TFTEA content. This result has been related to the micellar organization of TFTEA in the Nafion-TEA structure which seems to be more significant when the

membranes are elaborated by casting method. Moreover, *the position of matrix knee does not change with increasing TFTEA concentration in casting based membranes* unlike swelling based membranes which could be related to the *lower impact of TFTEA on the long range crystalline order in Nafion-TEA*.

DMA results show that *casting based membranes present better thermo-mechanical properties compared to swelling based membranes above 150°C* and sustain a storage modulus of 1MPa in the temperature range of 150-180°C. Moreover, the former present a very strong  $\beta$  relaxation with increasing TFTEA content and  $\alpha$  relaxation corresponding to pure Nafion-TEA is always present though with reduced intensity in the  $\tan\delta$  profiles even at high TFTEA content.

Furthermore, *both the kinds of doped membranes present conductivities of similar orders*.

The *gas-permeability coefficients of casting based TFTEA doped membranes have been found lower* to that of swelling based ones. This result supports the hypothesis that casting based doped membranes exhibit better long range crystalline order of PTFE chains.

In addition, both the kinds of doped membranes exhibit *similar sorption behavior* (e.g. an increase in water uptake with increasing TFTEA content) though the results from GAB modeling suggest that morphology developed by casting is more favorable for the sorption of water molecules in middle range activity.

Fuel cell tests show that *casting TFTEA doped membranes gives current density of 0.85A/cm<sup>2</sup> at 100°C using 100% humidified gases* followed by *a gradual decline in the performance with time*. Gradual loss in the performance has been related to the mechanical degradation, chemical degradation in the presence of peroxy radicals and elution of TFTEA from the membrane. The results of degradation study demonstrated *good chemical stability of TFTEA in the presence of peroxy radicals*. However, *Nafion-TEA membrane exhibited loss of Triethylammonium entity in the presence of peroxy radicals*. In order to further understand the degradation phenomena associated with amine neutralized Nafion<sup>®</sup> membranes, it will be very interesting to investigate systems based on different amines and at different temperatures as well as different water vapor pressures.

In a nutshell, membranes elaborated by *casting method present overall better performance compared to swelling based doped membranes* in regard of their high temperature-fuel cell application.



## References:

1. Gebel, G.; Aldebert, P.; Pineri, M.; *Macromolecules* **1987**, 20, 1425-1428.
2. Moore, R.B.; Martin, C.R.; *Macromolecules* **1988**, 21, 1334-1339.
3. Su, S.; Mauritz, K.A.; *Macromolecules* **1994**, 27, 2079-2086.
4. Van der Heijden, P.C.; Rubatat, L.; Diat, O.; *Macromolecules* **2004**, 37, 5327-5336.
5. A. Sacca, A.; Carbone, A.; Pedicini, R.; Portale, G.; D'Ilario, L.; Longo, A.; Martorana, A.; Passalacqua, E.; *Journal of Membrane Science* **2006**, 278, 105-113.
6. Fujimura, M.; Hashimoto, T.; Kawai, H.; *Macromolecules* **1981**, 14, 1309-1315.
7. Moore, R.B.; Cable, K.M.; Croley, T.L.; *Journal of Membrane Science* **1992**, 75, 7-14.
8. Moore, R.B.; Phillips, A.L.; *Journal of Polymer Science: Part B: Polymer Physics* **2006**, 44, 2267-2277.
9. Fan, Z.; Harrison, D.J.; *Analytical Chemistry* **1992**, 64, 1304-1311.
10. Broka, K.; Ekdunge, P.; *Journal of Applied Electrochemistry* **1992**, 27(2), 117-123.
11. Vengatesan, S.; Cho, E.; Kim, H.J.; Lim, T.H.; *Korean Journal of Chemical Engineering* **2009**, 26(3), 679-684.
12. Lin, J.; Wu, P.H.; Wycisk, R.; Pintauro, P.N.; Shi, Z.; *Macromolecules* **2008**, 41, 4284-4289.
13. Greaves, T.L.; Drummond, C.J.; *Chemical Society Review*, **2008**, 37, 1709-1726.
14. Iojoiu, C.; Judeinstein, P.; Sanchez, J.Y.; *Electrochimica Acta* **2007**, 53, 1395-1403.
15. Shao, Y.; Yin, G.; Wang, Z.; Gao, Y.; *Journal of Power Sources* **2007**, 167(2), 235-242.
16. Zhang, J.L.; Xie, Z.; Zhang, J.J.; Tanga, Y.H.; Song, C.J.; Navessin, T.; Shi, Z.Q.; Song, D.T.; Wang, H.J.; Wilkinson, D.P.; Liu, Z.S.; Holdcroft, S.; *Journal of Power Sources* **2006**, 160, 872-891.
17. Tarasevich, A.R.; Sadkowsky, M.; Yeager, E.; *Comprehensive Treatise of Electrochemistry* (Plenum New York **1983**), 7, 301-398.
18. Inaba, M.; Yamada, H.; Tokunaga, J.; Tasaka, A.; *Electrochemical and Solid-State Letters* **2005**, 7(12), A474-476.
19. Qiao, J.; Saito, M.; Hayamizu, K.; Okada, T.; *Journal of the Electrochemical Society* **2006**, 153(6), 967-974.
20. Ramaswamy, N.; Hakim, N.; Mukerjee, S.; *Electrochimica Acta* **2008**, 53, 3279-3295.
21. Holber, M.; Johansson, P.; Jacobsson, P.; *Fuel Cells* **2011**, 11(3), 459-464.
22. Collier, A.; Wang, H.J.; Yuan, X.Z.; Zhang, J.J.; Wilkinson, D.P.; *International Journal of Hydrogen Energy* **2006**, 31(13), 1838-1854.
23. Schiraldi, D.A.; *Journal of Macromolecular Science, Part C: Polymer Reviews* **2006**, 46(3), 315-327.
24. Borup, R.; Meyers, J.; Pivovar, B.; Kim, Y.S.; Mukundan, R.; Garland, N.; Myers, D.; Wilson, M.; Garzon, F.; Wood, D.; Zelenay, P.; More, K.; Stroh, K.; Zawodzinski, T.; Boncella, J.; McGrath, J.E.; Inaba, M.; Miyatake, K.; Hori, M.; Ota, K.; Ogumi, Z.; Miyata,

- S.; Nishikata, A.; Siroma, Z.; Uchimoto, Y.; Yasuda, K.; Kimijima, K.I.; Iwashit, N.;  
Chemical Reviews **2007**, 107, 3904-3951.
25. Chen, C.; Fuller, T.F.; Polymer Degradation and Stability **2009**, 94, 1436–1447.
26. Murphy, S. M.; Sorooshian, A.; Kroll, J. H.; Ng, N. L.; Chhabra, P.; Tong, C.; Surratt, J. D.;  
Knipping, E.; Flagan, R. C.; Seinfeld, J. H.; Atmospheric Chemistry and Physics Discussion  
**2007**, 7, 289-349.
27. Di Noto, V.; Negro, E.; Sanchez, J-Y; Iojoiu, C.; Journal of American Chemical. Society  
**2010**, 132, , 2183-2193.
28. [http://www.hanhonggroup.com/ir/ir\\_en/B15841.html](http://www.hanhonggroup.com/ir/ir_en/B15841.html); FTIR spectrum of  
Trifluoromethanesulfonic acid (CAS Number 1493-13-6).
29. FTIR spectrum of Trifluoromethanesulfonic anhydride (CAS Number 358-23-6); Sigma-  
Aldrich.

## 4. Casting method based Nafion-TEA membranes doped with different per- fluorinated anion based Ionic liquids

In the previous chapter, it has been shown that TFTEA doped membranes based on casting method can have significantly different morphology and consequently functional properties compared to swelling based membranes only due to the difference in the way of their elaboration. In order to further understand how a perfluorinated anion based PCIL can place itself in the matrix of Nafion-TEA and affect the morphology of Nafion-TEA matrix, doped membranes based on Nafion-TEA and PCILs containing a perfluorinated anion of different chain lengths were elaborated by casting method and characterized in similar fashion as in previous chapters.

Hence this chapter primarily focuses on the effect of different perfluorinated anion based PCILs on the morphology and functional properties of the doped membranes elaborated by casting method. The PCILs utilized for this study include: Triethylammonium Perfluorinated Butane Sulfonate (PFBuTEA) and Triethylammonium Perfluorinated Octane Sulfonate (PFOcTEA) (chemical structure shown in figure 1). The results obtained with PFBuTEA and PFOcTEA based doped membranes have been analyzed and compared with TFTEA based membranes. Table 1 shows certain important characteristics of all the PCILs which have been utilized in this work.

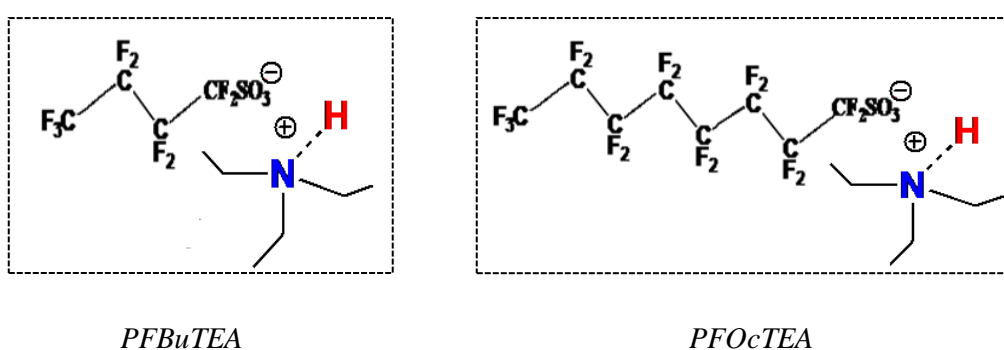


Figure 1: Chemical structure of the PCILs used in this study

<i>PCIL</i>	$\sigma \times 10^2$ (S/cm) at 110°C	$T_m(^{\circ}\text{C})$	$T_d(^{\circ}\text{C})$
<i>TFTEA</i>	1.89	34	376
<i>PFBuTEA</i>	1.10	61*	383
<i>PFOcTEA</i>	0.1	54	390

\**PFBuTEA* shows two sharp melting peaks: first melting peak at 28°C and second melting peak at 61°C

Table 1: Thermal properties and ionic conductivity values for different PCILs

#### 4.1: Characterization and comparison of Nafion-TEA membranes based on different PCILs

In this chapter, following will be discussed systematically:

- ❖ Firstly the effect of the nature of each PCIL (i.e. TFTEA, PFBuTEA and PFOcTEA) and their percentage content on the morphology of Nafion-TEA membranes will be discussed, followed by a comparison of the evolution of the morphology of these different doped membranes.
- ❖ Afterwards, a correlation of their morphology with various functional properties will be described.

The membranes were cast with different weight percentages depending on the PCIL and they were found to be stable against leaching phenomenon. The different concentrations obtained and related  $\lambda$  values are shown in table 2. The volume percent concentration of the ionic liquids in the membranes could not be calculated due to the difficulty in measurements of densities of PFBuTEA and PFOcTEA (because of their high melting point).

<i>Sample code</i>	<i>% PCIL (by weight)</i>	<i>Moles of PCIL/ moles of -SO<sub>3</sub><sup>-</sup>HN(C<sub>2</sub>H<sub>5</sub>)<sub>3</sub> of Nafion-TEA (<math>\lambda</math>)</i>
<i>Nafion-TEA+5%TFTEA</i>	<i>5</i>	<i>0.25</i>
<i>Nafion-TEA+10%TFTEA</i>	<i>10</i>	<i>0.78</i>
<i>Nafion-TEA+15%TFTEA</i>	<i>15</i>	<i>0.98</i>
<i>Nafion-TEA+20%TFTEA</i>	<i>20</i>	<i>1.12</i>
<i>Nafion-TEA+10%PFBuTEA</i>	<i>10</i>	<i>0.33</i>
<i>Nafion-TEA+20%PFBuTEA</i>	<i>20</i>	<i>0.78</i>
<i>Nafion-TEA+30%PFBuTEA</i>	<i>30</i>	<i>1.28</i>
<i>Nafion-TEA+40%PFBuTEA</i>	<i>40</i>	<i>1.9</i>
<i>Nafion-TEA+5%PFocTEA</i>	<i>5</i>	<i>0.11</i>
<i>Nafion-TEA+10%PFocTEA</i>	<i>10</i>	<i>0.22</i>
<i>Nafion-TEA+20%PFocTEA</i>	<i>20</i>	<i>0.5</i>
<i>Nafion-TEA+30%PFocTEA</i>	<i>30</i>	<i>0.86</i>
<i>Nafion-TEA+40%PFocTEA</i>	<i>40</i>	<i>1.33</i>
<i>Nafion-TEA+50%PFocTEA</i>	<i>50</i>	<i>2</i>

Table 2: Concentration and  $\lambda$  values for Nafion-TEA membranes doped with different PCILs

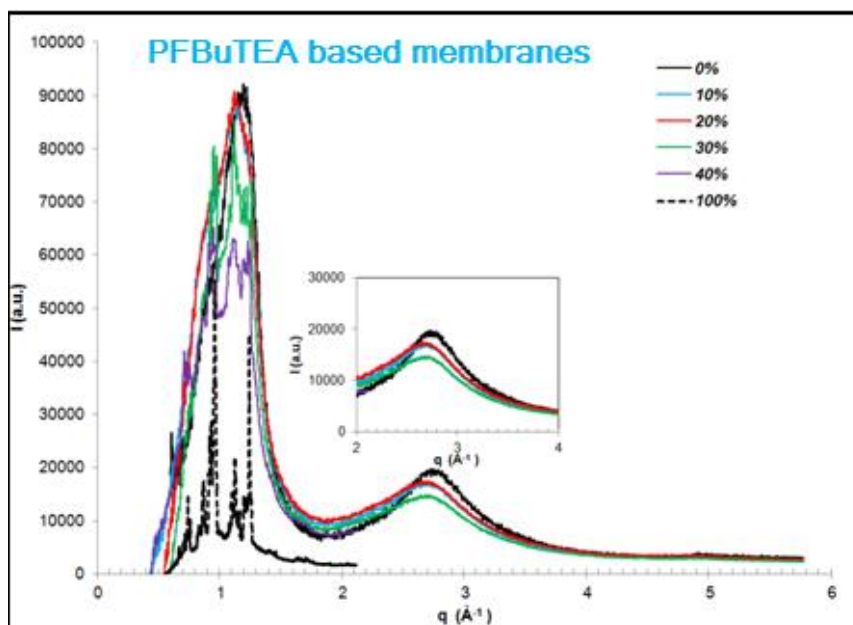
#### a. Morphology

The impact of different ionic liquids in terms of their chemical structure as well as percentage content on the morphology of Nafion-TEA has been explored on various length scales using WAXS and SANS in similar pattern as in the previous chapter. The sample preparation and the measurements were carried out under the same conditions which were employed for the TFTEA doped membranes.

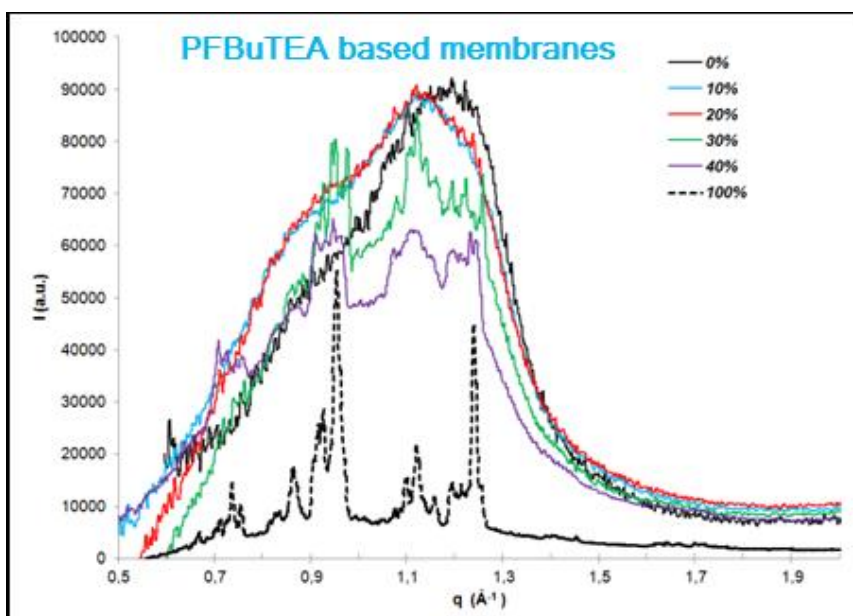
### Molecular scale

The *impact of different PCILs* on the morphology of Nafion-TEA in terms of *packing of perfluorinated chains* as well as the *inter-atomic correlation along the hydrophobic main-chain* was studied using WAXS measurements. The WAXS profiles of Nafion-TEA membranes based on **PFBuTEA** and **PFOcTEA** are shown in figure 2((a)-(b)) and 3 ((a)-(b)) respectively. The main features of the spectra are described as follows:

1. First, we consider the crystalline peak present at  $q=2.8 \text{ \AA}^{-1}$  ( $d=2.24 \text{ \AA}$ ) for Nafion-TEA corresponding to the correlation distance between two  $-\text{CF}_2$  groups present on the same side in the helix structure along the perfluorinated chain. It is clearly visible in figure 2(a) & 3 (a) that it shifts slightly towards lower  $q$  value ( $q=2.67 \text{ \AA}^{-1}$ ;  $d=2.35 \text{ \AA}$ ) for both PFBuTEA and PFOcTEA doped membranes, unlike for TFTEA based membranes for which it didn't change at all. This shift appears from the lowest PCIL concentration and does not evolve afterwards with increasing PCIL concentration in the case of PFBuTEA based membranes. In the case of PFOcTEA based membranes, this peak shifts gradually with increasing concentration of the PCIL. This result points towards increasing distance between two consecutive  $-\text{CF}_2$  groups present on the same side in the helix structure along the perfluorinated chains. Thus, this increase in distance signifies *slight relaxation in the helix organization and hence slight elongation of PTFE chains*. This result is in contrast to the results of TFTEA doped membranes where no such effect was observed.
2. Considering the broad peak observed for Nafion-TEA at  $q=1.18 \text{ \AA}^{-1}$  ( $d=5.32 \text{ \AA}$ ), it can be seen in figure 2(b) and 3 (b) that it is shifted to lower  $q$  value ( $\sim 1.12\text{--}1.13 \text{ \AA}^{-1}$ ;  $d=5.56 \text{ \AA}$ ) in the presence of both the ionic liquids (PFBuTEA and PFOcTEA) unlike TFTEA for which the peak value shifted to slightly higher  $q$  value ( $q=1.2 \text{ \AA}^{-1}$ ;  $d=5.23 \text{ \AA}$ ). These results underline that the *presence of PFBuTEA and PFOcTEA results in less dense packing of perfluorinated chains of Nafion-TEA*. However, this shift towards lower  $q$  value is clearly visible for the membranes containing up to 20wt% of these PCILs and difficult to observe afterwards (*from 30wt% PCIL content*) because of the *appearance of many peaks corresponding to pure PFBuTEA and PFOcTEA in the same  $q$  range*. This means that when these PCILs are added in the membrane below a certain percentage content, they are probably completely dispersed in the Nafion-TEA matrix. Above this critical percentage content, there is either formation of domains of these PCILs in the Nafion-TEA membrane at this length scale or these PCILs arrange themselves in the nano-structure of Nafion-TEA in such a way similar to their organization in their pure form.



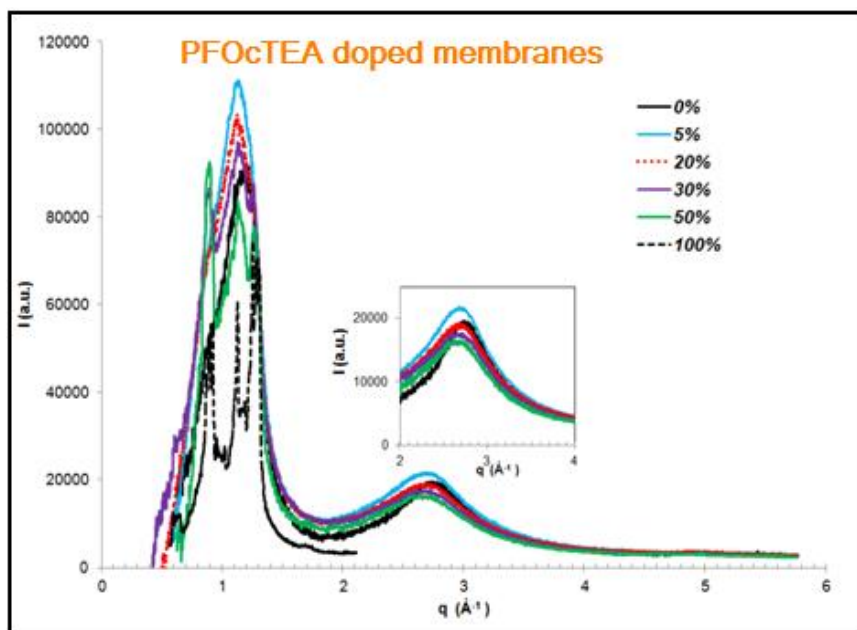
(a)



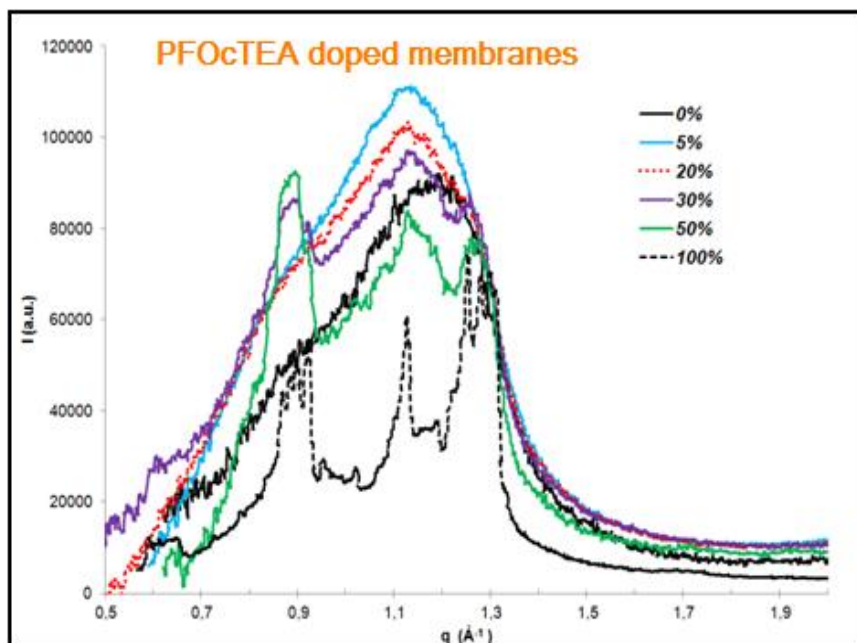
(b)

Figure 2: WAXS profiles of Nafion-TEA membranes doped with different wt% content of PFBuTEA; a). Full spectra; b). Zoom of full spectra in the  $q$  range of  $0.5\text{--}2\text{ \AA}^{-1}$

3. The halo observed at  $q \sim 0.80\text{ \AA}^{-1}$  is visible up to only 20 wt% content of both the PCILs and seems to be at same position as the virgin Nafion-TEA membrane. From 30 wt% of the PCILs, this halo is not visible due to its overlapping with the Bragg peaks of the respective PCILs.



(a)



(b)

Figure 3: WAXS profiles of Nafion-TEA membranes doped with different wt% content of PFOcTEA; a). Full spectra; b). Zoom of full spectra in the  $q$  range of  $0.5\text{--}2\text{ \AA}^{-1}$

From these experimental observations, following *conclusions* can be drawn:

- Both *PFBuTEA* and *PFOcTEA* doped membranes show similar evolution of WAXS profiles but different from that of *TFTEA* doped membranes.



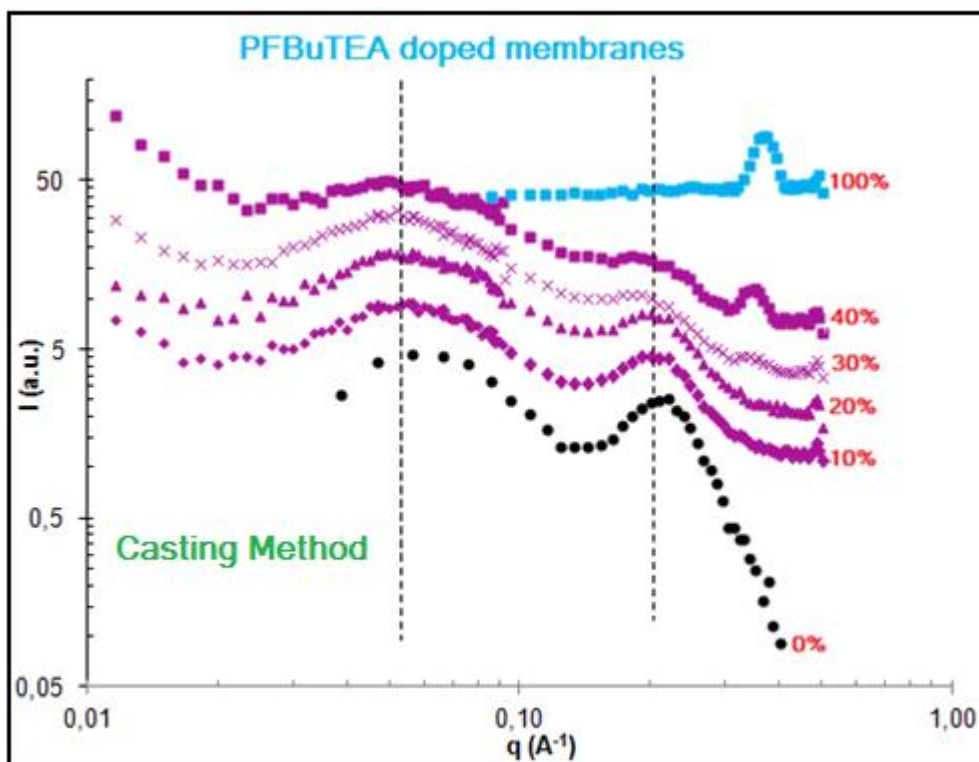
- Addition of PFBuTEA/PFOcTEA in Nafion-TEA with changes the intra-atomic co-relation along the PTFE main-chain and *slight relaxation/elongation in the helix organization PTFE main-chains* occurs, unlike the case of TFTEA doped membranes where it didn't change at all.
- The *local packing of the hydrophobic main-chains becomes less dense* on addition of PFBuTEA/PFOcTEA in Nafion-TEA matrix, unlike the case of TFTEA doped membranes where it improved.
- Appearance of Bragg peaks of PFBuTEA and PFOcTEA started from their 30 wt% content in the Nafion-TEA membranes signifying *formation of PCIL rich domains* in the membrane.

### Nanoscopy-mesoscopic scale

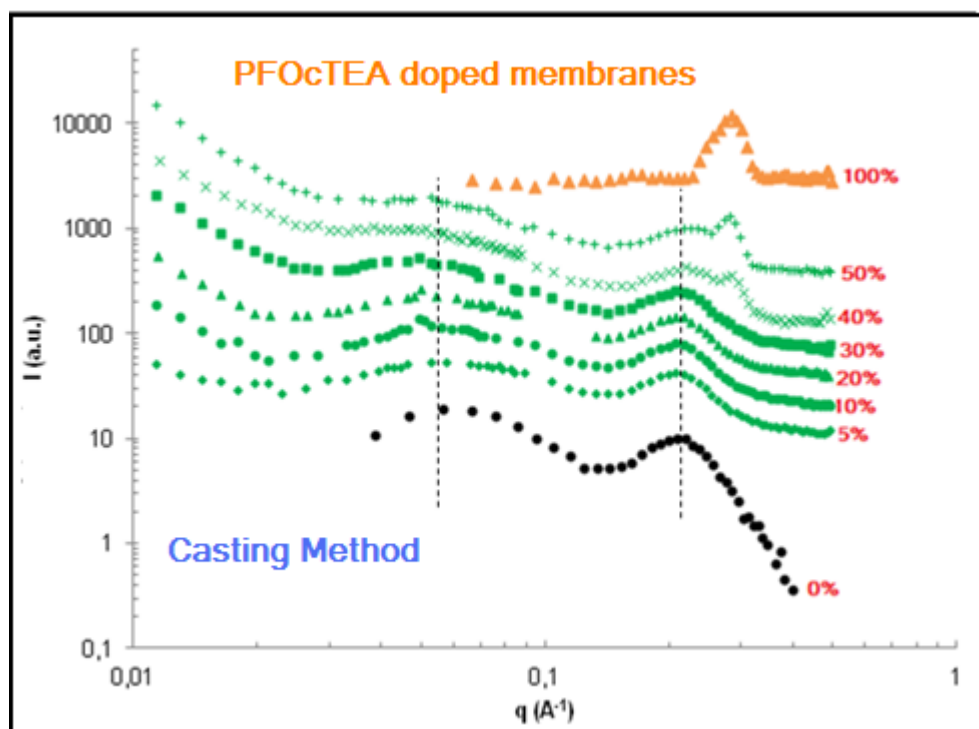
In order to further understand the impact of these two ionic liquids on the morphology of Nafion-TEA and compare with TFTEA at larger length scale, SANS measurements were carried out. The SANS profiles of PFBuTEA and PFOcTEA doped Nafion-TEA membranes on a log-log scale are presented in figure 4 (a) and (b) respectively. An offset has been applied for clarity.

With these two spectra, following points can be noted:

1. In the case of *PFBuTEA doped membranes*, both *the ionomer peak and the matrix knee do not change shape or position up to 20 wt% content of PFBuTEA*. On further increasing the content of PFBuTEA, a shift in the position of ionomer peak from  $q=0.21 \text{ \AA}^{-1}$  ( $d=30 \text{ \AA}$ ) for pure Nafion-TEA to  $q=0.182 \text{ \AA}^{-1}$  ( $d=34.5 \text{ \AA}$ ) for doped Nafion-TEA membranes is observed. However, matrix knee still remains at the same position with the same shape.
2. The SANS spectra of *PFOcTEA doped membranes* clearly shows *no change in the position as well as the shape of the ionomer peak and the matrix knee*. This trend is observed *whatever the percentage content of the PCIL* is in the doped membrane. This result is in contrary to that of TFTEA doped membranes in which a clear shifting and broadening of the ionomer peak and matrix knee were observed with increasing TFTEA content.



(a)



(b)

Figure 4: SANS profiles of Nafion-TEA membranes doped with different wt% content of (a). PFBuTEA ; (b). PFOcTEA

3. Moreover, *the intensity of the “small angle upturn” increases with increasing PCIL content* in both the cases. This is in contrast to the case of TFTEA doped membranes where it didn't change with increasing TFTEA content. This upturn at very small angle corresponds to the organization in the polymer at large scale ( $\sim 1000\text{\AA}$ ).
4. *Additional peak* is observed in the SANS profiles of these doped membranes from 30wt% content of these two PCILs (more clearly visible from 40 wt% content in the case of PFOcTEA). This peak is observed at  $q=0.35\text{ \AA}^{-1}$  ( $d=17.94\text{ \AA}$ ) for *PFBuTEA doped membranes* and  $q=0.284\text{ \AA}^{-1}$  ( $d=22.11\text{ \AA}$ ) for *PFOcTEA doped membranes* and increases in intensity with further increase in the PCIL content. This *additional peak corresponds to the Bragg peak of the pure PCILs*.

From these experimental observations, following *conclusions* can be drawn:

- The *nano-structuration of Nafion-TEA doesn't get destroyed in the presence of these two PCILs* even though these PCILs are composed of a long hydrophobic perfluorinated chain along with hydrophilic  $-\text{SO}_3-\text{H}^+\text{N}(\text{C}_2\text{H}_5)_3$  moiety.
- The appearance of the Bragg peaks of pure PCILs in the SANS profiles seems to be in correlation with the appearance of characteristic peaks of pure PCILs in the WAXS profiles as both of them start to appear from same wt% content of the PCIL i.e. 30wt% ( $\lambda \sim 1$ ). This appearance of Bragg peak at high percentage of these PCILs points towards the *formation of PCIL domains within the Nafion-TEA matrix*. Moreover, it seems that these PCIL domains are of enough large size. This is because Bragg peaks associated with a molecule like these PCILs can be observed only if it would form domains consisting of at least 3-4 layers. Furthermore, PCIL molecules seem to organize themselves within the polymer matrix in a fashion similar to their organization in pure form as Bragg peaks associated with these PCILs appear at similar position for both the cases i.e. in pure form as well as in the polymer matrix.
- There is *no significant increase in the size of ionic domains of Nafion-TEA in the presence of these PCILs* as the characteristic distance of the nano-phase separation (i.e. size of the ionic zone present between two hydrophobic ribbons/lamellae) doesn't change, unlike in the case of TFTEA doped Nafion-TEA membranes. This means that these two PCILs accommodate themselves in the Nafion-TEA structure without changing the nano-structuration of Nafion-TEA at this scale.

- There seems to be *no effect of these PCILs on the long range crystalline order of Nafion-TEA*, unlike TFTEA doped membranes.
- It seems that *change in the organization of Nafion-TEA occurs at larger length scale ( $\sim 1000\text{\AA}$ )* with increasing wt% percent content of PFBuTEA and PFOcTEA in the membrane.

After combining the information gained from WAXS and SANS on the morphology of PFBuTEA and PFOcTEA doped Nafion-TEA membranes based on casting method, we propose that these two ionic liquids accommodate themselves in the Nafion-TEA structure in the following ways:

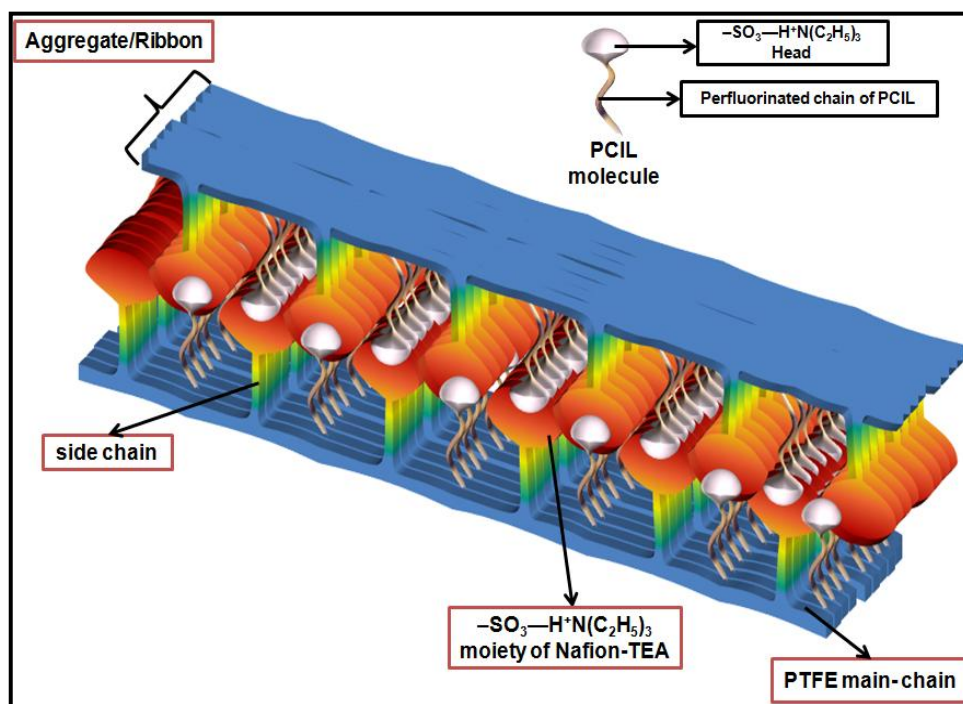
**1). PCIL present in moderate quantities ( $\lambda \leq 1$ ):** When the ionic liquid is present in moderate quantities ( $\lambda \leq 1$ ), the PCIL molecules could organize themselves in two ways:

(a). PCIL molecules organize themselves along the perfluorinated side-chains which are perpendicular to the surface of the lamellae/ribbons composed of PTFE chains. In other words, the PCIL molecules intercalate themselves between the side-chains and the perfluorinated chain-ends of the PCIL molecules in between the perfluorinated main-chains of the polymer. This type of organization facilitates loosening of the packing of perfluorinated PTFE main chains of the polymer (figure 6(a); the ionic entity “ $-\text{SO}_3-\text{H}^+\text{N}(\text{C}_2\text{H}_5)_3$ ” of the PCIL is shown smaller in size compared to that of Nafion-TEA in the picture for clarity). This type of PCIL organization could result in relaxation/elongation of perfluorinated main-chains as well (as deduced from the WAXS results).

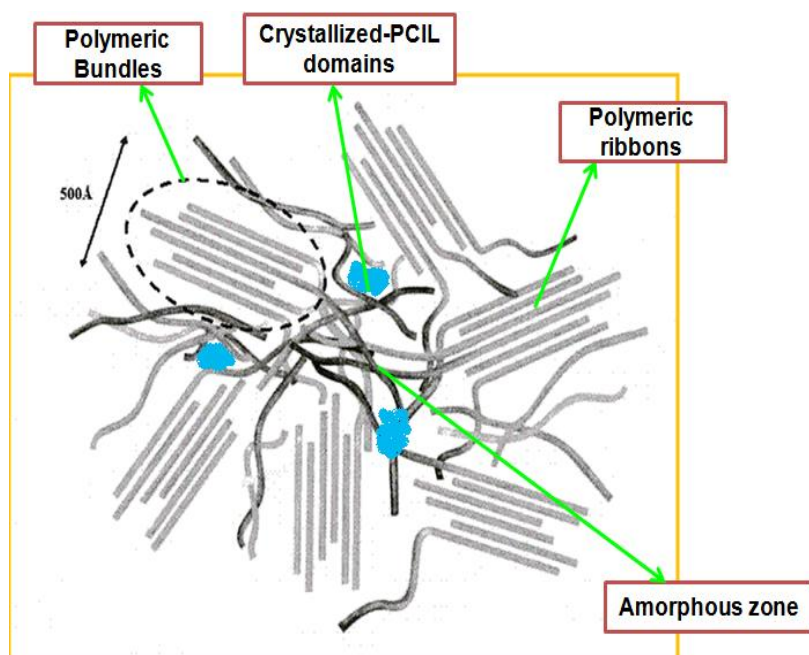
(b). Some of the PCIL molecules could possibly organize themselves in the amorphous inter-bundle or inter-ribbon zones in a fashion similar as the side-chains of the polymer and hence swell the system laterally and not perpendicularly.

**2). PCIL present in large quantities ( $\lambda \geq 1$ ):** When the ionic liquid is present in large quantities ( $\lambda > 1$ ), it could organize itself not only in the manner discussed in the above point, but could also form crystallized-PCIL domains in the inter-bundle amorphous region of Nafion-TEA and organize around the bundles (being able to be detected as pure PCIL molecules) as shown in figure 6 (b) and 6 (c). In the case of PFBuTEA based membranes, in addition to the different organizations of the PCIL discussed above, some of its molecules could also place themselves partially in the ionic domains and partially between the side-chains of Nafion-TEA in the case of  $\lambda \geq 1$  for PFBuTEA. This hypothesis is based on the fact that ionomer peak shifts to slightly smaller  $q$  values for the doped membranes with 30wt% or more of PFBuTEA signifying an increase in the size of ionic domains of Nafion-TEA.

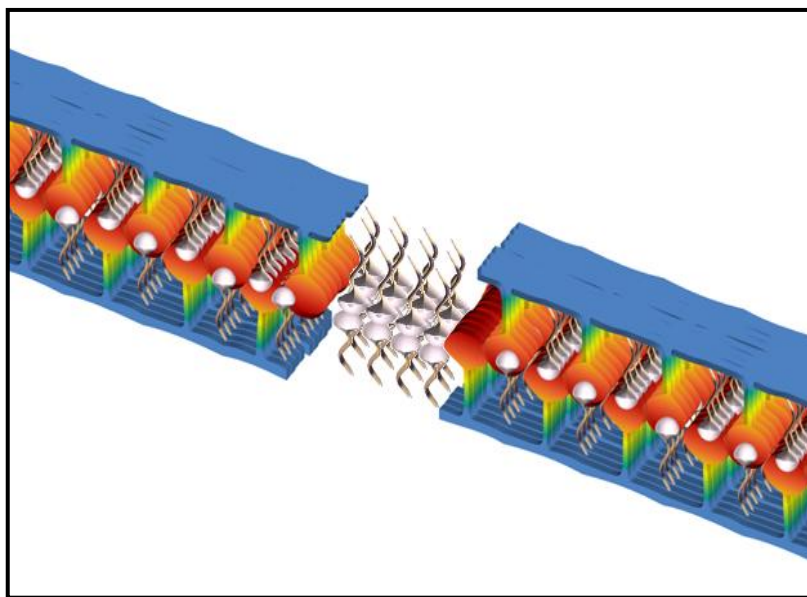
However, it could also be proposed that the organization/distribution of PFOcTEA/PFBuTEA molecules could be a mixture of all these possibilities from their moderate quantities in Nafion-TEA membrane.



(a)



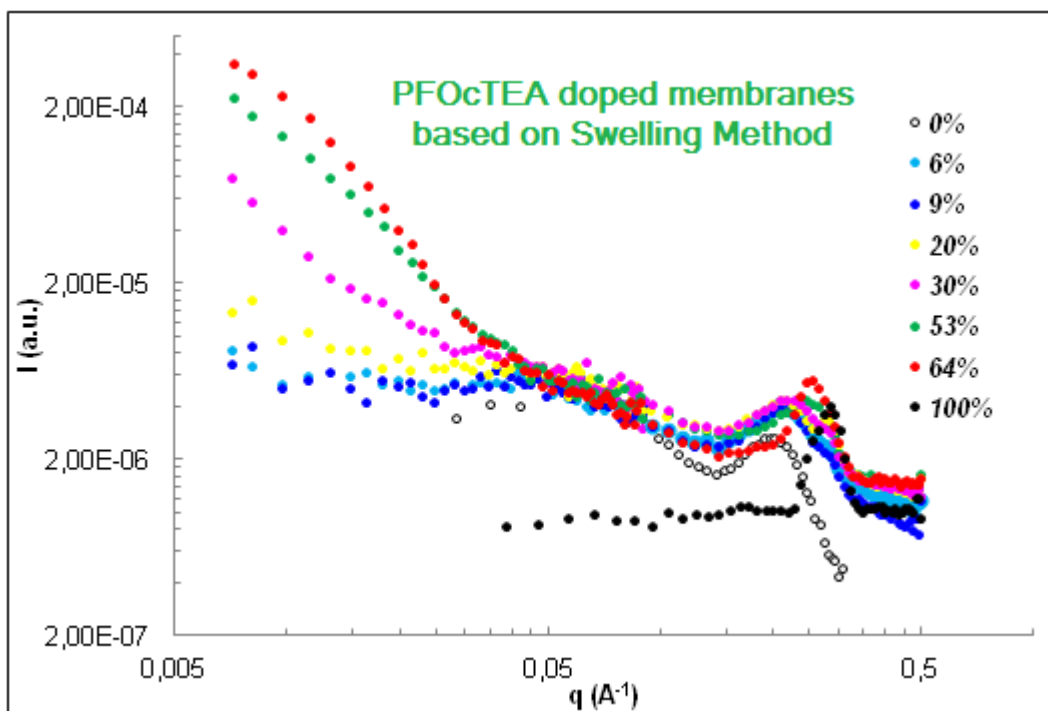
(b)



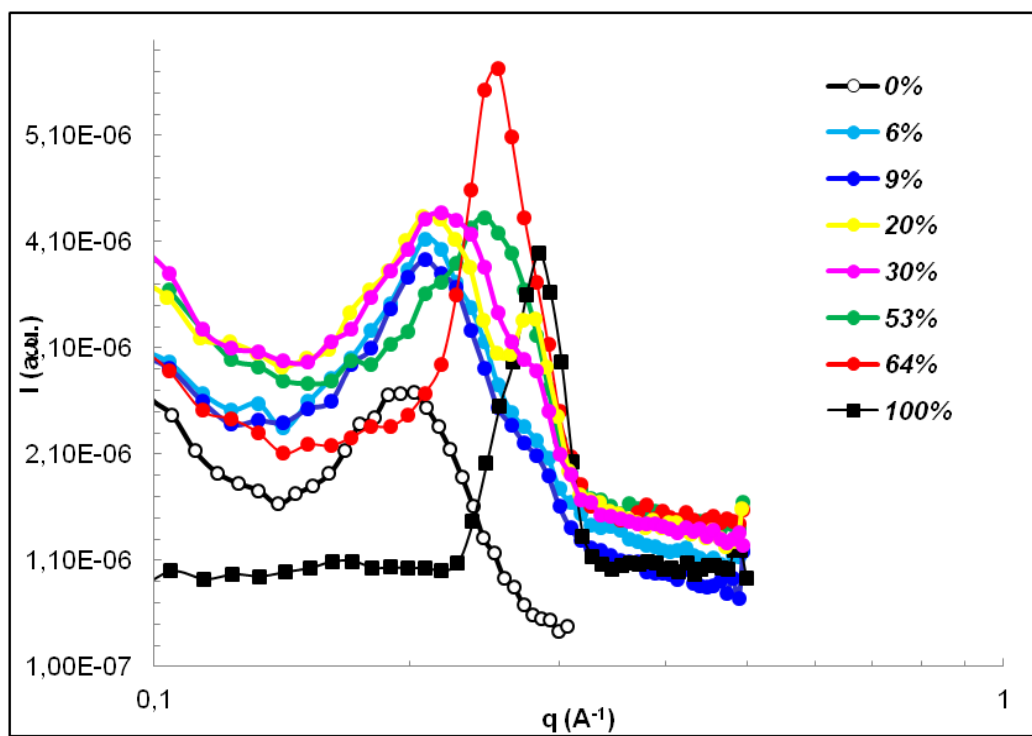
(c)

Figure 6: Organization and distribution of PFOcTEA and PFBuTEA in Nafion-TEA structure in different forms and at different length scales (The ionic entity “ $-\text{SO}_3-\text{H}^+\text{N}(\text{C}_2\text{H}_5)_3$ ” of the PCIL is shown smaller in size compared to that of Nafion-TEA in the picture for clarity.)

*The arrangement of PFOcTEA and PFBuTEA molecules in the structure of Nafion-TEA is quite different from that of TFTEA molecules.* Thus, in order to better understand if this peculiar arrangement of PFOcTEA and PFBuTEA molecules occurs either due to the chemical nature of the PCIL or due to the method of membrane elaboration, PFOcTEA doped Nafion-TEA membranes were prepared by swelling method (similar protocol of preparation as for TFTEA based membranes discussed in second chapter) and were characterized by SANS. These membranes based on swelling will be discussed only from morphological point of view in this section and will not be further discussed in other sections of this chapter. The SANS profiles of these PFOcTEA doped Nafion-TEA membranes based on swelling method are shown on a log-log scale in figure 5 (a) and (b).



(a)



(b)

Figure 5: SANS profiles of PFOcTEA doped Nafion-TEA membranes based on swelling method (a). Full Profile; (b). Focus on the large angle range (ionomer peak)

In the case of swelling based PFOcTEA doped membranes, following observations are made:

1. There is significant difference between casting and swelling based PFOcTEA doped membranes in the evolution of their **ionomer peak** with the PFOcTEA concentration. In the case of swelling based PFOcTEA doped membranes (figure 5 (b)), surprisingly, another small peak appears immediately along with the ionomer peak (at  $q = 0.282 \text{ \AA}^{-1}$ ;  $d = 22 \text{ \AA}$ ) on adding PFOcTEA in the membrane which corresponds to the **Bragg peak of PFOcTEA** ( $q = 0.284 \text{ \AA}^{-1}$ ). With increasing PFOcTEA content in the membrane, firstly the ionomer peak shifts to slightly larger  $q$  value and the neighbouring small peak becomes more intense (up to 20 wt%). Afterwards, when the concentration of PFOcTEA is enough high in the system (30-53 wt%), these two peaks start to superimpose with each other (due to gradual shifting of ionomer peak towards larger  $q$  value) to form one broad peak. Finally, when PFOcTEA is present in majority in the Nafion-TEA membrane (64 wt%), this broad peak becomes finer and resembles the Bragg peak of pure PFOcTEA though present at smaller  $q$  value ( $q = 0.247 \text{ \AA}^{-1}$ ;  $d = 25.4 \text{ \AA}$ ). Shifting of ionomer peak towards larger  $q$  value points towards **decrease in the size of ionic domains of Nafion-TEA on PFOcTEA addition** while appearance of **Bragg peak of PFOcTEA** corresponds to the **formation of PFOcTEA-rich domains**.
2. The **matrix knee** does not shift at all in swelling based membranes too as was the in the case of casting based membranes. This signifies that local crystalline order is not affected in both the cases.
3. The “**small angle upturn**” intensity increases with increasing PFOcTEA similarly to casting based membranes. However, the upturn seems to be **more prominent in the case of swelling based membranes** especially at high PFOcTEA concentrations.

From these observations, different effects of PFOcTEA addition into Nafion-TEA matrix can be accounted:

- It can be said that the SANS **profiles of swelling and casting based PFOcTEA doped Nafion-TEA membranes are quite similar** overall. This must be primarily due to the chemical nature of the PCIL. Thus, it can be said that PFOcTEA molecules **neither swell the ionic domains nor change long range crystalline order of Nafion-TEA** membranes for both swelling as well as casting method.
- However, **slight difference in the evolution of ionomer peak of Nafion-TEA and Bragg peak of PFOcTEA** in both the types should be due to the **difference in the elaboration method**. PFOcTEA has choice to distribute itself in a manner energetically more feasible in the casting



based membranes compared to swelling based membranes where PFOcTEA has to accommodate and orient itself in the pre-developed morphology of Nafion-TEA.

In the case of PFOcTEA doped membranes based on swelling method, three organization/distribution possibilities are proposed below:

1. PFOcTEA molecules intercalate themselves into the side-chains of the PTFE main-chains. This could also probably result in loosening of the packing as well as relaxation of helix structure of PTFE main-chains. PFOcTEA molecules seem to organize themselves all around the ribbons. However, their insertion in the side chain is not as perfect as in the case of casting based membranes.
2. PFOcTEA molecules could also organise themselves in the inter-bundle zones.
3. Moreover, PFOcTEA molecules could form crystallized domains in the amorphous inter-bundle domains. If a large number of molecules would organize in this way, it could exert pressure on the bundles thereby decreasing the distance between two bundles and hence decreasing the size of the ionic domains.

From all the experimental observations discussed in this section, it is clear that chemical nature of a PCIL plays great role in the final nano-structuration of Nafion-TEA. In addition, elaboration method could change a little bit the scenario of PCIL organization/distribution in the structure of the polymer. In order to further understand the systems based on PFOcTEA or PFBuTEA, it would be interesting to do the following experiments:

- ✚ Stretching of Nafion-TEA membrane at different degrees prior to PCIL addition and study of morphology afterwards.
- ✚ WAXS measurements under controlled humidity as well as at different temperatures.

#### ***b. Differential Scanning Calorimetry***

This characterization technique is an indirect method to gain information on the organization/structuration of an ionic liquid imbibed within a polymer matrix. As discussed previously, if the ionic liquid is completely dispersed in the polymer matrix, melting peak associated with the PCIL is not observed in the DSC thermogram. However, if aggregates of the PCIL are formed in the polymer matrix, a melting peak associated with the fusion of these PCIL aggregates could be observed through this technique. Moreover, higher the size of these PCIL aggregates within the polymer matrix; closer will be the value of their fusion temperature to the fusion temperature of pure

PCIL<sup>[1-3]</sup> (because of similar organization of the PCIL molecules in these aggregates compared to that in their pure form). Thus, in order to have more information about the organization and distribution of the PCILs in the doped membranes, DSC measurements were performed. In this study, the doped membranes were studied in the two temperature ranges (as mentioned below) in order to evidence Nafion-PCIL phase separation if any.

1). **Series I:** 15°C to 150°C with the heating rate of 2°C/minute

2). **Series II:** -50°C to 150°C with the heating rate of 2°C/minute

Two different temperature ranges for DSC measurements were chosen in order to be able to observe if any changes in the behavior corresponding to the organization/distribution of PCIL molecules is seen in different temperature ranges or not. This is important because some characterization measurements have been carried out starting from the room temperature, but some have been carried out starting from low temperatures (DMA measurements). Hence, these measurements could give us some idea about the validity of correlations of results from different characterization techniques. The results for PFBuTEA doped membranes and PFOcTEA doped membranes are presented in table 3 and 4 respectively.

<b>Series 1: 15 to 150°C at the heating rate of 2°C/minute</b>					<b>Series 2: -50 to 150°C at the heating rate of 2°C/minute</b>			
<b>PFBuTEA content (%)</b>	<b>Onset Fusion Temperature (°C)</b>		<b>ΔH (J/g)</b>		<b>Onset Fusion Temperature (°C)</b>		<b>ΔH (J/g)</b>	
	<b>Peak I*</b>	<b>Peak II**</b>	<b>Peak I*</b>	<b>Peak II*</b>	<b>Peak I*</b>	<b>Peak II**</b>	<b>Peak I*</b>	<b>Peak II**</b>
<b>100</b>	28	61	15.3	23.6	28	61	15.3	23.6
<b>10</b>	-	-	-	-	-	-	-	-
<b>20</b>	-	-	-	-	24.5	54.5	0.2	0.18
<b>30</b>	-	-	-	-	25.8	57	1.5	2.4
<b>40</b>	-	49.2	-	3.6	26	55 (broad peak)	2.9	5.9

Table 3: DSC results of Nafion-TEA+xwt% PFBuTEA membranes in two different ranges of temperatures of measurements

First, we consider the case of PFBuTEA doped membranes. From table 3, it can be seen that:

- In the temperature range of *Series I*, no melting peak corresponding to PFBuTEA is observed up to 30 wt% content of the PCIL in the membrane. However, further increase in the PCIL content in the membrane to 40 wt% results in appearance of a clear melting peak of PFBuTEA. This melting peak should correspond to the melting of PFBuTEA molecules organized in the form of aggregates within the membrane. Hence, this observation further corroborates the hypothesis done on the basis of WAXS and SANS results that PFBuTEA molecules form PCIL domains in the inter-bundle amorphous zones of Nafion-TEA at high PCIL concentration. It should be noted that the first fusion peak (onset temperature ~25°C) associated with PFBuTEA could not be observed because the device is not very well equilibrated in the beginning of the measurement.
- In the temperature range of *Series II*, the melting peaks corresponding to PFBuTEA start to appear from 20 wt% content of the PCIL in the membrane. Moreover, the onset temperatures of both the melting peaks increase and get closer to that of pure PCILs with increasing PCIL content in the membrane. In addition, the enthalpy changes associated with the fusion peaks also increase with increasing PCIL content. These results point out that the size of the PCIL domains/aggregates increases within the membrane with the PCIL content. Interesting thing to note is that the fusion peaks appear from lower concentrations of PFBuTEA in comparison to the measurements of series I and also in comparison to the WAXS and SANS measurements where the Bragg Peak associated with PFBuTEA started to appear from 30 wt% content of the membrane. We suppose that the cooling of samples to low temperatures induces crystallization of the small- amorphous PCIL aggregates present in the inter-bundle zones of the polymer. Hence, these unorganized PCIL molecules could organize themselves within the membranes during the cooling process which would eventually result in the appearance of the fusion peaks.
- Now, we compare the results obtained from the two series of measurements on the membrane with 40 wt% content of PFBuTEA. On comparing the onset temperature of the second fusion peak as well as the associated enthalpy change, it can be seen that both are higher in the case of series II measurements. Moreover, the fusion peak observed for the membrane in the series II measurement was much broader in comparison to that observed in series I. These results signify that:

*a).* the percentage of PCIL molecules crystallized is higher in the case of series II measurements.

*b).* the size distribution of these crystallized PCIL aggregates is more heterogeneous in the case of series II measurements.

Hence, this comparison further supports the assumption that we induce higher crystallization of PCIL domains on cooling the doped membranes to low temperatures.

Now, we consider the case of PFOcTEA doped membranes (Table 4).

<i>Series 1: 15 to 150°C at the heating rate of 2°C/minute</i>			<i>Series 2: -50 to 150°C at the heating rate of 2°C/minute</i>	
<i>PFOcTEA content (%)</i>	<i>Onset Fusion Temperature (°C)</i>	<i>ΔH (J/g)</i>	<i>Onset Fusion Temperature (°C)</i>	<i>ΔH (J/g)</i>
<b>100</b>	54.8	20.9	54.8	20.9
<b>10</b>	-	-	-	-
<b>20</b>	-	-	-	-
<b>30</b>	-	-	51	2.7
<b>40</b>	49	3,3	45	6.7
<b>50</b>	44.6 (Large peak)	4	36.7	10.1

*Table 4: DSC results of Nafion-TEA+xwt% PFOcTEA membranes in two different ranges of temperatures of measurements*

The behavior of these membranes in the two series of the measurements is described as follows:

- In the temperature range of **Series I**, PFOcTEA doped membranes present similar behavior as that of PFBuTEA doped membranes. The melting peak corresponding to PFOcTEA is observed from 40 wt% content of the PFOcTEA in the membrane. This observation is in accordance with the SANS and WAXS results. Thus, this fusion peak should correspond to the melting of crystallized PFOcTEA domains present probably in the inter-bundle amorphous zones of Nafion-TEA.

- In the temperature range of *Series II*, the melting peak corresponding to PFOcTEA starts to appear from 30 wt% content of the PFOcTEA in the membrane. The fusion peak starts to appear at lower PFOcTEA content in this case in comparison to series I which further supports the assumption that crystallization of PCIL domains is forced when the samples are cooled to lower temperatures. However, the onset temperature of the melting peak decreases and the peak becomes broader with increasing PFOcTEA content in the membrane. In addition, the enthalpy change associated with the fusion peak increases with increasing PCIL content. These results point out that the percentage of PCIL domains/aggregates increases within the membrane with the PCIL content but there is a heterogeneous size distribution of these crystallized PCIL aggregates.

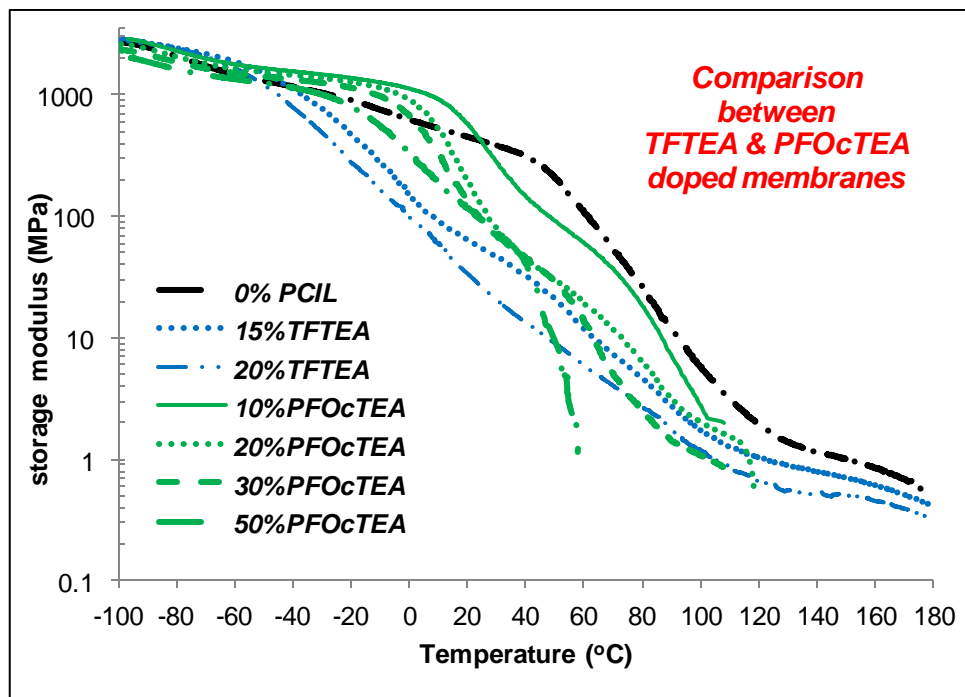
From these measurements, it is clear that PFBuTEA and PFOcTEA doped membranes exhibit Nafion-PCIL phase separation above a critical concentration of the PCIL in the membrane. Moreover, the degree of crystallinity of the PCIL aggregates formed in the inter-bundle amorphous zones of Nafion-TEA increases if the measurements are started from lower temperatures.

### *c. Thermo-mechanical properties*

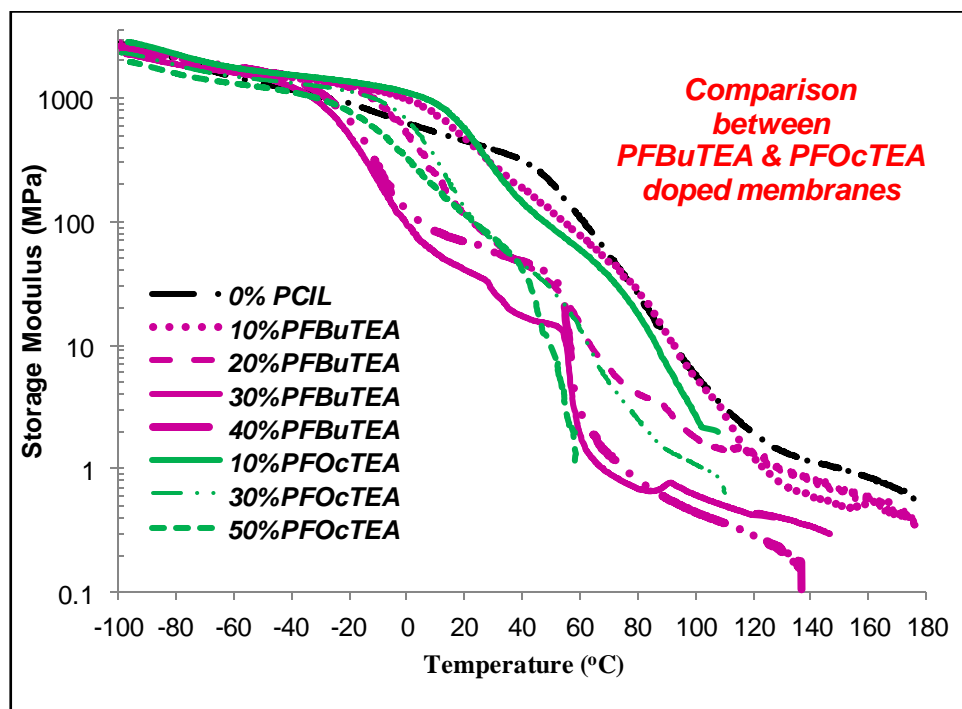
The evolution of thermo-mechanical properties of doped membranes based on PFOcTEA (in comparison to TFTEA based membranes) and PFBuTEA (in comparison to PFOcTEA based membranes) are shown in figures 7(a)-(b) and 8(a)-(b) as storage modulus versus temperature and  $\tan\delta$  versus temperature respectively.

#### *Storage Modulus versus Temperature*

Firstly, considering the evolution of thermo-mechanical properties of PFOcTEA doped membranes in comparison to TFTEA doped membranes (figure 7 (a)), it can be seen that PFOcTEA based membranes show different behavior compared to TFTEA based membranes. Two well –separated plateau are observed (corresponding to  $T_\beta$  and  $T_\alpha$  respectively) in the case of PFOcTEA doped membranes. While in the case of TFTEA doped membranes, these plateaux are much less evident and rather a continuous creeping of the membranes is observed with increasing temperature especially at high TFTEA concentration in the membrane.



(a)



(b)

Figure 7: Evolution of storage modulus vs temperature: a). PFOcTEA doped Nafion-TEA membranes in comparison to TFTEA doped Nafion-TEA membranes; (b). PFBuTEA doped Nafion-TEA membranes in comparison to PFOcTEA doped Nafion-TEA membranes

It could be pointed out that *PFOcTEA based membranes present better thermo-mechanical properties in comparison to TFTEA based membranes at low temperatures i.e. upto  $T_g$  (35-60 °C) and comparable storage moduli in the range of 80-120°C* for comparable PCIL content. However, *PFOcTEA doped membranes sustain only up to 120°C and collapse afterwards*. In contrary, TFTEA doped membranes shows a gel-like behavior and continue to sustain a constant storage modulus (~1MPa) in the temperature range of 120-180°C

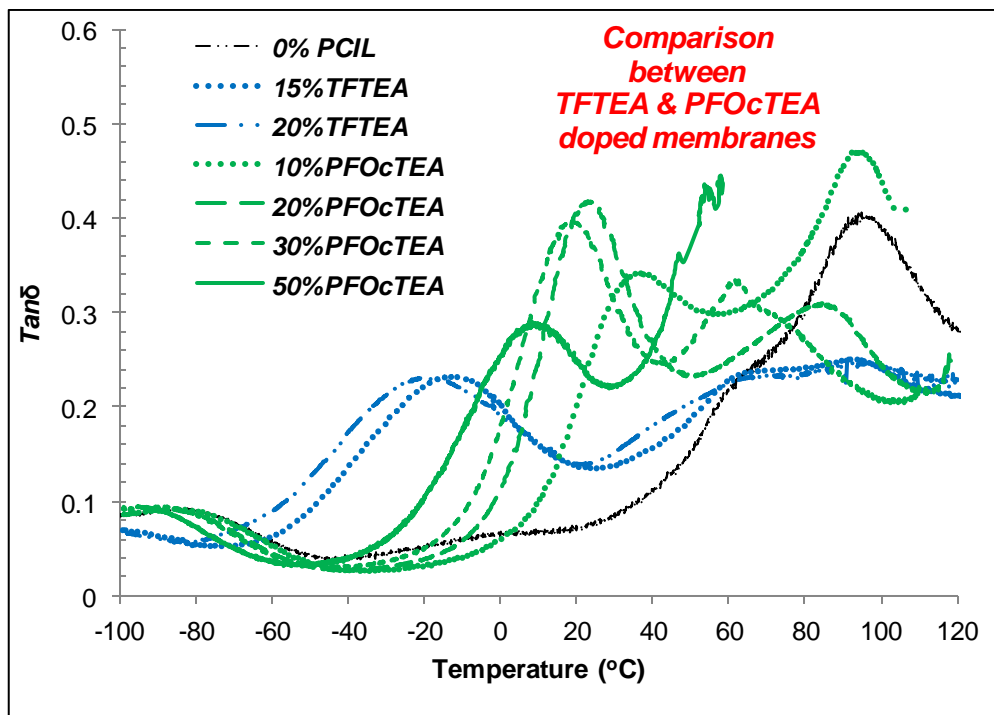
Now analyzing the case of *PFBuTEA doped membranes* (figure 7(b)), it is clear that these membranes show *thermo-mechanical properties similar to PFOcTEA doped membranes up to 120°C*. Above 120°C, where no PFOcTEA doped membrane sustains whatever the membrane composition is, PFBuTEA doped membranes sustain a plateau with storage modulus of approximately 0.3-1 MPa up to 140-180°C (depending upon PFBuTEA concentration). Thus, *PFBuTEA based membranes present thermo-mechanical behavior like a cross-linked gel in this temperature range similarly as TFTEA doped membranes above 120°C*. This behavior could be due to the fact that PFBuTEA has a perfluorinated anion of chain length intermediate to TFTEA and PFOcTEA. Hence, it is neither as hydrophilic as TFTEA nor as hydrophobic as PFOcTEA. Therefore, it would not probably act as a solvent for the crystallites in the Nafion-TEA at high temperatures like PFOcTEA due to its less stronger interactions with the hydrophobic domains of Nafion-TEA in comparison to that of PFOcTEA.

### *Tanδ versus Temperature*

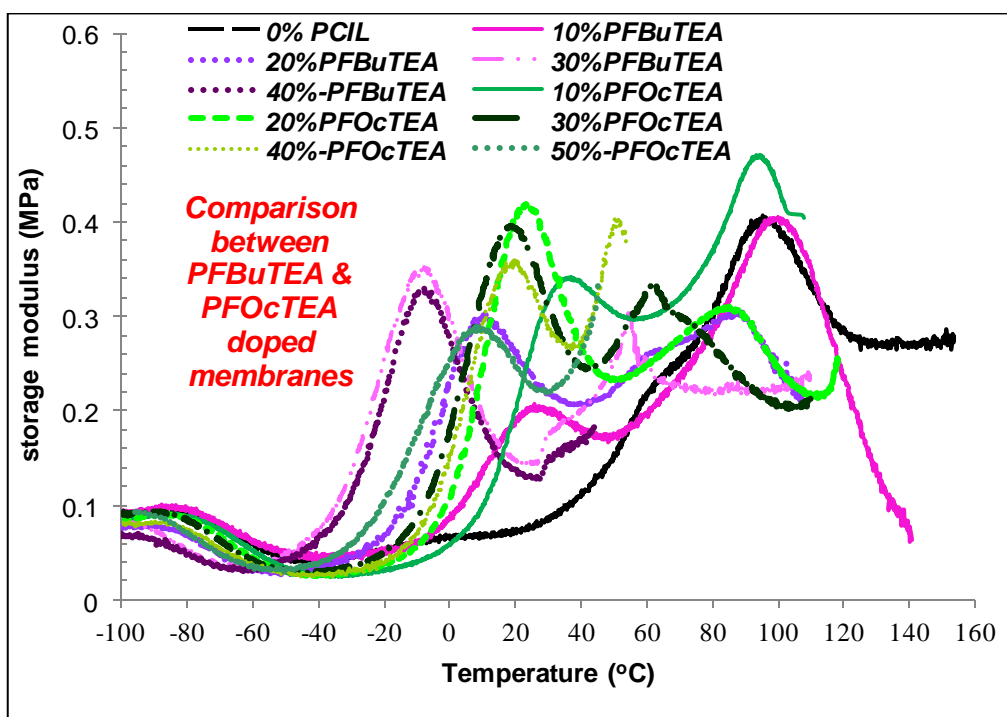
Now considering the evolution of Tanδ vs temperature, plots of doped membranes based on PFOcTEA (in comparison to TFTEA based membranes) and PFBuTEA (in comparison to PFOcTEA based membranes) are shown in figures 8(a) and (b) respectively.

From these plots, it seems that PFOcTEA and PFBuTEA doped membranes show similar behaviour and different from TFTEA doped membranes in certain aspects. The main features of these curves include:

1. The  *$\gamma$ -relaxation* observed for Nafion-TEA-casting membrane at -80°C *shifts very slightly to lower temperatures with increasing PCIL content in both PFBuTEA and PFOcTEA based doped membranes*. In the case of TFTEA based membranes, the shift in the relaxation peak is more significant. However, this shift is observed from 10wt% content of TFTEA and the peak does not shift further on increasing the concentration of TFTEA.



(a)



(b)

Figure 8: Evolution of  $\tan\delta$  vs temperature: a). PFOcTEA doped Nafion-TEA membranes in comparison to TFTEA doped Nafion-TEA membranes; (b). PFBuTEA doped Nafion-TEA membranes in comparison to PFOcTEA doped Nafion-TEA membranes



2. Taking into account the  ***$\beta$ -relaxation***, it is found to be very intense and large relaxation in the case of PFBuTEA as well as PFOcTEA doped membranes. It appears in the temperature window of -50 to 40°C for PFBuTEA doped membranes and -40 to 50°C for PFOcTEA doped membranes depending on the PCIL content. It shifts towards lower temperature on increasing PCIL content for both the casting based doped membranes. In addition, interesting point to note is that the intensity of the relaxation first increases on adding/increasing the PCIL content up to a certain concentration and then decreases above this concentration. This critical concentration is 30wt% for PFBuTEA doped membranes and 20wt% for PFOcTEA doped membranes. Now, we compare PFBuTEA and PFOcTEA doped membranes with TFTEA doped membranes. This relaxation emerged in the temperature range of -80 to 40°C in the case of TFTEA doped membranes. Additionally, it can be seen that the relaxation appears at lower temperatures. In addition, the peak is larger and the intensity of the peak is lesser in TFTEA doped membranes compared to other ones. Hence, ***depending on the length of the perfluorinated chain of the anion of the PCIL, two things can be pointed out regarding this  $\beta$ -relaxation:***

- a). The temperature window of the appearance of this relaxation shifts to higher temperature with increasing perfluorinated chain length of the anion.
- b). Longer the perfluorinated chain of the anion, stronger is the intensity of this relaxation.

However, it is interesting to note that  ***$\beta$ -relaxation*** is very intense in all the casting based membranes wherever the PCIL molecules chooses the organize itself (i.e. either in the ionic domains or intercalated with the hydrophobic side-chains or in crystallized form in the inter-bundle amorphous zones). This signifies that ***casting method allows more homogeneous organization of the hydrophobic chains.***

3. Concerning the relaxation appearing in the temperature range of the 50-110°C, it can be seen that there is ***only one relaxation ( $\alpha$ -relaxation) present in this temperature range for both PFOcTEA and PFBuTEA doped membranes.*** In contrary, TFTEA doped membranes present at least two overlapping relaxations in this temperature range. Moreover this  $\alpha$ -relaxation ***shifts to lower temperatures and decreases in intensity with the increasing content of PFOcTEA and PFBuTEA*** while very low shift in this relaxation was observed in the case of TFTEA doped membranes though intensity decreased with increasing TFTEA content.

On the basis of these results, the scenario of the thermo-mechanical responses of these doped membranes based on different PCILs could be described as follows:

1. Firstly, we consider the organization of PFBuTEA and PFOcTEA molecules as proposed in the previous section. The PCIL molecules have been assumed as intercalated with the pendant chains with their chain ends fixed between the PTFE chains of Nafion-TEA. Hence, *up to certain temperature (i.e. below  $T_\beta$ )* the intercalated PCIL molecules prevent the movement of side-chains as well as PTFE main chains of Nafion-TEA. Hence, *no flagrant plasticizing effect of PFBuTEA/PFOcTEA on Nafion-TEA* is visible at low temperature. As the  $T_\beta$  is reached, the perfluorinated chains of PFOcTEA become mobile and allow the movement of hydrophobic domains of Nafion-TEA along with plasticizing these hydrophobic domains resulting in a very strong  $\beta$ -relaxation. The position of  $\beta$ -relaxation is at higher temperature and is more intense in the case of PFOcTEA doped membranes. This is probably due to the fact that perfluorinated chains of PFOcTEA are better intercalated with the side chains and more fixed between the PTFE main-chains owing to its longer chain length. Thus, PFOcTEA molecules generate more restriction to the movements of the side-chains and PTFE main-chains of Nafion-TEA below  $T_\beta$ . But at  $T_\beta$ , it plasticizes more significantly the hydrophobic domains of Nafion-TEA and hence generating stronger response of hydrophobic chains of Nafion-TEA. Moreover, after a critical concentration, the intensity of  $\beta$ -relaxation decreases in the case of PFBuTEA and PFOcTEA doped membranes. This could be due to the fact that the PCIL molecules form PCIL aggregates in the inter-bundle amorphous zones in Nafion-TEA and hence do not contribute to the response of  $\beta$ -relaxation. Moreover, with increasing PCIL content, there is a decrease in the percentage mass of PTFE and fluorinated side-chains of the polymer which would result in lower intensity of  $\beta$ -relaxation.

While in the case of TFTEA doped membranes, TFTEA molecules significantly reduce the ionic interactions of the Nafion-TEA which results in easier sliding of the polymer chains and hence  $\beta$ -relaxation is observed at lower temperatures compared to that of PFBuTEA and PFOcTEA doped membranes.

2. In contrast, at  $T_\infty$  PFOcTEA molecules completely plasticize the membrane due to their interaction with the hydrophobic domains as well as the ionic domains of Nafion-TEA. Moreover, at high concentration of PFOcTEA (from 30wt% onwards), PCIL molecules are also present in crystallized form in the Nafion-TEA membrane. Once these crystals melt, they heavily plasticize both the hydrophobic as well as the hydrophilic domains of Nafion-TEA which results in deterioration of thermo-mechanical properties of doped membranes. In contrast, TFTEA based membranes sustain relatively better properties above 120°C. This must be because of polar nature of TFTEA (in comparison to PFOcTEA), dispersed in the form of aggregates mainly in the ionic domains limiting its plasticizing effect. Thus, the organized perfluorinated chains associated with the un-plasticized ionic functions of Nafion-TEA could restrict the complete flowing of the membrane and hence TFTEA doped membranes do not

collapse completely above 120°C. Interestingly, the behavior of PFBuTEA doped membranes is closer to TFTEA doped membranes above 120°C. This could be due to its lower dilution effect on the organized crystallites of Nafion-TEA in comparison to PFOcTEA due to its shorter perfluorinated chain length.

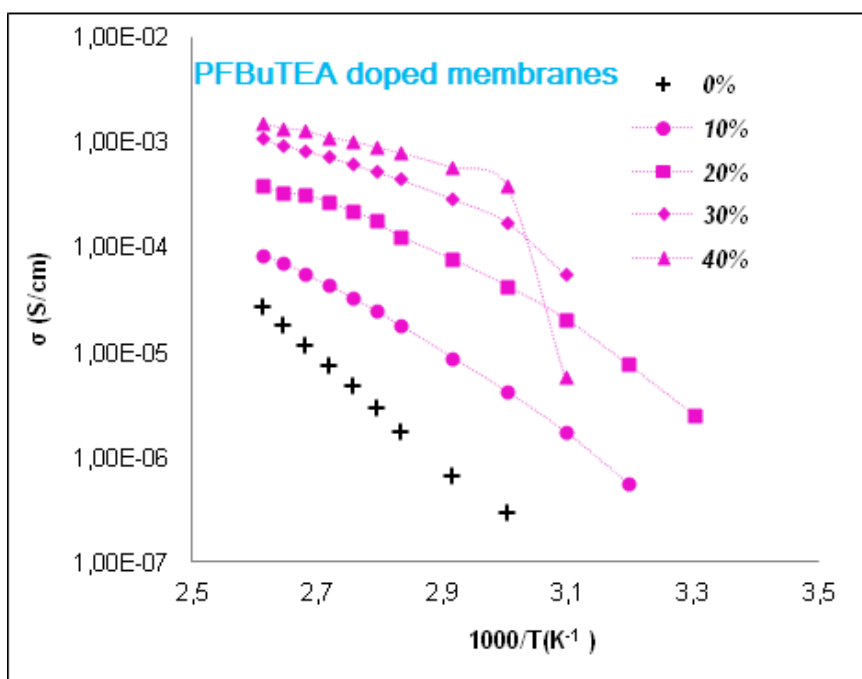
From these experimental observations on temperature dependent storage modulus and  $\tan\delta$  profiles of doped Nafion-TEA membranes based on different PCILs, following *conclusions* can be drawn:

- Distribution and organization of PCIL molecules in the morphology of Nafion-TEA have significant impact on the thermo-mechanical properties of the resulting membranes. This distribution and organization of PCIL molecules in turn depends on the chemical nature of the PCIL.
- Longer the chain length of the perfluorinated anion of the PCIL is, more similar are the thermo-mechanical properties to virgin Nafion-TEA membrane at temperatures lower than  $T_\alpha$  and complete collapse of the doped membrane above this temperature.

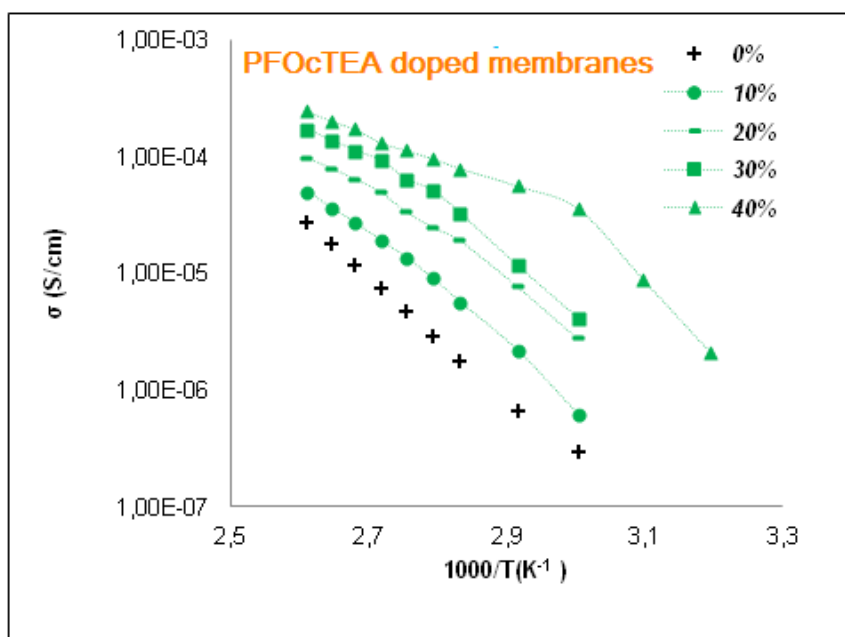
#### *d. Conductivity*

The conductivity measurements were carried out on PFBuTEA and PFOcTEA doped Nafion-TEA membranes in anhydrous conditions and their Arrhenius plots are shown in figure 9 (a) and (b) respectively. Both *PFBuTEA and PFOcTEA doped membranes present an increase in conductivity with increasing temperature as well as PCIL content.*

Moreover, *from 30wt% content*, an important difference in the conductivity values can be observed above 50 °C for PFBuTEA membranes and above 40 °C for PFOcTEA doped membranes i.e. a *sharp increase in conductivity is observed above these temperatures*. The appearance of Bragg peaks of PFBuTEA and PFOcTEA as shown in WAXS and SANS spectra also begins from 30wt% content (formation of crystallized PCIL domains). Moreover, these temperature values correspond to the  $T_m$  of these ionic liquids. Hence, this gap in the value of the conductivities above 30 wt% content is probably due to the fact that *crystallized PCIL aggregates* (which are around the adjacent bundles more precisely) *might limit the diffusion of ionic species within the percolated ionic domains of the membrane below their  $T_m$* . But, once these crystallites melt, a sharp increase in conductivity is observed due to increase in mobility and ionic species content of the system.



(a)



(b)

Figure 9: Conductivity vs temperature; a). PFBuTEA doped Nafion-TEA membranes; b). PFOcTEA doped Nafion-TEA membranes

In addition, there is only a slight difference in conductivity values of doped membranes between 30 and 40 wt% contents for both the PCILs which points towards the fact that the percolation of ionic domains could be almost optimum at 30wt% content of the PCILs. Conductivities of the order of

1.5mS/cm and 0.25mS/cm have been achieved with Nafion-TEA membrane containing 40 wt% PFBuTEA and 40 wt% PFOcTEA respectively.

Moreover, *comparisons of conductivities of doped membranes based on all the three PCILs* discussed so far i.e. TFTEA, PFBuTEA and PFOcTEA *in terms of mass percentage as well as  $\lambda$  value* are presented in figure 10 (a) and 10 (b) respectively. Moreover, conductivities of all the three ionic liquids pure form in function of temperature is shown in figure 11.

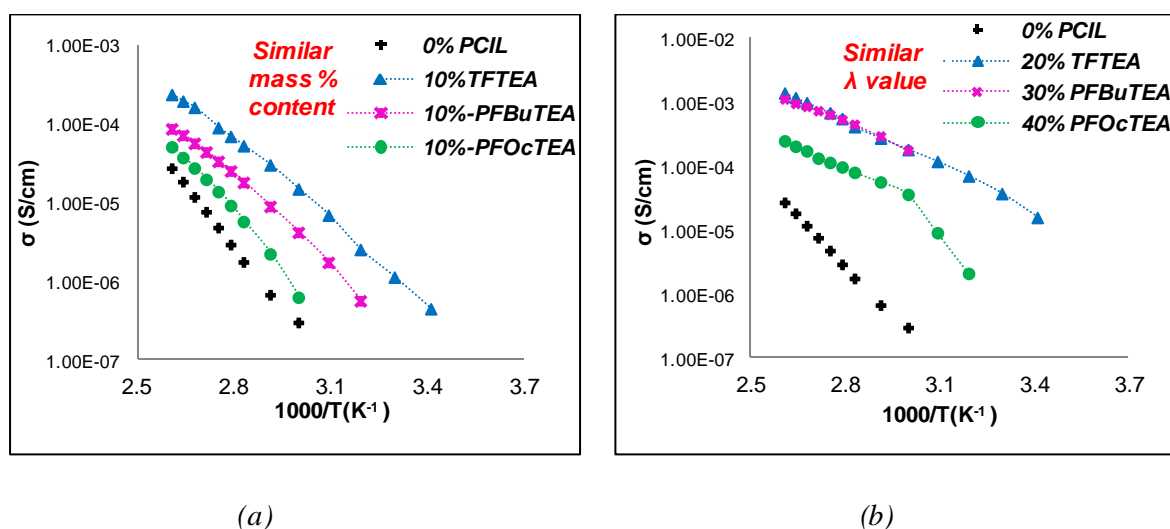


Figure 10: Conductivities of Nafion-TEA membranes doped with different PCILs; a). Equal mass percent content (10 wt%) of all the PCILs in Nafion-TEA membrane; b). Similar  $\lambda$  value of the PCIL (1.2-1.3 molecules of PCIL per ionic site of Nafion-TEA) in Nafion-TEA membrane

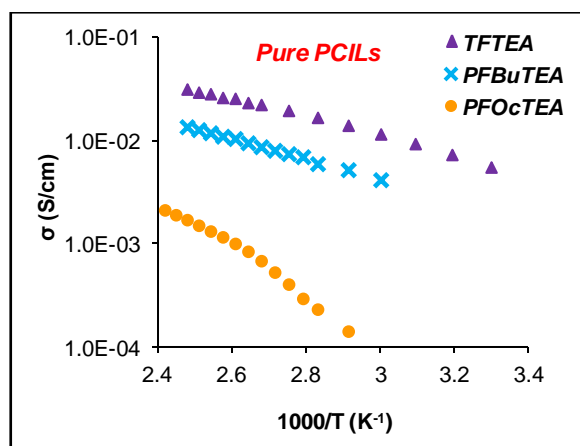


Figure 11: Comparison of conductivity of different PCILs in function of temperature

Considering *equal mass percentage*, the order of the conductivities for doped membranes with different PCILs is in the following order: **TFTEA>PFBuTEA>PFOcTEA**. This order is pretty logical as the number of ionic functions present in these membranes is also in the same order. Moreover, the conductivities of pure PCILs are in the same order.

Now, considering *similar  $\lambda$  value* of these PCILs, the results are discussed as follows:

1. **TFTEA and PFBuTEA based membranes present similar conductivity values and much higher in comparison to PFOcTEA doped membrane.**
2. On comparing the case of TFTEA and PFBuTEA, it is observed that the conductivity of TFTEA is 5 times higher than that of PFBuTEA at 110°C in pure form. But when PFBuTEA and TFTEA molecules are incorporated in the Nafion-TEA membrane, they show similar conductivity values at similar  $\lambda$  value. Moreover, the ionic function concentration in PFBuTEA doped membrane (total: 1.38 H<sup>+</sup>/kg; contribution of PFBuTEA: 0.75 H<sup>+</sup>/kg) is lesser than that of TFTEA doped membrane (total: 1.52 H<sup>+</sup>/kg; contribution of PFBuTEA: 1.05 H<sup>+</sup>/kg) at similar  $\lambda$  value, but still, both the membranes show similar conductivities.
3. Now considering the case of PFOcTEA the lower conductivity of PFOcTEA based membrane is probably due to higher viscosity, lower mobility and lower dissociation degree of PFOcTEA molecules as well as lower ionic function concentration in these membranes (total: 1.2 H<sup>+</sup>/kg; contribution of PFOcTEA: 0.6 H<sup>+</sup>/kg) lower compared to the membranes based on other two PCILs. However, it is pretty interesting to note that the TFTEA shows 25 times higher and PFBuTEA shows 10 times higher conductivity in comparison to PFOcTEA at 110°C in pure form. However, when these PCILs are incorporated in the Nafion-TEA membrane, the difference between the conductivities of the TFTEA/PFBuTEA and PFOcTEA doped membranes decreases to only 5 times for similar  $\lambda$  value.

Hence, from these observations, it can be said that the ***type of organization as well as distribution of PFBuTEA and PFOcTEA molecules in the structure of Nafion-TEA improves the ion conducting properties of PFBuTEA and PFOcTEA molecules.*** This is to say that: when PFBuTEA/PFOcTEA molecules are in pure form, they probably auto-organize in micellar/aggregates form. However, when PFBuTEA/PFOcTEA molecules are combined with Nafion-TEA, they intercalate into the side-chains of Nafion-TEA (with their ionic functions organized similarly as those of Nafion-TEA) rather than auto-organizing at least up to certain concentration. This change in organization of PFBuTEA/PFOcTEA molecules could possibly result in higher contribution of Grotthuss like mechanism for the conduction of protons/ionic species in the doped membrane in contrast to pure

PCILs in which the conduction of protons is believed to be facilitated by the diffusion of ammonium species mainly via vehicular mechanism<sup>[4]</sup>.

Moreover, *the phenomenon of creeping of membranes during the conductivity measurements was found to be negligible in the case of PFBuTEA and PFOcTEA doped membranes* while it was pretty significant in the case of TFTEA doped membranes. This is certainly due to the better thermo-mechanical properties of PFBuTEA and PFOcTEA based systems in comparison to TFTEA doped systems up to 120°C (as evidenced by DMA).

#### *e. Gas permeability*

The permeability coefficients of O<sub>2</sub> and H<sub>2</sub> gases measured at room temperature for Nafion-TEA membranes doped with different kinds of PCILs are shown in table 5. Concerning TFTEA doped membranes, it has been already discussed in the previous chapter that the variation in the permeability coefficients of O<sub>2</sub> and H<sub>2</sub> was low with increasing concentration of TFTEA. Now considering the *case of PFBuTEA and PFOcTEA*, it seems that these doped membranes show *similar permeability coefficients as TFTEA doped membranes* up to a *critical PCIL concentration* with no great change in the permeability values. However, *above this critical PCIL concentration, a sharp increase in the permeability coefficients* has been observed in both kinds of doped membranes. Moreover, further increasing the PCIL amount above this critical concentration only leads to small permeability variations afterwards. *This critical concentration seems to correspond to the appearance of Bragg peak of the PCIL in the SANS and WAXS spectra.* This result further corroborates the hypothesis of *formation of crystallized-PCIL domains in Nafion-TEA*. The sharp increase in the permeability coefficients of O<sub>2</sub> and H<sub>2</sub> on the formation of such domains could be due to the following *reasons*:

1. During membrane elaboration, the domains of PCILs get formed (but do not get crystallized due to high temperature of the system) with the polymeric zones all around and when cooled, these PCILs domains would crystallize resulting in their contraction which could lead to an increased free volume/porosity between these crystallized-PCIL domains and polymeric domains of Nafion-TEA.
2. Moreover, the perfluorinated chains of these PCILs are less entangled compared to perfluorinated-polymer chains of Nafion-TEA which would result in improved permeability of gases since these PCIL molecules (as these PCILs intercalate themselves with the side chains of Nafion-TEA)

3. Due to less efficient packing of perfluorinated chains of Nafion-TEA in presence of these PCIL molecules (evidenced from WAXS), permeability coefficients are expected to increase.

<i>PCIL</i>	<i>Weight percent of PCIL</i>	<i>PH<sub>2</sub></i> (barrer)	<i>PO<sub>2</sub></i> (barrer)
	0%	9.3	1.8
<i>TFTEA</i>	5%	9.6	2.0
	10%	8.8	1.9
	15%	6.2	1.7
	20%	6.5	1.9
<i>PFBUTEA</i>	10%	5.3	1.2
	20%	15.0	3.7
	40%	13.7	4.3
<i>PFOCTEA</i>	5%	9.3	1.7
	10%	8.7	1.8
	20%	9.8	2
	30%	9.7	2.2
	40%	16.0	4.7
	50%	17.7	5.3

Table 5: Permeability coefficients of Nafion-TEA membranes doped with different concentrations of various PCILs

#### *f. Water Sorption*

The water sorption behavior for Nafion-TEA membranes containing different ionic liquids (TFTEA, PFBuTEA and PFOcTEA) in various weight concentrations was analyzed at 25°C and discussed as a function of the respective properties of the Nafion-TEA matrix on one hand and of the PCILs on the other hand. All the materials studied in this chapter were made to undergo a consecutive cycle of sorption and desorption in order to check their stability towards exposure to water vapor and *no hysteresis phenomenon* was observed. A step by step analysis of the water sorption properties of the different materials and membranes is proposed hereafter.



### Comparison of the properties of the reference materials (PCILs, Nafion-TEA)

First of all, analyzing the *sorption behavior of the pure PCILs*, the *hydrophilicity trend* of these PCILs structure can be clearly observed in figure 12 (a) and (b) which is in the order as ***TFTEA>PFBuTEA>PFOcTEA***. TFTEA shows higher gain of water molecules especially above 0.3 water activity compared to PFBuTEA and PFOcTEA. Comparing PFBuTEA and PFOcTEA, both show similar sorption behavior up to 0.7 water activities and then the former shows higher water uptake than the latter above 0.7 water activities. This trend is pretty obvious from the chemical structure/nature of these PCILs i.e. ***higher the perfluorinated chain length of the anion of the PCIL, lower is the water uptake***. However, the difference in the water uptake of TFTEA and PFBuTEA is much more significant compared to the difference between that of PFBuTEA and PFOcTEA which underlines the *saturation of effect of the length of perfluorinated chain on the hydrophilicity of the PCIL* especially at low water activity. Figure 12 (a) and (b) also allow one to *compare the hydrophilicity of the PCILs with that of the reference Nafion-TEA matrix*. It can be seen in figure 12 (a) that Nafion-TEA presents lesser mass percentage gain of water compared to all the PCILs. However, considering the average number of water molecules gained per ionic site, the gain is comparatively *similar for both Nafion-TEA and PCILs at low activity* while *above 0.7 water activity*, the trend is as follows: ***TFTEA>>Nafion-TEA~PFBuTEA>PFOcTEA***.

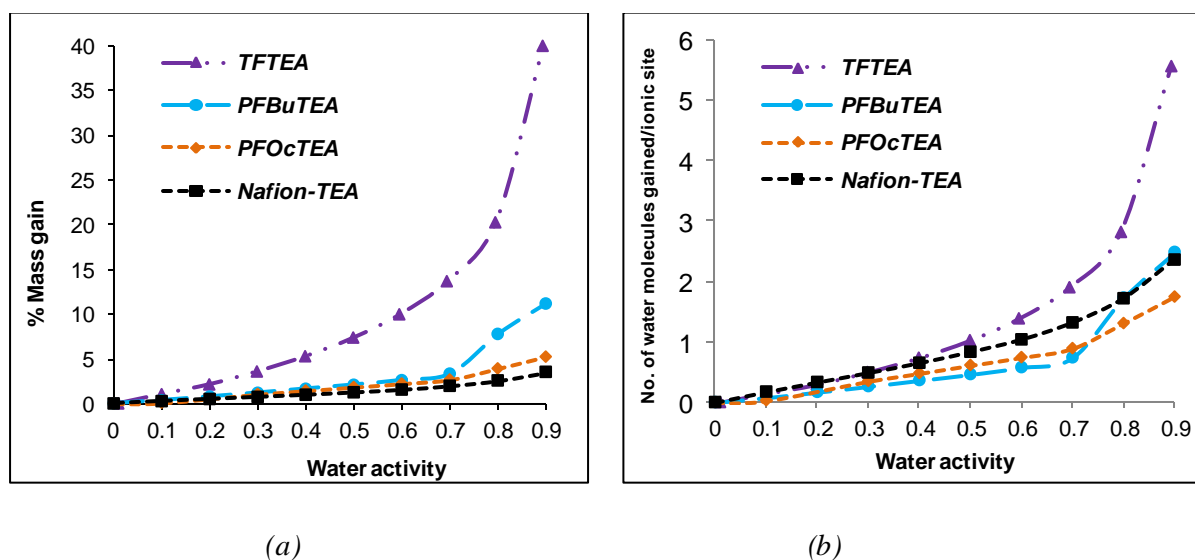


Figure 12: Water sorption isotherms of the different PCILs and of Nafion-TEA expressed as: a) in mass gain as a function of water activity; b) in number of water molecules gained per ionic site as a function of water activity.

It is noteworthy that the water sorption isotherm of PFBuTEA and PFOcTEA cannot be accurately modelled by GAB equation, contrary to that one of TFTEA, due to their particularly low water uptake values at low water activity in comparison to their much higher water uptake values at high water activity.

### Water sorption properties of the doped Nafion-TEA membranes

The sorption behavior of the doped membranes will now be discussed as a function of the nature and content of PCIL, considering the water uptakes expressed in % mass gain as a function of water activity. The percent mass gains of water for PFBuTEA and PFOcTEA doped Nafion-TEA membranes are presented in figure 13 (a) and figure 13 (b) respectively. All the doped membranes present a B.E.T.III type isotherm.

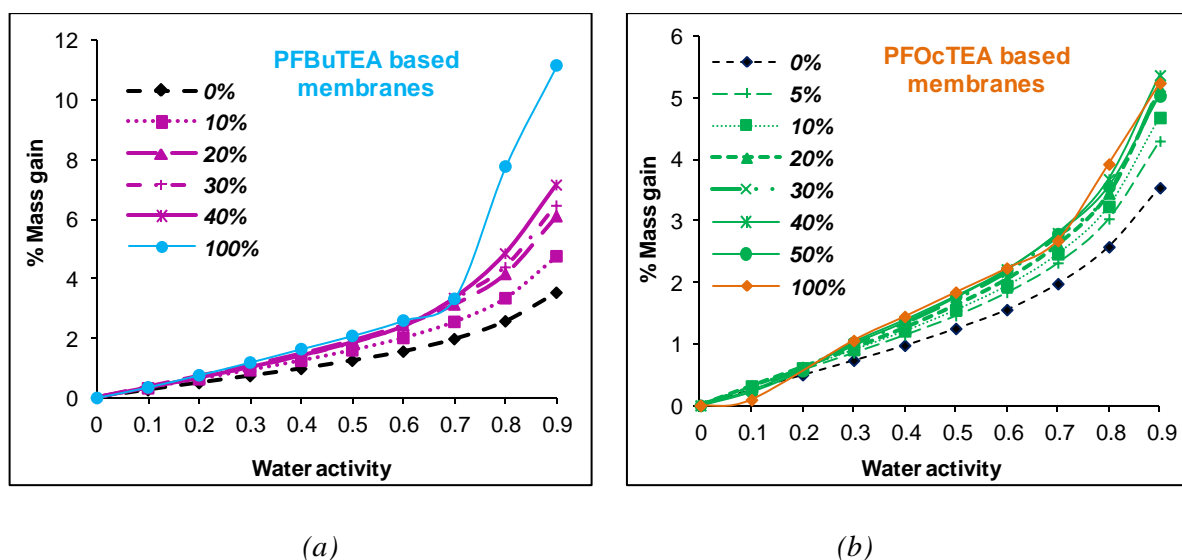


Figure 13: Water sorption behavior of Nafion-TEA membranes doped with various wt% contents of different PCILs; a): PFBuTEA; b): PFOcTEA

The influence on the water uptake of the respective PCIL content can first be discussed from figure 13(a) and Figure 13 (b). Concerning **PFBuTEA based membranes**, we have shown that PFBuTEA is characterized by a more important water uptake (expressed in mass gain) than Nafion-TEA matrix. As a consequence, the water uptake increases with the addition of PFBuTEA in the Nafion-TEA membrane for all the water activities (figure 13 (a)). However, the *increase in water uptakes is significant in all the range of water activity only for the membranes containing low amount of PFBuTEA and afterwards, the water uptake is not so much significant on further increasing the PCIL content* (i.e. above 20wt% of PFBuTEA). The *same trends are observed for PFOcTEA doped*

*membranes* (Figure 13 (b)). Indeed, a significant increase in water uptake on adding 5 and 10wt% PFOcTEA in Nafion-TEA is observed and a very little increase in water uptake is noticed afterwards on further the increasing PFOcTEA wt% content.

The water sorption isotherms expressed as the average number of water molecules gained per ionic site for PFBuTEA and PFOcTEA doped Nafion-TEA membranes are presented in figure 14 (a) and (b) respectively. It can be clearly seen that the *average number of water molecules sorbed per ionic site does not get strongly modified in the PCIL-doped Nafion-TEA matrix* in comparison to pure Nafion-TEA without any PCIL inside which is definitely due to the hydrophobic behavior of these PCILs.

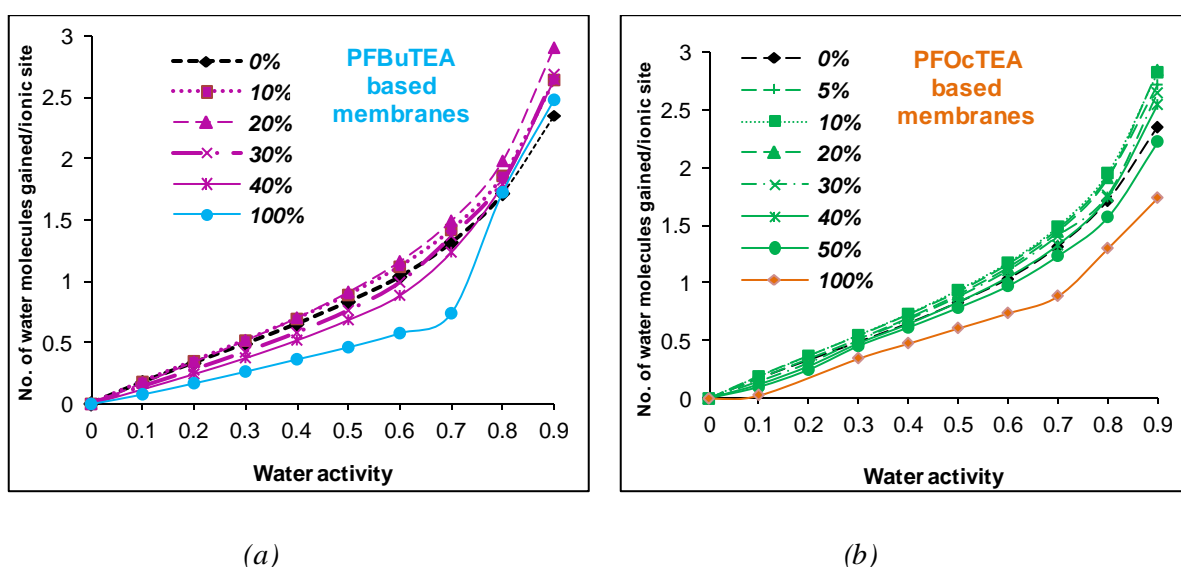


Figure 14: Number of water molecules gained per ionic site vs water activity for Nafion-TEA membranes doped with various wt% contents of different PCILs; (a):PFBuTEA doped membranes; (b): PFOcTEA doped membranes

In order to study more precisely the influence of the PCIL nature, the water sorption isotherms of the doped Nafion-TEA membranes based on TFTEA, PFBuTEA and PFOcTEA are compared in terms of equal weight percent content (10wt%) and similar  $\lambda$ /IEC value of the PCIL ( $\lambda \sim 0.8$  molecules of PCIL per ionic site of Nafion-TEA; IEC in the range of 1.08-1.16H<sup>+</sup>/Kg for all the membranes compared) in figure 15 (a) and 15 (b) respectively. In this comparison, the composition range has been chosen for which no significant formation of crystallized PCIL domains (of PFBuTEA/PFOcTEA) has been observed. Considering equal weight percent mass of all these PCILs in Nafion-TEA matrix, TFTEA based membrane present higher water uptake compared to PFBuTEA and PFOcTEA doped membranes which is due to higher ionic function concentration in the former compared to the latter

two. Now considering the % water uptake for similar  $\lambda$ /IEC value of the PCILs (figure 15 (b)), surprisingly, TFTEA ( $\lambda=0.78$ ; IEC=1.15H<sup>+</sup>/Kg) and PFBuTEA ( $\lambda=0.78$ ; IEC=1.16H<sup>+</sup>/Kg) doped membranes show similar water uptake even though TFTEA is much more hydrophilic in nature compared to PFBuTEA while PFOcTEA doped membrane ( $\lambda=0.86$ ; IEC=1.08H<sup>+</sup>/Kg) shows a little lesser water uptake which can be due to the more hydrophobic character of PFOcTEA compared to TFTEA and PFBuTEA as well as comparatively lower IEC of the membrane.

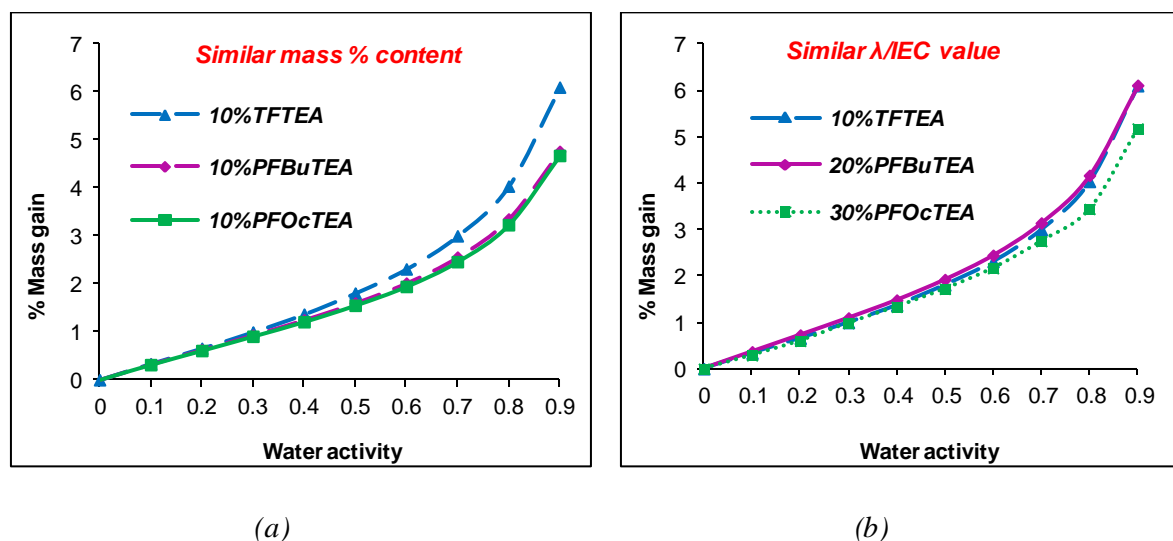


Figure 15: Comparison of water sorption isotherms of Nafion-TEA membranes doped with different PCILs; a). Equal mass percent content (10 wt%) of all the PCILs in Nafion-TEA membrane; b). Similar  $\lambda$  value of the PCIL ( $\lambda \sim 0.8$  molecules of PCIL per ionic site of Nafion-TEA; IEC in the range of 1.08-1.16H<sup>+</sup>/Kg for all the membranes compared) in Nafion-TEA membrane

Furthermore, the experimental isotherms related to Nafion-TEA+x% PFBuTEA/PFOcTEA have been compared with the calculated ones which have been calculated on the basis of an additive contribution of experimental isotherms of each component i.e. Nafion-TEA and PCIL {PFBuTEA and PFOcTEA} to the water sorption mechanism of the composite system.

Figure 16 (a) and (b) demonstrate the comparison between calculated and experimental isotherm of Nafion-TEA doped with 10 wt% of PFBuTEA and PFOcTEA respectively (at low PCIL content, in the range of PCIL content for which no Bragg peak was evidenced in WAXS/SANS spectra). For both the types of doped membranes, the experimental data are considerably higher in values than the calculated ones in the entire water activity range. This behavior confirms the *improvement in the hydrophilicity of the system when PFBuTEA/PFOcTEA and Nafion-TEA are combined together*. It

can be noted that for Nafion-TEA-TFTEA membranes, the experimental uptakes values were in good agreement with the calculated ones at low water activity and a little less important than the theoretical ones at high water activity.

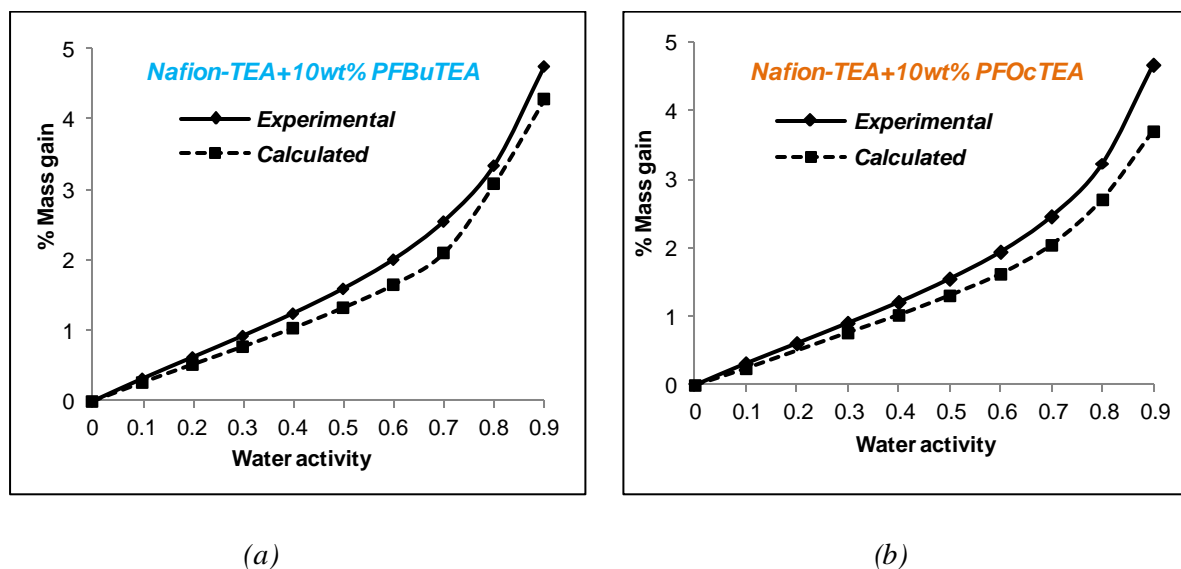


Figure 16: Comparison of Experimental & Calculated Water Sorption Isotherms (a): 10wt% PFBuTEA doped Nafion-TEA membrane; (b): 10wt% PFOcTEA doped Nafion-TEA membrane

It was interesting to further analyze the trends at high PFBUTEA and PFOcTEA content, in the range of PCIL content for which the Bragg peak was evidenced in SANS and WAXS spectra. Figure 17 (a) and (b) demonstrate the comparison between calculated and experimental isotherm of Nafion-TEA doped with 40 wt% PFBuTEA and 50 wt% PFOcTEA respectively. It is clear that the difference between experimental and calculated isotherms is less significant when PCILs (PFBuTEA and PFOcTEA) are present in high quantities compared to the one when PCILs are present in smaller quantities.

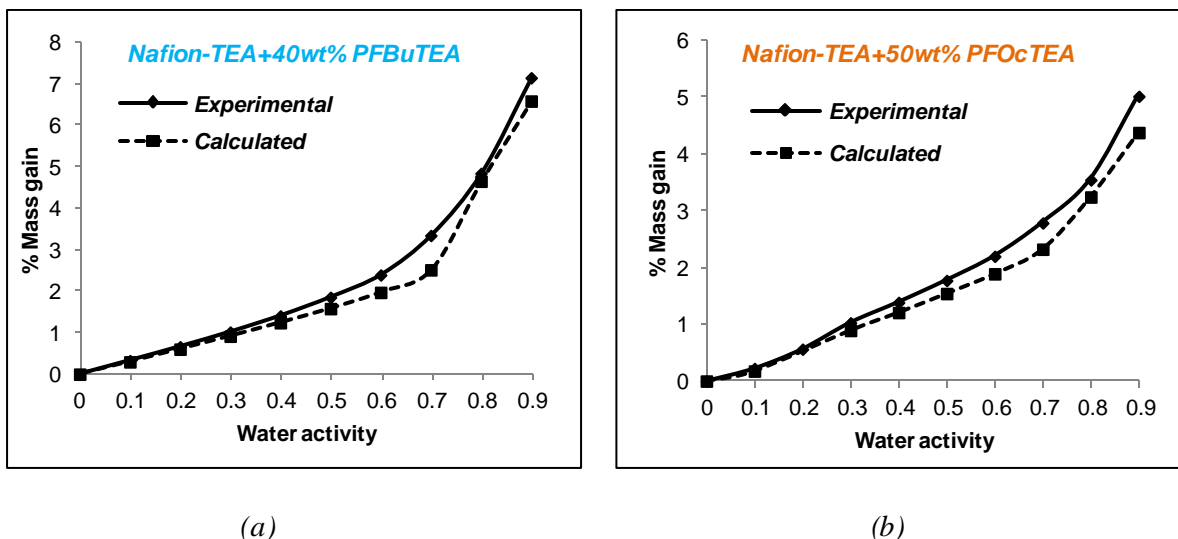


Figure 17: Comparison of Experimental & Calculated Water Sorption Isotherms (a): 40wt% PFBuTEA doped Nafion-TEA membrane; (b): 50wt% PFOcTEA doped Nafion-TEA membrane

*All the results obtained from this detailed water sorption analysis imply two things:*

1. Firstly, addition of PFBuTEA/PFOcTEA in Nafion-TEA improves the hydrophilicity of Nafion-TEA. This improvement is continuous with increasing PFBuTEA/PFOcTEA content up to 20 wt% content. Moreover, this improvement in the hydrophilicity of Nafion-TEA is higher than that predicted by the additive law. This could be due to the fact that PCIL molecules organize themselves in a manner similar to that of side chains of Nafion-TEA and different to the manner in which they organize in pure form (for e.g. micellar form) at least when present in low amount in the membrane. This might result in improved hydrophilic character of the PCILs and hence an overall improvement in the hydrophilicity of the doped membrane.
2. Afterwards, the formation of PCIL domains from 30wt% onwards (as evident from WAXS and SANS results) leads to decrease of the difference observed between experimental and theoretical water uptakes probably due to organization of PCILs in such domains similar to that of their pure form.

This *behavior is different to the one demonstrated by TFTEA doped Nafion-TEA membranes* (discussed in previous chapters) where *Nafion-TEA has a hindering effect on the water sorption capacity of TFTEA*; TFTEA being more hydrophilic than Nafion-TEA. This behavior seems to be due to:

- *More hydrophilic character of TFTEA compared to PFBuTEA and PFOcTEA*

- ***Difference in the morphology of TFTEA doped membranes compared to PFBuTEA and PFOcTEA doped membranes:*** In the case of PFBuTEA and PFOcTEA, PCIL arranges itself in three possible ways (hypothesized in the section of morphology) as follows:

- 1). Organization along the pendant side chains over the surface of the hydrophobic ribbons without modifying the size of ionic phase;
- 2). Organization between the adjacent bundles and hence swelling the system laterally (and not perpendicularly);
- 3). Formation of PCIL-domains possibly in amorphous inter-bundle phase of Nafion-TEA (probably only at high concentration).

Hence, the first two types of organization probably result in an overall plasticizing effect of the PCIL on the polymer matrix (i.e. loosen the packing of perfluorinated chains and reducing the tortuosity as well as crystallinity of the system) hence reducing constraint in the system thereby improving its water retaining capacity. However, ***formation of crystallized PCIL domains at high PCIL content (3<sup>rd</sup> possibility) results in lower accessibility of water molecules to the ionic functions*** and hence limiting the improvement effect of these PCILs on the hydrophilicity of Nafion-TEA matrix. Whereas in the case of TFTEA doped membranes, TFTEA organizes itself differently in the Nafion-TEA matrix (TFTEA interacts mainly with the ionic phase of Nafion-TEA percolating itself mainly at the hydrophobic-hydrophilic interface) probably which is why additivity law worked better in this case at low water activity and hydrophilicity of TFTEA was found to be hindered when inserted in Nafion-TEA matrix at high water activity.

#### **4.2: General Conclusion**

In this chapter, the impact of the chain length of the perfluorinated anion of the PCIL on the morphology and different functional properties of Nafion-TEA has been studied. ***PFOcTEA doped membranes have shown contrasting results to TFTEA doped membranes with PFBuTEA doped membranes presenting an intermediate behavior between the two.***

WAXS results have demonstrated that addition of PCILs with long perfluorinated chains i.e. PFOcTEA and PFBuTEA results in loosening of packing of perfluorinated chains and also slight elongation of the PTFE main-chains in contrast to the case of TFTEA where its addition results in even tighter packing of perfluorinated chains of Nafion-TEA. Furthermore, SANS results have shown that presence of ***PFOcTEA and PFBuTEA does not alter the nano-structuration of Nafion-TEA*** i.e. no changes in the size of ionic domains of the polymer as well as the characteristic distance associated

with the Matrix knee *in contrary to TFTEA doped membranes* in which swelling of mainly the ionic domains has been observed.

Keeping these results in mind, it has been proposed that *PFOcTEA and PFBuTEA molecules intercalate themselves with the side chains of the PTFE main chain* i.e. present laterally to the surface of the ribbons in Nafion-TEA and also between two adjacent bundles in lateral direction while *TFTEA percolates itself in the ionic domains of the polymer* and gets distributed heterogeneously due to its micellar organization (especially at high concentration). Furthermore, WAXS and SANS results from both the measurements have demonstrated the appearance of characteristic peaks of *PFBuTEA and PFOcTEA from 30 wt% onwards* which point towards with either the *formation of crystallized PCIL domains probably in the inter-bundle amorphous regions of the polymer* or these ionic liquids arrange themselves in the nano-structure of Nafion-TEA in the manner similar to its pure form.

DMA measurements have shown that *PFOcTEA doped membranes present relatively better thermo-mechanical properties than TFTEA doped membranes below  $T_{\alpha}$* . However, above  $T_{\alpha}$ , the former collapses while the latter sustains a constant storage modulus of 1MPa up to 180°C. PFBuTEA doped membranes show intermediate behaviour. The difference in thermo-mechanical response of PFOcTEA and TFTEA doped membranes arises mainly due to the difference in the polarity of these PCILs and their consequent organization in the structure of Nafion-TEA. Moreover, it has been observed that longer the perfluorinated chain of the anion is, more intense and sharper is the  $\beta$  relaxation of the polymer as well as the higher is the temperature of its appearance.

An increase in the conductivities of PFOcTEA and PFBuTEA doped membranes with increasing PCIL concentration and temperature has been observed. The order of conductivity (for similar  $\lambda$  value at high PCIL content) of these doped membranes based on different PCILs is as follows: TFTEA~PFBuTEA>PFOcTEA. The *similar conductivities of TFTEA and PFBuTEA based doped membranes at similar  $\lambda$  or IEC value could be related to the particular type of the organization of PFBuTEA in the structure of Nafion-TEA*.

Membranes with all the three PCILs present similar permeability coefficients of O<sub>2</sub> and H<sub>2</sub> gases up to 20 wt%. However, formation of pure PCIL domains at high PCIL concentration as observed with PFBuTEA and PFOcTEA results in sharp increase in the permeability coefficients.

Water sorption study has demonstrated that PFOcTEA and PFBuTEA doped membranes also present B.E.T.III type isotherms like pure Nafion-TEA membrane and TFTEA doped membranes. The order of water sorption capacity of these doped membranes based on the type of the PCIL inside is as follows: PFOcTEA<PFBuTEA<TFTEA. Although *PFOcTEA and PFBuTEA are more hydrophobic*



*than TFTEA, still their presence at weight content less to 20% results in a higher improvement in the water retaining capacity of Nafion-TEA than that predicted by the additive law.*

To summarize, it can be said that the chemical structure/nature of the PCIL plays a key role in the evolution of the morphology and hence functional properties of the host membrane (Nafion-TEA in this study).

***References:***

1. Rault, J.; Neffati, R.; Judeinstein, P.; European Physical Journal **2003**, B36, 627-637.
2. Ping, Z.H.; Nguyen, Q.T.; Chen, S.M.; Polymer **2001**, 42, 8461-8467.
3. Billamboz, N.; Nedelec, J.M.; Grivet, M.; A European Journal of Chemical Physics and Physical Chemistry **2005**, 6, 1126-1132.
4. Iojoiu, C.; Judeinstein, P.; Sanchez, J. Y.; Electrochimica Acta **2007**, 53, .1395–1403.

## 5. TFTEA doped membranes based on Polysulfones

The PCIL doped membranes based on Perfluoro Sulfonic Acid ionomers (e.g. Nafion<sup>®</sup>) do not show enough good thermo-mechanical properties required for the High Temperature-PEMFC technology. Besides, high manufacturing cost of PFSA based ionomers is another key issue. Thus, the idea is to replace Nafion<sup>®</sup> with hydrocarbon PEMs based on aromatic polymers, which have good physical properties and are inexpensive, and explore the PEM system based on a modified aromatic polymer in combination with a PCIL. Thus, in this work, we concentrate on PEMs based on modified Polysulfones doped with TFTEA.

Polysulfones was chosen as the host polymer for this work due to their very high thermal ( $T_g=180^{\circ}\text{C}$ ;  $T_d>400^{\circ}\text{C}$ ) and chemical stability which are required for the HT-PEMFC application. Since, Polysulfone is not an ionomer in itself, so it has to be modified chemically by grafting ionic functions on the back-bone of the polymer to transform it into an ionomer (as discussed thoroughly in the bibliographical chapter).

Thus, this work, *Polysulfone (Udel-form) chemically grafted with perfluoro alkyl sulfonic acid side-chains*, has been synthesized and investigated in combination with TFTEA. The chemical structure of modified Polysulfone (*neutralized with TEA*; referred as *PSPF-TEA*) utilized in this work is shown in figure 1.

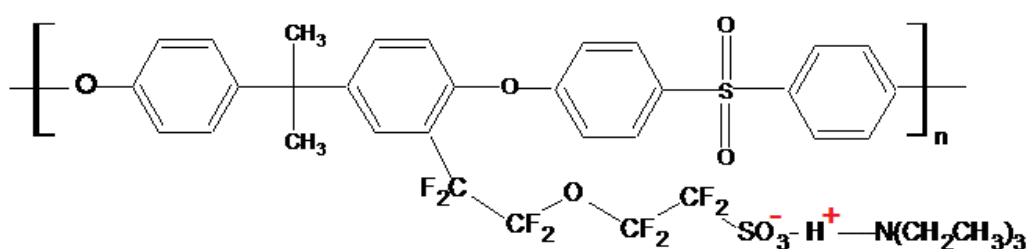


Figure 1: Chemical structure of the PSPF-TEA used in this study

This side-chain function was chosen to chemically modify the polymer because of the following reasons:

1. Combination of PCILs with unmodified Polysulfones results in very low compatibility between both the components.

- Moreover, directly sulfonated Polysulfones doped with PCILs result in systems with poor mechanical properties. This can be explained by the excessive plasticization effect of the PCIL on the polymer. The strong plasticization effect of the PCIL is due to the fact that there is no spatial separation between hydrophilic sulfonic groups and relatively hydrophobic polymer main-chain as the sulfonic acid groups are substituted directly on the main-chain (chemical structure of directly sulfonated Polysulfone-amine neutralized form shown in figure 2). Thus, the PCIL molecules interact heavily with both the ionic functions as well as the backbone chains resulting in the loss of morphology and hence mechanical stability (quite similarly as in the case of water molecules combined with directly sulfonated aromatic polymers). Thus, it is important to have nano-scale separation between hydrophobic and hydrophilic regions of the polymer to achieve enough good dimensional stability along with high proton conductivity. Keeping this point in mind, Polysulfone attached with ionic functions through perfluorinated ether side-chains was chosen as it has been shown in a previous work by Yoshimura et al. that Polysulfone (Radel form) modified with such kind of ionic functions exhibits nano-separation (separation between hydrophobic and hydrophilic domains) in the presence of water molecules<sup>(1)</sup>.
- This side chain function carrying sulfonic group resembles the side-chain of Nafion<sup>®</sup>. Hence, this could help us in comparing the impact of different kinds of polymer back-bone chains while keeping similar side-chain ionic functions on the consequent functional properties of the PCIL doped polymer electrolytes.

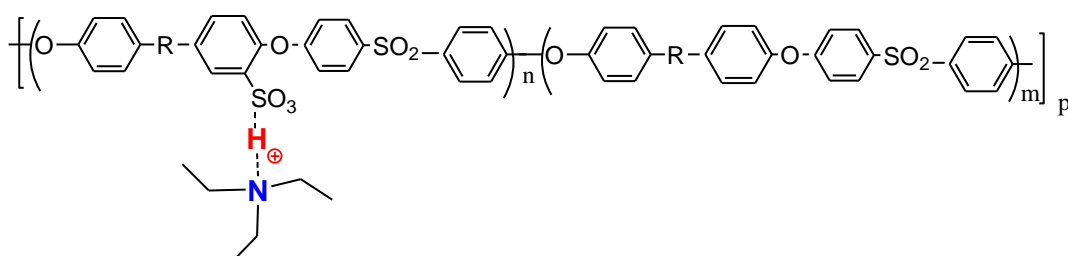


Figure 2: Chemical structure of the directly sulfonated Polysulfone neutralized with triethylamine

In this chapter, following will be discussed systematically:

- ❖ Synthesis of PSPF-TEA polymer and improvisations in the synthesis protocol
- ❖ Characterization of PEMs based on PSPF-TEA and TFTEA in terms of morphology, thermo-mechanical- properties and conductivity and comparison with the system based on Nafion-TEA+TFTEA.

### 5.1: Synthesis of PSPF-TEA

The synthesis of PSPF-TEA was done in four steps:

- Synthesis of the side-chain function*
- Bromination of Polysulfone(Udel form) at ortho-to-ether position*
- Grafting the side-chain function on the backbone of brominated-Polysulfone*
- Neutralization of PSPF-acid form with Triethylamine*

#### **a. Synthesis of the side-chain function**

The side chain function was synthesized by hydrolyzing the sulfonyl fluoride group of 1,1,2,2-Tetrafluoro-2-(1,1,2,2-tetrafluoro-2-iodoethoxy)ethanesulfonyl fluoride (PSA-F) into sulfonic acid function by using lithium hydroxide in THF as shown schematically in figure 3. The resulting product i.e. 1,1,2,2-Tetrafluoro-2-(1,1,2,2-tetrafluoro-2-iodoethoxy) ethane sulfonate is referred as PSA-Li.

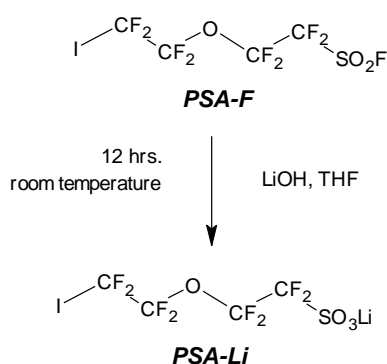
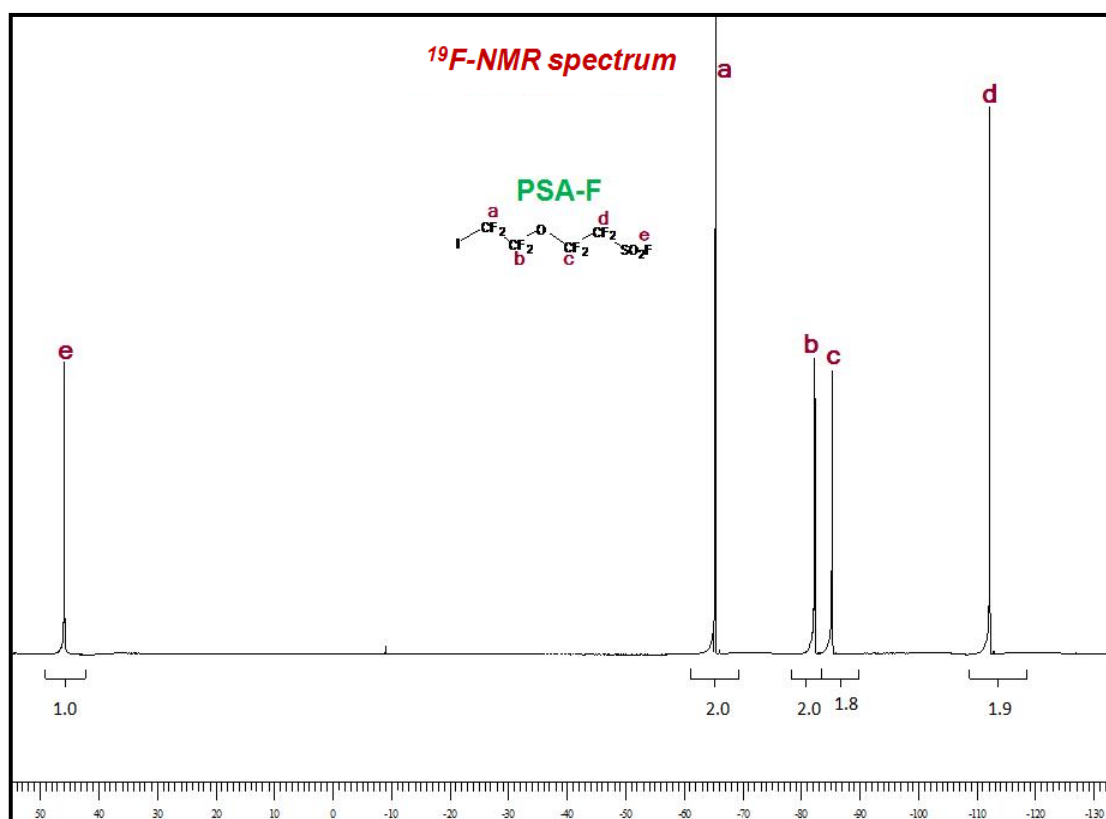
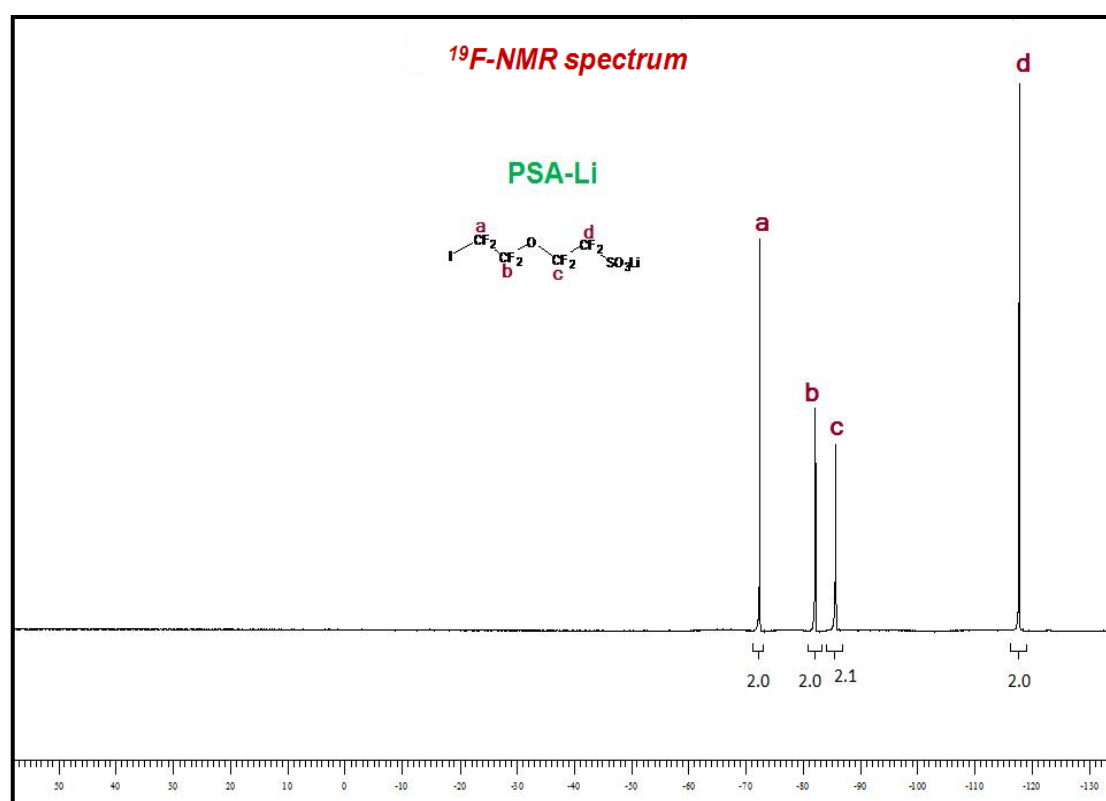


Figure 3: Schematic synthesis of PSA-Li

The  $^{19}\text{F}$ -NMR spectra of the starting and final product are shown in figure 4 (a) and 4 (b) respectively.



(a)



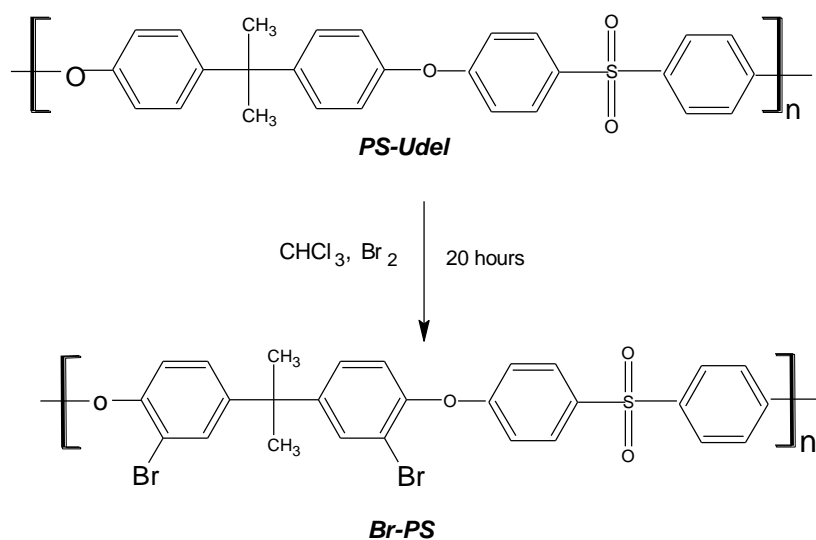
(b)

Figure 4:  $^{19}\text{F}$ -NMR spectra; a). PSA-F; b). PSA-Li

It can be clearly seen from the  $^{19}\text{F}$ -NMR spectra that the sulfonyl fluoride function of PSA-F is completely hydrolyzed into lithium sulfonate in PSA-Li since the peak at 45.8 ppm corresponding to fluorine atom of  $-\text{SO}_2\text{F}$  is no more present in the spectra of PSF-Li.

***b. Bromination of Polysulfone (Udel form) at ortho-to-ether position***

In order to graft the side-chain ionic function on the backbone of Polysulfone, polymer (Polysulfone-Udel/PS-Udel) was first brominated by using bromine with dichloromethane as solvent<sup>[2,3]</sup>. The reaction involved in the bromination step is shown in figure 5. The degree of bromination was varied by varying the amount of  $\text{Br}_2$  added during the bromination reaction. The reaction takes around 20 hours to finish.



*Figure 5: Schematic synthesis of brominated Polysulfone (Br-PS) from Polysulfone-Udel (PS-Udel)*

Bromination of Polysulfone is an electrophilic substitution reaction in which Bromine atoms attaches themselves selectively at ortho position to the aryl ether linkage in the arylene ether segment of the repeating unit due to the activation by electron-donating oxygen atoms. The ortho-ether position in the aryl sulfone segment is unreactive to bromination reaction due to electron-withdrawing nature of sulfonyl group. The degree of bromination was calculated by using the following relation between the peaks of  $^1\text{H}$ -NMR of the polymer:

*“Degree of Bromination” = integral of protons at 7.52 ppm/integral of protons at 7.87ppm*

The protons at 7.52 ppm correspond to protons located at ortho position to brominated site in the arylene ether segment (marked as “*d*” in the  $^1\text{H}$ -NMR spectrum) while the protons at 7.87 ppm correspond to protons in the aryl sulfone segment whose position is not affected before and after the reaction (marked as “*b*” in the  $^1\text{H}$ -NMR spectrum).

The bromination degree ranged between 40-100% in our case depending upon the amount of  $\text{Br}_2$  added during the reaction. The NMR spectrum of brominated Polysulfone with almost 80% of degree of bromination is shown in figure 6.

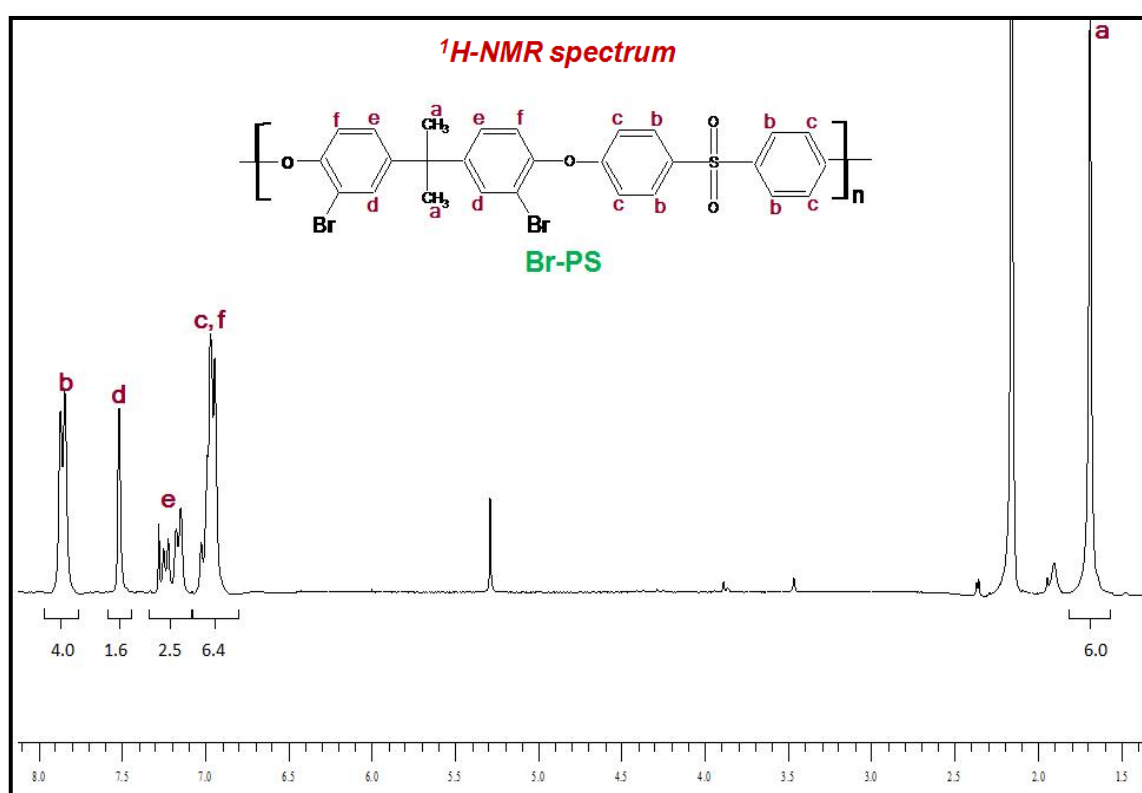


Figure 6:  $^1\text{H}$ -NMR spectrum of Br-PS with 80% degree of bromination

Afterwards, the brominated polymers with different bromination degrees were taken for the measurement of SEC-MALS technique (Size Exclusion Chromatography conjugated with Multi-Angle Light Scattering). Table 1 shows the values of number average molecular weight ( $M_n$ ) obtained for different polymers (PS-*x*-Br where *x* corresponds to the number of bromide groups per repeating unit of PS-Udel).



It can be seen from the table 1 that the brominated-Polysulfone with low bromination degree have lower  $M_n$  values in comparison to unmodified PS-Udel. This signifies that Polysulfone exhibited chemical degradation during the bromination process. This chemical degradation of the polymer is mainly due to prolonged exposure to hydrogen bromide (HBr) gas which is continuously produced during the reaction. Surprisingly, this phenomenon has not been accounted much in the works related to bromination of Polysulfone in the literature.

<i>Sample</i>	<i><math>M_n</math>(g/mol)</i>
<i>PS-Udel</i>	$2.717 \times 10^4$
<i>PS-0.8-Br</i>	$7.101 \times 10^3$
<i>PS-2-Br</i>	$2.823 \times 10^4$

Table 1:  $M_n$  values determined for PS-Udel with different bromination degrees using SEC-MALS

Thus, in order to prevent or decrease the degree of chemical degradation of Polysulfone due to the production of HBr gas during bromination, two ideas were considered mentioned as follows:

- Addition of a basic chemical product such as potassium carbonate into the reaction mixture in order to absorb HBr produced during the course of bromination reaction:*** the amount of Potassium Carbonate added was equi-molar to the amount of Bromine added.
- Increasing the rate of bromination reaction by addition of a solvent with dielectric constant and/or solvent quality better than dichloromethane:*** In this regard, dichloromethane:acetic acid (90:10;v/v) was chosen. Acetic acid has been frequently used as a solvent in the case of bromination of Polystyrene<sup>[4]</sup>.

The experimental conditions were kept otherwise similar to those employed in previous bromination reaction. These two types of bromination reactions were carried out with a pre-determined degree of bromination of 40-50% in order to see the preliminary effect of the presence of potassium carbonate/acetic acid on the rate of the reaction and chemical degradation exhibited by the polymer.

Firstly, it was observed that the bromination reaction took almost same time to finish in the case of system based on potassium carbonate while the ***reaction time drastically reduced to 2 hours in the case of acetic acid based reaction mixture***. In addition, both the types of brominated polysulfones

conceived 40% bromination degree. Furthermore, both the types of bromiated Polysulfones were taken for the measurement of molecular weight by SEC-MALS Technique Table 2 shows the number average molecular weight of Br-PS obtained from reaction systems based on Potassium Carbonate and acetic acid in comparison to Br-PS (with similar bromination degree) obtained without acetic acid/potassium carbonate in the reaction mixture.

<i>Sample</i>	<i>M<sub>n</sub> (g/mol)</i>
<i>PS-Udel</i>	$2.717 \times 10^4$
<i>PS-0.8-Br</i>	$7.101 \times 10^3$
<i>PS-0.8-Br</i> <i>(Carbonate)</i>	$1.391 \times 10^4$
<i>PS-0.8-Br</i> <i>(Acetic acid)</i>	$1.661 \times 10^4$

Table 2: *M<sub>n</sub>* values determined by SEC-MALS for brominated PS-Udel (bromiantion degree: 40%) obtained from the reaction systems based on Potassium Carbonate and acetic acid

It can be observed that the degree of chemical degradation phenomenon could be reduced to some extent but not totally avoided.

### c. Grafting the side-chain function on the backbone of brominated-Polysulfone

The bromination process of Polysulfone was followed by grafting the synthesized side-chain function (from I<sup>st</sup> step) PSA-Li on the backbone chain of the polymer by using Ullmann reaction at 120°C in the presence of Copper powder (*Note*: The brominated polymers obtained from bromination reaction without the presence of potassium carbonate or acetic acid in the reaction mixture were utilized for this reaction and all the results presented on this system will be based only on these polymers). The reaction involved in the synthesis is shown schematically in figure 7.

When the reaction was finished, the polymer was precipitated in 5N solution of hydrochloric acid. Thus, this reaction resulted in Polysulfone grafted with perfluorinated ether side-chains carrying sulfonic acid functions at the chain end (denoted as PSPF-H<sup>+</sup>).

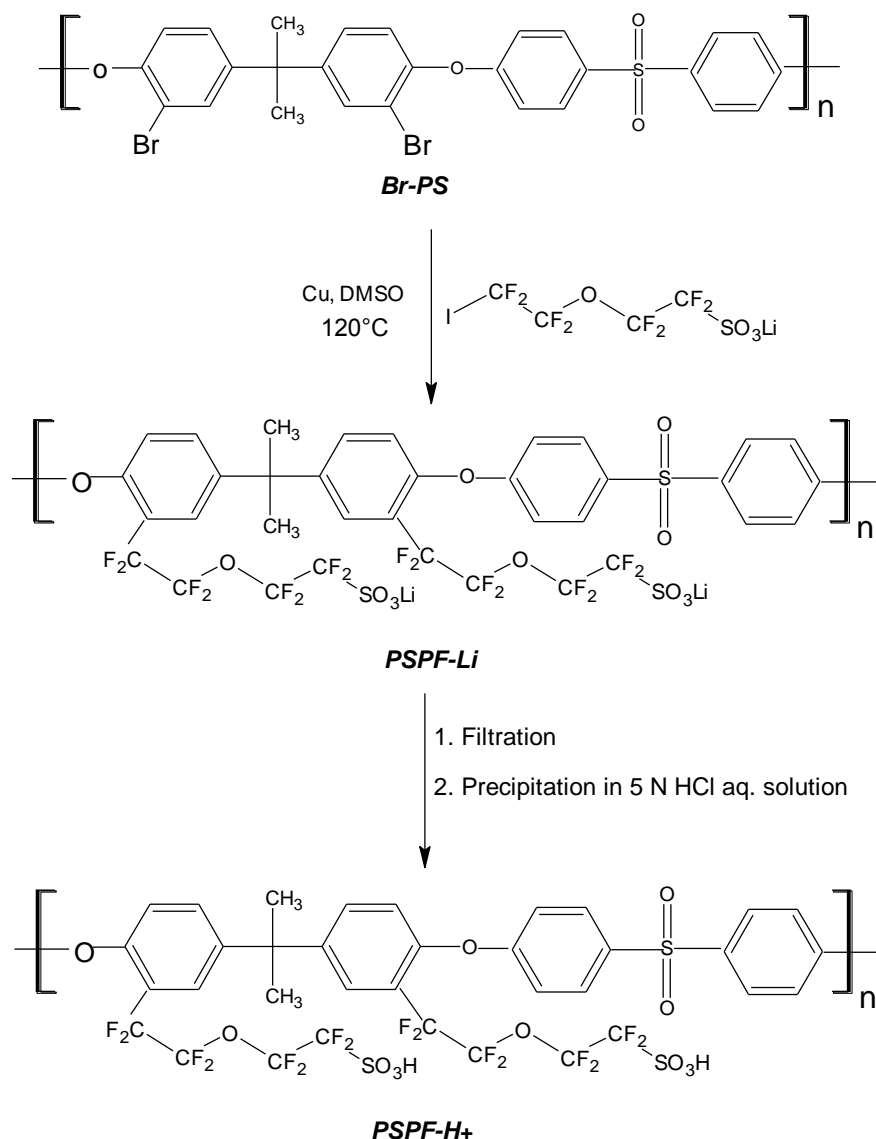
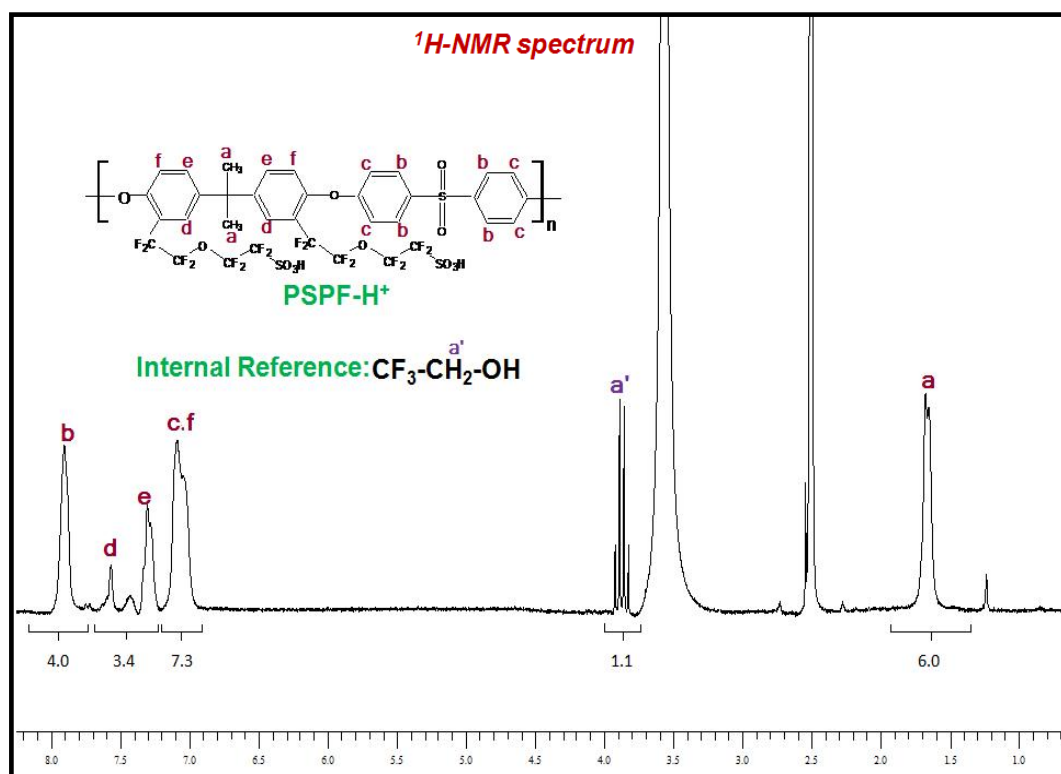
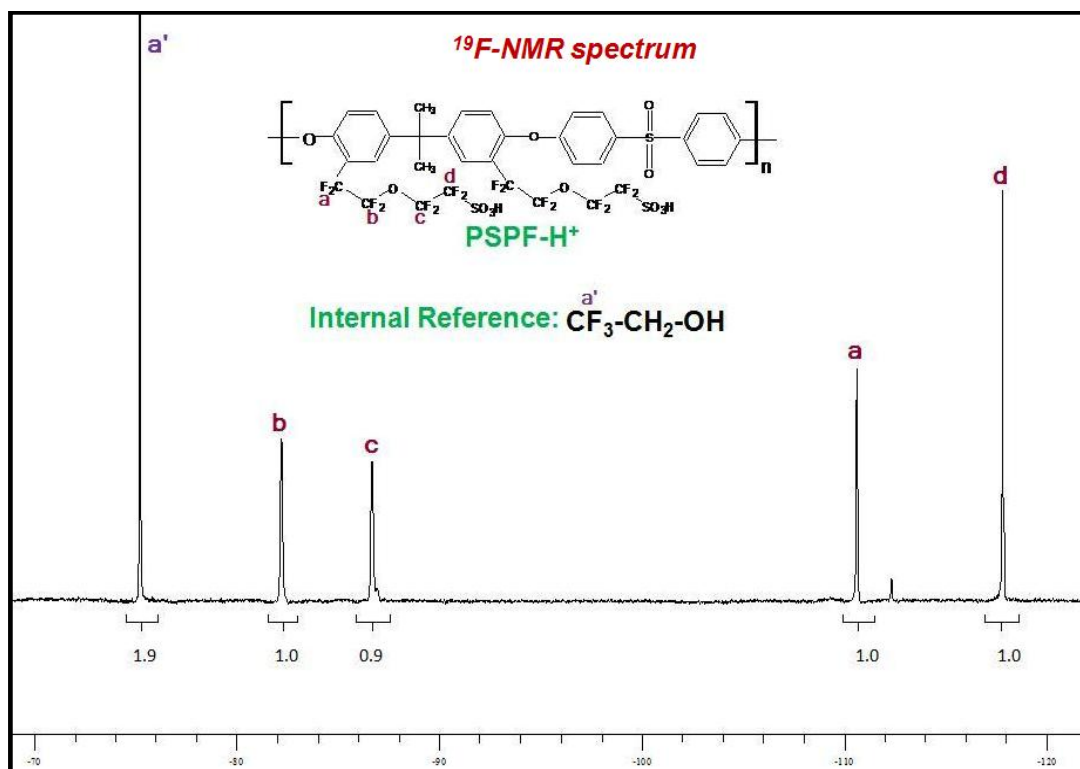


Figure 7: Schematic illustration of grafting of PSA-Li on the backbone chain of Br-PS using Ullmann reaction

The <sup>1</sup>H-NMR and <sup>19</sup>F-NMR spectra of PSPF-H<sup>+</sup> (prepared from Br-PS with approximately 40% bromination degree) are shown in figure 8 (a) and 8 (b) respectively. A small amount of internal reference (trifluoro ethanol) was added in the tubes prior to NMR measurements in order to verify the molar ratio of hydrogenated and perfluorinated parts of PSPF to find the degree of substitution of the side-chain function.



(a)



(b)

Figure 8: NMR spectra of PSPF- $\text{H}^+$ ; a).  $^1\text{H}$ ; b).  $^{19}\text{F}$

It can be seen from the spectra that the peak associated with  $-\text{CF}_2$  group of PSA-Li directly attached to the iodide shifts from -72.6 ppm to -110.6 ppm when it gets directly attached to the Polysulfone backbone by elimination of the iodide group. Moreover, after calculating the molar ratio between hydrogenated and perfluorinated parts of PSPF by using the peaks of internal reference, a ratio of about 40% is found which signifies that all the bromide groups of Br-PS were replaced by the side chain ionic functions.

PSPF- $\text{H}^+$  were obtained with different substitution degrees and complete replacement of bromide with the side-chain ionic function was found.

***d. Neutralization of PSPF-acid form with triethylamine***

The sulfonic acid groups of the resulting polymer i.e. PSPF-acid form were neutralized with Triethylamine in aqueous solution and lyophilized. Afterwards, the neutralized polymer (PSPF-TEA) was dried at 80°C under vacuum and stored under Argon atmosphere for further characterization.

The dried polymers with different substitution degrees were taken for the determination of their number average molecular weight ( $M_n$ ) by using SEC-MALS technique. Table 3 shows the values of  $M_n$  obtained for different polymers (PSPF-y-TEA where y corresponds to the number of TEA-neutralized sulfonic acid functions per repeating unit of PS-Udel). Further gain in the weight of the polymers on substituting the ionic functions signifies that no degradation occurred during the reactions of ionic function substitution as well as the neutralization process. Furthermore, the ***Ion Exchange Capacities (IEC)*** of these polymers were calculated by using the value of degree of ionic function substitution (which were calculated from the NMR spectra obtained in the presence of the internal reference “trifluoro ethanol”). The IEC values for the polymers with varying substitution degrees are also shown in table 3.

<i>Sample</i>	<i>M<sub>n</sub>(g/mol)</i>	<i>IEC (H<sup>+</sup>/Kg)</i>
<i>PS-Udel</i>	$2.717 \times 10^4$	-
<i>PSPF-0.8-Br</i>	$7.101 \times 10^3$	-
<i>PSPF-1.6-Br</i>	-	-
<i>PSPF-2-Br</i>	$2.823 \times 10^4$	-
<i>PSPF-0.8-TEA</i>	$1.493 \times 10^4$	1.06
<i>PSPF-1.6-TEA</i>	-	1.49
<i>PSPF-2-TEA</i>	$3.017 \times 10^4$	1.62

Table 3:  $M_n$  values determined for PS-Udel with different bromination degrees using SEC-MALS

## 5.2: PSPF-TEA+TFTEA

In this section, impact of TFTEA doping on the morphology as well as properties of PSPF-TEA will be discussed. All the membranes which will be discussed have been prepared by casting method. In the elaboration of these membranes, solvent evaporation was carried out at 60°C followed by annealing treatment of one hour at 150°C. The membranes were dried at 80°C under vacuum and stored in glove box for further analysis. The  $\lambda$  values as well as membrane property of doped membranes based on PSPF-TEA (with different degrees of ionic function substitution) and TFTEA are shown in table 4.

<i>Sample</i>	<i>% TFTEA (by weight)</i>	<i>% TFTEA (by Volume)</i>	<i>Moles TFTEA/ moles SO<sub>3</sub><sup>-</sup>- <sup>+</sup>HN(C<sub>2</sub>H<sub>5</sub>)<sub>3</sub> of PSPF-y-TEA  (<math>\lambda</math>)</i>	<i>Membrane property</i>
<b><i>PSPF-0.8-TEA</i></b>	0	0	0	<i>Brittle</i>
<b><i>PSPF-0.8-TEA+20%TFTEA</i></b>	20	20	0.76	<i>Brittle</i>
<b><i>PSPF-0.8-TEA+30%TFTEA</i></b>	30	30	1.3	<i>Flexible</i>
<b><i>PSPF-1.6-TEA</i></b>	0	0	0	<i>Brittle</i>
<b><i>PSPF-1.6-TEA+15%TFTEA</i></b>	15	15	0.76	<i>Brittle</i>
<b><i>PSPF-1.6-TEA+20%TFTEA</i></b>	20	20	1.1	<i>Flexible</i>
<b><i>PSPF-1.6-TEA+33%TFTEA</i></b>	33	33	2.12	<i>Very fragile</i>
<b><i>PSPF-2.0-TEA</i></b>	0	0	0	<i>Brittle</i>
<b><i>PSPF-2-TEA+30%TFTEA</i></b>	30	30	2.12	<i>Flexible</i>

Table 4: Concentration and  $\lambda$  values for different casting based PSPF-y-TEA+zwt% TFTEA membranes (Density of all the PSPF-y-TEA are taken as 1.4 g/cm<sup>3</sup>)

Firstly, the morphology results obtained from SANS measurements will be discussed followed by discussion on thermo-mechanical properties and conductivities.

#### ***a. Morphology***

The morphology of the membranes was studied by using SANS measurements. The membranes were analyzed in the  $q$  range of 0.04-0.4 Å<sup>-1</sup> in order to observe if the polymer exhibits any hydrophilic-hydrophobic nano-separation in the absence and/or presence of TFTEA. All the membranes based on PSPF-TEA were utilized in dry state and the cells were prepared in the Argon atmosphere in order to avoid any effect of water presence on the morphology of the membranes. PSPF-y-H<sup>+</sup> membranes (y=0.8 and 2) were also prepared (and utilized in dried form) in order to provide reference membranes for the triethylamine neutralized membranes. Furthermore, these membranes in acidic form were swollen with water (~27 wt%) prior to SANS measurements and measurements were done in order to compare the impact of presence of water with that of TFTEA on the evolution of SANS spectra of PSPF membranes. Unfortunately, many of the membranes especially with low substitution degree were quite brittle and hence could not be analyzed using SANS. Figure 9 demonstrates the SANS spectra of different membranes in the  $q$  range of 0.04-0.4 Å<sup>-1</sup>.

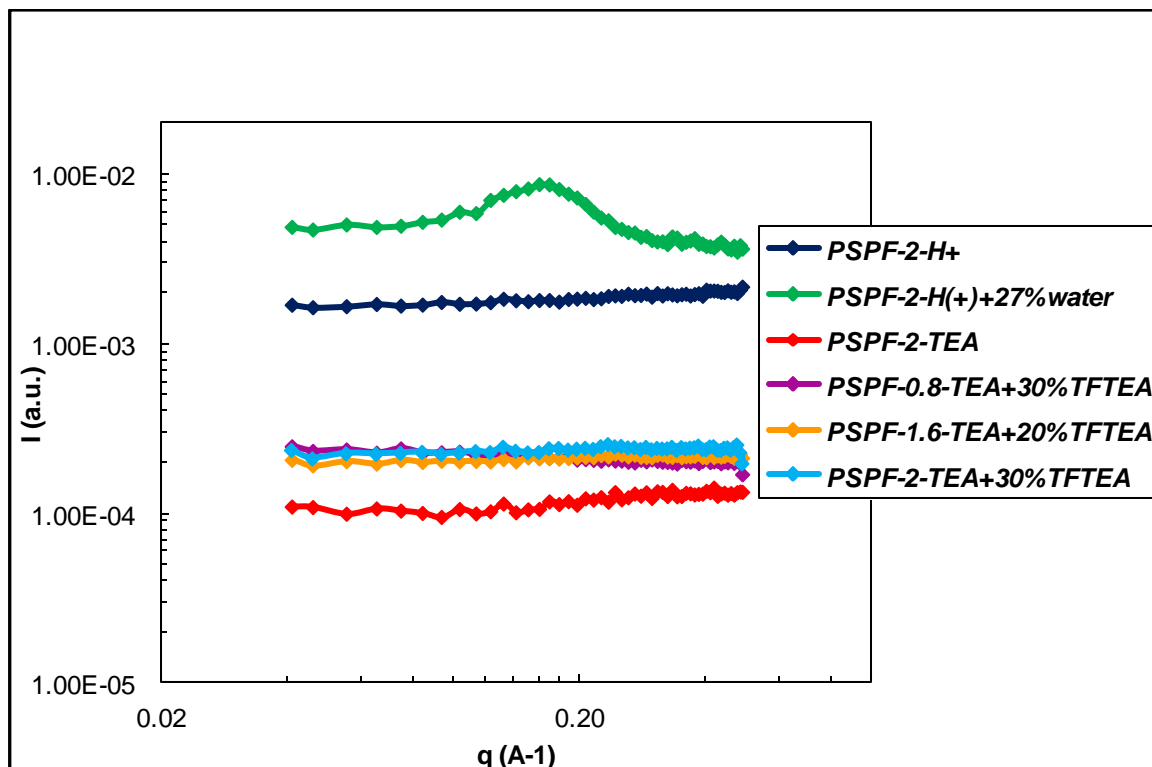


Figure 9: SANS spectra of different membranes based on PSPF in the  $q$  range of 0.04-0.4  $\text{\AA}^{-1}$

From figure 9, following observations can be made:

1. Firstly, we compare the SANS profile of dry PSPF in acidic form (PSPF-2- $\text{H}^+$ ) with that of Nafion<sup>®</sup> in acidic form (Nafion- $\text{H}^+$ ). It can be seen that *PSPF-2- $\text{H}^+$  does not exhibit any peak in dried state in this  $q$  range similarly as Nafion- $\text{H}^+$*  (discussed in the second chapter). This result is similar to that obtained in the literature for dry Polysulfone (Radel form) modified with the same ionic function<sup>(1)</sup>.
2. Now, we compare the SANS profile of dry PSPF-TEA with that of dry Nafion-TEA. It has been thoroughly discussed and explained in the second chapter that dry *Nafion-TEA exhibits a distinct ionomer peak at  $q=0.202 \text{ \AA}^{-1}$  ( $d=31 \text{ \AA}$ ), suggesting a string-like organization of Triethylammonium cations at the hydrophobic/hydrophilic interface*. However, PSPF-TEA does not exhibit any peak in this  $q$  range. This signifies that either:
  - a. *PSPF-TEA does not exhibit any nano-separation at the hydrophobic/hydrophilic interface.*
  - b. *The contrast between the side-chain ionic functions and the main-backbone chain is not enough to generate a well-marked peak.*



3. On swelling ***PSPF-2-H<sup>+</sup> membrane in water (water content~27 wt%), a well-defined peak is observed at  $q=0.17 \text{ \AA}^{-1}$  corresponding to a distance of  $39.6 \text{ \AA}$*** . Yoshimura et al. obtained similar result for modified Polysulfone (Radel form; modified with same ionic function) in the presence of water molecules i.e. they observed formation of ionic domains of characteristic size of  $37 \text{ \AA}$  in modified polymer containing 38wt% of water<sup>[1]</sup>. However, the size of ionic domains seems to be larger in our case even with lower quantity of water present in our membrane. This is probably due to the fact that ***Polysulfone–Radel form is more rigid compared to Polysulfone-Udel form. The higher rigidity of the former results in more restricted aggregation of side-chain ionic functions in the modified form is more restricted in it and hence smaller size of ionic domains***.
  
4. Finally, we consider the case of PSPF-TEA membranes doped with different degrees of TFTEA. It can be seen that PSPF-y-TEA membranes in the presence of TFTEA do not still exhibit any peak. From this observation, it seems that ***PSPF-y-TEA membranes doped with TFTEA do not exhibit any nano-seperation of hydrophilic-hydrophobic domains in the presence of TFTEA*** in contrary to the presence of water probably due to strong plasticizing effect of TFTEA on both the main-chain as well as the side-chain ionic function of PSPF-TEA. The problem of contrast does not appear to be an issue behind this result because the system based on PSPF-H<sup>+</sup> and water present an ionomer peak while PSPF-TEA and TFTEA does not, though the contrast (between main-chains and ionic domains) should be better in the latter.

#### **b. Thermo-mechanical properties**

Membranes based on PSPF-y-TEA with intermediate substitution degree of side-chains (around 1.6 per repeating unit) and TFTEA were utilized to evaluate the thermo-mechanical properties of this system by using DMA. However, it could be carried out on only on one membrane i.e. membrane containing 20 wt% TFTEA since the virgin membrane as well the membranes with lower TFTEA contents were very brittle and the membrane with higher TFTEA content was too flexible and fragile for the measurements. The storage modulus versus temperature plot of this membrane is shown in figure 10.

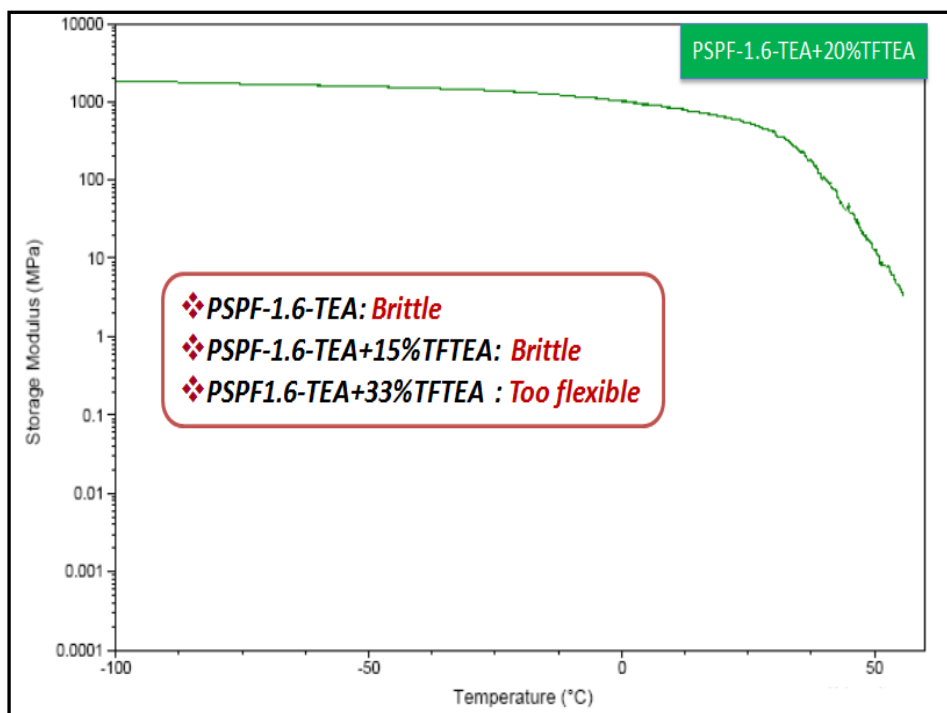


Figure 10: Storage modulus vs Temperature plot of PSPF-TEA+20wt%TFTEA membrane

It can be seen from the plot that the membrane starts to lose its mechanical strength from 40°C. This behavior underlines *strong plasticizing effect of TFTEA on the matrix of PSPF-TEA*. The strong plasticizing effect of TFTEA must be due to the following reasons:

1. The ionic functions are randomly distributed in PSPF-TEA.
2. Moreover, TFTEA could interact not only with the ionic functions but also with the backbone of the polymer.

Apart from strong plasticizing effect of TFTEA on the matrix of PSPF-TEA, *the low molecular weight of the modified polymer could be another reason for its insufficient mechanical/thermo-mechanical properties*.

### c. Conductivity

The conductivity measurements were carried out on the same set of membranes utilized also for the DMA measurements (i.e PSPF-y-TEA with y=1.6 ionic functions per repeating unit). The measurements were carried out on the dried membranes in the same fashion as mentioned in the previous chapters in order to avoid any impact of water molecules on the conductivity values. The ionic conductivities of the PSPF-TEA membranes doped with different concentrations of TFTEA are

shown in figure 11. In order to compare different TFTEA doped membranes, ionic conductivities of Nafion-TEA and TEA neutralized directly-sulfonated Polysulfone in combination with different concentrations of TFTEA (SPS-1.4-TEA+30wt% TFTEA) with similar  $\lambda$  values are included in figure 11.

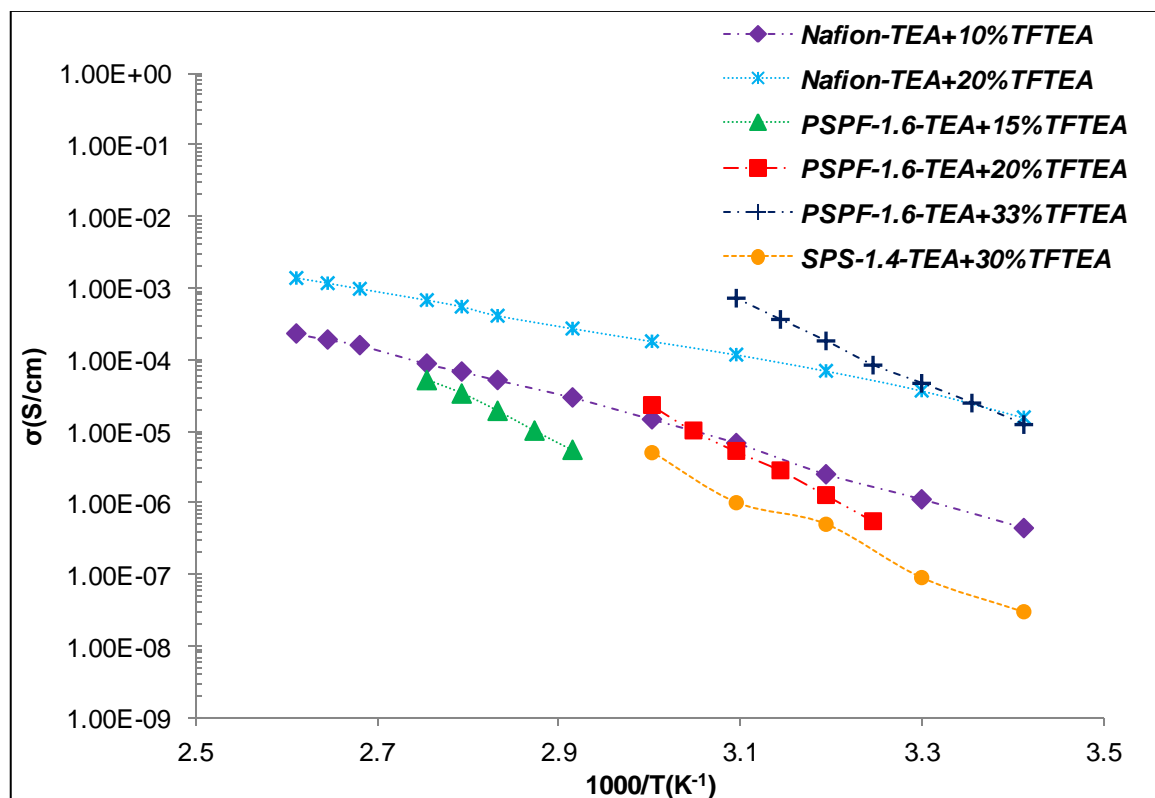


Figure 11: Ionic conductivity of neutralized PSPF with different percentage of TFTEA (PSPF-TEA+x wt%TFTEA)

On comparing PSPF-TEA based doped membrane with SPS-TEA based doped membrane, it is observed that *PSPF-TEA based doped membrane (33 % TFTEA weight fraction; 33 % TFTEA volume fraction) shows much better conductivities in comparison to doped membranes based on directly-sulfonated Polysulfone membranes ((33 wt% TFTEA fraction; 26 wt% TFTEA volume fraction)) for comparable TFTEA volume fraction.*

(Note: IEC value for SPS-1.4-TEA is  $2.53\text{H}^+/\text{kg}$  while it is  $1.49\text{H}^+/\text{Kg}$  for PSPF-1.6-TEA)

On comparing Nafion-TEA and PSPF-TEA with *similar  $\lambda$  values and volume fractions* of TFTEA, for e.g., 1.12 for Nafion-TEA based membrane (20wt% TFTEA content) and 1.1 for PSPF-1.6-TEA (20wt% TFTEA content), it seems that *PSPF-TEA based doped membrane show inferior conductivities in comparison to Nafion-TEA based doped membrane up to their  $T_g$  values.* Moreover, above their  $T_g$ , PSPF-TEA based doped membranes collapse completely and thus, ionic

conductivities at higher temperatures could not be accessed for this system. Interestingly, on comparing *PSPF-TEA membrane doped with enough high TFTEA content (weight Fraction: 33%; volume fraction: 33%) show conductivity values slightly higher than those obtained with Nafion-TEA containing optimum TFTEA concentration (weight Fraction: 20%; volume fraction: 24%) up to their  $T_g$* . The important issue is that the  $T_g$  values of PSPF-TEA based doped system are lower in comparison to Nafion-TEA based doped system due to stronger plasticizing effect of TFTEA on the former.

(Note: IEC value of PSPF-1.6-TEA is higher than that of Nafion-TEA).

### 5.3: General Conclusion

In this work, membranes based on modified Polysulfone in combination with TFTEA have been investigated.

From the synthesis point of view, it has been observed that the *bromination of Polysulfone results in significant chemical degradation of the polymer due to its exposure to Hydrogen Bromide gas* produced during the reaction. The degree of chemical degradation was reduced by adding Potassium Carbonate into the reaction mixture to absorb HBr gas produced during the reaction. Alternatively, the prolonged exposure of the polymer can be reduced by *improving the rate of the bromination reaction by the addition of Acetic Acid into the reaction mixture*. These results are really preliminary. Hence, improvisations on the protocol of bromination of Polysulfones have to be investigated in more details.

Concerning the characterization of these membranes, SANS results have shown that the *size of ionic domains are larger in modified Polysulfone based on Udel form in comparison to Radel form* in the presence of similar amount of water molecules. However *PSPF-TEA does not present any peak in undoped or doped form* which signifies no nano-phase separation between hydrophilic and hydrophobic domains.

Moreover, DMA results have shown a *very strong plasticizing effect of TFTEA on the PSPF-TEA matrix*.

The conductivities of *PSPF-TEA+TFTEA system are better than those of directly sulfonated Polysulfone+TFTEA membranes* for similar sulfonation degrees and volume fractions of TFTEA at all the temperatures. Moreover, their conductivities are *lower to those of Nafion-TEA+TFTEA for similar  $\lambda$  values and volume fractions*. However, comparable conductivities are observed at high contents of TFTEA in PSPF-TEA in comparison to that of optimum system based on TFTEA and

**Nafion-TEA.** The key problem is that the conductivities could be measured only up to the  $T_g$  value of PSPF-TEA based membranes and their  $T_g$  values were much lower compared to those of Nafion-TEA based membranes with similar  $\lambda$  values.

This performance of PSPF based doped membranes must be primarily due to the reason that the ionic functions are randomly distributed within the membrane and consequently TFTEA is dispersed completely in the chemical structure of the membrane. This results in flagrant plasticization effect of TFTEA. Hence, in order to improve the performance, it is important to separate hydrophobic and hydrophobic domains of the polymer. In order to separate the ionic domains from the hydrophobic domains, it would be interesting to synthesize block co-polymers in which only one of the blocks would be functionalized with the side-chain ionic function to interact with the PCIL molecules while the other non-functionalized block would not present any interaction with the PCIL and hence would contribute to the mechanical stability of the system.

***References:***

1. Yoshimura, K.; Iwasaki, K.; *Macromolecules* **2009**, 42, 9302-9306.
2. Bonfanti, C.; Lanzini, L.; Sisto, R.; Valentini, C.; *Journal of Applied Polymer Science* **1997**, 64(10), 1987–1997.
3. Lafitte, B.; Jannasch, P.; *Journal of Polymer Science: Part A: Polymer Chemistry* **2005**, 43, 273–286.
4. Jhon, Y.K.; Semler, J.J.; Genzer, J.; *Macromolecules* **2008**, 41, 6719-6727.

## General Conclusions and Perspectives

---

The objective of this thesis project was to study the Polymer Electrolyte Membranes (PEM) based on nano-structured ionomers in combination with different Proton Conducting Ionic Liquids (PCIL), *a system capable of ionic conduction in anhydrous state*, for the application of High Temperature-PEMFCs.

This system has been dealt by the research community to some extent and has shown very promising results for the HT-PEMFC application. However, a clear relation between the chemical nature of the PCIL/polymer electrolyte on the morphology (at different length scales) and various functional properties of the system has had not been shown. Moreover, various key functional properties such as gas-permeation, water sorption and degradation phenomena associated with such kind of system had not been studied in detail.

*Thus, in this work, influence of the chemical structure of functional polymers and PCILs on the evolution of morphology as well as functional properties of the system has been largely studied. Different characterization techniques have been used which allowed us to study the response of our system at different length scales i.e. molecular, nanoscopic-mesoscopic and macroscopic scales.*

In the *first chapter* of the work, PEMs based on neutralized Nafion<sup>®</sup> and Triethylammonium Triflate (TFTEA) have been studied.

It has been shown that neutralization of acidic sites in Nafion<sup>®</sup> 117 membrane by triethylamine (TEA) has significant effect on the morphology as well as functional properties of Nafion<sup>®</sup>. *Nafion<sup>®</sup> neutralized with triethylamine (Nafion-TEA) exhibits a single layer string-like organization of inter-digitated TEA cations at the hydrophobic-hydrophilic interface when in anhydrous state.* The presence of these bulky alkyl ammoniums at the hydrophobic-hydrophilic interface results in weak dipole-dipole interactions in place of strong hydrogen bonds among the ionic functions in Nafion<sup>®</sup>. Consequently, the mobility of perfluorinated main chains in the polymer increases and so does the permeability of oxygen and hydrogen gases. Moreover, the neutralization of sulfonic acid functions by TEA results in pretty low water uptakes by the membrane at 25°C.

Afterwards, impact of TFTEA doping levels on the properties of Nafion-TEA has been evaluated.

*TFTEA molecules, like water molecules, interact mainly with the ionic functions of Nafion-TEA.* That is why the evolution of nano-structure of Nafion-TEA with TFTEA concentration is very similar to that of acidic Nafion<sup>®</sup> swollen by water. However, a more *heterogeneous distribution of TFTEA in*

*Nafion-TEA, probably due to the micellar organization of TFTEA in the membrane*, has been proposed *at high TFTEA content (above 18 wt%)*. Concerning thermo-mechanical properties, a *plasticizing effect of the ionic liquid on the Nafion-TEA matrix* has been observed and this phenomenon amplifies with the increasing content of ionic liquid within the polymer.

The gas permeability of the doped Nafion-TEA membranes is very close to that of virgin Nafion-TEA membrane. However, introduction of the ionic liquid within the Nafion-TEA membranes significantly boosts the ionic conductivity under anhydrous conditions. Moreover, the *hydrophilicity of the Nafion-TEA membrane improves with increasing TFTEA content*.

The *second part* of this thesis work has permitted us to establish the fact that the *elaboration method of these PCIL doped membranes play a significant role in the evolution of some of their key functional properties*. The methods of elaboration chosen in this study for comparison were *Swelling* and *Casting*.

Firstly, results have pointed towards more densely and homogeneously organized morphology in casting based Nafion-TEA at molecular and nanoscopic-mesoscopic length scales. This improved morphology of Nafion-TEA when recast could explain why the *casting based membrane presents better thermo-mechanical properties above 150°C* and sustains a storage modulus of approximately 1 MPa in the temperature range of 150-190°C while Nafion-TEA prepared from extruded-Nafion® 117 membrane collapses completely above 150°C.

Conductivity of recast Nafion-TEA is comparatively lower than that of extruded Nafion-TEA below 100°C and similar afterwards probably due to denser packing of ionic functions and lower mobility of the side chains in the former up to  $T_g$  (~100°C).

Gas permeability coefficients of gases have been found lower while water uptake at 25°C has been found higher for casting based membrane compared to the extruded one at middle water activity ratios.

Concerning TFTEA doped membranes based on these two methods of elaboration, *casting based membranes show better performance overall*. For instance, the packing of perfluorinated chains have been found more compact along with lower impact of TFTEA on the long range crystalline order in Nafion-TEA in the case of casting based doped membranes. In addition, *casting based membranes present better thermo-mechanical properties in comparison to swelling based membranes above 150°C and sustain a storage modulus of ~1MPa in the temperature range of 150-180°C*. Furthermore, gas-permeability coefficients of casting based TFTEA doped membranes have been found to be lower to that of swelling based ones. Both these results seem to be related to the better results on morphology for the casting based membranes as mentioned firstly. In terms of anhydrous ionic conductivities and water sorption, both the types of membranes show similar evolution with increasing TFTEA content.



However, it seems that *the casting based membranes exhibit heterogeneous swelling of ionic domains of Nafion-TEA at lower concentrations of TFTEA compared to swelling based doped membranes.*

Keeping in mind better overall performance of casting based TFTEA doped membranes, *fuel cells test were carried out on the casting based one giving a current density of 0.85A/cm<sup>2</sup> at 100°C using 100% humidified gases.*

In the *third part* of the work, it has been clearly observed that the *morphology of the doped membranes and hence consequent functional properties depend a lot on the chemical structure of PCIL incorporated within the membrane.* The different PCILs incorporated within the Nafion-TEA membrane by casting method for this study were: Triethylammonium Perfluorinated Butane Sulfonate (PFBuTEA) and Triethylammonium Perfluorinated Octane Sulfonate (PFOcTEA) and compared with TFTEA based membranes.

*From the morphological point of view, flagrant differences have been found in the membranes based on PFOcTEA and PFBuTEA in comparison to TFTEA based membranes.* Keeping all the results in mind obtained from the morphological characterization at different length scales, it has been proposed that PFOcTEA and PFBuTEA molecules intercalate themselves with the side chains of the PTFE main chain i.e. present laterally to the surface of the ribbons in Nafion-TEA and also between two adjacent bundles in lateral direction while TFTEA locates itself mainly in the ionic domains of the polymer and gets distributed heterogeneously due to its micellar organization (especially at high concentration). In addition, *PFOcTEA and PFBuTEA doped membranes exhibit the formation of crystallized PCIL domains probably in the inter-bundle amorphous regions of the polymer starting from 30 wt% content of these PCILs in the membranes.*

Consequently, the evolution of functional properties is also a bit different in these systems.

For instance, PFOcTEA doped membranes present relatively better thermo-mechanical properties than TFTEA doped membranes below  $T_g$ . However, above  $T_g$ , the former collapses while the latter sustains a constant storage modulus of ~1MPa up to 180°C. PFBuTEA doped membranes show intermediate behaviour probably due to the intermediate perfluorinated chain of the anion in PFBuTEA between TFTEA and PFOcTEA.

Indeed, the ionic conductivities and water uptakes for TFTEA doped membranes is higher than those based on PFBuTEA and PFOcTEA based membranes for same mass percent content and/or  $\lambda$  value due to the higher ionic function concentration in TFTEA doped membranes as well as the more hydrophilic nature of TFTEA. But, interestingly, *PFBuTEA doped membranes show comparable*

*conductivities to TFTEA doped membranes for similar  $\lambda$  value (at high PCIL content) even if TFTEA is way higher conductive than PFBuTEA in pure form. Moreover, PFOcTEA molecules also present better ionic conductivity when present within the membrane in comparison to its pure form.*

The same trend goes for the water uptakes i.e. *water uptakes of both, PFOcTEA/PFBuTEA doped membranes, are higher than that predicted by the additive law.* This means that PFOcTEA/PFBuTEA gain higher amount of water when incorporated into the membrane in comparison to their pure form. While in the case of *TFTEA doped membranes, the water sorption capacity is limited by the hindering effect of Nafion-TEA matrix.*

This *improvement in the ionic conductivities and water uptakes of PFOcTEA/PFBuTEA based membranes* seems to be due to the *specific organization of PFOcTEA/PFBuTEA molecules in the Nafion-TEA matrix* which enhance their ionic conduction as well as their hydrophilicity in the membranes.

Unfortunately, it has been observed that the Nafion-TEA membranes (doped/un-doped) have been found more susceptible to the attack of peroxy radicals in comparison to Nafion<sup>®</sup> membrane (acidic form). Moreover, the thermo-mechanical properties of Nafion<sup>®</sup> based PCIL doped membranes are not enough good for the application of High Temperature-PEMFCs.

Thus, in the next (and the *last part*) of this thesis work, the idea of replacing Nafion<sup>®</sup> with a modified aromatic polymer i.e. *Polysulfone in these PCIL based systems* has been explored. In this work, Polysulfone has been grafted with perfluoro alkyl sulfonic acid functions prior to combination with TFTEA.

From the synthesis point of view, it has been seen that the *bromination step involved in the process of modification leads to chemical degradation of Polysulfone* due to evolution of hydrogen bromide gas during the reaction. Various strategies such as *addition of acetic acid or potassium carbonate into the reaction mixture during bromination reaction* have been examined in order to prevent/minimize the phenomenon of chemical degradation. *Drastic improvement in the rate of the reaction by the addition of acetic acid* and an overall minimization of the degradation has been observed but could not be completely avoided. After all the steps, Polysulfone carrying perfluoro alkyl sulfonic acid functions was neutralized with triethylamine (denoted as PSPF-TEA) in similar fashion as done for Nafion-TEA prior to elaboration of doped membranes with TFTEA.

However, *PSPF-TEA did not present any nano-structuration in the presence of TFTEA in contrary to the presence of water molecules.* Moreover, the thermo-mechanical properties were found inferior

to that of Nafion-TEA based doped membranes. Their *ionic conductivities have been found superior to that of directly sulfonated Polysulfone based doped membranes inferior to that of Nafion-TEA based doped membranes for similar  $\lambda$  values and volume fractions of TFTEA*. However, comparable conductivities are observed at high contents of TFTEA in PSPF-TEA in comparison to that of optimum system based on TFTEA and Nafion-TEA up to the  $T_g$  value of the former. Moreover, the  $T_g$  value of PSPF-TEA based doped membranes are much lower in comparison to that of Nafion-TEA based ones. The reason behind such behavior must be the strong interaction of TFTEA with the ionic functions of PSPF-TEA which are randomly distributed in the polymer. Moreover, backbone chain of PSPF-TEA is less hydrophobic in comparison to that of Nafion-TEA. Both these factors result in *strong plasticizing effect of TFTEA on the PSPF-TEA matrix*.

### Perspectives

This work has opened gate for many *perspectives*. Firstly, it will be very interesting to study the morphology as well as the functional properties of Nafion-TEA based systems in the presence of controlled humid conditions and at different temperatures as well.

Considering the fact that Nafion<sup>®</sup> membranes neutralized with triethylamine show specific morphology at the interface, it will be intriguing to study the impact of other amines on the resulting organization of the ionic functions at the hydrophobic-hydrophilic interface.

Moreover, the morphology of the membranes could significantly depend on the solvent and annealing conditions utilized in the casting of PCIL doped membranes, hence, it will be interesting to play with the solvents as well as the experimental conditions employed for the casting of these membranes.

Concerning fuel cell tests, it is important to utilize electrodes (in the MEA assembly) which are adapted for high temperature functioning of PEMFCs. Thus, in future, the fuel cell performance of PCIL based membranes should be evaluated by using suitable electrode assembly system.

Concerning degradation phenomenon associated with Nafion-TEA membranes, it will be very interesting to further understand the degradation mechanism and impact of neutralization on the rate of membrane degradation. The possible ways of going further in understanding could be varying the chemical structures of amines or degree of neutralization of the membranes or experimental conditions (such as temperature, relative humidity) to evaluate the behavior of such amine neutralized membranes.

Also, since Polysulfone with randomly distributed ionic function side-chains exhibited strong plasticizing effect of the PCIL, it will be intriguing to replace randomly modified Polysulfones with

block copolymers of Polysulfones containing hydrophobic and hydrophilic blocks and combine them with different PCILs to explore their possibility as an alternative system for the future of HT-PEMFCs.

## 6. Experimental Part

---

In this chapter, detailed descriptions of various experimental as well as characterization procedures carried out during the course of thesis work are presented. The chapter has been divided into 2 parts described as follows:

- ❖ First section of this chapter will be focused on the synthesis of various PCILs. Moreover, the experimental methods employed for the modification and preparation of membranes based on Nafion® as well as modified Polysulfone with/without PCILs will be discussed in this section.
- ❖ In the second section, detailed description of procedures employed to characterize the membrane (with/without the PCILs) will be given.

### 6.1: Synthesis

#### *a. PCIL synthesis*

PCIL synthesis was carried out by reaction of the acid (Triflic acid(TF)/Perfluorobutane sulfonic acid(PFBS)/Pefluoro octane sulfonic acid(PFOS)) with distilled Triethylamine (TEA) with molar ratio TEA/Pure Acid=1.05 in deionized water at room temperature in an ice bath for 20-30 minutes. TEA utilized for PCIL preparation (as well as other purposes discussed in the succeeding sections) was received from *Sigma-Aldrich*. TF (from *Sigma-Aldrich*) and PFBS (from *Fluorochem*) were available in pure form while PFOS was available in the form of aqueous solution (PFOS: ~40% w/w in water from *Fluka*).

In the case of TF based PCIL, water was evaporated from the synthesized PCIL named as trifluoromethane sulfonate of Triethylammonium (TFTEA) using rotavap. After removal of water, activated charcoal and methanol were added to TFTEA and stirred for some time followed by filtration to remove impurities or unreacted products. Methanol was then evaporated followed by drying at 110°C under vacuum for 48 hours.

In the case of PFBS/PFOS based PCILs, the synthesized PCILs named as Triethylammonium Perfluorinated Butane Sulfonate (PFBuTEA) & Triethylammonium Perfluorinated Octane Sulfonate (PFOcTEA) were lyophilized in order to remove the water. Afterwards, these PCILs were dried at 110°C under vacuum for 48 hours.

All the PCILs synthesized namely TFTEA, PFBuTEA and PFOcTEA were stored in glove box under argon atmosphere after the drying treatment. The purity of the PCILs was confirmed by NMR technique and Differential Scanning Calorimetry (DSC) techniques and the water content of the PCILs was determined by using Karl-fischer measurements.

In order to do NMR measurements, a *Bruker AVANCE 300* NMR spectrometer at frequencies of 300.12 MHz for protons and 282.39 MHz for  $^{19}\text{F}$  measurements was used. An amount of ~10mg of each PCIL was taken in 0.5 ml of a deuterated solvent (DMSO and  $\text{D}_2\text{O}$ ) for the analysis.

The DSC measurements were carried out by using a *TA instruments' DSC 2920-Modulated DSC*. Around 5-7 mg of the samples were placed in DSC aluminum crucibles and sealed in argon atmosphere prior to the measurements. The measurements were carried out in the temperature range of  $-100^\circ\text{C}$  to  $150^\circ\text{C}$  with  $5^\circ\text{C}$  per minute of heating rate using modulation of  $0.6^\circ\text{C}$  every 60 seconds under argon atmosphere.

#### **b. Preparation of Nafion-TEA**

##### **Nafion-TEA-extruded**

Commercially available Nafion<sup>®</sup> 117 membrane (from *Acros*) was treated in refluxing 2M nitric acid aqueous solution for 1 hr (to reactivate all the ionic sites) followed by washing with deionized water up to neutral pH. This membrane is denoted as Nafion- $\text{H}^+$ . Then, membrane was kept in 1M TEA in water/ethanol solution (50:50 v/v) under mild stirring at room temperature overnight followed by washing the membrane to neutral pH. The treatment with TEA solution allows the neutralization of the reactivated acidic ionic sites. The neutralized Nafion<sup>®</sup> 117 membrane (referred as Nafion-TEA) was dried at  $80^\circ\text{C}$  under vacuum for 48 hrs and stored in glove box under argon atmosphere.

##### **Nafion-TEA-casting**

Commercially available Nafion<sup>®</sup> 117 membrane was cut into morsels and stirred in 1M Lithium Hydroxide aqueous solution overnight in order to exchange all the acidic sites with Lithium to prevent any degradation in the succeeding steps. Afterwards, the morsels were washed with deionized water to neutral pH. The washed morsels were then kept in a heat-resistant beaker with water/ethanol solution (50:50 v/v) and a bar magnet. This beaker was installed in a reactor, closed and heated to  $250^\circ\text{C}$ . The pressure of the system in the reactor increased to 25 bars. The system was left under such pressure and temperature conditions along with mild stirring for 7 hours. Finally, a solution of Nafion<sup>®</sup> was obtained. This solution was filtered using a PTFE filter (0.25  $\mu\text{m}$  pore size) and lyophilized afterwards. The powder of Nafion<sup>®</sup> (in Lithium form) obtained from lyophilization was stirred in 1M nitric acid

aqueous solution for 12 hours to exchange all the lithium sulfonate sites into sulfonic acid sites. Then, the powder was filtered and washed to neutral pH using a sintered glass filter. TEA was added in an aqueous mixture of Nafion-H<sup>+</sup> powder (with molar ratio TEA/sulfonic acid site of Nafion<sup>®</sup> =3) in order to neutralize the acidic sites. Addition of TEA led to formation of a viscous suspension/solution of Nafion-TEA in water which was then lyophilized to obtain powder of Nafion-TEA. The powder of Nafion-TEA was then dried at 80°C under vacuum for 48 hours and then stored in glove box in argon atmosphere.

To prepare Nafion-TEA-casting membrane, a 10% (w/v) solution of Nafion-TEA powder in Dimethylacetamide was prepared. This solution was filtered using a PTFE filter (0.25 µm pore size) and subsequently degasified using a pump. The degasified solution was pour into a petri-dish and heated at 60°C for 48 hours to evaporate the solvent followed by an annealing treatment of one hour at 150°C. The resulting membrane was finally dried at 80°C under vacuum for 48 hours to evaporate any trances of solvent left in the membrane and stored in glove box for further experiments.

### **c. Preparation of Polysulfone (Udel) carrying pendant perfluoro alkyl triethylammonium sulfonate chains (PSPF-TEA)**

The synthesis of PSPF-TEA was done in four steps described as follows:

#### **Synthesis of the pendant perfluoro alkyl sulfonic acid functions**

Firstly, the pendant side chain function was synthesized. This side chain function was synthesized by hydrolyzing the sulfonyl fluoride group of 1,1,2,2-Tetrafluoro-2-(1,1,2,2-tetrafluoro-2-iodoethoxy)ethanesulfonyl fluoride (PSA-F; from *Apollo Scientific*) into sulfonic acid function by using lithium hydroxide in THF. In this experiment, PSA-F (1 mol) and mono-hydrate lithium hydroxide (2.2 mol) were stirred in THF (30-40 ml) in a round bottom flask at room temperature overnight. Then, the mixture was filtered by using filter paper in order to eliminate remaining lithium hydroxide as well as lithium fluoride which was formed during the reaction. The filtrate was then concentrated by evaporating the solvent using Rotavap. Afterwards, the product was dissolved in acetonitrile in order to remove remaining traces of lithium fluoride from the product since lithium fluoride is insoluble in acetonitrile. The solution was then filtered using filter paper followed by solvent evaporation. Finally, NMR of the final product was done in deuterated-DMSO to evaluate its purity.

### **Bromination of Polysulfone(Udel form) at ortho-to-ether position**

The second step involved bromination of Polysulfone (Udel form). The apparatus (comprised of a three-necked round bottom flask and a glass condenser) was very well dried firstly by heating and secondly by using high argon flow in order to eliminate traces of water molecules present in the system before starting the experiment. This experiment was done in dichloromethane as solvent which was refluxed for 4 hours in the presence of calcium hydride in a distillation column to eliminate the water molecules present in it and recovered prior to the bromination reaction. In this experiment, bromine (1.5-3 mol depending on the bromination degree required) was added drop-wise to a stirred solution of Polysulfone (1 mol) in dichloromethane (100 ml) at 45°C under refluxing conditions. The reaction was carried out under argon atmosphere and the hydrogen bromide produced during the reaction was absorbed into 2M solution of sodium hydroxide by a continuous flow of Argon through the apparatus. The duration of the reaction was around 20 hours (for all the degrees of bromination). Afterwards, the brominated polymer was recovered by pouring the dichloromethane solution into methanol (200-300 ml). The recovered polymer (Br-PS) was dried at 60°C under vacuum for 48 hours and stored in glove box under Argon atmosphere afterwards.

In order to improve the rate of the reaction, the above reaction was carried out in the presence of Acetic acid. The conditions and the set up were kept same as mentioned in the above experiment. The amount of acetic acid was kept as 10% of the total volume of the solvent taken for the reaction.

Also, the same reaction was carried out in the presence of potassium carbonate under same experimental conditions and set up. Potassium carbonate was dried at 175°C under vacuum for 24 hours and stored in argon atmosphere before use. The amount of potassium carbonate added was equimolar to the amount of bromine added during the reaction.

The products from all the reactions were analyzed by using NMR technique. The measurements were done in deuterated-chloroform.

The molecular weights of the brominated polymers with different bromination degrees were determined by using SEC-MALS technique (DAWN EOS<sup>®</sup> from Wyatt Technology). A 1% (w/v) solution of the polymer in DMF+0.1M NaNO<sub>3</sub> was utilized. The solution of the polymer was filtered by using PTFE filter (0.45 µm pore size) before measurements. The molecular weight was calculated by imposing a known value of differential of refractive index in function of concentration of the solution (dn/dc: variation in the refractive index of a solution for a given variation in the concentration of the solution; expressed as ml/g). The molecular weight determination was carried out by using coupled SHODEX GPC-KD-806M + GPC-KD-804 columns at 40°C



### *Grafting the side-chain function on the backbone of brominated-Polysulfone*

The bromination process of Polysulfone was followed by grafting the synthesized side-chain function (from I<sup>st</sup> step) PSA-Li on the backbone chain of the polymer by using Ullmann reaction at 120°C in distilled dimethylsulfoxide (DMSO). Br-PS with different bromination degrees were utilized for this reaction in order to have Polysulfone with different degrees of substituted side-chain function. DMSO was vacuum distilled at 100°C and stored over thermi-molecular beads (to absorb traces of water) under argon atmosphere. The apparatus was very well dried firstly by heating and secondly by using high argon flow in order to eliminate traces of water molecules present in the system before starting the experiment.

In this experiment, copper powder with mesh size: 150 (from *Alfa aesar*) and molar quantity of 8 moles was added into a solution of brominated Polysulfone (1 mol) in DMSO (60 ml) and the reaction mixture was stirred for 2 hours at 120°C. Afterwards, a solution of PSA-Li (molar quantity dependent on the degree of bromination of Polysulfone ranging between 1-2.4 mol) in DMSO (10 ml) was added drop-wise into the reaction mixture and the system was stirred for 6 hours at 120°C. Then, the solution was filtered (by using filter paper first followed by PTFE filter with pore size of 0.25µm) to remove copper particles. The filtrate was precipitated in a 5N HCl solution. The precipitated polymer was washed first by 5N HCl solution several times and then by water up to neutral pH. Then, the polymer was dried in an oven at 80°C for several hours followed by drying at 80°C under vacuum for 48 hours. The final product (PSPF-H<sup>+</sup>) was analyzed by NMR technique and the measurements were done in deuterated-DMSO.

### *Neutralization of PSPF-H<sup>+</sup> with triethylamine*

Finally, the sulfonic acid sites of PSPF-H<sup>+</sup> were neutralized with triethylamine by stirring PSPF-H<sup>+</sup> (1 mol) and triethylamine (1.5 M) together in deionized water (50 ml). The system became like a suspension after stirring for 30 minutes. It was then lyophilized and finally powder of PSPF-TEA was obtained. The powder was dried at 80°C under vacuum for 48 hours and stored in glove box under argon atmosphere.

The molecular weights of the grafted polymers with different substitution degrees were determined in similar manner as for brominated ones by using SEC-MALS.

*All the NMR measurements mentioned in this section were done by using a Bruker AVANCE 300 NMR spectrometer at frequencies of 300.12 MHz for protons and 282.39 MHz for <sup>19</sup>F*

**measurements.** An amount of ~10mg of each sample was taken in 0.5 ml of deuterated solvent ( $\text{CDCl}_3$ , DMSO and  $\text{D}_2\text{O}$ ) for the analysis.

#### *d. PCIL-based-Membrane elaboration*

##### Swelling method

Nafion-TEA membranes (prepared from extruded Nafion<sup>®</sup> 117 membranes) were swollen with different concentrations of PCILs (by weight) at 80-85°C by dipping Nafion-TEA membranes in PCILs for different periods of time in argon atmosphere. The PCIL weight fraction (with respect to the total weight) within the PCIL-based membranes was determined gravimetrically.

In the case of TFTEA doped membranes, the rate of uptake of TFTEA by Nafion-TEA is fast in the first hour and then reaches a maximum percentage of uptake (24 wt%) after 20 hours. The membrane containing more than 24 wt% TFTEA was prepared by swelling at 95°C.

In the case of PFOcTEA doped membranes, the uptake of PFOcTEA by Nafion-TEA increases up to ~40 wt% in first 3 hours. The content of PFOcTEA in Nafion-TEA reached to a flagrant amount of 65 wt% in 24 hours.

The membranes obtained with different concentrations were always stored in glove box and taken for different types of characterization later.

##### Casting method

Nafion-TEA powder prepared from commercially available Nafion<sup>®</sup> 117 membrane (protocol thoroughly discussed in the case of Nafion-TEA-casting) was utilized to cast the membranes in combination with the PCILs.

In order to cast Nafion-TEA+x wt% PCIL membranes, different w/w proportions of Nafion-TEA powder and the PCILs were collected in recipients in the glove box and taken outside to the ambient conditions. Then, a 10% (w/v) solution was prepared by dissolving these proportionate mixtures of Nafion-TEA powder and the PCILs in dimethylacetamide. This solution was filtered using a PTFE filter (0.25  $\mu\text{m}$  pore size) and subsequently degasified using a pump. The degasified solution was pour into a petri dish and heated at 60°C for 48 hours to evaporate the solvent followed by an annealing treatment of one hour at 150°C. The resulting PCIL doped Nafion-TEA membrane was finally dried at 80°C under vacuum for 48 hours to evaporate any trances of solvent left in the membrane and stored in glove box for further experimental analysis.

Membranes based on PSPF-H<sup>+</sup> and PSPF-TEA with/without TFTEA were elaborated and dried in the same manner as described for TFTEA doped Nafion-TEA membranes.

## **6.2: Membrane Characterization**

### **a. Study of leaching phenomenon**

This study was particularly carried out on swelling based TFTEA doped Nafion-TEA membrane. In this study, Nafion-TEA membranes were swollen with TFTEA under argon atmosphere at 80°C to the maximum concentration (around 24%). Afterwards, a sample was kept in argon atmosphere at 20°C while another one was kept in ambient atmosphere at the same temperature. The membranes were regularly weighed after being blotted (with paper and a little bit of heating in order to melt the solidified TFTEA on membrane surface). The weight measurements were carried out until stable weights were achieved. TFTEA leaching was observed only for the membranes containing more than 21wt%. Thus, in the case of swelling based TFTEA doped membranes, the characterization was carried out principally with membranes presenting a maximum doping level of 20wt%. However, some experiments have been performed with higher doping levels but only with freshly prepared samples.

### **b. Density measurements**

The density of the membranes was measured by using *METTLER TOLEDO*'s density kits (using the buoyancy technique) at room temperature (21°C) with toluene as the solvent (in fact, a very poor has to be chosen for this measurement).

### **c. Wide Angle X-ray Scattering (WAXS)**

The WAXS measurements were carried out on the *Philips X'pert* diffractometer in transmission geometry (Bragg-Brentano) using Copper X-ray tube ( $\lambda_{\text{Cu}}=1.5406 \text{ \AA}$ ). The membranes were cut in the form of a rectangular sample in the glove box and stored in closed recipients. The recipients were opened and open cells were prepared prior to WAXS measurements. Afterwards, the measurements were carried out in ambient conditions. The scan step was 0.04° (in 2 $\theta$ ) in the range of 4.02° to 89.94°. The diffractometer was equipped with a 800 channel multi-detector with a step of 0.02°. For the incident beam optic, a fixed aperture of the divergence slit 1/2° was chosen and for the diffracted beam an aperture of 1° was chosen.

#### **d. Small Angle Neutron Scattering (SANS)**

SANS measurements for all the membranes were carried out on the *PAXE* spectrometer (Laboratoire CEA-CNRS Léon Brillouin, Orphée reactor, Saclay, France). 12 mm diameter disc-like samples of all the undoped/PCIL-doped membranes were cut in a glove box and kept in sealed recipients (to avoid any contact with humid air). The quartz neutron cells were prepared prior to SANS measurements, closed quickly and maintained at room temperature. In some cases, cells were prepared directly in the glove box, sealed with para-film and taken out for the measurements.

Concerning SANS measurement on the swelling based Nafion-TEA membrane with 20wt% TFTEA in the presence of water, the disc of the membrane was cut in the glove box and afterwards taken out in the ambient atmosphere to add water (10% of total weight of the membrane) on its the surface 24 hours prior to SANS measurement and the cell was closed immediately.

Regarding SANS measurements of water swollen PSPF-H<sup>+</sup>, disc of dried polymer was cut in the glove box and stored in a closed recipient. Afterwards, the membrane disc was swollen with water in the ambient conditions and quartz cells were prepared prior to the measurements.

The neutron scattering intensity was measured as a function of the scattering vector  $q$  defined as:  $q=(4\pi/\lambda)\sin(\theta/2)$  where  $\lambda$  is the wavelength of the incident neutron beam and  $\theta$  is the total scattering angle. The detector was tilted with respect to the incident beam direction. Two configurations were used to cover the angular range from  $8.5 \cdot 10^{-3}$  to  $0.6 \text{ \AA}^{-1}$  ( $\lambda=7.5\text{\AA}$ ,  $D=5\text{m}$  and  $\lambda=5\text{\AA}$ ,  $D=1.3\text{m}$ , where  $D$  is the sample-to-detector distance). The SANS spectra were corrected for detector efficiency and background subtraction. Absolute intensities were obtained by measuring a water-sample for calibration (1 mm thick in Helma cell).

#### **e. Differential Scanning Calorimetry (DSC)**

The Modulated-DSC measurements of all the membranes were done using a TA instruments' DSC 2920-Modulated DSC. The measurements were carried out in the temperature range of  $-50^{\circ}\text{C}$  to  $150^{\circ}\text{C}$  with  $5^{\circ}\text{C}$  per minute of heating rate using modulation of  $0.6^{\circ}\text{C}$  every 60 seconds under argon atmosphere.

#### **f. Dynamic Mechanical Analysis (DMA)**

The thermo-mechanical properties of the different membranes were studied using a *TA Instruments' DMA2980*. The measurements were carried out in the temperature range of -100°C to 150°C with preloaded force of 0.01N using an amplitude of 15-20µm (depending on the membrane), 200% Force track and a frequency of 1Hz. The storage and loss modulus of the composite membranes were determined in the given temperature range.

#### **g. Conductivity in anhydrous condition**

The conductivity measurements of the membranes were carried out with Electrochemical Impedance Spectroscopy using an *HP 4192A* Impedance Analyzer in the frequency range of 5-13 MHz. The membranes were placed between two stainless steel electrodes in a Swagelok cell (*shown in ANNEXE 1*) having Teflon joints and spacers and the cells were prepared and closed in the glove box under Argon atmosphere to avoid any contact with humid air. The conductivity measurements were carried out in the temperature range of 20-150°C with temperature equilibrated for 2 hours prior to conductivity measurements by using the program SIMPATI in a *VOTSCH VTM 4004* oven.

The water content of anhydrous Nafion-H<sup>+</sup> and Nafion-TEA was determined by using NMR technique before the conductivity measurements on these membranes. In order to do this, cells containing around 1-1.5gm of membrane morsels were prepared in the glove box, closed well and taken for NMR measurements afterwards.

#### **h. Conductivity in humid conditions**

The conductivity measurements were carried out for swelling based TFTEA doped Nafion-TEA membranes at different relative humidity values (0.1-0.9) as well as temperatures (25°C, 40°C and 80°C). The conductivity measurements were done with Electrochemical Impedance Spectroscopy using a *MATERIAL MATES' 7260* Impedance Analyzer in the frequency range of 5-13 MHz. The conductivity measurements on the membranes were carried out in a *VOTSCH VC 4018* oven equipped with the ventilation system to control the relative humidity as well as temperature through a program (*SIMPATI*) during the measurements. The cells were prepared in the ambient conditions and doped membranes were adjusted between silver electrodes of the cell and then the cells were connected to the device. At each temperature value, membranes underwent a cycle of increasing vapor pressure from 0.1 to 0.9 (0.1 to 0.8 in the case of measurements at 80°C). Between each increase in the vapor pressure, there was a gap of 12 hours and conductivities were measured every hour to determine the equilibrium conductivity value.

#### **i. Gas-permeation Analysis**

Permeation measurements for all the membranes were performed at 20°C for H<sub>2</sub> and O<sub>2</sub> gases. The gas purity was higher than 99%. After a preliminary high-vacuum desorption step, the membrane (effective area 3 cm<sup>2</sup>) was submitted to an upstream gas pressure fixed at 3 bars. The pressure variations in the downstream compartment were measured as a function of time with a *Datametrics* pressure sensor. The permeability coefficients expressed in barrer units (1 barrer = 10<sup>-10</sup> cm<sup>3</sup><sub>STP</sub>.cm.cm<sup>-2</sup>.s<sup>-1</sup>.cm<sub>Hg</sub><sup>-1</sup>) were calculated from the slope of the steady-state line. The precision on the permeability value was estimated to be better than 5%.

#### **j. Water Sorption Analysis**

Dynamic vapor sorption analyzer, *DVS Advantage* (Surface Measurement Systems Ltd., London, UK) was used to determine the water sorption isotherms of the films. The vapor partial pressure was controlled by mixing dry and saturated nitrogen, using electronic mass flow controllers. The experiments were carried out at 25°C and the initial weight of the samples was approximately 50 mg. The samples were pre-dried in the DVS Advantage by exposure to dry nitrogen until the dry weight of the samples was obtained. A partial pressure of water was established within the apparatus and the water uptake was followed as a function of time. The equilibrium was considered to be reached when changes in mass with time (dm/dt) were lower than 0.0002 for 5 consecutive minutes. Then, vapor pressure was increased in suitable activity up to 0.9 by step of 0.1. The cycle was ended by decreasing the vapor pressure in steps to obtain, also, desorption isotherms. The sorption rate was estimated at each water activity by the half sorption time  $t_{1/2}$  normalised to the film thickness.

#### **k. Fuel cell tests**

Casting based TFTEA doped Nafion-TEA membranes (TFTEA doping level~20wt%) were utilized to carry out fuel cell tests. The Membrane Electrode Assembly (MEA) based on this doped membrane was prepared by using the protocol of *Paxitech*<sup>®</sup> Company. It involved pressing the doped membrane between the active layers (composition of active layer is confidential) under pressure of 30bar at 140°C for five minutes. The fuel cell performance was evaluated at 100°C using 20%, 50% and 100% humidified gases and 1 atm relative pressure.

In order to evaluate the performance of this membrane, the MEA was mounted into the cell and equilibrated at 100°C for some time to acquire the Open Circuit Voltage (OCV) value. In the measurements with 20% and 50% humidified gases, OCV values could not be measured. While in the

measurements with 100% humidified gases, an OCV value of approximately 0.95 V was achieved. Afterwards, it was further stabilized at 0.6 V for several hours using 100% humidified gases to acquire a constant value of drawn electric current. The drawn electric current increased slowly and it took 12 hours to reach a constant value. Then, the MEA was subjected to a round cycle of voltage in the range 0.9-0.3V and drawn electric current was registered. The duration of the each cycle of the applied voltage was 3 hours. This cycle was repeated several times.

### **1. Degradation study**

The chemical stability of TFTEA against different concentrations of hydrogen peroxide at 110°C has been evaluated by using a *Varian Unity* NMR spectrometer at frequencies of 399.96 MHz for protons and 376.30 MHz for  $^{19}\text{F}$  measurements was used NMR spectroscopy ( $^1\text{H}$ ;  $^{19}\text{F}$ ).

All the solutions of hydrogen peroxide utilized in this study were prepared from 30% w/w (9.79 M) aqueous solution of hydrogen peroxide (which is commercially available from the *OM Group*).

In this study, 1M deuterated-aqueous solutions of TFTEA were prepared and equal quantities (3ml) were put in a set of 4 small glass recipients. These recipients were kept in an oven at 110°C during the course of the study. Equal quantities (i.e. 10 $\mu\text{l}$ ) of 0.25M deuterated-aqueous solution of hydrogen peroxide were injected into these 4 recipients the first day. The second day, 10  $\mu\text{l}$  content of hydrogen peroxide was injected into recipient number 2, 3 and 4 while recipient 1 was injected with 10  $\mu\text{l}$  of deuterated water in order keep the concentration of all the solution equal. The third day, 10  $\mu\text{l}$  content of hydrogen peroxide was injected into recipient number 3 and 4 while recipient 1 and 2 were injected with 10  $\mu\text{l}$  of deuterated water content. The last day, 10  $\mu\text{l}$  content of hydrogen peroxide was injected into recipient number 4 while recipient 1, 2 and 3 were injected with 10  $\mu\text{l}$  of deuterated water. Thus, the recipient number 1 contained minimum amount of hydrogen peroxide while recipient number 4 contained maximum amount of hydrogen peroxide. Another recipient with TFTEA solution (3 ml) containing only deuterated water (and no hydrogen peroxide solution) was also kept in the same condition to be utilized as reference and its concentration was changed every day by addition of 10  $\mu\text{l}$  of deuterated water content till the last day of the experiment. The recipients were closed very well in order to avoid evaporation of any of the degradation products from the system. All the recipients were removed from the oven after 4 days and taken for NMR spectroscopic measurements.

Furthermore, in order to verify if the concentration of TFTEA remains equal or not before and after exposure to hydrogen peroxide, equal quantities of solutions of TFTEA (0.3 ml) before and after the

study were analyzed in the presence of a known amount of internal reference i.e. trifluoro ethanol using NMR technique.

The evolution of chemical stability of the membranes in the presence of peroxy radicals was studied by using a *NICOLET MAGNA-IR 760* spectrometer (ATR-FTIR and FTIR-Transmission mode).

In the first study, membranes based on Nafion-TEA and Nafion-TEA doped with 14wt% TFTEA (both based on commercial Nafion<sup>®</sup> 117 membrane) were taken and cut into small films. These films were then hung over a bath of hydrogen peroxide solution (10% w/w) using a PTFE stand and glass capillaries in a closed glass dessicator heated at 80°C in an oven. Afterwards, these films were removed from the dessicator at regular intervals in the time span of 40 days. ATR-FTIR technique was utilized to follow the degradation phenomena of these membranes. All the samples were dried at 80°C under 30mbar for 48 hours prior to ATR-FTIR measurements. ATR-FTIR spectra of both the membranes (after drying under the same conditions mentioned above) were also recorded before starting the degradation study in order to keep them as the reference spectra.

In order to check the stability of membranes under humid conditions, without the presence of hydrogen peroxide, another study was carried out on the same type of membranes i.e. Nafion-TEA and Nafion-TEA doped with 14wt% TFTEA (both based on commercial Nafion<sup>®</sup> 117 membrane). In this study, films of both the types of samples were hung over a bath in a closed glass dessicator heated at 80°C in similar fashion as in the previous study and were removed from the dessicator at regular intervals in the time span of one month. The only difference was that the bath was filled with pure water instead of hydrogen peroxide solution. Similar drying treatment was carried out on all the samples prior to ATR-FTIR measurements as mentioned in the previous study.

Furthermore, in order to study the membranes with by using FTIR in transmission mode, very thin membranes (Nafion-TEA and Nafion-TEA+20wt% TFTEA) with thickness in the range of 20-25 µm were prepared by casting method. Special sample holders with a window were prepared from PTFE (*shown in ANNEXE 2*) for this study in order to clamp the membranes and directly record their FTIR spectra (transmission mode) before and after exposure to hydrogen peroxide solution so as to avoid any problems in their handling during the study. These PTFE sample holders were hung using a PTFE stand kept over a bath of hydrogen peroxide solution in the dessicator. In this study, a 20% w/w hydrogen peroxide solution was utilized to accelerate the degradation phenomena. In addition, the solution was renewed in the system with a speed of 10µl/s by using a pumping system. Moreover, the dessicator was heated at 80°C by circulation of hot water in the outer surface of the two parts of the dessicator to acquire homogeneous temperature in the system (*set up shown in ANNEXE 3*). This study was carried out over a period of 10 days and samples were removed at regular time intervals for FTIR



measurements (in transmission mode). The membranes were dried at 80°C under pressure of 30 mbars for 48 hours prior to the measurements of FTIR spectrum in transmission mode (both before and after exposure hydrogen peroxide solution).

## Résumé (in French)

---

### *Contexte :*

Les membranes échangeuses de protons (PEM) ont été largement étudiées pour l'application pile à combustible (PEMFC). Actuellement, les matériaux les plus connus pour la technologie PEMFC sont à base des ionomères perfluorés, dont la plupart appartiennent à la famille Nafion<sup>®</sup>. Les Ionomères sont utilisés pour la fabrication des membranes mais également de la couche active des électrodes. Ce type de matériaux impose une température de fonctionnement de la PEMFC inférieure à 80°C, à des températures plus élevées les performances du système chutent brutalement dû à la perte de conductivité ionique de l'ionomère. Le rendement électrique d'une PEMFC ne dépasse pas 50%. La gestion thermique, notamment pour les voitures, représente un vrai problème. Néanmoins, la plupart des constructeurs d'automobiles conditionnent la réussite des piles à combustible à la conception de piles très performantes à des températures supérieures à 100°C.

A cet égard, quelques approches ont été explorées par la communauté scientifique. Ces approches comprennent des électrolytes obtenus par l'ajout dans une matrice polymères d'une molécule conductrice de protons de type acide phosphorique ou des solvants à haut point d'ébullition tels que les imidazoles ou les liquides ioniques à conduction protonique (PCIL). Les membranes à base de PCILs sont très prometteuses, en raison de leur forte conductivité ionique et stabilité à haute température dans des conditions anhydres. Cependant, la performance de ce système dépend fortement de la structure chimique des polymères et des PCILs, de la concentration de PCIL dans la membrane et en particulier des interactions entre le PCIL et le polymère. Afin d'avoir un système PEMFC performant, une forte conductivité, une bonne stabilité thermique, chimique et électrochimique à haute température, une excellente tenue thermomécanique, une faible perméabilité aux gaz, une prise d'eau limitée sont requises pour la membrane polymère. Pour répondre à toutes ces exigences, une membrane nano-structurée, possédant des domaines hydrophobes et des domaines hydrophiles (ioniques) co-continus, est exigée. Dans ces membranes les nano-domaines hydrophobes sont principalement responsables des propriétés mécaniques alors que les nano-domaines hydrophiles assurent principalement la conductivité ionique.

Dans ce travail, une étude approfondie sur l'évolution de la morphologie et les propriétés fonctionnelles de systèmes électrolytes polymères, en fonction de la concentration et de la structure de PCIL, a été effectuée.

Les membranes ont été synthétisées par gonflement ou coulée-évaporation, l'impact de la méthode d'élaboration sur les propriétés de ces membranes dopées a été étudié.

Egalement, des études préliminaires sur les performances de ces membranes dans la pile à combustible et sur les phénomènes de dégradation en présence de peroxyde d'hydrogène ont été effectuées.

La matrice polymère, principalement étudiée, dans cette thèse est le Nafion<sup>®</sup>. Cependant, afin d'améliorer la stabilité thermomécanique, des matrices polysulfones fonctionnels ont été synthétisées et explorées.

### *Etat de l'art sur les liquides ionique à conduction protonique et ses membranes.*

Les membranes Polymère fonctionnel + liquide(s) ionique(s) conducteurs de protons (PCIL) sont considérées comme une approche intéressante pour l'application PEMFC fonctionnant à haute température grâce aux propriétés des PCILs telles que : la conductivité ionique élevée, la faible pression de vapeur, une large variété structurale, une haute stabilité thermique et électrochimique pour en énumérer quelques-unes [148149].

Les liquides ioniques sont des sels fondus possédant un point de fusion inférieur à 100°C. De nombreux liquides ioniques sont à l'état liquide à la température ambiante et certains d'entre eux cristallisent à des températures très basses. De toute évidence, les liquides ioniques qui sont liquides à température ambiante offrent plus d'avantages par rapport à ceux qui ont des points de fusion relativement élevés. Les liquides ioniques sont généralement composés d'un cation organique tel que l'alkylammonium, l'alkylphosphonium, l'alkylsulfonium, le 1,3-dialkylimidzolium, l'alkylpyridinium, l'alkyltriazolium etc. Les anions utilisés pour préparer les liquides ioniques peuvent être poly-nucleus comme  $\text{Al}_2\text{Cl}_7^-$ ,  $\text{Fe}_2\text{Cl}_7^-$ ,  $\text{CuCl}_3^-$  etc. ou mono-nucleus comme  $\text{BF}_4^-$ ,  $\text{PF}_6^-$ ,  $\text{CF}_3\text{SO}_3^-$ ,  $\text{CH}_3\text{SO}_3^-$  ( $\text{CF}_3\text{SO}_2$ ) $_2\text{N}^-$ ,  $\text{CF}_3\text{CO}_2^-$  etc.

Les liquides ioniques sont connus pour former des agrégats de grande taille par interactions dipôle-dipôle ou par des liaisons d'hydrogène. Par conséquent, l'organisation structurale dépend principalement de la nature des cations et des anions présents dans le PCIL. Par exemple, si l'anion est à base nitrate les liquides ioniques montrent la formation d'agrégats de grandes tailles contrairement au PCIL à base de l'anion lactate ou formiate. Les PCIL à base de monoalkylammonium ont tendance à former des agrégats de grande taille quelle que soit la longueur de la chaîne alkyle, tandis que ceux à base de di-et tri-alkylammonium présentent une tendance limitée à la formation d'agrégats stables en raison de l'encombrement stérique et du plus faible nombre d'atomes hydrogène capables de former

des liaisons hydrogène. La formation des agrégats nuit généralement à la conductivité {150}. Les liquides ioniques s'organisent sous forme de micelles ou de lamelles {151}.

Pour une application PEMFC, le liquide ionique doit être capable de conduire les protons. Le tableau 1 présente les différentes caractéristiques de PCILs. Peu de groupes de recherche ont mené des études détaillées sur l'impact de la structure de cation et anion sur les propriétés de PCIL afin d'évaluer leur utilité pour l'application PEMFC.

Acide	Amine	T <sub>g</sub> (°C)	T <sub>f</sub> (°C)	T <sub>d</sub> (°C)	σ *
<b>Bis(trifluoromethylsulfonyl)imide (TFSI)</b>	Pyrollidine	-	35	373	3.96
	Pyridine	-	60.3	314	3.04
	Pyrazine	-	53.6	229	3.38
	Butylamine	-	16.2	352	1.04
	Triéthylamine	-	3.5	350	3.23
	Bis(méthyléthoxy)amine	-73	30	-	2.1**
	Diméthyléthylamine	-42	66	377	4.6***
	Diéthylméthylamine	-67	24	375	4.1***
	Imidazole	-	73	379	2.7
	Piperazine	-	172.7	358	-
	Benzimidazole	-	101.9	368	1.3
	1,2,4-Triazole	-	22.8	287	2.2
<b>Triflic Acid (TF)</b>	Ethylamine	-	173	400	a
	Diéthylamine	-	127	390	-
	Triéthylamine	-58	36	380	3.1
	Dipropylamine	-	136	390	a
	Tripropylamine	-	160	380	a
	Dibutylamine	-	140	390	a
	Tributylamine	-	128	353	-
	Trihexylamine	-83	-1	361	0.2***
	Diméthylethylamine	-117	41.6	360	5.6***
	Diéthylméthylamine	-	-13	360	4.3***
	Bis(méthylethoxy)amine	-	55	300	2.7
	Pyrollidine	-	157	395	a
	Methylpyrollidine	-	103	382	3
	Pyridine	-	145	390	a
	Methylpyridine	-	101	380	2.8

\* Conductivité à 130°C ( $10^{-2}$  S/cm); \*\* Conductivité à 100°C ( $10^{-2}$  S/cm); \*\*\* Conductivité à 120°C ( $10^{-2}$  S/cm)

<sup>a</sup> Conductivité inférieure à 0.1 ( $10^{-2}$  S/cm)

Table 1: Caractéristiques des PCILs en fonction de la nature du cation et de l'anion<sup>(152-154)</sup>

La température de fusion  $T_f$  de tous les PCILs varie entre -15 et 175°C en fonction de l'anion et du cation. Les  $T_f$  sont généralement plus faibles pour les PCIL provenant de l'anion TFSI. Les PCILs à base d'amines tertiaires (exemple : Triéthylamine; TEA) montrent les  $T_f$  les plus faibles alors que les PCILs à base d'amines secondaires cycliques présentent les points de fusion les plus élevés. La température de dégradation de tous les PCILs varie dans la gamme 300-400°C en fonction de l'anion et du cation, mais elle augmente, généralement, avec l'augmentation de la différence de pKa entre l'acide et l'amine.

Les valeurs de conductivité ionique de PCILs sont dans la plage de 0,1 à  $6 \cdot 10^{-2}$  S/cm. En règle générale, la conductivité ionique de PCIL à base de TFSI est supérieure à celle obtenue avec TF. Toutefois, leurs conductivités sont similaires au-dessus de leurs points de fusion. Si on compare l'effet de différentes amines, les PCILs à base de TEA montrent des conductivités supérieures dans un large intervalle de température par rapport aux PCILs à base d'autres amines. Iojoiu et al. ont également mené des études sur l'étude du mécanisme de conduction des différentes PCILs à base d'alkyl ammonium en utilisant la RMN sous gradient de champ pulsé {154}. Il a été observé que les coefficients de diffusion de protons acides et de radical alkyl d'ammonium sont similaires et plus grands que celui de l'anion indiquant que le proton est transporté par l'amine sous forme d'ammonium via le mécanisme véhiculaire.

On recense dans la littérature quelques études sur la synthèse de membranes à base de mélanges : PCILs+ matrice polymère (telle que le Nafion<sup>®</sup>, les polymères aromatiques sulfonés, etc.) et leurs performances pour l'application HT-PEMFC ont été évaluées. La méthode la plus couramment employée pour l'incorporation d'un PCIL dans la matrice polymère est la "méthode de gonflement" qui consiste à immerger la membrane dans le PCIL à des températures élevées.

Doyle et al. a exploré premièrement la possibilité d'utilisation de ces matériaux pour l'application HT-PEMFC {156}. Ils ont étudié le système à base du Nafion<sup>®</sup> (en forme  $H^+$  et  $Li^+$ ) + 1-butyle, 3-méthyle imidazolium triflate (BMITf) ou 1-butyle, 3-méthyle imidazolium tétrafluoroborate (BMIBF<sub>4</sub>). Ils ont rapporté des conductivités de l'ordre de 0,06 S / cm à 0,11 S / cm (de 150 à 180 ° C) et ont affirmé qu'il n'y avait pas d'échange de cations entre les sites acides du Nafion<sup>®</sup> et les liquides ioniques.

Benette et al. ont principalement axé leurs recherches sur la compréhension de l'effet des liquides ioniques sur la morphologie du Nafion® 117 par diffraction des rayons X (SAXS) et ont utilisé le modèle proposé par Gierke et al. pour discuter leurs résultats{159}. Ils ont préparé des membranes à base de PCILs tels que le 1-éthyl-3-méthylimidazolium trifluorométhanesulfonate (EMI-Tf) et le 1-éthyl-3-méthylimidazolium bis (trifluorométhanesulfonyl) imide (EMI-Im) et de Nafion® (sous forme protonée) par la méthode de gonflement. Ils ont indiqué que l'incorporation de EMI-Im, qui est de nature hydrophobe, détruit la structuration de la membrane Nafion® alors que l'addition d'EMI-Tf conduit à une augmentation de la taille des clusters ioniques.

Schmidt et al. ont concentré leurs travaux sur l'étude de l'effet des liquides ioniques sur les propriétés mécaniques et thermiques du Nafion® 117 (sous forme protonée) {161}. Ils ont rapporté un effet plastifiant des liquides ioniques sur le Nafion® et ont suggéré que plus l'hydrophobie et la taille de l'anion (du liquide ionique) sont grandes plus l'effet plastifiant du PCIL sur la matrice de Nafion® est fort.

Sanchez et al. a réalisé pour la première fois des études sur les membranes PCILs + Nafion® sous forme neutralisée {163.164}. La neutralisation des sites acides du Nafion® avec la même base que celle utilisée pour la préparation du PCIL a été effectuée pour éviter un processus d'échange de cations entre le Nafion® et le PCIL.

Dans leur travail, ils ont combiné le Nafion® sous forme neutralisée avec le triéthylammonium et des PCILs tels que le méthane sulfonate d'ammonium (MSTEA) et le triflate d'ammonium (TFTEA) par la méthode de gonflement. Une amélioration des propriétés thermiques du Nafion® a été rapportée en raison de la neutralisation des sites acides sulfoniques. En outre, ils ont signalé une conductivité anhydre de 10 mS/cm pour des membranes à base de TFTEA et 14mS/cm pour des membranes à base de MSTEA avec une forte plastification de membranes à haute concentration en PCILs. En outre, ils ont signalé une amélioration des propriétés mécaniques du Nafion® en le neutralisant avec une diamine en raison d'un phénomène de réticulation physique. Plus tard, ils ont démontré une meilleure conductivité des membranes anhydres imbibées avec un PCIL à base d'une diamine, en raison d'une forte contribution du mécanisme de Grotthuss dans la conduction du proton.

Vito di Noto et al. ont réalisé une étude approfondie sur le système Nafion-TEA + TFTEA par spectroscopie FTIR et Raman afin de comprendre les interactions entre les PCIL et la matrice polymère et l'organisation du PCIL au sein de la matrice{165}. Une diminution de la cristallinité de la phase hydrophobe du Nafion® a été proposée en raison de la neutralisation avec une amine et l'addition de liquide ionique. L'étude Raman a montré que les anions TF s'agrègent pour former des micelles. Le

mécanisme de conduction protonique dans ce type de système n'est pas encore totalement élucidé. Il a été proposé que les PCILs comme le TFTEA forment de micelles anioniques conduisant à l'obtention de nano-domaines appelés MTA dans les domaines hydrophiles de Nafion® et la migration des protons se fait par un phénomène de sauts entre les ions ammonium, les anions sulfonates du polymère et les MTA {166}.

De même, Wantanabe et al. ont combiné un polyimide sulfoné (neutralisé avec la diéthylméthylamine) avec le triflate diéthylméthylammonium (DEMAT) en utilisant la méthode de coulée-évaporation {167}. Ils ont rapporté l'effet plastifiant de DEMAT sur la matrice polyimide à des concentrations élevées (> 67wt%). Une conductivité ionique supérieure à  $10^{-3}$  S/cm à 40°C a été rapportée pour la membrane formée d'un ionomère d'une capacité d'échange ionique (CEI) de 2,15 et 1,41 meq / g contenant plus de 67% en poids de DEMAT. En outre, ils ont signalé une augmentation de la perméabilité à l'hydrogène et à l'oxygène de la matrice ionomère avec l'incorporation de DEMAT. Cependant, les coefficients de perméabilité sont du même ordre de grandeur que ceux qui sont reportés pour le Nafion® à l'état humide.

### **Motivation et objectifs de mes travaux de thèse:**

L'état de l'art sur les membranes à base de liquides ioniques à conduction protonique montre des propriétés très prometteuses de ces matériaux pour l'application pile à combustible, PEMFC, fonctionnant au-delà de 120°C. Cependant la plupart des études portent sur les liquides ioniques à base d'imidazole (ou imidazolium ?) qui se sont avérés moins performants dans les PEMFC que ceux à base d'ammonium dû à l'adsorption de l'imidazole sur le catalyseur de Pt. Il résulte de la majorité des données bibliographiques que les PCILs plastifient le polymère hôte ce qui peut avoir des effets négatifs sur la stabilité thermomécanique des membranes. Les propriétés des membranes sont très dépendantes de la structure du polymère et du PCIL mais aucune étude n'a clairement montré l'impact des différentes structures chimiques ou de la composition de la membrane sur la morphologie et les propriétés fonctionnelles. De plus, aucune étude n'a été consacrée aux propriétés de transport (telles que la sorption d'eau, la perméabilité aux gaz) et aux phénomènes de dégradation de ces membranes, ces études étant pourtant indispensables pour l'application pile à combustible.

La compréhension de l'effet produit par l'addition du PCIL sur la morphologie et les propriétés électrochimique, thermomécanique, de transport, etc. des membranes est exigée afin de concevoir des PEMFC performantes et d'adapter la structure et les propriétés des matériaux composant la membrane.

Ainsi, l'objectif de ma thèse a été de réaliser une étude approfondie sur l'influence de :

- la structure chimique de PCILs
- la concentration de PCIL
- la structure de polymères
- la méthode d'élaboration

sur l'évolution de la morphologie et des propriétés de la membrane.

Différentes techniques seront utilisées afin de caractériser la membrane à différentes échelles : moléculaire, nanoscopique-mésoscopique et macroscopique.

Afin de valider l'utilisation de ces membranes dans les piles à combustible, des tests préliminaires dans une mono-cellule sont également réalisés. L'une des principales causes de dégradation de la membrane est due à la formation des peroxydes lors du fonctionnement de la pile. Afin d'évaluer l'impact des peroxydes sur la stabilité des membranes, des études ont été réalisées en présence d'eau oxygénée.

### ***Résultats et discussion***

Les résultats de mes travaux de thèse sont présentés à travers 4 chapitres. Dans les trois premiers chapitres le Nafion neutralisé est utilisé comme matrice polymère. Le Nafion 117 a été neutralisé avec la même amine que celle utilisée pour la préparation des PCILs afin :

- d'améliorer sa compatibilité avec le PCIL,
- d'éviter l'échange cationique avec le PCIL
- d'améliorer la stabilité thermique des membranes gonflées {1,2}.

Les PCILs sont des alkyle d'ammonium qui semblent être plus adaptés pour l'application visée en raison d'une plus forte conductivité ionique et d'une absorption à la surface de l'électrode de Pt moindre par rapport aux PCILs à base d'imidazolium {3}.

Dans le dernier chapitre des Ionomères à base de polysulfone ont été synthétisés et étudiés en présence du liquide ionique.



**Objectif :**

L'objectif de ce chapitre est d'étudier l'impact de la concentration de liquide ionique, TFTEA, sur la morphologie des membranes de Nafion<sup>®</sup> neutralisé et implicitement sur leurs propriétés intrinsèques (comme la conductivité, les propriétés thermomécaniques, la perméabilité aux gaz et la sorption d'eau). La présence de l'eau est pratiquement inévitable dans les conditions de fonctionnement d'une PEMFC ainsi l'impact de l'humidité relative sur la morphologie et les conductivités de ces membranes a été également évalué.

Ce chapitre est divisé en trois parties :

- 1. le Nafion<sup>®</sup> neutralisé (Nafion-TEA) a été caractérisé et comparé au Nafion<sup>®</sup> 117 sous forme acide (Nafion-H<sup>+</sup>).
- 2. l'impact de la quantité de PCIL, sur la morphologie et les propriétés intrinsèques des membranes a été largement discuté.
- 3. l'impact de l'eau sur l'évolution de la morphologie et de la conductivité des membranes a été évalué.

Les structures chimiques de Nafion-TEA et TFTEA sont montrées dans la figure 1.

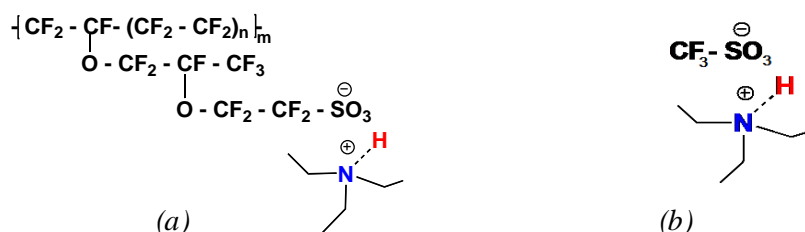


Figure 1: Structures chimiques des: a). Nafion-TEA; b). TFTEA

**Le Nafion<sup>®</sup> neutralisé (Nafion-TEA) : morphologie**

L'analyse SANS du Nafion-TEA nous a permis de supposer une organisation spécifique des cations de triéthylammonium (TEA) dans la matrice polymère. La différence entre la distance caractéristique, extraite du pic ionomère du Nafion<sup>®</sup> sous forme acide à l'état sec ( $d_0$ ) et du Nafion-TEA sec ( $d_{\text{TEA}}$ ) correspond à la taille du cation TEA (4 Å), suggérant une organisation « string like » des cations TEA localisés à l'interface hydrophobe-hydrophile. Cette organisation est représentée dans la figure 2.

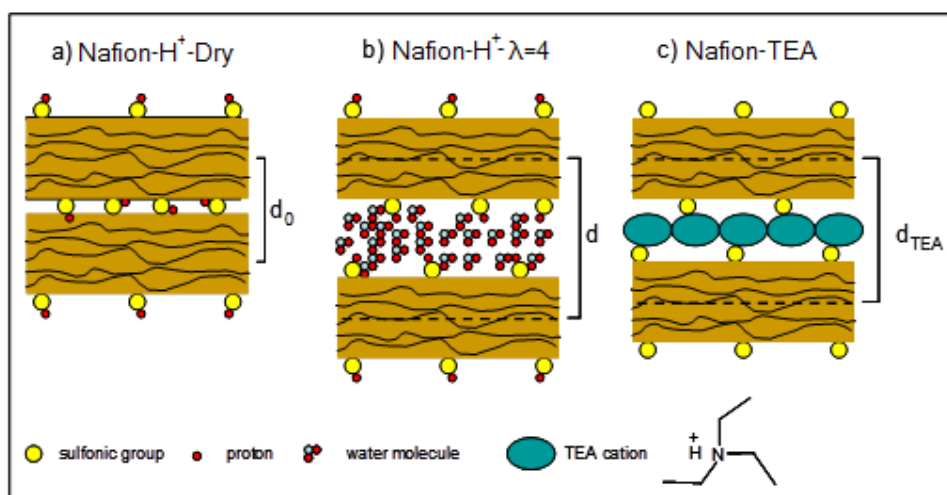


Figure 2 : Représentation schématique de l'interface hydrophobe / hydrophile de a) Nafion- $H^+$  sec; b) Nafion- $H^+$  à faible teneur en eau ; c) Nafion-TEA sec

### Membranes dopées : morphologie et propriétés

Pour les membranes dopées, l'évolution de la nano-structure du Nafion-TEA avec la concentration en TFTEA est très similaire à celle du Nafion<sup>®</sup> acide gonflé par l'eau. Cependant, des pics plus larges à haute teneur en TFTEA sont observés (pour des fractions volumiques d'eau ou de liquide ionique identiques), ce qui indique une répartition plus hétérogène du TFTEA dans la matrice Nafion-TEA à forte concentration en TFTEA probablement en raison d'une organisation micellaire de TFTEA dans la membrane.

Il a été démontré par analyse mécanique dynamique (DMA) que le TFTEA plastifie le Nafion-TEA induisant une plus grande mobilité des chaînes principales perfluorées. Ce phénomène s'amplifie avec l'augmentation de la concentration en TFTEA.

L'augmentation de la concentration de TFTEA dans les membranes accroît significativement la conductivité ionique en milieu anhydre (figure 3 (a)).

Il a été également montré que si la perméabilité aux gaz du Nafion-TEA est plus élevée par rapport au Nafion- $H^+$ , l'ajout de TFTEA dans le Nafion-TEA n'a en revanche pas d'influence sur la perméabilité dans la gamme de concentration en TFTEA considérée.

L'absorption d'eau par le Nafion-TEA est très faible par rapport au Nafion- $H^+$  et elle n'est pas dominée par la présence de sites spécifiques de sorption (isotherme BET III). Cependant, l'addition de liquide ionique conduit à une augmentation de la prise d'eau comme le montre la figure 3 (b).

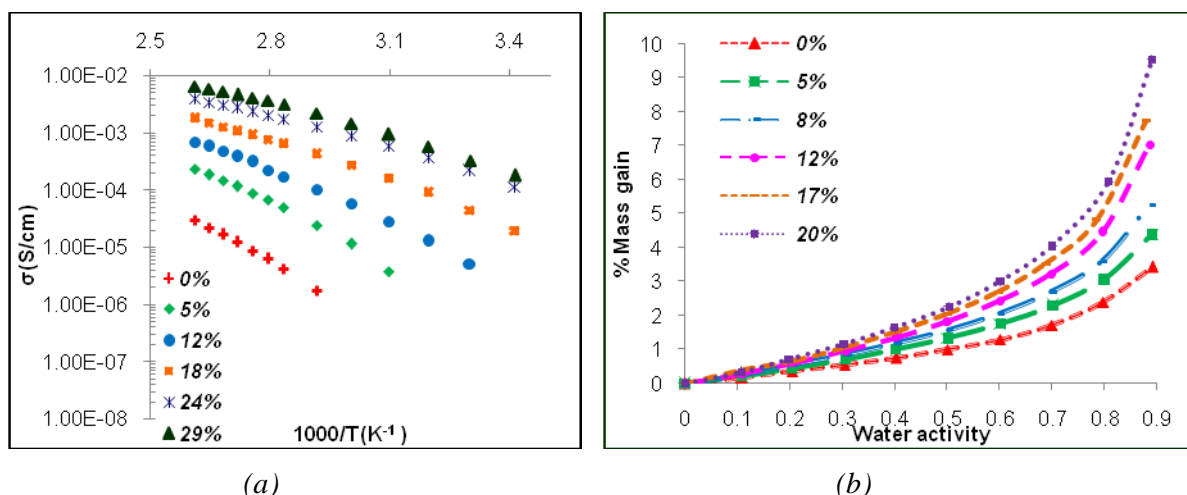


Figure 3 : Nafion neutralisé dopé avec différentes quantités de TFTEA (Nafion-TEA + x% TFTEA) :  
a). conductivité ionique ; b). sorption d'eau

### L'impact de l'eau

Concernant l'impact de l'hydratation, il a été démontré que la présence d'eau en faible quantité (faible humidité relative) augmente considérablement la conductivité ionique des membranes dopées avec TFTEA. En outre, la présence de molécules d'eau semble se traduire par un gonflement plus élevé des domaines ioniques et une meilleure nano-séparation des phases hydrophile-hydrophobe.

### Chapitre 3: Elaboration des membranes à base de Nafion-TEA et TFTEA. Comparaison entre les méthodes d'élaboration : gonflement / coulée évaporation

Objectif :

Evaluer l'impact de la méthode d'élaboration (gonflement ou coulée-évaporation) sur la morphologie et les propriétés des membranes dopées par TFTEA.

En effet, par le procédé de gonflement le liquide ionique gonfle une membrane pré-structurée de Nafion-TEA alors que par le procédé de coulée-évaporation la membrane est formée à partir d'une solution : Nafion-TEA + TFTEA + solvant polaire, l'organisation et la formation de la membrane hybride ayant lieu au cours de l'évaporation du solvant. Les principales différences entre ces deux méthodes sont illustrées dans la figure 4.

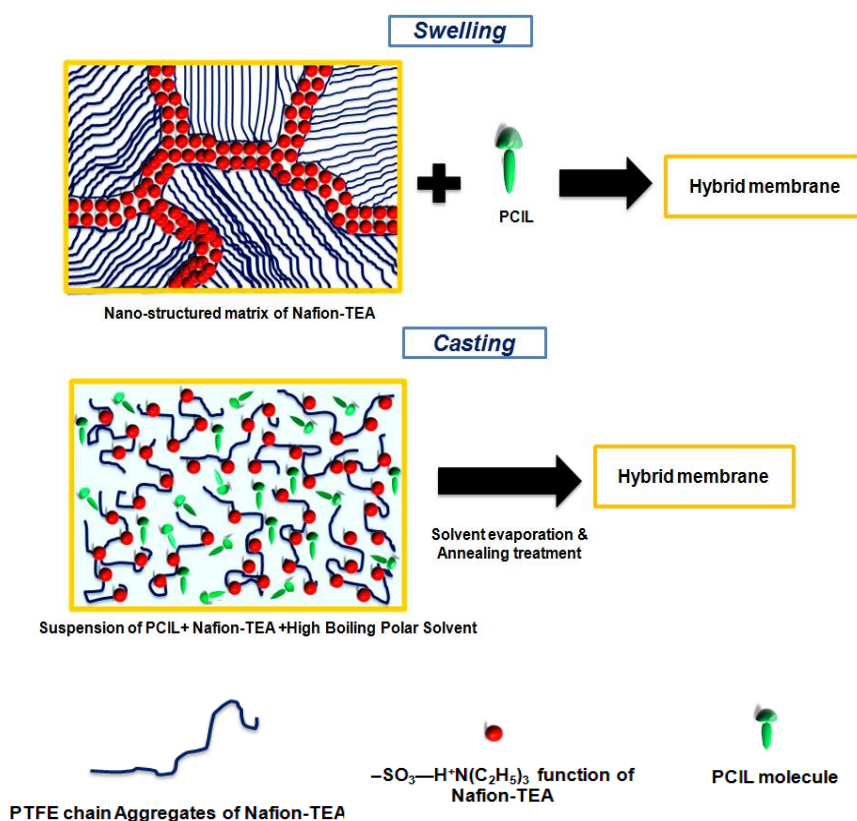


Figure 4: Comparaison de deux méthodes d'élaboration des membranes Nafion-TEA dopées : gonflement (swelling), coulée-évaporation (casting)

Ce chapitre a été divisé en trois parties:

1. les différentes propriétés des membranes Nafion-TEA préparées par le procédé de coulée-évaporation (Nafion-TEA-casting) sont comparées à celles des membranes Nafion-TEA obtenues à partir du Nafion 117 commercial (extrusion).
2. les propriétés des membranes de Nafion-TEA dopées avec TFTEA et préparées par coulée-évaporation ou gonflement sont largement discutées et comparées.
3. les performances des membranes dopées ont été évaluées dans la pile à combustible. Les phénomènes de dégradation de la membrane en présence de radicaux peroxydes ont été étudiés.

### ***Nafion-TEA : méthode d'élaboration***

La comparaison structurale à différentes échelles des deux membranes Nafion-TEA (obtenues par coulée-évaporation et par extrusion) a été réalisée par WAXS et SANS. Les conclusions sont présentées ci-dessous :

- A l'échelle cristallographique, dans la membrane de Nafion obtenue par coulée-évaporation (Nafion-casting) les chaînes perfluorées de Nafion-TEA sont ordonnées de manière plus dense
- A l'échelle nanoscopique, les différences sont négligeables. Ainsi, on peut supposer que les domaines ioniques de la membrane Nafion-TEA-casting sont disposés et organisés de manière assez similaire à celle du Nafion-TEA-extrudé.
- A l'échelle mésoscopique, les cristallites caractéristiques du squelette PTFE semblent être mieux organisées et / ou de plus grande taille dans le Nafion-TEA obtenu par coulée – évaporation.

Les études DMA ont montré que la membrane Nafion-TEA-casting présente des meilleures propriétés thermomécaniques au-dessus de 150°C et maintient un module de conservation d'environ 1 MPa dans la plage de températures de 150-190°C pendant que le Nafion-TEA extrudé s'effondre complètement à 150°C.

La conductivité de la membrane Nafion-TEA-casting est plus faible que celle du Nafion-TEA extrudé au-dessous de 100 °C.

Les coefficients de perméabilité aux gaz sont inférieurs pour la membrane obtenue par coulée-évaporation.

En ce qui concerne les propriétés de sorption d'eau, la prise d'eau par la membrane Nafion-TEA casting est légèrement plus élevée dans la plage d'activité d'eau de 0,1 à 0,8 et très proche à l'activité de 0,9. Toutefois, la diffusion de l'eau est beaucoup plus lente pour le Nafion-TEA casting. Tous ces résultats sont en accord avec les résultats de morphologie et ils renforcent l'hypothèse que les membranes obtenues par coulée-évaporation sont plus ordonnées et présentent un plus fort taux de cristallinité et / ou des cristallites de plus grande taille.

### **Membranes dopées**

La comparaison entre les membranes dopées (avec TFTEA) conduit à plusieurs conclusions :

- A l'échelle cristallographique, un empilement plus dense des chaînes perfluorées a été mis en évidence (en utilisant la technique de WAXS) pour les membranes obtenues par coulée-évaporation.
- A l'échelle nanoscopique, il a été montré par SANS que les membranes obtenues par coulée-évaporation présentent un gonflement des domaines ioniques supérieur et / ou plus hétérogène. Ce résultat pourrait être attribué à l'organisation micellaire de TFTEA dans la structure du Nafion-TEA qui semble être plus importante lorsque les membranes sont élaborées par coulée-évaporation (montré dans la figure 5).
- A l'échelle mésoscopique, les pics caractéristiques de la matrice observés par SANS n'évoluent pas avec l'augmentation de la concentration de TFTEA.

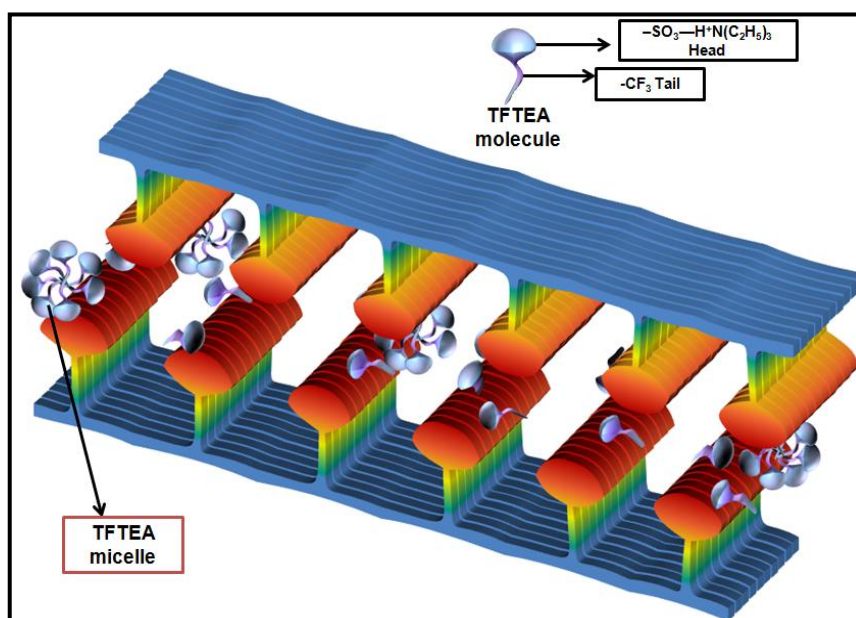


Figure 5 : Distribution inhomogène et organisation micellaire de TFTEA dans les domaines ionique de Nafion-TEA

Les spectres DMA montrent que les membranes obtenues par coulée-évaporation présentent de meilleures propriétés thermomécaniques : le module de conservation est supérieur avant  $150^\circ\text{C}$  et des modules d'au moins 1MPa sont maintenus jusqu' à  $180^\circ\text{C}$  alors que les membranes obtenues par gonflement s'effondrent avant  $150^\circ\text{C}$  (la température de fluage étant liée à la concentration de TFTEA).

Les deux types de membranes dopées présentent des conductivités assez similaires. Les coefficients de perméabilité aux gaz des membranes dopées obtenues par coulée-évaporation sont inférieurs à ceux des membranes préparées par gonflement, ce résultat renforçant l'hypothèse que les membranes Nafion-TEA + TFTEA obtenues par coulée-évaporation présentent un empilement plus dense des chaînes PTFE.

Les deux types de membranes dopées présentent un comportement similaire en sorption de vapeur d'eau (une augmentation de l'absorption d'eau avec les quantités croissantes de TFTEA), même si les résultats de la modélisation GAB suggèrent que la morphologie développée par coulée est plus favorable pour la sorption de molécules d'eau.

### **Tests en pile, dégradation**

Lors des tests en pile, des densités de courant de  $0.85\text{A}/\text{cm}^2$  à  $0.6\text{V}$  et  $100^\circ\text{C}$  (humidité relative 100%) sont obtenues pour une membrane contenant 20% de TFTEA. Cependant après quelques jours de fonctionnement une perte graduelle des performances a été observée, liée probablement à la dégradation mécanique et/ou la dégradation chimique en présence de radicaux peroxyde et l'élution de TFTEA de la membrane.

Les études sur la dégradation en présence de peroxydes ont montré une très bonne stabilité chimique de TFTEA. En revanche, le Nafion-TEA semble perdre ses cations, triéthylammonium, et se transformer en Nafion- $\text{H}^+$  après quelques jours d'exposition aux peroxydes. Egalement, il a été mis en évidence l'apparition d'anhydrides avec une cinétique beaucoup plus accélérée par rapport aux résultats publiées sur la dégradation du Nafion- $\text{H}^+$ .

En conclusion générale, les membranes élaborées par procédé de coulée-évaporation présentent une meilleure performance globale par rapport à des membranes élaborées par gonflement.

### ***Chapitre 4: Membranes obtenues par coulée évaporation. Influence de la structure de PCIL***

Objectif :

Dans le chapitre précédent, il a été démontré que la méthode d'élaboration a un fort impact sur la morphologie et les propriétés des membranes. Afin de mieux comprendre comment un PCIL à base d'anion perfluoré interagit avec la matrice Nafion-TEA et quel est son impact sur la morphologie et les propriétés, des membranes Nafion-TEA dopées avec différents PCILs ont été élaborés par coulée-

évaporation. En plus de TFTEA, deux liquides ioniques ont été utilisés, la différence étant donnée par la longueur de la chaîne perfluorée de l'anion.

Les PCILs utilisés sont les suivantes: Perfluorobutane sulfonate de triéthylammonium (PFBuTEA) et perfluorooctane sulfonate de triéthylammonium (PFOcTEA) (les structures chimiques étant représentées dans la figure 6). Les résultats obtenus avec des membranes dopées avec PFBuTEA d'une part et PFOcTEA, d'autre part, ont été analysés et comparés aux résultats issus de membranes à base de TFTEA.

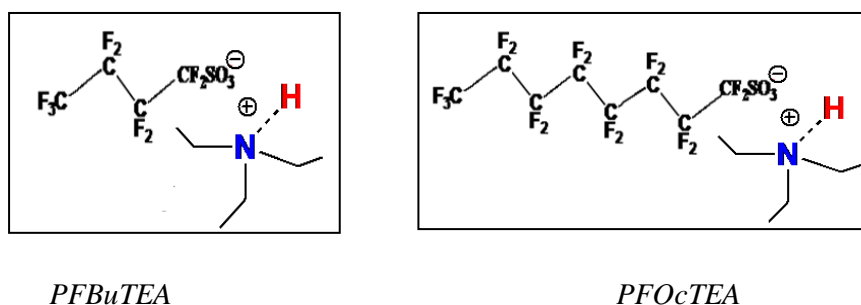


*Figure 6: Structures chimique de PFBuTEA et PFOcTEA*

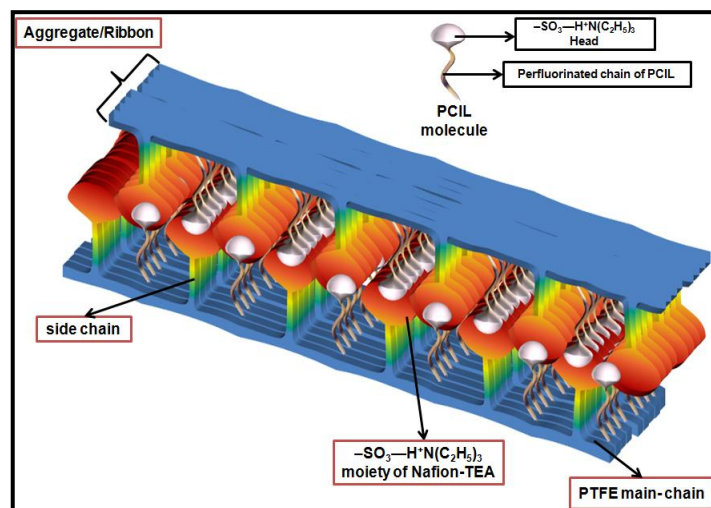
- A l'échelle cristallographique, il a été observé par WAXS que la densité des chaînes perfluorées est plus faible pour les membranes dopées avec le PFOcTEA et PFBuTEA par rapport à celles dopées avec le TFTEA. En plus, la structure hélicoïdale du Nafion est légèrement allongée dans le cas des membranes dopées avec des PCILs à plus longue chaîne perfluorée.
- A l'échelle nanoscopique et mésoscopique, les résultats de SANS ont montré que les PCILs : PFOcTEA et PFBuTEA ne modifient pas la nano-structuration de Nafion-TEA. Aucun changement de la taille des domaines ioniques ainsi que de la distance caractéristique associée à la matrice polymère, avec l'augmentation de la concentration du PCIL dans la membrane, n'a été observé contrairement aux membranes à base de TFTEA dans lesquelles un important gonflement des domaines ioniques avait été enregistré.

A partir de ces résultats, pour expliquer la structuration de la membrane en fonction du liquide ionique nous supposons que :

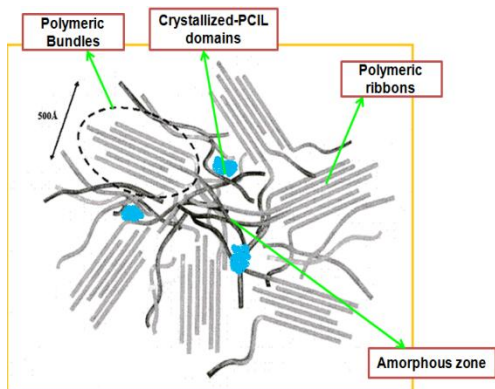
- les chaînes perfluorées de PFOcTEA et PFBuTEA ont la possibilité de s'insérer entre les chaînes latérales de Nafion à la surface des rubans de Nafion-TEA (figure 7 (a)) alors que le TFTEA se disperse de façon plus ou moins homogène dans les domaines ioniques du polymère.



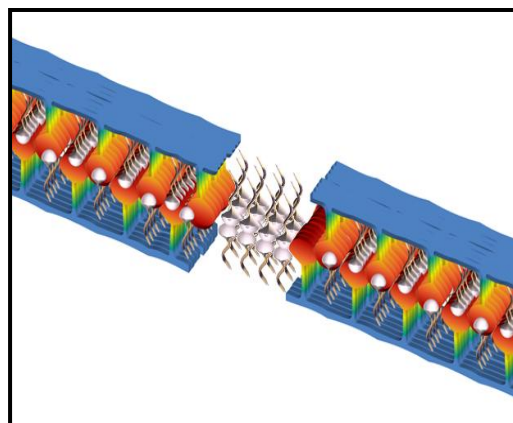
En plus, les résultats issus des analyses WAXS et SANS ont montré l'apparition de pics de Bragg caractéristiques pour le PFBuTEA et le PFOcTEA à partir de 30% en poids. Ces pics de Bragg mettent en évidence la formation de domaines PCIL cristallisés, probablement dans les régions amorphes inter-agrégats du polymère, où les liquides ioniques s'organisent de la même façon que dans le liquide pur (figure 7 (b) et (c)).



(a)



(b)



(c)

Figure 7: Organisation et répartition des PCILs PFOcTEA et PFBuTEA dans le Nafion-TEA (pour plus de clarté, l'entité ionique " $-\text{SO}_3-\text{H}^+\text{N}(\text{C}_2\text{H}_5)_3$ " du PCIL apparaît de plus petite taille par rapport à celle de Nafion-TEA)

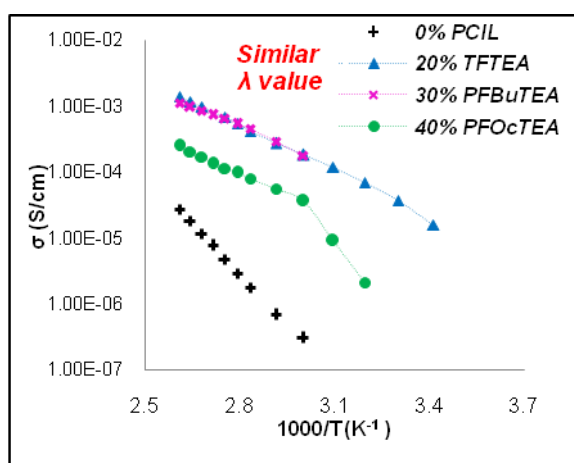
Les analyses DMA ont montré que les membranes à base de PFOcTEA présentent des meilleures propriétés thermomécaniques que les membranes à base de TFTEA à des températures inférieures à  $T_\alpha$ . Cependant, au-dessus de  $T_\alpha$ , les membranes à base de PFOcTEA s'effondrent tandis que les membranes à base de TFTEA présentent un module de 1 MPa jusqu'à 180 °C. Les membranes à base de

PFBuTEA présentent un comportement intermédiaire. Le comportement thermomécanique très différent des membranes doit s'expliquer par la structure et la polarité des PCILs.

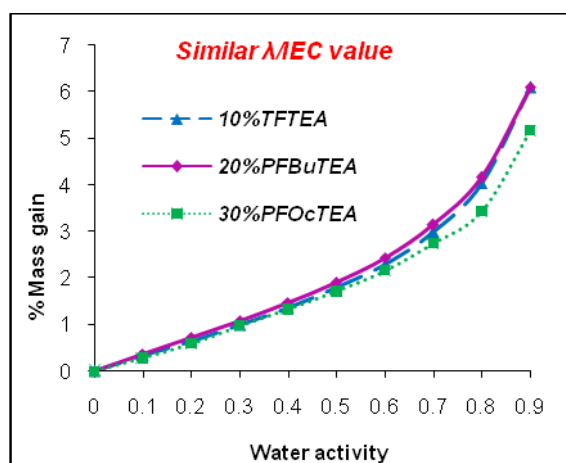
Les conductivités tant pour les membranes à base de PFOcTEA que pour celles à base de PFBuTEA sont dépendantes de la concentration. Pour les trois PCILs l'ordre de conductivité est le suivant: TFTEA ~ PFBuTEA > PFOcTEA (figure 8 (a)). Le fait d'observer des valeurs de conductivité très proches pour les membranes à base de TFTEA et PFBuTEA, malgré les conductivités beaucoup plus élevées de TFTEA pur par rapport à PFBuTEA, pourrait s'expliquer par la répartition et l'organisation de ces deux PCILs dans le Nafion-TEA.

Les coefficients de perméabilité à O<sub>2</sub> et H<sub>2</sub> sont très proches pour les trois types de membranes contenant jusqu'à 20% de PCIL en poids et ils sont peu dépendants des quantités de PCIL introduites. Cependant, à des concentrations plus élevées, les coefficients de perméabilité augmentent de façon significative probablement dû à la cristallisation des PCILs dans la matrice polymère.

Les études de sorption d'eau ont démontré que les membranes à base de PFOcTEA et PFBuTEA présentent des isothermes de sorption de type BET III comme le Nafion-TEA et les membranes dopées avec TFTEA (figure 8 (b)). La capacité de sorption d'eau de ces membranes dopées en fonction du type de PCIL est la suivante: PFOcTEA < PFBuTEA < TFTEA. PFOcTEA et PFBuTEA sont plus hydrophobes que TFTEA et même plus hydrophobe que le Nafion-TEA. Cependant une fois que ces PFBu-TEA et PFOC-TEA sont incorporés dans la membrane, leur contribution au phénomène de sorption est plus élevée qu'à l'état pur ce qui explique pourquoi les valeurs expérimentales de prise d'eau d'une membrane contenant 20% PCIL sont supérieures aux valeurs obtenues par la loi d'additivité. Ce comportement est probablement dû à l'organisation des molécules PFOcTEA/PFBuTEA dans la matrice Nafion-TEA qui doit être assez différente comparée à celle des liquides ioniques purs.



(a)



(b)

Figure 8 : Comparaison a). de la conductivité ionique, b).des isothermes de sorption de l'eau ; du Nafion-TEA dopé avec différents PCILs pour un même nombre de molécules de PCIL par site ionique de Nafion-TEA

Pour résumer, on peut dire que la structure chimique / nature du PCIL joue un rôle clé dans l'évolution de la morphologie et les propriétés fonctionnelles de la membrane (Nafion-TEA dans cette étude).

### Chapitre 5: Membranes à base de polysulfone et PCIL

Objectif :

Dans les chapitres précédents, nous avons montré que les propriétés thermomécaniques sont dépendantes de la structure du PCIL et de la méthode d'élaboration. Toutefois, des nouvelles matrices polymères doivent être développées afin d'obtenir des membranes stables du point de vue thermomécanique à haute température. Dans ce contexte, pendant ma thèse j'ai développé des Ionomères aromatiques fonctionnalisés avec des fonctions ioniques perfluorosulfonées similaires à celles du Nafion®.

Parmi les polymères aromatiques, le polysulfone a été choisi en raison de sa très grande stabilité thermique ( $T_g = 180\text{ }^{\circ}\text{C}$ ;  $T_d > 400\text{ }^{\circ}\text{C}$ ) et chimique qui sont toutes deux requises pour l'application HT-PEMFC. Le travail a porté sur un polysulfone commercial (UDEL) qui a été ultérieurement modifié pour attacher la fonction ionique sur la chaîne de base.

La structure chimique du polysulfone modifié (neutralisé avec la TEA, dénommé PSPF-TEA) est montrée sur la figure 9.

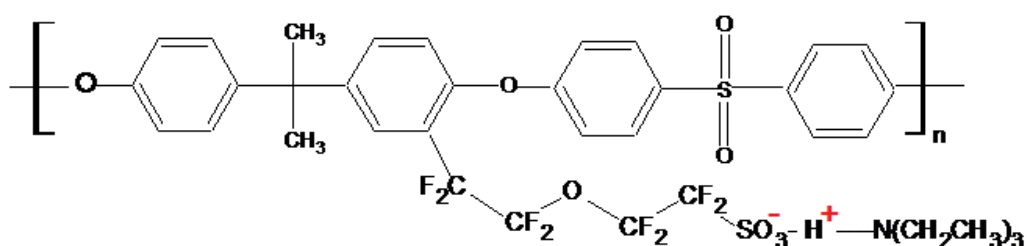


Figure 9: Structure chimique du Polysulfone-modifié PSPF-TEA

Ce chapitre est divisé en deux parties :

- 1). Optimisation du protocole de synthèse de PSPF-TEA
- 2). Caractérisation des membranes à base de PSPF-TEA et TFTEA en termes de morphologie, de propriétés thermomécaniques et conductivité

La synthèse est réalisée en trois étapes :

Bromation

Réaction d'Ulmann

Acidification et neutralisation des fonctions acides

Pendant la synthèse nous avons été confrontés au problème de coupures de chaînes lors de la réaction de bromation, sûrement dû à la présence de produit secondaire de réaction, HBr, et à la présence de la liaison éther sur la chaîne de base du polymère. Ainsi, afin de réduire cette réaction secondaire, différents protocoles ont été explorés : comme l'ajout de carbonate de potassium dans le milieu réactionnel ou l'ajout d'acide acétique.

Par les deux méthodes des nettes augmentations de la masse molaire ont été obtenues, mais les conditions restent encore à améliorer afin de complètement éliminer cette réaction parasite.

Les membranes ont été préparées par coulée-évaporation.

Malgré la présence d'une fonction ionique similaire à celle du Nafion et la présence d'un pic Ionomère bien défini pour PSPF acide, qui montre la nano-structuration du polymère en domaines hydrophile/hydrophobes, on observe que l'ajout de TFTEA dans la matrice polymère fait disparaître le pic ionomère. Nous supposons que les chaînes de base de PSPF-TEA, n'étant pas aussi hydrophobe que les chaînes PTFE du Nafion, interagissent avec le TFTEA et ainsi le liquide ionique est dispersé dans toute la membrane.

De plus, les résultats de DMA ont montré un effet fort de plastification par le TFTEA sur la matrice PSPF-TEA.

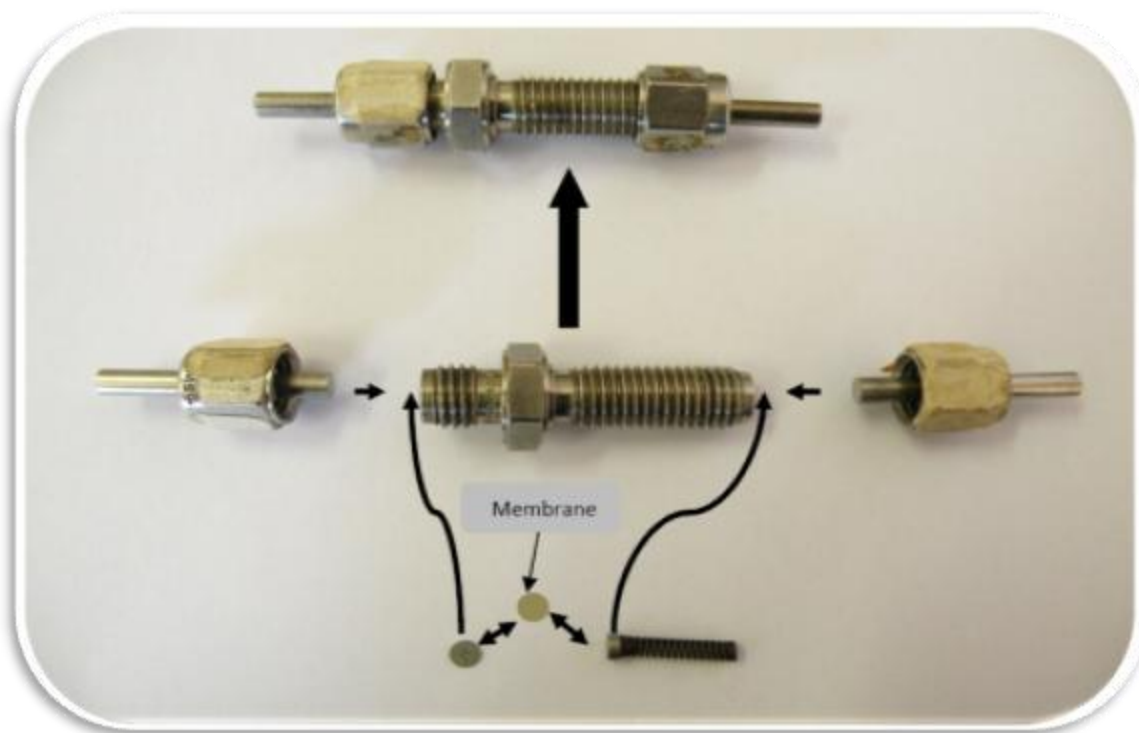
Les conductivités des systèmes PSPF-TEA + TFTEA sont supérieures à celles des membranes polysulfone sulfoné + TFTEA (aux mêmes degrés de sulfonation et mêmes fractions volumiques de TFTEA) à toutes les températures. Cependant, les conductivités restent inférieures à celles de Nafion-TEA + TFTEA pour des valeurs de  $\lambda$  ou fractions volumiques de TFTEA similaires.

En conclusion, cette étude a montré des tendances et pistes prometteuses liées à l'incorporation de PCILs dans des matrices polymère aromatique modifiée. Néanmoins la faible tenue thermomécanique reste un des freins majeurs pour l'application. Ce comportement est probablement dû à la fonctionnalisation statistique des polymères et à la dispersion dans la masse du polymère des espèces PCIL. Il en résulte des effets de plastification flagrants du polymère par le TFTEA. Par conséquent, afin d'améliorer les performances, il est important de séparer les domaines hydrophobes et hydrophiles du polymère. Pour séparer les domaines ioniques des domaines hydrophobes, il serait intéressant de synthétiser des copolymères à blocs dans lesquels un bloc serait fonctionnalisé et l'autre bloc choisi de façon à ne pas interagir avec le PCIL.

## ANNEXE 1

---

*Swagelok cell utilized for conductivity measurements at elevated temperature  
under anhydrous conditions*



## ANNEXE 2

---

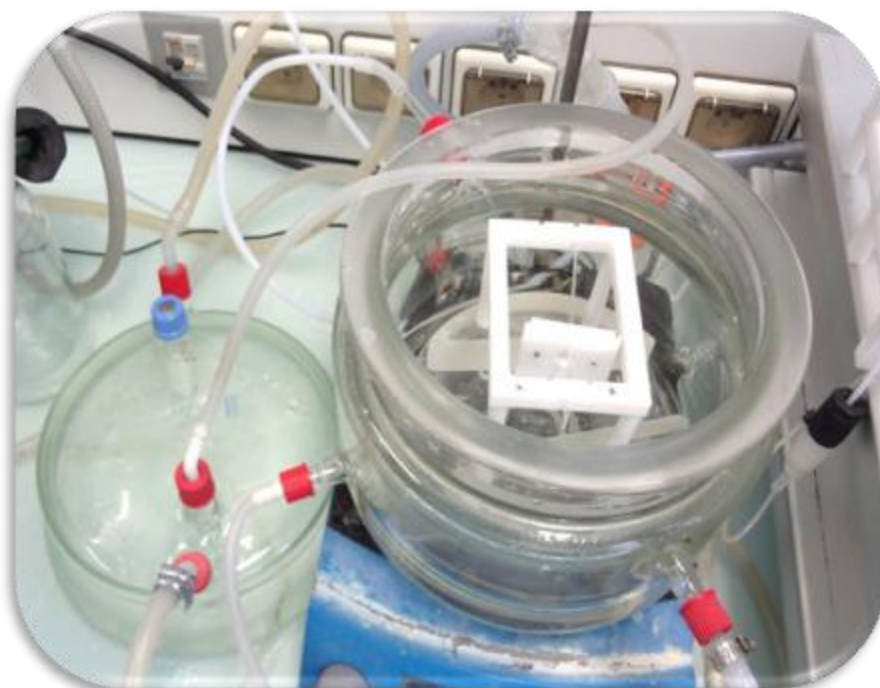
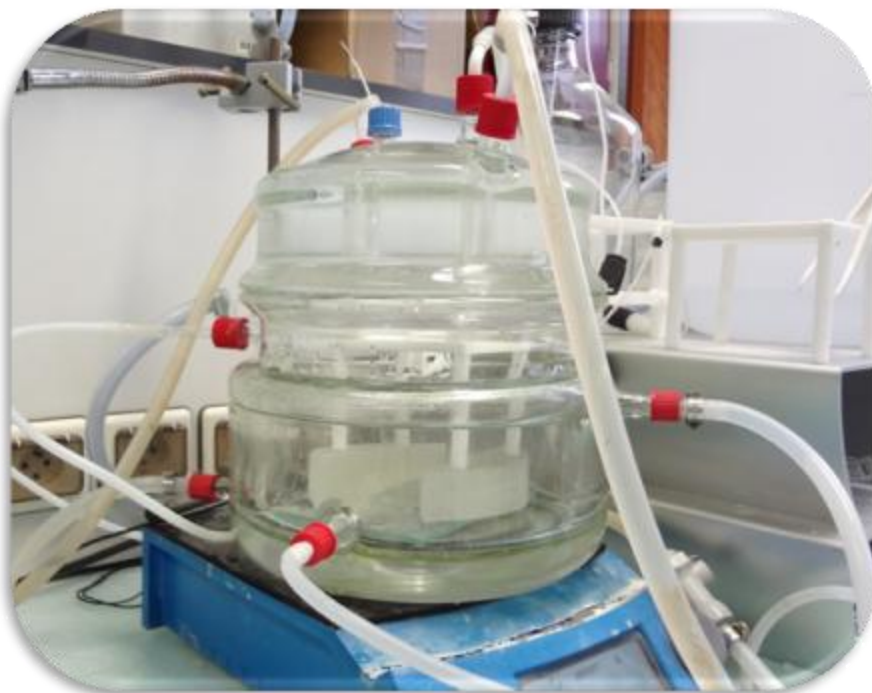
*PTFE sample holder equipped with a window: To hold thin membranes during degradation experiments and perform FTIR measurements in transmission mode before and after the experiments without dismounting the membranes*



## Annexe 3

---

*Experimental set-up utilized to perform degradation experiment with thin membranes*





**Summary:** The polymer electrolyte membranes based on Proton Conducting Ionic liquids (PCIL) are very promising systems for the high temperature-PEMFC technology owing to their good ionic conductivity and stability at temperatures above 100°C. The objective of this thesis work is to achieve a profound study on the evolution of morphology and consequent functional properties of the PCIL based polymer electrolyte membranes in function of: i). concentration of the PCIL, ii). the method of elaboration and iii). chemical structure of the PCIL. To demonstrate the potential of these membranes in HT-PEMFC, preliminary tests have been carried out in the fuel cell stack and degradation phenomena associated with PCILs and membranes in the presence of hydrogen peroxide have been studied. The first part of this work is focused on the characterization of Nafion® membranes neutralized with triethylamine (Nafion-TEA) and swollen with triethylammonium Triflate (TFTEA). It has been shown that Nafion-TEA exhibits a single layer string-like organization of inter-digited Triethylammonium cations at the hydrophobic-hydrophilic interface when in anhydrous state. The introduction of TFTEA into Nafion-TEA membrane does not destroy its nano-structuration but significantly boosts the anhydrous ionic conductivity and hydrophilicity of the system. The second part of this work has permitted us to establish the fact that doped membranes prepared by casting method have better organization and better thermo-mechanical properties compared to those obtained by swelling method. Third part of this work focuses on the impact of the chemical nature of the PCIL on the morphology and functional properties of Nafion-TEA membranes. It has been demonstrated that the PCILs with long perfluorinated chain length do not modify the nano-structuration of Nafion-TEA membranes at all. This has a strong impact on the ion-conducting, water-sorption and thermo-mechanical properties of the membrane. In the last part, aromatic ionomers were synthesized in order to replace Nafion-TEA in such PCIL based system. Despite the similar structure of the side chain of the synthesized aromatic ionomers and Nafion®, the membranes based on aromatic ionomers and TFTEA do not present any nano-structuration. Moreover, the plasticizing effect of TFTEA is more noticeable in the case of aromatic ionomers probably due to a random distribution functions in the ionic polymer membrane.

**Keywords:** High Temperature-PEMFCs; Ionic liquids; Polymer electrolytes; Nano-structuration; thermo-mechanical properties transport properties

**Résumé :** Les membranes à base de liquides ioniques à conduction protonique (PCIL) sont très prometteuses comme électrolytes des piles à combustible haute température (HT- PEMFC) du fait de leur forte conductivité et stabilité à des températures supérieures à 100°C. L'objectif de cette thèse est de réaliser une étude approfondie sur l'évolution de la morphologie et des propriétés fonctionnelles, des membranes à base de liquides ioniques, avec i) la concentration en PCIL, ii) la méthode d'élaboration et iii) la structure chimique du PCIL. Afin de prouver la potentialité de ces membranes dans le HT-PEMFC, des tests préliminaires en pile sont réalisés et les phénomènes de dégradation des PCIL et des membranes en présence de peroxyde d'hydrogène sont étudiés. La première partie de ce travail est focalisée sur la caractérisation des membranes de Nafion® neutralisées avec le triéthylamine (Nafion-TEA) et gonflées avec triflate de triéthylammonium (TFTEA). Il a été montré que dans le Nafion-TEA sec, les cations présentent une organisation de type « string like » à l'interface hydrophobe-hydrophile. L'introduction du TFTEA dans la membrane Nafion-TEA ne détruit pas sa nano-structuration, mais augmente de manière significative la conductivité ionique du système. La deuxième partie de ce travail nous a permis d'établir que les membranes dopées élaborées par coulée-évaporation présentent une meilleure organisation et une meilleure tenue thermomécanique par rapport à celles obtenues par gonflement. La troisième partie de ce travail est focalisée sur l'étude de l'impact de la nature chimique du PCIL sur la morphologie et les propriétés fonctionnelles des membranes de Nafion-TEA. Il a été démontré que les PCILs avec longues chaînes perfluorées ne modifient pas la nano-structuration du Nafion-TEA. Ceci a un impact fort sur les propriétés de conductivité, de sorption d'eau et sur les propriétés thermomécaniques de la membrane. Dans la dernière partie, des Ionomères aromatiques ont été synthétisés afin de remplacer le Nafion-TEA. Malgré la structure similaire de la chaîne latérale des Ionomères aromatiques et du Nafion®, les membranes à base d'Ionomères aromatiques et TFTEA ne présentent aucune nano-structuration. De plus l'effet plastifiant du TFTEA est plus notable dans le cas des Ionomères aromatiques probablement du fait d'une distribution aléatoire des fonctions ioniques dans la membrane polymère.

**Mot-clé :** PEMFC-Haute Température ; Electrolyte Polymère ; Liquide Ionique ; Nano-structuration ; Propriétés de Transport ; Propriétés Thermomécanique.